Modelling particle movement and sediment transport in rivers

Adrian Kelsey, BSc, MEng

This thesis is submitted for the degree of Doctor of Philosophy

at Lancaster University.

September 1993

"That's funny ," said Pooh. "I dropped it on the other side," said Pooh, "and it came out on this side! I wonder if it would do it again?" And he went back for some more fir-cones.

It did. It kept on doing it.

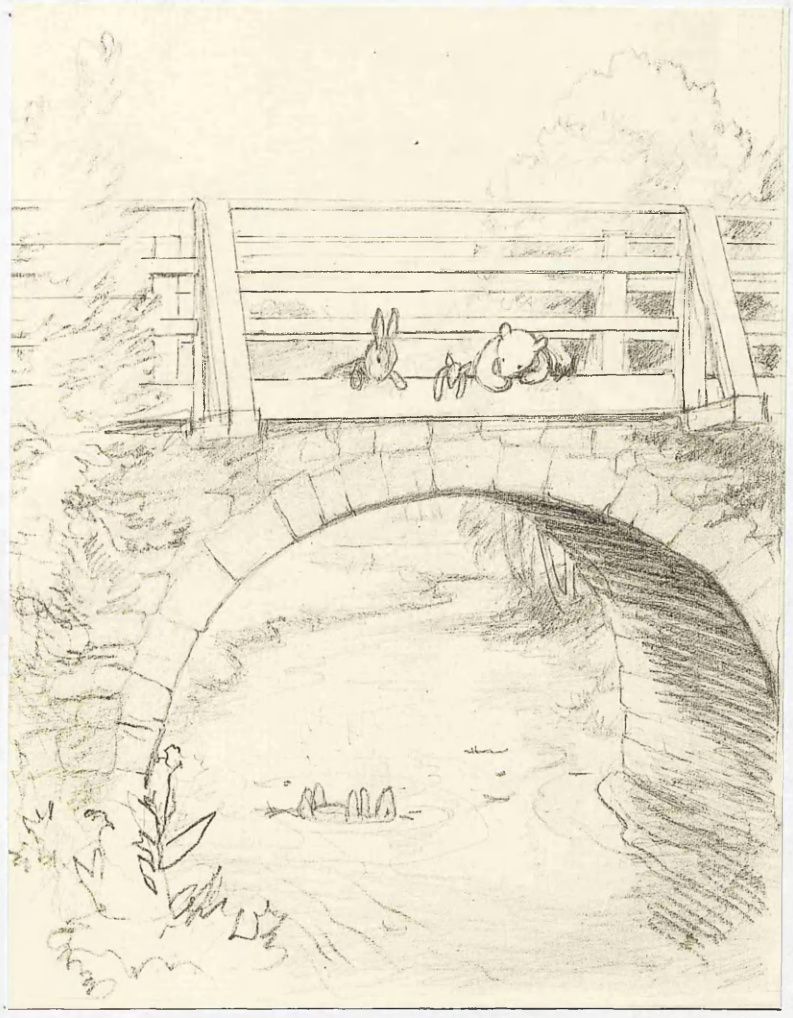

Looking very calm, very dignified, with his legs in the air, came Eeyore from beneath the bridge.

"It's Eeyore!" cried Roo, terribly excited.

"Is that so?" said Eeyore, getting caught up by a little eddy, and turning slowly round three times.

.....

"Not round and round," said Eeyore. "It's much more difficult. I didn't want to come swimming at all today," he went on, revolving slowly. "But if, when in, I decide to practise a slight circular movement from right to left - or perhaps I should say," he added, as he got into another eddy, "from left to right, just as it happens to occur to me, it is nobody's business but my own."

There was a moment's silence while everybody thought.

The House at Pooh Corner. A.A. Milne, 1928.

Modelling particle movement and sediment transport in Rivers

Adrian Kelsey, BSc, MEng.

Submitted for the degree of Doctor of Philosophy at Lancaster University

September 1993.

Models of fluvial bedload sediment transport have been developed at two scales: individual particle movement and mass transport of sediment. The model of the movement of individual sediment particles includes the stochastic influences due to the flow and the structure of the bed. This model was used to calculate distributions of particle movement. These were then used to calculate sediment transport over a mobile bed including the effects of the stochastic influences on particle movement.

The model of individual sediment particle movement includes descriptions of initiation of motion, rolling, non-contact motion and impact. The movements of sediment particles are calculated under the influence of turbulent velocity fluctuations, using a particle tracking method. Movements of initially coincident fluid and sediment particles are calculated, fluid movement due to mean flow and velocity fluctuations, sediment particle movement due to the fluid. The influence of fluid on sediment is continued until no correlation remains, either due to the separation of fluid and sediment or to elapsed time. At this point new conditions for the fluid are calculated.

Observations of particle movements in sediment transport show a range of particle movements for the same conditions, due to the stochastic influences of the structure of the bed and the turbulent flow. The particle model was used to calculate distributions of particle movements by repeated calculations of particle tracks on a parallel processing computer. These distributions were used to describe the behaviour of particles, fraction entrained, time in motion and distance travelled. The distributions were used to calculate the rate of sediment transport and the effects of sediment transport over a mobile bed. Their use in these calculations allowed the influence of stochastic processes at the scale of individual particle movements to influence the calculated sediment transport.

Table of contents

List of figures

List of tables

Acknowledgements

I would like to express my thanks to all my supervisors, Keith Beven and the late Cath Allen at Lancaster and Paul Carling at the Institute of Freshwater Ecology, Windermere. The supervision and guidance they gave has led eventually to the production of this thesis. The work described in this thesis was carried out while in receipt of an NERC studentship, for which I am grateful.

I would like to thank the members of the Fluid Dynamics & Hydrology Group for all their help, hindrance and the brewing of innumerable mugs of tea. Finally I would like to thank family and friends for their support during this thesis and especially during the lengthy write up.

Chapter 1

Introduction

1.1 Introduction

Transport of sediment involves the movement of many individual particles; sediment transport is the sum of the motion of all these individual particles. The movement of sediment particles does not occur in isolation. When sediment transport occurs it must be driven by a fluid. The resulting flow is a 2-phase flow, air and sediment for aeolian sediment transport; water and sediment for fluvial sediment transport. The process of sediment transport involves interactions and feedbacks between the 2 phases.

The type of sediment transport considered here is bedload transport of sediments in fluvial environments. When considering sediment transport in rivers a distinction is usually made between suspended load and bedload transport of sediment. In suspended transport sediment particles are supported by turbulent fluctuations in the flow, moving large distances between contacts with the bed. In bedload transport sediment particles are supported by the bed either directly, by sliding or rolling, or indirectly by conservation of momentum at impacts; this type of movement is called saltation. Though supported by contact with the bed this type of movement can be affected by turbulent velocity fluctuations. For bedload transport, in addition to the two phases of fluid and sediment there is a third component to the sediment transport process, that is the presence of a mobile boundary at the interface of fluid and sediment. In fluvial sediment transport the flow is driven by the component of gravity acting in the direction of flow. The flow over the mobile boundary imposes a shear stress on the boundary. When the shear stress due to the flow is below a critical value

the bed is at rest. As the shear stress increases it reaches a value such that the shear force acting on the bed is sufficient to mobilise the particles that form the bed.

The work described in this thesis is concerned with the modelling of bedload transport of sediment in rivers. Trying to describe sediment transport, qualitatively or quantitatively, in order to explain observations or to supply descriptions to model processes reveals a complex system of interactions and feedbacks. These interactions and feedbacks between flow and sediment occur over a wide range of scales, spatial and temporal.

Descriptions of sediment transport may be made at the level of individual particles or of groups of particles. In this thesis the approach taken to modelling the movement of sediment is to develop a particle based description of the movement of sediment particles. Such an approach acknowledges the discrete nature of the transport of sediment. The particle level is the smallest scale of the sediment transport process, such models can therefore incorporate the smallest scale processes of sediment transport. The use of particle based models allows stochastic process descriptions to be used and lend themselves to the inclusion and modification of different processes within an overall structure.

These particle based models and the data produced from them are then used as the basis for calculating mass movement of sediment particles in sediment transport. The models developed allow calculations to be performed at the larger scale of sediment transport while including the effects of processes occurring at smaller scales. The ultimate aim in developing models of sediment transport is to develop models which included the modification of the mobile bed, leading to the development of bedforms.

This approach to modelling sediment transport, calculations of single particle movements, then scaling these to the mass movement of sediment transport was made possible by the availability of relatively cheap parallel processing computers. The

performance of many similar calculations can be simply and efficiently implemented on parallel processing computers, making use of this power. This makes possible the calculation of the movements of many sediment particles, and allows the increase in scale from the calculation of the movement of single particles to the calculations of sediment transport.

In this introductory chapter three sections will be presented. The first gives a description of the range of scales, and the features representative of these scales in the transport of sediment. The modelling of sediment transport over mobile beds in rivers will then be considered. Finally a brief outline of the pattern of the rest of the thesis will be presented.

1.2 Scales of sediment transport

The range of scales associated with bedload sediment transport can be seen in the nature of the bed over which transport occurs and in the flow causing the transport to occur. The scales of the bed over which transport occurs are linked with scales of the flow and associated with temporal and spatial variations which occur in the rate of sediment transport. Sediment transport rate exhibits variation at all scales, due to the processes driving the transport and features of the transport (Gomez *et al.*, 1989, Hoey, 1992).

The scales of the bed start with the individual particles forming the bed and increase in scale through bedforms to larger variations in the quantities of bed material contained in reaches. In the flow causing sediment transport, the smallest scales are the turbulent fluctuations in the velocity of the flow. The scales involved increase from those due to secondary flows within a river through the storm scale hydrographs causing sediment transport events on to seasonal variations in flow. At all these scales there is temporal and spatial variability in the records of sediment transport.

The continuous record of counts of bedload particles moving past a detector at Squaw Creek, Montana, USA, described in Bunte (1992), showed both a response to a hydrograph and considerable variation between measurement intervals. The continuous records of sediment transport in flumes, described in Gomez *et al.* (1989), show large variations in transport rate, even with the steady flows used in these experiments. Measurement of bed heights and observations of the bed, performed at the same time as the measurement of sediment transport, linked variation in sediment transport rate with the passage of bedforms. The increasing scale of bedforms from ripples through secondary dunes to primary dunes caused fluctuations of decreasing frequency.

The discrete nature of sediment transport makes the behaviour of individual particles the smallest scale of the system to be studied. Even within the description of sediment particles a range of scales are present, from fine material, which would usually be carried in suspension by the flow, through sand and gravel which would move as bedload in saltation or, with increasing particle size, by sliding or rolling.

Single particles interact with the bed, other particles in motion and the flow. At this scale the interactions and cause of variation can be seen, though describing individual processes of particle movement can be difficult and the complete movement of particles harder still. The availability of a particle for transport is affected by its position on the bed, the relation of its size to the local bed, particle size and geometry, and the degree to which the surrounding bed acts to shield a particle from the flow. The variability possible in these geometries can be seen in the measurements made by Kirchner *et al.* (1990), for water worked surfaces in flumes, and Buffington *et al.* (1992), for water worked surfaces in river beds. In addition to these variations the packing geometries formed by particles in the bed can also influence the availability of a particle for entrainment into the flow; examples of this are structures, such as the clusters described in Reid *et al.* (1992). The availability of sediment for transport can also be affected by armouring (Parker & Sutherland, 1990) where the surface coarsens

due to transport leaving the sub-surface composition finer than the surface composition.

In addition to the considerations of the bed and its influence on the availability of a particle for movement there is the influence of the flow. While a particle cannot move until the forces necessary to mobilise it occur these can happen under a range of flow conditions. A particle can be mobilised when the mean flow conditions are insufficient to cause entrainment or remain immobile for a time when mean conditions are sufficient to cause entrainment. Such variation can occur due to the presence of turbulent fluctuations in the flow and specifically the presence of structures within the turbulence. The importance of such structures can be seen in observations of the fluvial environment described by Drake *et al.* (1988) and the marine environment described by Williams (1990) and is discussed further later.

The combination of bed structure and turbulent flow leads to complex interactions describing the movement of particles. A review of observations of particle movement, theory describing particle movement, and methods of modelling such effects is found in Chapters 2 and 3 of this thesis.

The increasing size of scales associated with sediment transport, spatial and temporal, described in Gomez *et al.* (1989) and Hoey (1992), start with the interaction of particle and flow described above. The interactions occurring at these scales lead to instantaneous variation in the rate of sediment transport. At the next scale, Hoey (1992), describes particle clusters, boulder steps and gravel ribs as typical features, i.e. local features caused by packing arrangements of particles which make a group of particles more stable than the individual particles forming the group. Gomez *et al.* (1989) identify the movement of bedforms, such as dunes, as the probable cause of variation in the rate of transport of sediment at this scale. These features and variations in transport rate are associated with temporal scales of the order of hydrographs, causing sediment transport events to occur. Beyond these scales the

features associated with variations in the rate of transport by Gomez *et al.* (1989) and Hoey (1992) are gravel sheets, bars and other large scale coherent features. The time scales associated with these variations are seasonal or even longer.

Observations of the distances travelled by similar size particles, in flumes, under steady flow conditions, showed a range of distances travelled (Einstein, 1937). Observations of the movement of sediment particles in rivers also found ranges of particle movements for single events (Hassan *et al.*, 1991, Schmidt & Ergenzinger, 1992). The stochastic influences due to the flow and the bed acting at the scale of individual particles act during mass transport of sediment. These influence the movement of the individual particles, and since it is the sum of the movements that constitute the transport of sediment, this is also affected.

1.3 Approaches to modelling

The description of sediment transport in the previous section showed that there are a range of scales involved in the sediment transport process and that there are variations in the transport rate at each of these scales, linked to stochastic processes at that scale and smaller scales. The work described in this thesis considers sediment transport at two scales, the first is the scale of the movement of individual particles, the second is the scale of mass movement of sediment particles. At the scale of individual particles the stochastic influences are known, though including them in a model of particle movement can still be difficult. However these influences also carry over into larger scales and having included their effects at one scale the change to mass transport should, if possible, be made including these effects.

Since some of the elements of sediment transport are stochastic even a deterministic model that accurately describes elements of the sediment transport processes will not be able to reproduce the full range of observed behaviour. At the scale of individual particles the stochastic influences on particle movement come from

the turbulent velocity fluctuations in the flow and the structure of the bed. The stochastic elements in particle movement have been included in models of particle movement by using distributions to describe components of the model. These distributions can either be used as a source of random numbers in calculations or to assign probabilities to events. In Naden (1987a), probabilities for particle entrainments are calculated based on the distribution of forces acting due to velocity fluctuations. Models of particle movement which include impact with the bed as a process have introduced a stochastic element into the calculation of particle movement by the inclusion of a random element in the description of the bed. Wiberg & Smith (1985) used impact heights selected from a random distribution between the minimum and maximum possible impact heights, Sekine & Kikkawa (1992) calculated a bed structure with particle heights determined from a random distribution.

As the scale at which sediment transport is being studied increases, the detail of the descriptions used must decrease, to keep calculations manageable. Calculations of sediment transport therefore move from discrete descriptions for processes such as initial motion to continuum descriptions for rate of transport. This change can be seen in the models of particle movement of Wiberg & Smith (1985) and Sekine & Kikkawa (1992). Both of these models of particle movement include a stochastic element based on impact with the bed and results calculated using them have been successfully compared with observations. The models of particle movement have also been used as the basis for the development of expressions for the rate of transport of sediment (Wiberg & Smith, 1989, Sekine & Kikkawa, 1992). In order to use the data from the model of particle movement in the calculation of sediment transport the range of values of particle movement calculated for the movement of individual particles were reduced to a mean concentration profile in Wiberg & Smith (1989) and mean quantities describing dimensions of trajectories in Sekine & Kikkawa (1992).

Particle based models have been used in models of sediment transport processes because of the discrete nature of the sediment transport process. Particle

models have also been used in other fields of study related to the environment, in particular to the modelling of the dispersion of tracers and pollutants (Zannetti, 1990, Allen, 1982). In these applications the method used is particle tracking, the movements of particles, representing the pollutant or tracer, are calculated, based on local flow conditions and stochastic influences of the flow. The method is used because the process being modelled is Lagrangian and stochastic. Particle tracking models are explicitly Lagrangian and stochastic effects, important in the dispersion process, such as those , due to turbulent velocity fluctuations, can easily be imposed on the movement of particles. The data requirements to use such a model, such as descriptive statistics of the turbulence, are also simple in principle, though not necessarily easy to supply.

Existing models of the movement of sediment particles as bedload only include stochastic elements in the model due to the impact with the bed. Observations of particle movement show that turbulent velocity fluctuations have a significant influence on particle movement. The adoption of a particle tracking approach to modelling the interaction of particle movement and fluid allows the development of a model of sediment particle movement which includes the stochastic influence of turbulent velocity fluctuations as well as the effects of impact with the bed. This approach is used in the development of the model of particle movement described in this thesis.

The other scale considered in this thesis is the mass movement of sediment particles over a mobile bed. As has already been described for the rate of transport of sediment, increasing the scale means that features present at one scale can often only be represented by simple statistics, such as the mean, rather than the range of values that they take. Another reason for the interest in particle tracking as a method for calculating the dispersion of tracers is that the result is obtained by calculating the movement of many particles independently. The passage of passive tracers does not modify flow, therefore the mean flow component and distributions for the fluctuations need only be specified at the start of calculations. This type of calculation can easily be

implemented on parallel processing computers, calculations for the same conditions can be repeated many times, on individual processors, without the need for communication between processors. The development of parallel computers has led to development of particle tracking methods and enabled calculations to be performed with large numbers of particles.

Calculations of sediment transport based on particle movements are more complicated. Sediment particles are not passive tracers, they modify the flow and interact with each other. The number of particles involved in mass transport of sediment is large and the description of the motion is more complicated than that for passive tracers, requiring the numerical solution of ordinary differential equations, rather than an analytical solution. The combination of non-independent calculations and greater computational requirements make direct calculation of the movement of sediment particles very computationally intensive. Such calculations have been performed for deterministic systems, where the bed was the only stochastic influence, (Jiang & Haff, 1993) but this calculation was in two dimensions for only 100 particles. By comparison, calculations involving dispersion of passive tracers have been made in three dimensions using 20,000 particles (Hankin pers. comm.).

There are more difficulties involved in increasing the scale of a calculation of the movement of sediment particles than there are scaling problems modelling the dispersion of a passive tracer. In describing and modelling of sediment transport one theme has been the development of deterministic equations describing processes. However an alternative approach has been to acknowledge the stochastic nature of the process and, rather than using deterministic descriptions, use distributions to describe particle movement. This was the approach taken to the calculation of sediment transport by Einstein (1937).

The use of distributions based on calculations of particle movement can be used to model sediment transport. Such calculations allow the use of a model of particle

movement including stochastic influences to be used for the calculations of particle movement, make effective use of parallel computing facilities and allow the influence of processes at one scale to be felt at larger scales. Such an approach deals with the problem associated with the development of models of sediment transport over a mobile bed identified earlier and is used here in the development of models of sediment transport.

1.4 Summary of contents

The contents of this thesis are split into two parts, describing the movement of sediment particles and mass transport of sediment particles respectively.

The first part of the thesis is concerned with the movement of individual sediment particles. In this part a model of the movement of sediment particles is developed and then tested. In Chapter 2, observations of the movement of sediment particles and the theory describing these movements are reviewed. In Chapter 3, previous models of particle movement are described, along with the necessary descriptions of flow and the bed. Based on the work reviewed in these chapters, Chapter 4 describes a model of the movement of single sediment particles. The model takes into account observations and theory in the choice of processes included in the model. The descriptions of processes take into account representations from previous models and their limitations. The final chapter of this part, Chapter 5, describes the testing of the model and compares results calculated with the model, with those observed experimentally.

The second part describes the transport of sediment. In this part of the thesis the mass movement of sediment particles is considered, leading to descriptions of the rate of sediment transport and a model of sediment transport and bed modification. The descriptions of the mass movement of sediment particles take into account the stochastic nature of the sediment transport process. Chapter 6, reviews particle based

models of sediment transport and the stochastic descriptions they contain. In Chapter 7, calculated ranges and distributions of particle behaviour are examined. Finally in Chapter 8 a rate of sediment transport expression and a model of sediment transport over a mobile bed are described. These models both use the distributions of particle behaviour described in the previous chapter.

The final chapter of the thesis, Chapter 9, contains conclusions about the work described in the rest of the thesis and recommendations for future work.

Part I

Movement of sediment particles

Chapter 2

Movement of sediment particles, observation and theory

2.1 Introduction

This part of the thesis, Part I, describes the movement of particles in fluvial sediment transport, in particular the movement of single particles. The flow in which such transport occurs is turbulent. The sediment particles under consideration are those moving as bedload. Particles moving as bedload are supported by contact with the bed, either directly, when sliding or rolling, or by impacts with the bed, when saltating. This type of motion is in contrast with suspended motion of particles where particles are supported by the fluctuations in the flow and can travel an indefinite distance between contacts with the bed. Turbulent fluctuations in the flow can affect the motion of particles even when they are moving as bedload, influencing particularly the initiation of particles into motion and modifying particle trajectories.

The aim of this work was to develop a particle based model of the bedload movement of sediment particles in fluvial systems, including the effects of turbulent fluctuations on particle motion. Such a model could be used to study transport processes and the interactions of particles and the fluvial system. It could also be used to examine particle behaviour qualitatively, and to calculate quantitative descriptions of particle movement such as distance and speed of travel.

The first three chapters of this part of the thesis share a common structure, with each chapter containing sections describing the nature of the flow, sediment movement and the bed. This breakdown of fluvial sediment transport is used in Leeder (1983) to describe the elements of, and the feedbacks occurring in sediment transport in open channel flows. Leeder (1983) emphasises the importance of the inter-relationships and feedbacks present in fluvial sediment transport (see Figure 2.1a) and that considering

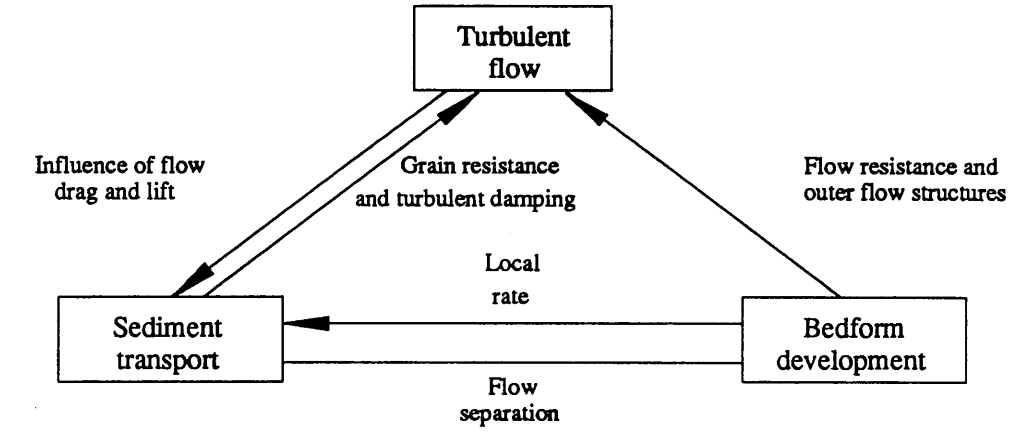

a)

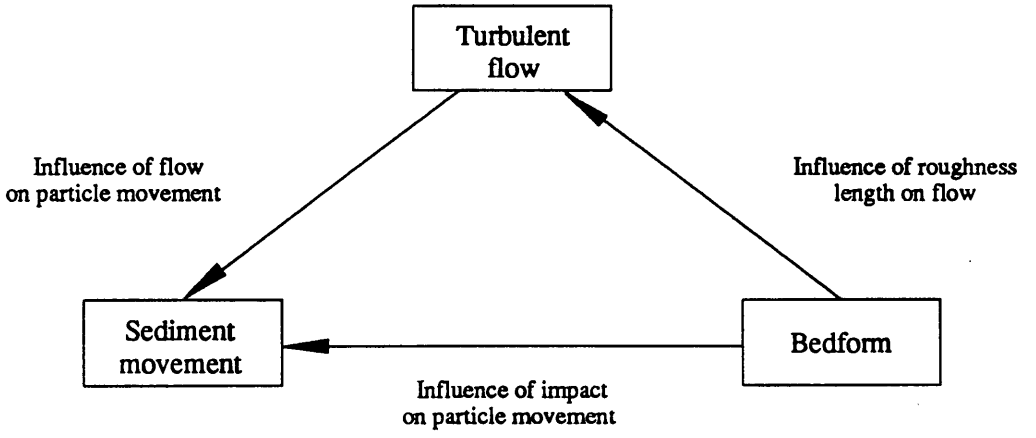

b)

Figure 2.1 Feedbacks and interactions in fluvial sediment transport

portions of the sediment transport process in isolation will not necessarily give results applicable to the whole. By only considering the movements of single particles and ignoring interactions between moving particles the description of the movement of particles in sediment transport is greatly simplified, but still contain all the elements forming the sediment transport process. When bulk movements of sediment occur, the feedbacks are due to the bulk nature of the processes; when only single particles are in motion these feedbacks are reduced to interactions (see Figure 2.1b). Any feedbacks between sediment particles and bedform and bedform and flow cannot be considered because there is no way for the movement of a single particle to modify the bedform. Feedback between sediment movement and the flow can be considered in that the particle will extract momentum from the flow causing the flow to be modified. However for a single particle in a fluvial environment, where the density of particle and fluid are of the same order of magnitude the effect this will have on the flow can be assumed to be negligible.

While the aim of this work was to model the movement of sediment particles in fluvial systems there have been other studies of particles movement in fluids. The movement of sediment particles in aeolian systems and more generally the movement of particles in fluid have been studied. The information from these studies is described where it is relevant to the present work.

2.2 Flow

In rivers in which sediment transport is occurring the flow will be turbulent. An appropriate description of the flow will therefore take into account its turbulent nature and the effects this may have on the transport of sediment.

An idealised turbulent flow can be described by the continuity and Navier-Stokes equations. For steady, incompressible flow, a reasonable assumption for open channel flow, these can be written:

$$\frac{\partial u_i}{\partial x} = 0$$

$$\rho\left(u_j \frac{\partial u_i}{\partial x_j}\right) = \rho F_i - \frac{\partial p}{\partial x_i} + \mu \nabla^2 u_i$$

where u_i is the velocity in direction x_i, F_i is the body force in direction x_i, ρ is the fluid density, p is the pressure and μ is the dynamic viscosity. For a 3-dimensional flow , i = 1,2,3 directions, x_i correspond to x, y, z directions and the corresponding velocities u_i to u, v, w. The x axis is taken to be in the mean streamwise direction, the y axis the cross stream direction and the z axis to be vertical, Figure 2.2. In the Navier-Stokes equation the term on the left hand side represents the acceleration force on the fluid; the first term on the right hand side represents the body force acting, the second the pressure or inertial force and the third term the viscous forces acting. In many applications assumptions can be made simplifying these full equations leading to a simpler description of the system under consideration.

Turbulent flow in rivers contains a wide range of spatial and temporal scales, from the smallest, associated with viscous dissipation of energy to the largest, determined by the channel geometry. In order to simplify the description of the system, the velocity and other properties can be decomposed into mean and fluctuating components, using the Reynolds decomposition

$$u_i = U_i + u_i'$$

where U_i are the mean velocity components and u_i' the fluctuating components in direction x_i. This decomposition can be substituted into the equations of continuity and the Navier-Stokes equations, these can then be time averaged and rearranged to give the Reynolds equations.

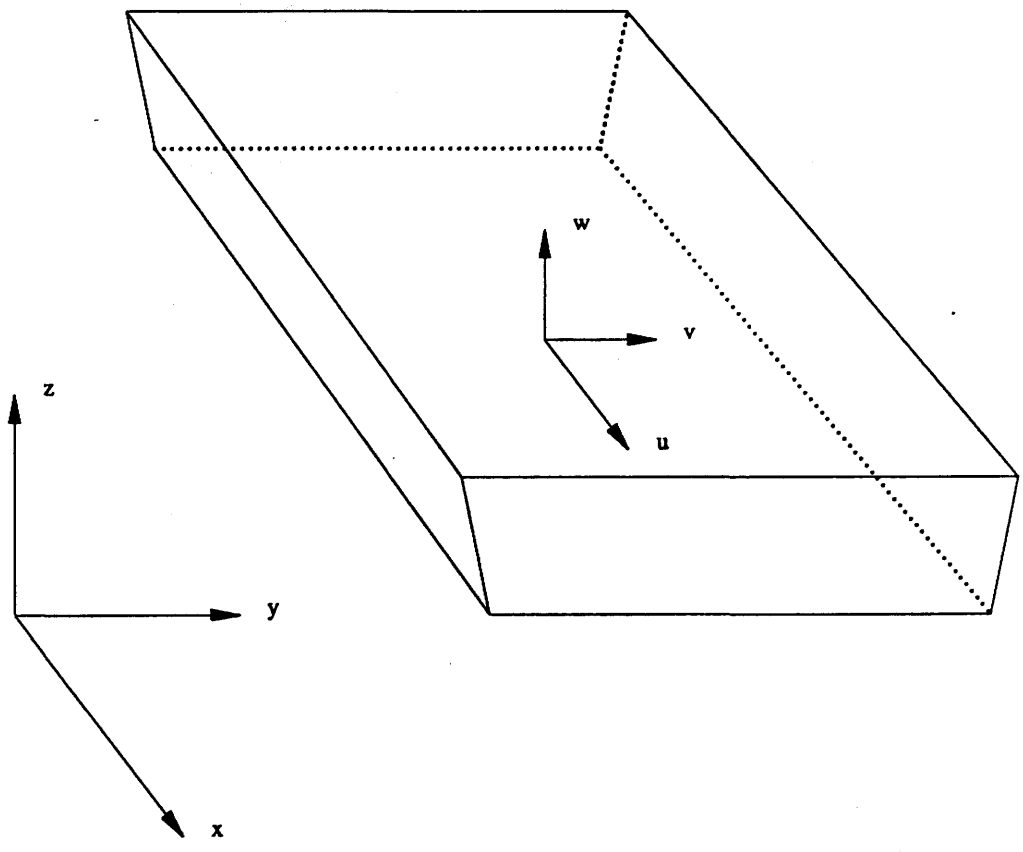

Figure 2.2 Coordinate system

$$\rho\left(U_j \frac{\partial U_i}{\partial x_j}\right) = \rho F_i - \frac{\partial \bar{p}}{\partial x_i} + \frac{\partial}{\partial x_i}\left(\mu \frac{\partial U_i}{\partial x_j} - \rho \overline{u_i' u_j'}\right)$$

where the overbars represent time average quantities. Though this simplifies the equations the descriptions so produced are for the mean flow and contain more terms than there are equations, introducing a closure problem. The extra terms are the products of the fluctuating terms, the Reynolds stresses.

These descriptions of turbulent flow are completely general, the nature of the flow steady or unsteady is not specified. Turbulence itself is a 3-dimensional phenomenon. However, although flow in straight channels or laboratory flumes includes cross-stream currents due to the influence of boundaries and in rivers also due to upstream influences the dominant flow is the streamwise component of flow. Likewise while cross-stream velocity fluctuations exist their magnitude is less than the streamwise fluctuations and their influence when describing processes such as bursting and sweeping is not as important as that of the vertical fluctuations. Thus the effects of features in the turbulence, important in the transport of sediment, can be broadly represented in terms of the mean flow and a 2-dimensional representation of the turbulent velocity fluctuations. Once such a model has been tested in 2 dimensions the possibility of its extension to 3 dimensions remains. If along with the reduction to 2 dimensions the flow is considered to be steady then the Reynolds equations can be stated in the form

$$\rho\left(U\frac{\partial U}{\partial x}+W\frac{\partial U}{\partial z}\right)= \rho F_x - \frac{\partial \overline{p}}{\partial x} + \frac{\partial}{\partial z}\left(\mu\frac{\partial U}{\partial z}-\rho\overline{u'w'}\right)$$

The Reynolds decomposition of turbulent flow, as well as enabling a simplified form of the Navier-Stokes equations to be derived for the mean flow components, suggests the approach of describing the mean flow and superimposing the effects of turbulent fluctuations on this mean flow.

2.2.1 Mean flow component

A description of the mean flow component can be derived from dimensional considerations and asymptotic matching. The dimensional analysis of turbulent flow described here is 2-dimensional. While flow in channels contains secondary, cross-stream components, the mean velocity profile described here has been found to give a good fit to data for rivers (Carling, 1991) and is appropriate to describe flow in laboratory flumes. The analysis is for uniform steady flow and is based on a consideration of the length scales acting through the depth of the flow. The boundary layer is considered in three regions: a viscous or roughness sub-layer, in which the length scale is related to the viscosity; an inertial sub-layer, scaled by the roughness length scale, and an outer wake region, where the scaling is from the boundary layer (Raupach *et al.*, 1991). The form of the velocity profiles in each of these regions can be derived from the variables which affect the velocity profile in that region. Between inner and outer regions the blending of the velocity profile must be smooth and continuous, the flow in the inertial sub layer, the main region of interest for bedload

movement of particles, is therefore described by the logarithmic velocity profile for turbulent flow over a rough boundary

$$\frac{U}{U_*} = \frac{1}{\kappa} \ln\left(\frac{z}{z_0}\right)$$

where U_* is the mean bed shear velocity, κ is von Karman's constant, z is the height above the zero velocity height and z_0 is the roughness length scale, as derived in Raupach *et al.* (1991), for a solid surface and by Nakagawa *et al.* (1988) for a permeable surface. Thus for any depth, we can describe the mean velocity component acting on a particle in motion over a rough surface, the assumption of a 2-dimensional system with uniform flow limiting the other mean velocity components to zero.

2.2.2 Fluctuating flow component

The action and importance of the fluctuating components of velocity on sediment particles can be seen from observations of particle motion. Sediment transport is usually described as either suspended or bedload transport. In suspended transport particles are completely supported by the fluctuations of the flow and can therefore travel an indefinite distance without contact with the bed. In bedload transport the particles are directly supported by the bed either directly, by rolling or sliding, or by impacts between movements away from the bed. Movement of particles as bedload is usually regarded as being unaffected by turbulence. However since suspended transport is usually only taken to start when the flow is fully capable of carrying particles in suspension, at any stage below this condition a particle may be affected by turbulence without becoming fully suspended. There are two ways that particles which would travel as bedload may be affected by turbulence without becoming fully suspended, both of these occur due to the nature of the fluctuations in turbulent flow close to a boundary. The first is that a particle may start to move when the mean bed shear stress is below that for particle motion since fluctuations can cause instantaneous values of higher shear stress. The second is that the trajectories of

particles which are basically moving as bedload in saltation can have their trajectories altered by turbulent fluctuations, changing the distance travelled between contacts with the bed. This behaviour is called "modified" saltation by Hunt & Nalpanis (1985).

In laboratory studies of flow over smooth walls (Kline *et al.*, 1967) it was observed that low speed streaks existed on the wall. These structures periodically broke down, ejecting fluid from the wall in what they called a "burst". Observation by Grass (1971) showed that a similar bursting process was present in flow over a rough boundary, though the mechanisms involved were not necessarily the same. The turbulent fluctuations are not simply random uncorrelated signals but contain coherent structures which transport significant quantities of mass, heat and momentum. The bursting process was part of a "burst-sweep" cycle, in which low speed fluid "burst" or was "ejected" from the near wall region; this was then followed by a "sweep" or "inrush" of high speed fluid from the surrounding region. Analysis of measurements of turbulence in the wall region to examine bursting & sweeping were made using quadrant analysis; the quadrants are defined by the horizontal and vertical velocity fluctuations, u', w', Figure 2.3. The analysis calculates the contribution to the Reynolds stress from each of these quadrants (Lu & Wilmarth, 1973); the largest contribution to the total stress comes from bursting, followed by sweeping. The frequency, duration and contribution to total stress from each quadrant were also examined by Lu & Wilmarth (1973).

This analysis showed that a majority of the shear stress occurred in a minority of the time and occurred in the quadrants associated with bursts and sweeps. The bursting and sweeping was not continuous; but there would be a period of high shear stress followed by a period where the signal was relatively quiescent. The behaviour of the turbulence signals was related to the presence of coherent structures in this near wall layer, these eddies would detach from the wall causing the observed signals. This analysis was made on laboratory measurements in the near wall region. Analysis of measurements of turbulence made on the River Severn (Heslop *et al.*, 1993) show

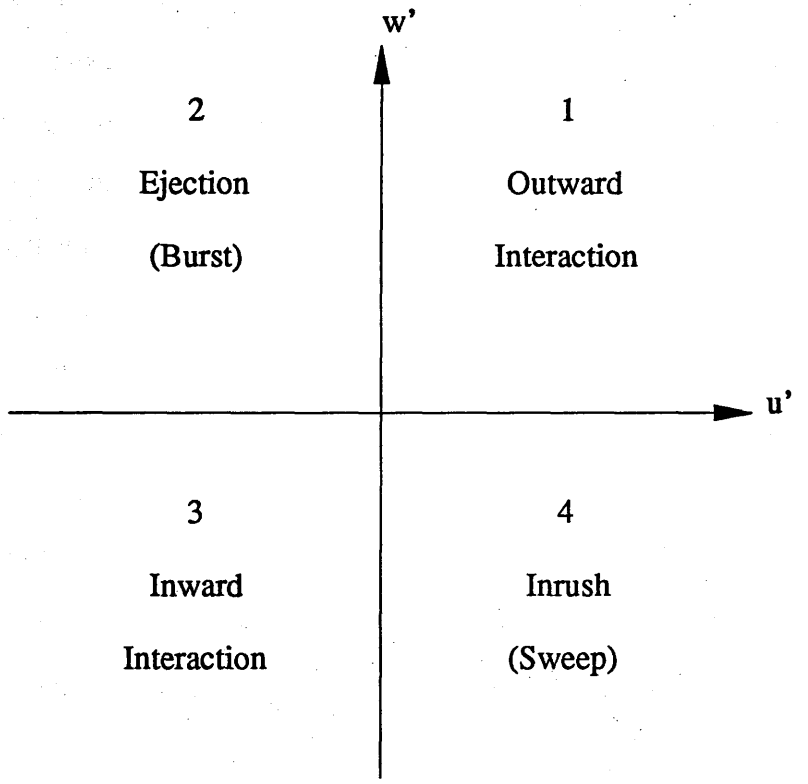

Figure 2.3 Definition and names of quadrants

similar behaviour, an intermittent shear stress signal, with large contributions to shear stress from the burst and sweep quadrants, though for measurements far above the bed. The duration of the contribution to the total stress from each quadrant for this data were also analysed (Holland, pers. comm.), see Table 2.1. The field measurements are of a qualitatively similar form of behaviour but the exact relation between the small scale near wall structures and the larger scale features extending throughout the flow depth in rivers is not clear. These different scales have been linked by Jackson (1976), speculating that boils seen on the surface of rivers are the geophysical equivalent of bursts. However an alternative explanation is put by Levi (1983, 1991), that boils are caused by eddy shedding at the river bed and their periodicity can be explained by a universal Strouhal law. Relating bursting and sweeping structures to particle movement, it would be expected that sweeping would be important in initial motion of sediment while bursting would be important in the modification of saltation.

Observations of particle motion by Drake *et al.* (1988) in Duck Creek, Wyoming, reveal a system in which 70% of the movement of particles occurs in 9% of the time. The transport was observed to occur in discrete events; these events were termed 'sweep-transport' events. They started with simultaneous entrainment of a large fraction of the available surface material, followed by a period of enhanced entrainment and transport, before gradually decaying to normal transport rates. They were termed sweep-transport events since they resembled observations of sweeps, visualised using sand in laboratory experiments, and because of the high speeds of propagation and particle movement, since sweeps involve downward motion of high speed flow. Observations from the marine environment, made in the Solent by Thorne *et al.* (1989) and further analysed in Williams (1990), combine simultaneous observations with video, hydrophone and electromagnetic current meters. The observed behaviour of the sediment was similar to that observed by Drake *et al.* (1988). The addition of the simultaneous measurements of turbulent fluctuations indicate an intermittent structure

Quadrant	Reynolds Stress $\overline{uw}$		Duration	
	m^2s^{-2}	%	seconds	%
1	0.215	-1.43	3.0	0.5
2	-9.250	61.68	86.8	14.47
3	0.829	-5.53	14.4	2.4
4	-5.273	35.16	69.0	11.5

Data from the River Severn (Holland pers. comm.)

Table 2.1 Contributions to shear stress by quadrant

in the turbulence signal, as observed in laboratory experiments, and a correspondence between sediment transport and sweep events in the turbulence record.

The evidence for the effects of bursting on particle trajectories comes from laboratory experiments. Francis (1973) and Abbott & Francis (1977) observed the movement of particles moulded from gravel shapes, though of varying density, across a fixed gravel bed, formed from particles of the same size fraction. The movement of particles was recorded at 1/40 second intervals for a range of transport stages. The particle tracks were analysed to determine the mode of transport. The transport stage was defined as the ratio of mean bed shear velocity, U_*, to critical bed shear velocity for the initiation of particle motion, U_{*cr}. The value of critical shear velocity for initiation of particle movement was calculated using a value of Shields stress, τ_{*cr} = 0.06, the critical bed shear velocity was calculated

$$U_{*cr} = \sqrt{\tau_{*cr} g \frac{(\rho_s - \rho)}{\rho} d}$$

where g is the acceleration due to gravity, ρ_s and ρ are the sediment and fluid densities and d is particle diameter. The definition of suspension used in their study was that a particle travelled in suspension when it experienced upwards acceleration between contacts with the bed. This ignores saltations in which the downward acceleration of particles is reduced by turbulent fluctuations without ever becoming directed upward. The results of the observations of Abbott & Francis are shown in Figure 2.4a, from which it can be seen that at a transport stage of U_*/U_{*cr} = 1.0 approximately 10% of the saltations are suspended, while at a transport stage of U_*/U_{*cr} = 3.0 approximately 70% of the saltations are suspended. In the corresponding graphs of saltation length and height, Figures 2.4b & 2.4c, the effect this has on the distance travelled in a single trajectory can be seen, with suspended trajectories always showing larger values of maximum height and distance travelled. The observed effects on particle tracks can be seen in Figure 2.5a, showing the falling limb of trajectories, particularly track 15, and in Figure 2.5b, which shows the effects of turbulence on falling and rising limbs of

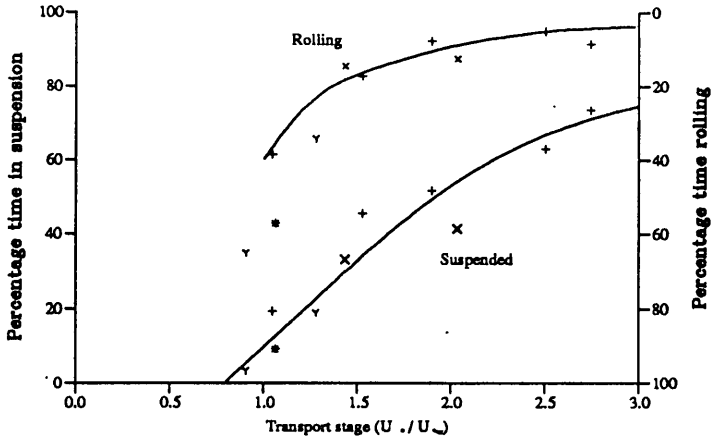

a) Percentage of time travelling in mode

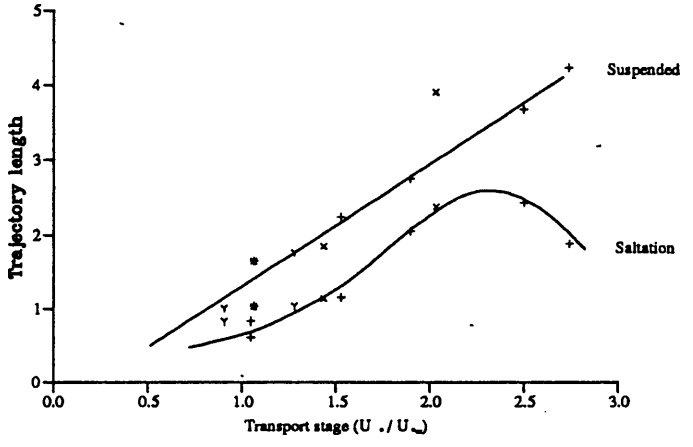

b) Trajectory lengths

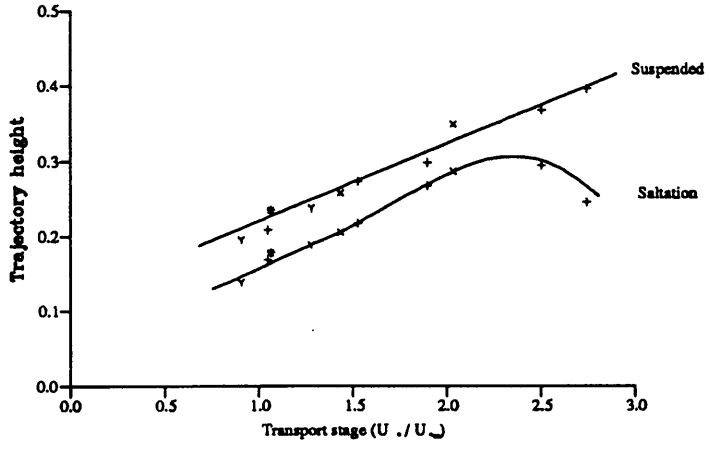

c) Trajectory heights

+ particle density = 1.24
× particle density = 1.43
Y particle density = 1.80
* particle density = 2.57

Figure 2.4 Observed particle behaviour (Abbott & Francis, 1977)

Units non-dimensionalised with respect to flow depth

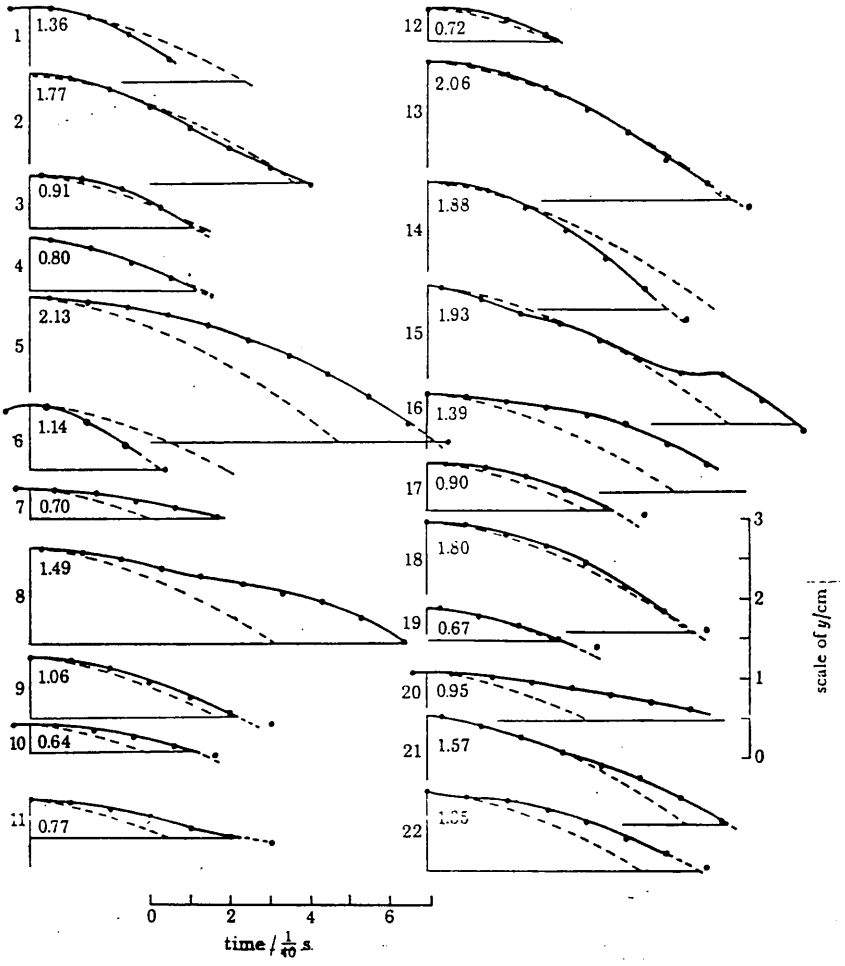

a) Observed particle heights on falling limb of trajectories

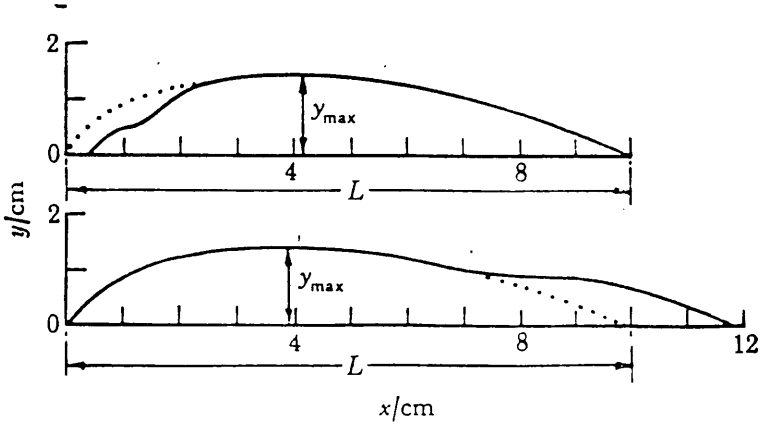

b) Effect of impulses from flow received before and after crest of trajectory

Figure 2.5 Observations of particle trajectories (Abbott & Francis, 1977)

trajectories. The observed trajectories show particles following normal saltation paths with step changes whose effects persist through the rest of the trajectory, as would be expected if a burst structure, which persisted through time and space, impinged on the particle position.

The observations of Fernandez Luque & van Beek (1976) also showed the effects of turbulence on particle trajectories; particles travelled almost in suspension Figure 2.6 at a transport stage, $U_*/U_{*_{cr}}$, of approximately 0.84. Observations of the movement of particles over a rough surface have also been made by Sumer & Deigaard (1981). These experiments use particles that have almost neutral buoyancy and the particles are almost travelling in suspension; they show a repeating pattern of particles being lifted, dropping, then lifted again, a motion consistent with the intermittent presence of bursting structures in the flow, lifting particles, which then slip from the structure, as it is also decaying.

2.3 Sediment movement

Movement of particles as bedload can be considered in terms of the constituent processes; initiation of motion, movement and impact/deposition. Analyses of a series of films of particle movement in Drake *et al.* (1988) describe the different types of particle behaviour that were observed during particle motion, Table 2.2. In trying to describe the movement of sediment particles in fluvial systems, observations and descriptions of the movement of sediment particles from aeolian systems provide a useful source of information. However it must be remembered that the relative density of the sediment in air is of order 1,000 while in water it is of order 1. This difference causes important variations in the behaviour of transported particles.

In fluvial sediment transport the flow being considered is open channel flow, that is flow with a free surface. For such a flow, the cause of the flow is the component of gravity, g, acting in the direction of the flow, due to the slope of the

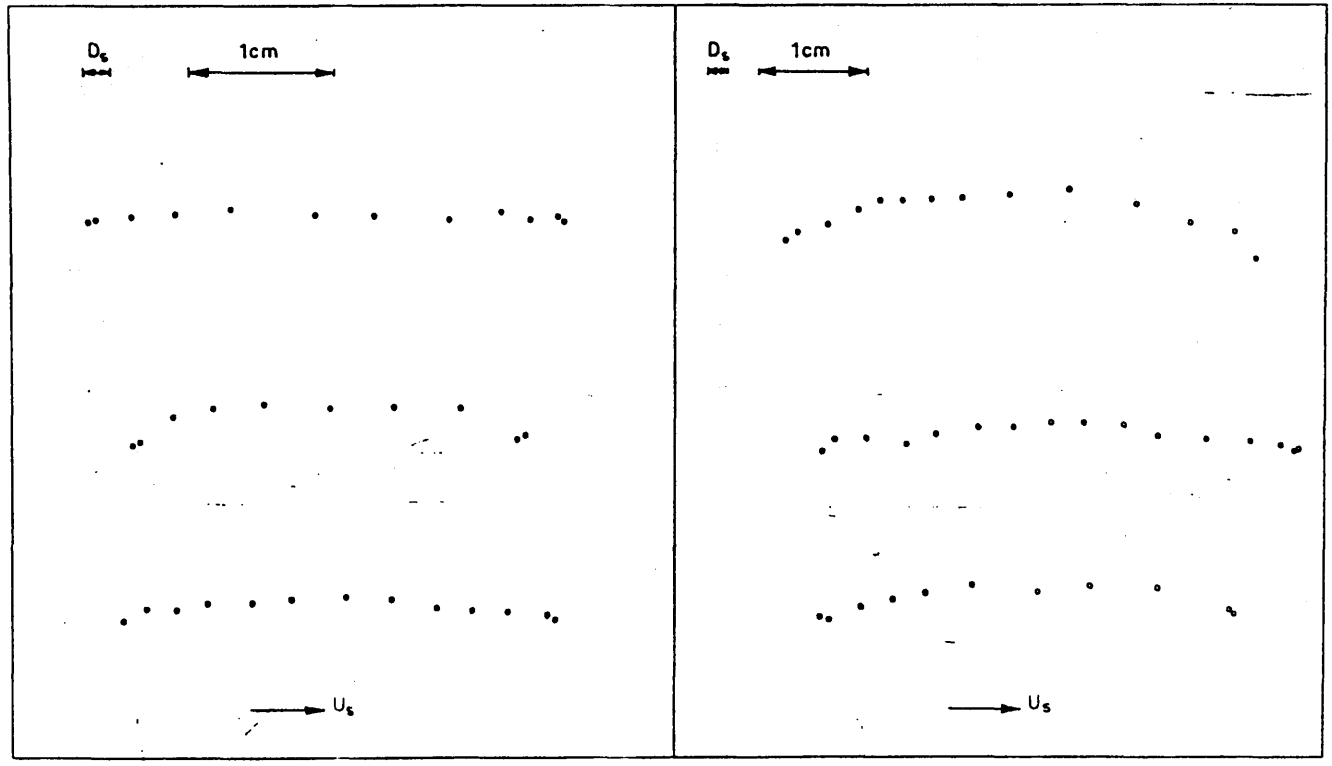

1/ψ = 0.0506, $\bar{u}_s$ = 0.186 m/s, $\bar{u}_B$ = 0.149 m/s
FIG 14a

1/ψ = 0.0539, $\bar{u}_s$ = 0.214 m/s, $\bar{u}_B$ = 0.171 m/s
FIG. 14b

Figure 2.6 Observations of particles almost in suspension (Fernandez Luque & van Beek, 1976)

Process Type		
Initial Motion	Movement	Distrainment
Roll-over	Sliding	Collision
Lift-off	Rolling	Gradual deceleration
Impact	Saltating	

Table 2.2. Types of particle behaviour observed by Drake *et al.* (1988)

channel, S. In most open channel flows the slope can be regarded as small, the components of gravity acting parallel and normal to the slope can then be taken as

$g_x \approx gS$

$g_z \approx g$

a further result of the slope being small is that the effect of gravity on the stability of grains in the bed can be ignored (Yalin, 1977).

For steady uniform flow, the assumptions used to derive the mean velocity profile in Section 2.2.1, velocity is constant and there are therefore no net forces acting on the fluid. The force acting on the boundary per unit width can be calculated

$F_{boundary} = \rho h l g_x$

where ρ is the fluid density, h is the flow depth and l is the streamwise length of the bed. For zero net force in the direction of motion this must equal the shear stress acting on the boundary, τ. The shear stress can be written

$\tau = \rho U_*^2$

where U_* is the mean bed shear velocity. Since the slope , S, of the channel only affects the flow, either the shear stress, τ, or shear velocity, U_*, can be used in its place. It is the shear force due to the flow, acting on the particles forming the boundary, that initiates movement of particles. If the shear force exerted exceeds that acting to keep a particle at rest the particle will start to move, the shear stress at which this occurs is called the critical shear stress, τ_{cr}, or critical shear velocity, U_{*cr}, its value has already been discussed in Section 2.2.2.

2.3.1 Initiation of motion

Initial motion of particles can occur due to either fluid forces or to the impact of particles already in motion. The former is obviously of importance in any system in which movement of sediment occurs, since particle movement must be caused by fluid forces. The latter is of much less importance in fluvial systems than in aeolian systems,

where two thresholds of initial motion are present, that due to flow and a lower threshold for that due to impact.

2.3.1.1 Due to fluid forces

For movement to occur due to fluid forces, the drag and lift forces exerted on a particle by the flow must be sufficient to overcome the forces due to gravity and the structure and packing of the particles in the bed. These forces can either be overcome by lift forces acting to lift a particle directly, as observed by Drake *et al.* (1988) for small particles, or by a pivoting motion, more normal for gravel particles, observed by Carling *et al.* (1992) and Drake *et al.* (1988). The initial motion of particles is therefore dependent on the fluid behaviour near the bed, turbulent flow structure, the nature of the bed, flow separation, form drag, the relative grain size, with its influence on the pivoting angle and also on the particle exposure and projection (Richards, 1990).

2.3.1.2 Due to impact

The alternative method of entrainment is by impact. At the end of a trajectory particles can rebound from the bed with a large part of their energy intact, while sufficient energy can be absorbed by bed particles to enable their entrainment. In aeolian systems this leads to two thresholds for motion: a higher threshold for motion due to fluid forces and a lower for motion due to impact. Motion, once started, can therefore persist after the flow conditions are not sufficient to entrain particles of themselves. This is a result of the high relative density of sediment in air. Drag force due to the flow is proportional to the fluid density. This is low for air, therefore a high velocity is required to reach the threshold to initiate motion, but once in motion the fluid forces retarding a particle at the end of its trajectory are also small, so more energy is retained until the impact. In fluvial systems the low relative density of sediment means that lower velocities can cause the particle to be entrained and that the

drag force retards a particle more before impact. The observations of Drake *et al.* (1988) showed impact to be an insignificant cause of entrainment in water .

2.3.2 Movement of particles

Once a particle has been entrained it can move by sliding, rolling or saltation and suspension out of contact with the bed, in order of distance travelled in a given time. While sliding does occur its importance to total sediment transport on rough natural beds is limited by the small distances of movements in which it is involved. Rolling is a more significant process; however, there are problems in describing the motion. While the particle is rotating its actual motion is a series of pivots about contact points with the bed (see Figure 2.7, from the data of Drake *et al.*, 1988) and it is often the start of non-contact movements rather than a complete movement in its own right. The different forces involved in the non-contact motion of particles, saltations, 'modified' saltations and suspensions are similar. These are the movements in which the furthest distances are travelled. The dividing line between a rolling and a non-contact motion is hard to define. Here, the non-contact motion of particles is described first, and rolling after.

2.3.2.1 Non-contact motion

To calculate the movement of sediment particles requires an appropriate equation of particle motion. In describing particle motion the most important variations to consider are the particle Reynolds number, $Re_p = u_r d/\nu$, where u_r is the relative particle velocity, d is the particle diameter, ν is the kinematic viscosity and the relative density of the sediment, ρ_s/ρ, where ρ_s is the sediment density and ρ is the density of the fluid.

The Reynolds number indicates the relative importance of viscous and inertial forces. At low particle Reynolds numbers, the flow round the particle is Stokes flow, the effects of viscous forces predominate and the appropriate drag force to consider as

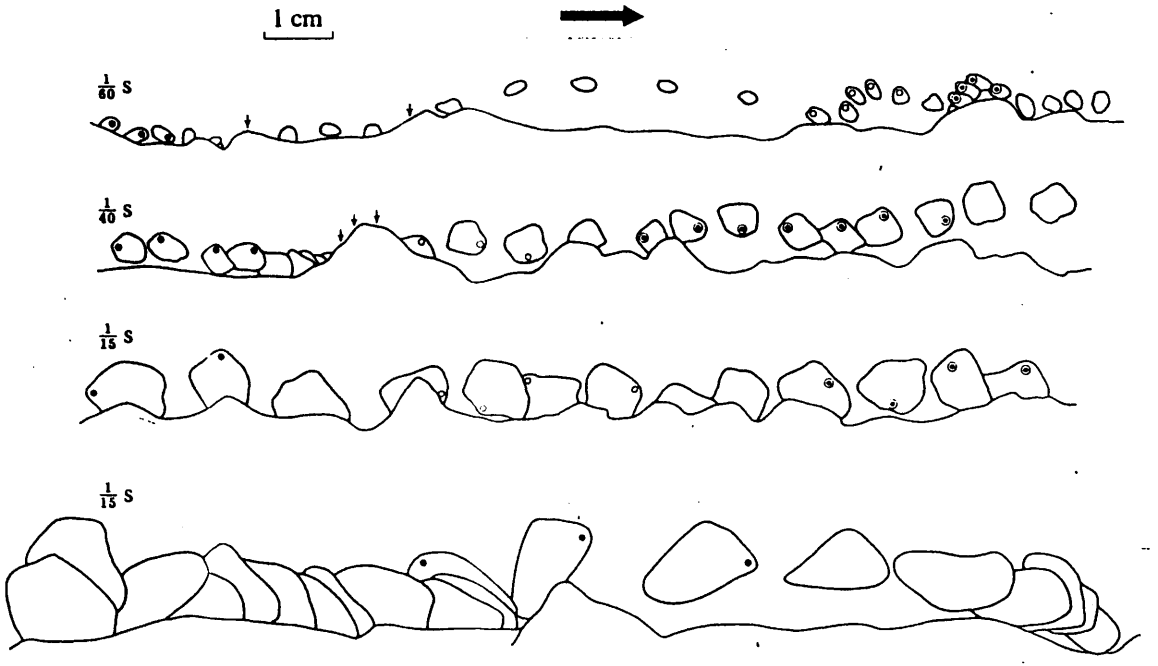

Figure 2.7 Obse vations of particle movement near the bed (Drake *et al.*, 1988)

acting is the Stokes drag. Descriptions of this type of particle motion were independently derived by Basset (1888), Boussinesq (1903) and Oseen (1927) for particles moving under the influence of gravity in a fluid at rest. These equations were extended by Tchen (1947) to those for a small particle moving in a fluid with variable velocity. This solution is not exact and the nature and effects of the assumptions have been discussed by Hinze (1959). More recently Maxey & Riley (1983) produced an alternative derivation and description of the movement of small particles in a turbulent flow, describing the limitations of earlier derivations. Stokes flow only applies for $Re_p \leq 1$, so particles must either be small or have small relative velocities. These equations can be used to describe the movement of fully suspended particles in the fluvial environment or particle movement in the aeolian environment, but are not appropriate to describe the movement of particles as bedload in fluvial environments.

For higher particle Reynolds numbers Graf (1971) extended the equations of Tchen (1947) on a term by term basis, substituting forms of each term appropriate for high particle Reynolds number. This description has the disadvantage that the magnitude and relative importance of terms varies with the particle Reynolds number; in particular there is no allowance for lift in the original equations, since in Stokes flow velocity shear produces no resultant force (Maxey & Riley, 1983), whereas at higher particle Reynolds number lift forces can occur.

At high Reynolds numbers inertial forces dominate and, except in boundary layers, the viscous forces can be ignored. The assumption of inviscid flow, along with that of irrotational flow leads to Euler's equation and Bernoulli's equation. These can often be solved using potential flow solutions. This type of analysis is that found in classical hydrodynamics; descriptions of particles moving in an unbounded ideal fluid, with the fluid at rest, in motion and gradually accelerating can be found in Batchelor (1967) and Newman (1978), which includes rotation of the particle in the analysis.

The instantaneous force on a body moving without rotation due to the pressure, p, acting on its surface is

$$\tilde{F} = -\int p\,\tilde{n}\,dA$$
$$= \rho\int \frac{\partial\phi}{\partial t}\tilde{n}\,dA + \tfrac{1}{2}\rho\int q^2\,\tilde{n}\,dA - \rho\int \tilde{g}.\tilde{x}\,\tilde{n}\,dA$$

where the second equation is obtained by substituting Bernoulli's equation for the dynamic pressure in the first equation. The integrations are performed over the surface A, coincident with the surface of the body, n is the normal to this surface, ϕ is the velocity potential, q is the magnitude of the velocity, g is the acceleration due to gravity and ~ over a character represents a vector quantity. The final term represents the buoyancy and can be ignored in analysis of the effects of particle movement in this context. This expression for the force acting on a particle is for fixed axes; converting to axes moving with the particle gives an expression

$$F_i = \int\left(\tfrac{1}{2}q^2 - u_{pj}u_j\right)n_i\,dA + \rho\frac{du_{pj}}{dt}\int \Phi_j\,n_i\,dA$$

where u_p is the particle velocity and Φ is the new velocity potential based on coordinates at the position of the particle. The first term represents the force on a body in steady motion, while the second term is non-zero only when the particle is accelerating.

The first term for a particle in steady motion predicts a zero force on the particle. This is because the pressure distribution over the surface of the particle, calculated using Bernoulli's equation, is symmetrical; this result is called d'Alembert's paradox. In reality in the boundary layer near the particle surface viscous forces are important and the assumptions on which the analysis is based cease to apply. The streamlines about the particle cease to be symmetrical due to the effects of friction. The pressure recovery on the downstream surface is not complete, so a drag force is present even before flow separation occurs.

Integration of the second term leads to an expression for the force due to particle acceleration

$$F_i = -\rho V C_{A\,ij} \frac{\mathrm{d}u_{pj}}{\mathrm{d}t}$$

where V is the volume of the particle and $C_{A\,ji}$ is a coefficient called the coefficient of added mass. For a non-symmetrical particle the added mass coefficient is dependent on the direction of movement of the particle. The force is the product of a mass and an acceleration, representing a mass term which must be added to the mass of a particle to predict its behaviour, hence the coefficient is called the added mass coefficient. The force is due to the acceleration of fluid because of the movement of the particle.

For a fluid which is accelerating slowly and uniformly relative to the scale of the body a further term can be added to the acceleration reaction term. The expression for the acceleration becomes

$$F_i = -\rho V C_{A\,ij} \frac{\mathrm{d}u_{pi}}{\mathrm{d}t} + \rho V \frac{\mathrm{d}u_i}{\mathrm{d}t}\left(C_{A\,ij} + \delta_{ij}\right)$$

where δ_{ij} is the Kronecker delta.

Though the inviscid, irrotational flow solution fails to predict the presence of a drag force acting on a particle in steady motion the force due to particle acceleration exists, the coefficient of added mass and its variation were measured by Odar & Hamilton (1964). For a symmetrical particle the calculated added mass coefficient simplifies to a single value, for a sphere the theoretical value is 0.5 (Newman, 1978). The measurements of Odar & Hamilton (1964) found that the added mass coefficient, C_A, for a sphere in a fluid at rest, varied with an acceleration number, Ac, defined

$$Ac = \frac{u_p^{\,2}}{d\,\dfrac{\mathrm{d}u_p}{\mathrm{d}t}}$$

The added mass coefficient, C_A, varied from the theoretical value of 0.5 for an acceleration number approaching zero, to a constant value of 1.05 above an acceleration number of 1.

The fact that the ideal flow solutions do not include any particle boundary layer effects and hence no mechanism for lack of recovery of pressure or even flow separation, limits their direct use in the calculation of particle motion. Wiberg & Smith (1985) show a derivation for the motion of a particle in a flow where the particle Reynolds number, Re_p, is much greater than one. The equation of particle motion that they derive is:

$$
\begin{aligned}
-(\rho_s + C_A\rho)\frac{d\langle u_{ri}\rangle}{dt} = &-(\rho_s - \rho)\frac{d\langle u_{ri}\rangle}{dt} \\
&-(\rho_s - \rho)g_i \\
&+\rho\frac{C_D}{2}\frac{\pi d^2}{4}|u_{ri}|u_{ri} \\
&+\rho\frac{C_L}{2}\frac{\pi d^2}{4}\left[\left(u_{ri}^2\right)_{TOP} - \left(u_{ri}^2\right)_{BOTTOM}\right]
\end{aligned}
$$

where $C_D$and C_L are the coefficients of drag and lift respectively and u_r is the relative velocity of the particle, u - u_p, with $\langle\ \rangle$ representing an average over the particle. In this equation the drag and lift forces due to the pressure were retained by equating the pressure terms from an ideal flow solution with the form of the terms derived from dimensional analysis (See Appendix, Wiberg & Smith, 1985). This expression for the lift force takes into account the difference in velocities between top and bottom of the particle, falling away to zero as the velocity gradient across the particle falls to zero. Once this has been done the values of the coefficients of drag and lift as determined from experiment can be substituted to give the drag and lift forces in the equations. The value of coefficient of drag for an isolated sphere has been determined experimentally across a wide range of values of particle Reynolds numbers, being

viscous dominated at low particle Reynolds and dominated by form and pressure drag at high particle Reynolds numbers. The value of the coefficient of lift is not as well defined, it is composed of more than one term, a wall effect and a force due to rotation of the particle. The relative contributions of these terms vary and in constraining a system to enable one component to be measured the possibility of measuring others may be removed.

A similar equation of particle motion is developed by Murphy & Hooshiari (1982), they sum the terms due to the forces known to act on particles in motion. They split the lift into a term due to spin and a term due to the wall effect, giving an expression for the particle motion containing more terms than that of Wiberg & Smith (1985). Though the effect of these terms is considered separately the magnitude of the terms is still determined from empirical values for the coefficient of lift for each of these terms and so does not differ greatly from the expression of Wiberg & Smith (1985).

2.3.2.2 Contact motion

Particles in contact with the bed can move by either sliding or rolling, with the forces described in the previous section acting to cause the movement. While classical analyses for both these types of motion exist there are problems in applying these to a fluvial environment with a rough bed.

An observed motion can easily be characterised as sliding; yet, its relation to the sliding of a block on a surface, a situation which can easily be described mathematically, is not obvious and the appropriate coefficients have not been measured. On a rough bed, however, the distance travelled in sliding motion will always be small with respect to other modes of motion occurring. The rolling motion is more significant in terms of distance travelled, though again the relation between spheres rolling on spheres, as used in physics examples, and the movement along the

bed of a river is hard to define, especially if neither of the particles involved is spherical. Rolling motion is also important in initial motion from rest and after impacts (Abbott & Francis, 1977), determining the conditions at the start of saltation, that is the conditions when a particle loses contact with the bed rather than those when motion starts. The observations of Francis (1973) likened the movement of a bed particle, just before it lost contact with the bed, to rolling without slipping, this can be analysed for spheres to give equations for the particle rotational acceleration, such an analysis is given in Appendix 1.

2.3.3 Impact / Deposition

The impact process is the basis of both the continuation of particle motion and the cessation of particle motion. In continuing motion, the fraction of particle momentum conserved at an impact influences the initial conditions of the next saltation. While in the cessation of particle motion, it determines under what condition the particle ceases to move.

Cessation of motion of particles has been observed to be caused by different mechanisms, and these depend on the mode in which the particle is moving. After saltation and sliding, particles can be stopped by collisions with other particles which were close to head on (Drake *et al.*, 1988). After rolling, deposition usually follows deceleration of the particle, particle speed dropping until it falls into a crevice or cannot clear the next obstacle (as observed by Francis, 1973, Drake *et al.*, 1988).

Observations of the impact process have been made by Gordon *et al.* (1972) in a 2-dimensional flume using spheres as the mobile particles, travelling over a mobile bed of spheres. These results showed a loss of the normal component of momentum on impact, with tangential momentum being conserved. Observations by Abbott & Francis (1977) showed no coupling between pre- and post-impact particle trajectory. However their observations usually included a period of rolling between trajectories, which could explain this decoupling (Naden, 1987b).

Observations of impact in the aeolian environment have been made by Willetts & Rice (1985), observing the transport of sand in a wind tunnel; Werner (1987), observed the impact of single grains of quartz; Mitha *et al.* (1986), simulated quartz grains using ball bearings, observing the impact of a ball bearing into a bed formed of ball bearings. In addition to these observations numerical simulations of the impact process in aeolian saltation have been made by Werner & Haff (1988) and Anderson & Haff (1988). In these numerical experiments the effects of the impact of particles into a bed of discs, free to move horizontally and vertically, were examined. The aim of all this work was to determine appropriate splash functions to use in models of aeolian sediment transport. The splash function relates the effect of an impacting grain to the resulting outgoing grains. The splash functions determined from observations and those from numerical simulation give qualitative agreement (McEwan *et al.*, 1992). Outgoing grains due to an aeolian impact consist of the grain rebounding from the impact and a number of other grains ejected from the bed as a result of the impact.

Observations of the fluvial environment indicate that ejection of grains from the bed due to impact was rare (Drake *et al.*, 1988). If only rebounding grains were considered, the observations show particles impacting at low angles and rebounding at much higher angles with a reduced velocity (McEwan *et al.*, 1992). Simple geometric models such as that of Rumpel (1985) modelled the impact between a moving particle and a single bed particle in a bed which was not mobile but was also not rigid, that is, the momentum of impact could be dissipated without modifying the bed. In such a case a perfect collision would conserve all the tangential momentum while the normal component of momentum would be transferred to the bed, Figure 2.8. A model of this type predicts the observed increase in angle of the rebounding particle along with the reduction of particle velocity. Such a collision shows a decreasing ratio of outbound to incident particle velocities as the angle between particle centres increased. Since the leaving angle increases with angle between particle centres, analysis of the observed ratio of particle velocities

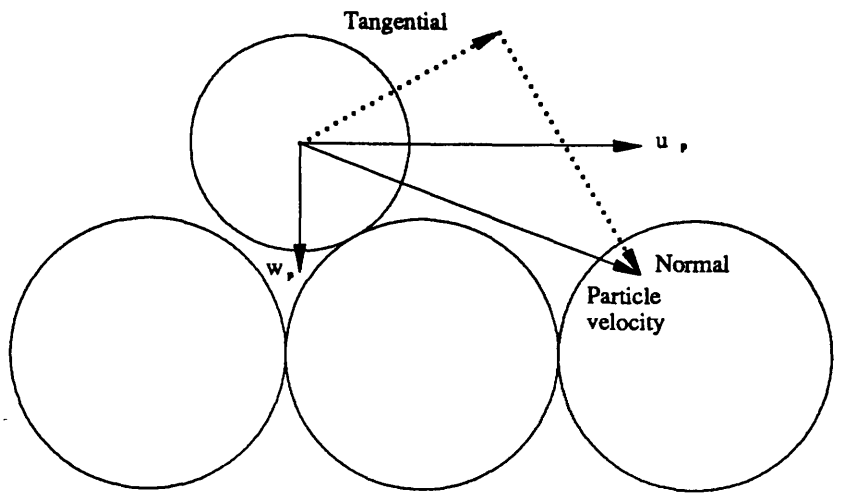

a) Velocity components immediately before impact

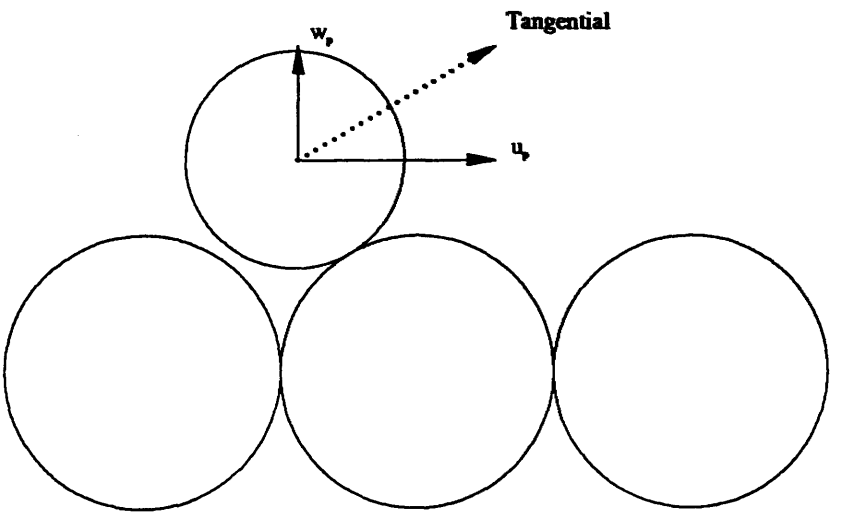

b) Velocity components immediately after impact (Rumpel, 1985)

Figure 2.8 Change in particle velocity at impact (Rumpel, 1985)

should show a negative correlation. McEwan *et al.* (1992) using the data of Willetts & Rice (1985) found this to be the case.

The numerical simulations described in Werner & Haff (1988) and Anderson & Haff (1988) were performed for discs constrained to move in two dimensions in an aeolian environment. Calculations were performed to determine the effects of the impact of individual discs. Similar calculations have been performed for a fluvial environment and are described in Jiang & Haff (1993); these allow for the effects of a high density fluid by increasing the damping amongst the particles. The calculations were performed for the effects of a shearing flow on the bed, rather than being driven by the impact of individual particles. The effects of the shearing flow were calculated on any particles exposed to the flow; the effects of interactions of particles were calculated between all particles. Though the interactions of particles were calculated and the model of these interactions is described, the results of individual impacts are not described. Since the model is of mass movement of sediment particles the details of the shearing flow and interactions of particles are described in Section 6.2.5.

2.3.4 Two-phase flow

By examining the movement of only single particles in water the interaction between flow and particle is reduced to the influence of the flow on the particle. Any momentum extracted from the flow is small and has little effect on the flow profile.

By contrast, turbulent eddies in the flow can affect the motion of particles. However particles in a flow do not respond immediately to a change in the surrounding velocity field but respond over a period of time, the relaxation or characteristic response time. The response time was defined by Hinze (1972) as the time required for the relative particle velocity to fall to half its initial value. For a high particle Reynolds number this gives an expression for the response time

$$t_r = \frac{d}{K u_{r\,initial}} \left(\frac{\rho_s}{\rho} + C_A \right)$$

where $u_{r\,initial}$ is the initial value of the relative particle velocity, K is of O(1) and is related to the expression for drag and C_A is the added mass coefficient.

$$K = \frac{C_D}{2} \frac{\pi}{4}$$

where C_D is the coefficient of drag for the particle. For a sediment particle in water ρ_s/ρ is O(1), and equating $u_{r\,initial}$ to σ_u, the standard deviations of the velocity fluctuations gives an expression

$$\frac{\sigma_u t_r}{\Lambda} \propto \left(\frac{\rho_s}{\rho} + C_A \right) \frac{d}{\Lambda}$$

where Λ is the length scale of the eddies. Thus if

$$\frac{d}{\Lambda} < \frac{1}{\left(\frac{\rho_s}{\rho} + C_A \right)}$$

the motion of eddies will influence particles.

The slow response of heavy particles to turbulent fluctuations has an effect other than causing relative motion and hence additional fluid forces acting on the particle. Since a heavy particle is always in motion relative to the fluid the flow sampled by the particle varies continuously. This has been called the ' crossing trajectories' effect by Csanady (1963). A heavy particle will not remain in an eddy as a fluid particle would, but leave it; the autocorrelation of the velocity of a heavy particle will therefore fall more rapidly than that of a fluid particle which will show the correlation of the flow itself.

2.4 Bed

In rivers the bed affects and is affected by the flow. Simplifying the system under consideration to one in which only the movement of single particles is considered removes the possibility of the bed being modified. In the fluvial environment, Sekine & Kikkawa (1992) found that the position of particle centres formed a Gaussian distribution about a mean bed height. In Furbish (1987) and Robert (1988) detailed measurements of the variation of bed surface heights, in the cross stream and streamwise directions respectively, and statistical descriptions of these are given. These studies describe the roughness heights present directly without attempting to characterise the bed in terms of the distribution of particle sizes present. Robert (1988) found two scales present within the measurements of bed roughness, corresponding to the grain roughness scale and the scale of small structures on the bed. These measurements were made in either rivers or flumes with a mobile bed, after it had been worked by a flow.

The observations that have been made of the movement of individual particles moving in isolation have been either for fixed beds, with the particle forming the roughness glued in place, or for a bed below its threshold for initial motion and hence with no bed particles moving. The range of the roughness elements used in these experiments has also been simplified, to either a single size (spheres: Meland & Norrman, 1966, Murphy & Hooshiari, 1982) or a single size fraction (gravel: Francis, 1973, Abbott & Francis, 1977). Under these circumstances the bed roughness can be characterised by a single length scale, derived from the particle size.

Observations have been made with mobile beds, in flume by Fernandez Luque & van Beek (1976), and in the field by Drake *et al.* (1989) and Williams (1990). The observations of Fernandez Luque & van Beek (1976) were of a mobile bed formed of a single type and size of sediment particle, the bed can therefore still be characterised using a single length scale. The observations of Drake *et al.* (1989) and Williams

(1990) were for a bed formed of a range of particle sizes, in Drake *et al.* (1989) only qualitative descriptions of particle behaviour were given, while in Williams (1990) distributions showing ranges of conditions present are shown but the behaviour of individual particles is not.

2.5 Conclusions

The movement of sediment particles as bedload in fluvial sediment transport occurs in turbulent flow over a rough bed. Observations of the movement of sediment particles, in the laboratory and in the field, show that turbulent velocity fluctuations in the flow influence the movement of sediment particles, the initiation of motion and the subsequent trajectory. The importance of the effects of velocity fluctuations on particle movement make this a component of the movement of sediment particles that should be taken into account when considering the components to include in a model. The flow description in a model should therefore be capable of including both mean and fluctuating velocity components.

The components of the movement of sediment particles can be broken down into initiation of motion, movement and deposition. Any model of the movement of sediment particles needs to contain these components. The components can be either deterministic or stochastic, using suitable distributions. The presence of different types of motion and their relative importance must also be considered. Movements of particles away from the bed, that is suspensions or saltations, are the most significant forms of motion for distance covered. Rolling and sliding are much less important in terms of distance travelled, however rolling is still significant because of its importance at the beginning of movements, determining the initial conditions for saltation and, at the end of movement, influencing when deposition occurs.

The bed is important in the sediment transport process, supplying particles and modifying the flow. For single particle movements it is the processes interacting with

the bed, rather than the bed itself, that need to be described, since the movement of the particles cannot modify the bed. The initiation of motion and position of impact require particle positions, not detailed models of the bed structure. The flow calculations require a roughness length scale, again not a detailed model of bed structure. The model of impact needs to be based on consideration of the bed structure, but for single particle movement the effects of bed structure on the impact are supplied by consideration of the conservation of momentum at impact. A model of the bed is required in models of particle movement, but for models of single particle movement it can be represented by a simple fixed geometry.

Chapter 3

Modelling the movement of sediment particles

3.1 Introduction

In this chapter modelling of the movement of sediment particles will be discussed, principally in the fluvial environment but with some reference to the aeolian environment. Modelling of the movement of sediment particles requires the description of different systems, components of particle movement and processes acting to modify the particle movement. In some cases, particularly initial motion of sediment, the process is modelled in its own right and not just as a component of the movement of particles and these models will be discussed along with their use in models of particle movement. Other than the particle movement itself the major consideration is the representation of turbulence and its effect on particle movement. This will involve the consideration of dispersion due to turbulence of passive and non-passive tracers and how this can be modelled.

3.2 Flow

In Chapter 2 descriptions of turbulent flow were introduced; here, methods of using those descriptions to model turbulence are discussed and also how previous models of the movement of sediment particles represent turbulence.

A full solution of turbulent flow would require solution of the Navier-Stokes equation; methods that solve these equations are called Direct Numerical Simulation methods, DNS. The use of DNS is limited by the fineness of the mesh on which the solution must be calculated, determined by the smallest turbulent length scales, and the correspondingly small time intervals at which these solutions must be performed. The requirements for memory space and computational speed which these impose, limit the

application of DNS to low Reynolds number flows, unlike those found in rivers, e.g. the channel Reynolds number of 3000 in Komori *et al.* (1993), for a smooth walled channel. A slightly less computationally intensive approach, though still preferably performed on a supercomputer, is Large Eddy Simulation, LES. In this method the full Navier-Stokes equations are solved for large eddies while a sub-grid scale model is used to supply the effects of smaller eddies which are not calculated explicitly (Thomas *et al.*, 1992). Initial applications of this type of model to open channel flow are being made (Thomas *et al.*, 1992), specifically modelling data from the SERC Flood Flume, but the computing power required will limit applications for some time to come.

Even with the solution of the full Navier-Stokes equations used in LES the sub-grid scale eddies which are of interest in modelling the effects of turbulence on sediment particle movement have been lumped together, therefore in any approach to modelling flows the stochastic element of the sub-grid scale flows must be reintroduced. If statistics to describe the turbulent fluctuations are available this problem can be approached by the summation of mean and fluctuating components, the reverse of the Reynolds decomposition. Therefore the modelling of the mean flow component will be considered, followed by superimposing the effects of fluctuating flow components, the approach taken in describing the flow in Chapter 2.

3.2.1 Mean flow modelling

In solving for the mean flow the choice is between solving for a non-depth averaged solution to the Reynolds equations or to use a simplification of the Reynolds equations amenable to analytical solution, or to use the logarithmic velocity profile for turbulent flow over a rough boundary. Solutions to the 2-dimensional Reynolds stress equations have been used by Ungar & Haff (1987) and Werner (1990). As with any solution of the Reynolds equations these require a turbulence model to solve the closure problem. They use an eddy viscosity model,

$$\mu_t = \rho \left| \frac{\partial u}{\partial z} \right| l^2$$

combined with Prandtl's mixing length hypothesis, that is

$l = \kappa z$

the mixing length is proportional to the height, z, above the surface. Though the theory behind the mixing length hypothesis is not correct, its empirical application has been found to produce acceptable results without complicated computation (Werner, 1990). The form of the equations used included the effects of a body force, due to particle drag, on the flow velocity profile. For a steady flow with zero pressure gradient the velocity profile became the logarithmic velocity profile, derived from dimensional considerations in Section 2.2.1. Calculations of the motion of single particles in water do not need to include this term, since the momentum extracted by particles in water is much less significant than that in air. The direct use of a logarithmic velocity profile was the technique used by Sekine & Kikkawa (1992) and Murphy & Hooshiari (1982) to describe the flow in their models of particle movement in water.

3.2.2 Fluctuation modelling

The effects of turbulent velocity fluctuations on dispersion of a tracer can be introduced into a calculation if velocity fluctuations can be superimposed on the mean flow. Particle tracking calculations offer a way of performing this operation. In this approach the trajectories of a large number of particles are calculated on an iterative basis. The local conditions in time and space at the start of an iteration are used to define the magnitude and form of a velocity distribution. From this distribution a value is selected at random and used to calculate the particle behaviour over the next iteration. The approach was first used to calculate the dispersion of passive tracers in the atmosphere (Zannetti, 1990). The ability of the approach to reproduce observed behaviour from simple statistical parameters, its grid free nature and relatively small requirements for computing power have led to its wider application. In the simplest

form of particle tracking a single value for the velocity fluctuation is used for the integral time scale of the turbulence (Allen, 1982). The value for the velocity fluctuation, u', at each iteration, is then independent of the previous iteration and can be calculated from a random distribution

$$u'(t) = f(\sigma_u)$$

where $f(\sigma_u)$ is a distribution whose magnitude is determined by the standard deviation of the velocity fluctuation, σ_u. In more complex forms time intervals smaller than the integral time scale are used at each iteration and the autocorrelation function of the turbulence is included in the expression for the velocity fluctuation

$$u'(t+\Delta t) = R(\Delta t)u'(t) + f(\sigma_u)$$

where

$$R(\Delta t) = \exp\left(-\frac{\Delta t}{T_L}\right)$$

and $f(\sigma_u)$ is a random component. The use of an exponential function to represent the autocorrelation was first used by Taylor (1921); observations show it to give a good fit to actual curves (MacInnes & Bracco, 1991). The velocity fluctuation at time $t+\Delta t$ therefore contains a term correlated with the velocity fluctuation at the previous iteration along with a new random component.

The method has been further developed to include correlation between the different components of the velocity fluctuations (Zannetti, 1990) and inhomogeneity of the turbulence (Tampieri *et al.*, 1992). Though its data requirements are simple, most measurements made at the appropriate scale are Eulerian, while the particle tracking method is Lagrangian in nature and should use Lagrangian statistics. Empirical expressions for these statistics are available to calculate atmospheric dispersion (Hanna, 1982); measurements exist for open channel flow over a smooth bed, for neutrally buoyant spheres (Sullivan, 1974) and for the dispersion of particles on the surface of an open channel flow over a rough bed (McQuivey & Keefer, 1971).

Since most measurements of turbulence that have been made are Eulerian an alternative to using directly measured Lagrangian parameters would be to try and find a relation between Eulerian and Lagrangian statistics for a flow. Unfortunately no simple measure suggests itself and the problem of mapping from Eulerian to Lagrangian appears to be best approached from empirical analysis, either from direct field measurements of Eulerian and Lagrangian statistics like those performed for atmospheric dispersion (Hanna, 1979, 1981), from comparison of simulation with measured dispersion data (Heslop & Allen, 1989, Allen, 1992), or numerical simulation of a turbulence field (Lynov *et al.*, 1991, Fung *et al.*, 1992).

For atmospheric dispersion, point readings of turbulence were made, for Eulerian statistics, along with the tracking of balloons, for Lagrangian statistics. The statistics of both sets of measurements were then calculated and related (Hanna, 1979, 1981). The comparison of simulated dispersion was made with measurements of the dispersion of dye performed on the River Severn, the simulations were made using turbulence statistics based on measurements made at the same time as the dye dispersion measurements (Heslop & Allen, 1989, Allen, 1992).

Lynov *et al.* (1991) generated a random flow field using vortex elements each of which acted on every other to produce the turbulent structures. This structure was then analysed to produce Eulerian and Lagrangian statistics. Fung *et al.* (1992) used a large number of Fourier modes to generate a flow field. Eddies were formed at two scales, a large scale where the eddies moved independently and randomly, and a small scale where the movement of the eddies was influenced by the movement of the larger eddies. The calculated flow field was then analysed to produce the Eulerian and Lagrangian statistics. The relation between Eulerian and Lagrangian statistics from such calculations is still empirical not analytical.

If neither direct measurements nor empirical conversion factors are available then other methods of producing the transformation must be employed. One such

approach mentioned in Pasquill & Smith (1983) is to extend the 'frozen eddy' hypothesis of Taylor (1938). The 'frozen eddy' hypothesis states that the turbulence moving past a point can be considered as a frozen structure being advected past by the mean velocity of the flow. If this is the case then Eulerian temporal measurements at a point can be mapped onto Eulerian spatial measurements, the Eulerian integral length scale can be calculated

$$L_E = U\,T_E$$

where U is the mean flow velocity and T_E is the Eulerian integral time scale. This has become a standard method of converting measured Eulerian integral time scales to the Eulerian integral length scale. This idea is extended to produce pseudo-Lagrangian scales by assuming that the traversing of the Eulerian length scale by the turbulent velocity fluctuations, here represented by the standard deviation of the fluctuation, returns a Lagrangian time scale

$$T_L = \frac{L_E}{\sigma_u}$$

where σ_u is the standard deviation of the velocity fluctuations. This approach was used by Sullivan (1971) to calculate appropriate time scales for particle tracking calculations. In his model this was combined with a description of an eddy as a region the size of the turbulent integral length scale with a constant value of velocity fluctuation.

3.2.2.1 Applications and types of particle tracking

Applications of particle tracking have been made in modelling atmospheric dispersion (Thompson, 1971, Zannetti, 1990). The technique has also been applied in open channel flow (Sullivan, 1971), estuarine (Allen, 1982) and marine environments (van Dam, 1993). For open channel flows attempts have been made to produce better quality measurements to define the turbulence in open channel flow (e.g. Heslop & Allen, 1989) and also to make use of suitable computing resources such as parallel

computers (Allen, 1992) which, particularly for passive tracers, offer significant possibilities for performance enhancement. Of particular relevance to the present work particle tracking has also been extended to calculate the behaviour of heavy, (non-passive) tracer particles (see Section 3.3.4 below).

3.3 Sediment movement

3.3.1 Initiation of motion

Modelling of initial motion of sediment is pursued in its own right as a method of predicting the onset of sediment transport and as a way of reconstructing the magnitude of events necessary to cause observed transport behaviour. Therefore the modelling of initial motion will be described, followed by the approaches used when modelling the movement of sediment particles.

In fluvial sediment transport, for reasons given in Chapter 2, attention is concentrated on initiation of motion due to fluid forces. There are two basic approaches to modelling initiation of motion of particles. One is the modelling of a force balance, an explicit statement of the forces acting and hence the balance of forces required to initiate particle movement; the other is dimensional analysis, also derived from forces acting on the bed but with a simplification of the force balance.

3.3.1.1 Dimensional analysis

The parameter used to describe whether particles will be entrained by a flow is called the Shields stress, τ_*, derived using dimensional analysis by Shields (1936),

$$\tau_* = \frac{\rho U_*^2}{g(\rho_s - \rho)d}$$

where ρ and ρ_s are the fluid and sediment densities, U_* is the mean bed shear velocity, g is the acceleration due to gravity and d is the diameter of the particle being entrained. This parameter was derived from dimensional reasoning, balancing drag force on a

particle due to the flow, acting to entrain it, against the particle weight, causing it to remain at rest (Raudkivi, 1990). To use Shields stress in a calculation a value of the non-dimensional group must be calculated empirically. The value of the critical Shields stress for initial motion of particles, τ_{*cr},was determined experimentally for particles being entrained from a flat bed. Shields' results were plotted as τ_* *vs.* Re_{*_p}, showing a constant value of $\tau_{*cr} \approx 0.06$ for $\mathrm{Re}_{*_p} > 100$. Though this provides an average value for initial motion there will be scatter about this line due to different particle positions within the bed and different compositions of bed material. Although the Shields stress is a general description it is still necessary to use data to determine the value applicable in a particular situation.

3.3.1.2 Pivoting analysis

In a force balance analysis of initial motion the forces acting on the particle due to the flow are calculated to see whether they are sufficient to overcome the force due to gravity, Figure 3.1. For the simple system shown in Figure 3.1 where all the forces are assumed to act through the centre of mass of a sphere the particle moves if the following inequality becomes true

$$F_x \cos\theta_p + F_z \sin\theta_p > mg \sin\theta_p$$

where m is the mass of the particle, g is the acceleration due to gravity, θ_p is the pivoting angle and F_x and F_z are the horizontal and vertical components of fluid force respectively, calculated from the forces due to drag and lift, F_D and F_L,

$$F_x = F_D \frac{(u-u_p)}{\sqrt{(u-u_p)^2+(w-w_p)^2}} - F_L \frac{(w-w_p)}{\sqrt{(u-u_p)^2+(w-w_p)^2}}$$

$$F_Z = F_D \frac{(w-w_p)}{\sqrt{(u-u_p)^2+(w-w_p)^2}} + F_L \frac{(u-u_p)}{\sqrt{(u-u_p)^2+(w-w_p)^2}}$$

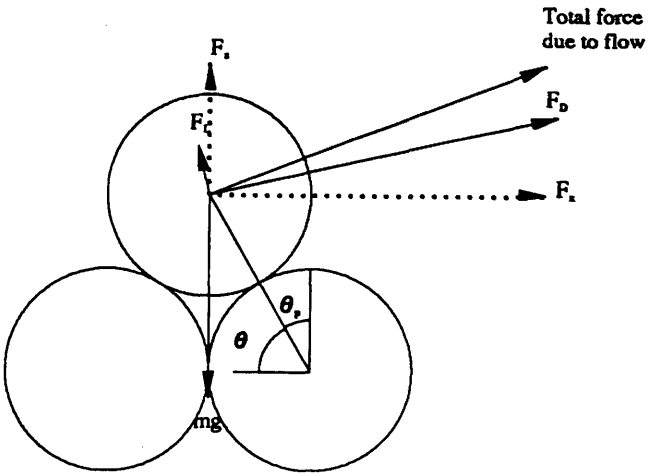

a) Forces acting (solid lines), horizontal & vertical components (dotted lines)

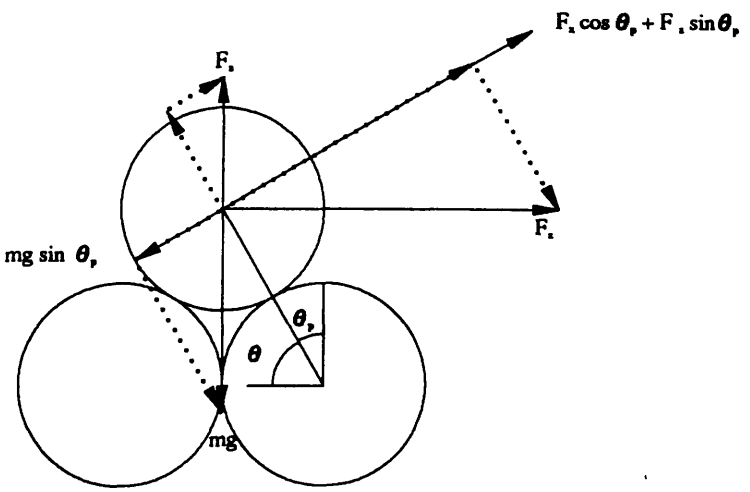

b) Force balance for initiation of motion

Figure 3.1 Balance of forces due to flow and gravity for initiation of motion

This approach was used by White (1940) and has been used with a number of different sets of assumptions: James (1990) produced a general pivoting model, allowing for offset positions for action of the forces and fractional exposed areas, and reviewed available data for the required parameters, which lead to a simplification of the model; Naden (1987a) included the effects of different arrangements of particles and turbulent fluctuations in the flow; Wiberg & Smith (1987) the effects of heterogeneous sediments; Komar & Li (1986) and Carling *et al.* (1992) the effects of different particle shapes and sizes. The range of variations illustrate the reason for trying to find a physically based description of the process of entrainment, to try and enable the development of a model to be used in any situation. They also illustrate the problem that each of these models includes some, not all, of the possible variables and even with these simplifications and such a relatively simple problem the selection of appropriate values for parameters is difficult.

3.3.1.3 Application of initial motion models

In models of particle movement in fluvial systems the initial movement of particles from rest has not always been included. Van Rijn (1984) and Sekine & Kikkawa (1992) used observations to scale an initial particle velocity and direction. Wiberg & Smith (1985) and Naden (1987a) used force balance models of particle motion though in different ways. In Wiberg & Smith (1985) a pivoting model of particle entrainment was used to supply the initial conditions of position and velocity, at the start of a particle trajectory. In Naden (1987a) different structures formed by particles were analysed using a pivoting model to calculate the velocities required to entrain particles from each structure. A description of turbulent fluctuations, assuming a Gaussian distribution, was then used to calculate the probabilities of entrainment for a particle in a flow. The exact particle velocity at the start of a trajectory was not required in this model.

3.3.2 Movement

As in the description of particle movement in Chapter 2, when calculating particle movement there is a split between non-contact motion and movement in contact with the bed at the start of a particle movement or between movements. There are also different ways of treating the modelling of particle movement depending on the use to which the calculation is to be put. For example, Naden (1987b) used empirical relations to calculate particle movements; van Rijn (1984) only calculated single saltations.

3.3.2.1 Non-contact motion

In Naden (1987b) experimental data were analysed to produce empirical expressions for height and length of saltation and particle velocity; the possibility of suspended saltations due to turbulent fluctuations was also included. This approach was used since theoretical models gave a range of answers and the aim of the study was the modelling of bed topography due to sediment transport, not the mechanics of sediment transport.

In all the other models of the movement of sediment particles considered here some form of the equations of particle motion were solved numerically to calculate the movement of particles in saltation. Differences between the models come from the inclusion or otherwise of terms in the equation of particle motion and from the different values of coefficients used in the equations.

In Reizes (1978), Sekine & Kikkawa (1992) and Jiang & Haff (1993) only the effects of forces due to drag and gravity were considered. Sekine & Kikkawa (1992) experimented with the effects of the forces due to lift and fluid acceleration but found the effects of these to be only slight. Van Rijn (1984) added the lift force due to shear, using the model of Saffman (1965). This model of lift force was for flow where

viscous forces predominated but it was assumed that it could also be used in a turbulent flow. The coefficient of lift in the model of van Rijn (1984) was used to match the calculated and observed particle trajectories In the van Rijn model only single saltations were calculated, using empirically set initial particle velocities to calculate characteristic saltation heights and lengths and particle velocities for different transport stages. Murphy & Hooshiari (1982) and Wiberg & Smith (1985) used all the terms described in the previous chapter to calculate particle motion, even though the contribution due to individual terms may be small.

3.3.2.2 Contact motion

The calculation of contact motion was not always included in models of particle movement. Van Rijn (1984) and Sekine & Kikkawa (1992) set the initial particle velocities empirically, eliminating this problem. In Wiberg & Smith (1985) the contact motion was expressed as a pivoting movement and in Sekine & Kikkawa (1988) a non-slip rolling model was used. In the particle simulation of Jiang & Haff (1993) the possibility of rolling existed due to the way particle interactions were modelled, including rotational motion of particles in addition to translational motion. The calculations performed showed that while particles rotated, contact with the bed was intermittent; this is similar to the behaviour observed by Drake *et al.* (1988).

3.3.3 Impact / Deposition

The models of impact and deposition used in models of particle motion depend on the overall description of the particle movement. Naden (1987b) used a balance between tangential and gravity forces to determine whether a particle was trapped or continued to move. This model did not require the calculation of initial conditions for a saltation since the height and length of saltations were determined from empirical equations and each saltation was considered to be independent of the previous saltation, based on the observations of Abbott & Francis (1977).

In the models of Wiberg & Smith (1985) and Sekine & Kikkawa (1992) the conditions at the start of the next saltation were required. Both used a single coefficient to represent the reduction in velocity at the impact. In Wiberg & Smith (1985), the value of this coefficient was set to match experimental data of Abbott & Francis (1977). The coefficient was set to a value of 0.4 to match a saltation, then this value was used in other calculations. Sekine & Kikkawa (1992) used a value of 0.65, based on experimental data and the fitting of their calculations to experiment. Reizes (1978) describes a 3 dimensional impact model with particle rotation for no-slip and slip conditions but does not state the values of the coefficients of slip and restitution used in the calculations. While Murphy & Hooshiari (1982) calculated a coefficient of restitution of 0.25 for a bed of loose marbles, further analysis of impact wasn't performed because of the difficulty of analysing the impact angles from their photographs. In all these calculations the initial conditions for saltations were calculated from the final velocity of the previous saltation using a coefficient of restitution.

In Wiberg & Smith (1985), the conditions for a particle to cease moving were failure to clear the next particle. This could occur with impact at either extreme, that is low or high. Sekine & Kikkawa (1992) allowed the possibility of a particle being trapped in a pocket in the bed, bouncing off particles until the amount of energy dissipated caused it to cease to move.

In aeolian models of particle motion the results of impacts have been described in terms of 'splash' functions, empirical relations linking the impact of a particle with the numbers of particles ejected and the velocities with which these particles were ejected. These empirical relations are based on models described in the previous chapter, with coefficients set from numerical simulations (Anderson & Haff, 1988) or experiment (Werner, 1990; McEwan *et al.*, 1992).

3.3.4 2 phase flow

The modelling of the interaction of heavy particles with turbulent flow using particle tracking has been approached in two ways: modification of the time scale over which correlation is preserved and the tracking of fluid and heavy particles independently while checking correlations.

A modification to account for the reduced correlation time scale due to the 'crossing trajectories' effect was proposed in Csanady (1963), for homogeneous turbulence. When a particle has a low terminal velocity and small inertia the particle follows the fluctuations of the flow. The velocity fluctuations which affect the particle are due to eddy decay and the correlation time scale for the particle with the flow tends to the Lagrangian time scale, T_L. For a particle with large terminal velocity the particle cuts through the turbulence and the time scale tends to L_E / u_t, where L_E is the Eulerian integral length scale and u_t is the terminal velocity of the particle. The change in correlation is due to the movement of the particle through the fluctuations, represented by the time the particle takes to traverse the Eulerian length scale. The time scale of Csanady (1963) interpolates between the Lagrangian integral time scale, T_L, for small particle terminal velocities responding to fluctuations and the Eulerian time scale defined above, L_E / u_t, for particles with large terminal velocities which do not respond to fluctuations in the flow

$$T_L^* = \frac{T_L}{\sqrt{\left(1+\left(\frac{\beta u_t}{\sigma_w}\right)^2\right)}}$$

where β is the ratio $\sigma_w T_L/L_E$, which is of O(1). This time scale was used by Sawford & Guest (1991), modified to take account of variation in length scale in different directions for inhomogeneous turbulence, to simulate motion of heavy particles. This

approach of modifying the time scale has been used to calculate the effects of turbulence in modifying aeolian saltation. The expression due to Csanady (1963) was found not to reproduce all observations with a single value of β. Hunt & Nalpanis (1985) and Anderson (1987) therefore used a slightly different form

$$T_L^* = \frac{T_L}{\left(1 + A\left(\frac{u_r}{\sigma_w}\right)^{\frac{2}{3}}\left(\frac{T_L}{\Delta t}\right)^{\frac{1}{3}}\right)}$$

where A is a constant of O(1) used to match the calculated paths to the results of Snyder & Lumley (1971). This form of the modified time scale accounts for the spatial gradients of turbulence and was based on an expression for the cross-correlation of velocities over a small interval, δz, (Hunt & Nalpanis, 1985)

$$\overline{w(z+\delta z)w(z)} = w^2(z) - A_1 \frac{\sigma_w^{\frac{4}{3}}}{T_L^{\frac{4}{3}}} \delta z^{\frac{4}{3}}$$

where for time Δt

$\delta z = u_r \, \Delta t$

These expressions for T_L^* can then be used in expressions for the first order autocorrelation function as used in passive particle tracking

$$R(\Delta t) = \exp -\left(\frac{\Delta t}{T_L^*}\right)$$

The alternative approach of tracking fluid and particle and checking time and distance to ensure that the scales have not been exceeded is described in Shuen *et al.* (1986). In this model values for the velocity fluctuations of an eddy were selected and particles were assumed to interact for the eddy lifetime, or the time spent in the eddy. A more complex model used by Zhuang *et al.* (1989) includes random changes when moving from eddy to eddy and changes correlated in time and space with the eddy scales within the eddy. An application of the 'particles in eddies' approach has been

made for open channel flow by Yvergniaux & Chollet (1989). In this model the results were compared with the data for movement of particles in suspension of Sumer & Diegaard (1981), rather than the effects of turbulence on saltating particles.

3.4 Bed

Bed descriptions suitable for modelling the movement of single particles depend on the system being modelled and the complexity of the model being used. The model of Sekine & Kikkawa (1992) uses a 3 dimensional impact model and therefore requires a 3 dimensional representation of the bed. That of Wiberg & Smith (1985) only uses a 2 dimensional impact model and therefore a 2 dimensional representation of the bed is all that is required. In both of these models the particles from which the bed is formed are spheres, the same simplification being made in describing particle movements.

The bed representation has been used as a method of introducing a stochastic element into otherwise deterministic models by Wiberg & Smith (1985) and Sekine & Kikkawa (1992). In Wiberg & Smith (1985) the impact position is determined by selection of a height from a uniform random distribution at the time of impact. Sekine & Kikkawa (1992) generate a surface of particles with equal horizontal spacing in the streamwise and cross-stream directions and a vertical position determined from a Gaussian distribution. These methods are used to generate bed descriptions based on simple particle descriptions. More complex descriptions are possible, for example Robert (1991) simulates bed roughness using a range of sizes and shapes of particles, reproducing the statistics of measurements of actual bed roughness, though the model is not used as the description of a bed in a model of particle motion.

As was mentioned in the previous chapter the observations of single particle motion were made over static beds of single size ranges. The descriptions of the bed above describe natural or water worked bed material. Where the bed is static and

made up of material of a single size, simpler descriptions can be used, such as square and hexagonally packed spheres (Reizes, 1978).

3.5 Conclusions

In Chapter 2 the influence of turbulent velocity fluctuations in the flow on the movement of sediment particles was described. In this chapter methods of modelling turbulent velocity fluctuations in the flow, and of calculating the effects of the interaction of these fluctuations with heavy particles are described. The methods described make it possible to include the effects of turbulent velocity fluctuations on calculated particle movements and should therefore be included in the model of particle movement. A model of the mean flow velocity and a description of the scales of turbulence above rough beds in open channels suitable for use in a particle tracking must therefore be included in the model of particle movement.

The modelling of particle motion requires a description of the initiation of motion of particles and values for the initial conditions at the start of saltations. Any model of particle movement in contact with the bed must be able to supply these values. Descriptions of non-contact particle movement and impact must be included to allow complete particle movements to be described .

The final component of the model is a description of the bed; if only single particle movements are being calculated no modification of the bed can occur. Any effects due to mobility of the bed must be included in the model of particle impact.

Chapter 4

A model of the movement of single sediment particles in turbulent flow in the fluvial environment

4.1 Introduction

A model of the movement of single sediment particles in turbulent flow is described in this chapter. The aim of this work is to develop a model able to include the effects of turbulent fluctuations of the flow on particle movement. The representation of other processes is therefore made at a level that reproduces essential processes without necessarily reaching the complication of the process models described in the previous chapter. The possibility of substituting different process models at a later date always remains available.

The equations used to describe the particle motion and all the calculations performed were in a non-dimensionalised form. The parameters used to non-dimensionalise quantities were the fluid density, ρ, the flow depth, h, and the mean bed shear velocity, U_*.

All the components of the model, flow (mean and fluctuating), and particle processes, are treated in 2 dimensions (downstream and vertical). The use of a more complicated description of the flow would require the use of a more complicated flow solver with higher computer overheads. Given the dominance of downstream and vertical flow components for transport in the simple flows considered here and the fact that the basic types of behaviour can be observed in 2 dimensions this is not considered an undue simplification at this stage.

The use of 2-dimensional flow constrains the only possibilities for 3-dimensional effects to those which affect the initial conditions of a movement, i.e. those for initial particle motion and impact. Reizes (1978) and Sekine & Kikkawa (1992) include a 3-dimensional description of particle impact in their models of sediment particle movement. Use of such a model does extend the possible uses of a model of sediment particle movement, e.g. the calculation of sediment transport around bends (Sekine & Parker, 1992). The effects of 3-dimensional impact are not important with respect to reproducing the effects of a turbulent flow when that flow is only being modelled in 2 dimensions and are therefore not included in this model.

The other simplification used throughout the descriptions of particle processes is the replacement of particles by spheres of equivalent diameter. This makes the formulation of the descriptions simpler; describing the motion and behaviour of a sphere is a difficult problem; attempting to describe the behaviour of any other shape is much harder, for example the added mass coefficient of anything other than a symmetrical body is dependent on the direction of movement. Computing geometries of interacting particles, important in the calculation of initial motion and impact, is also a simpler problem for spheres than for other shapes, even regular shapes.

In addition to the description of the components of the model there is also a description of the implementation of the model. The structure of the program, the routines used to generate the random number sequences and how the calculations were performed on different machines is discussed.

4.2 Flow

The flow experienced by particles is calculated from a mean flow onto which is superimposed a fluctuating component, Figure 4.1.

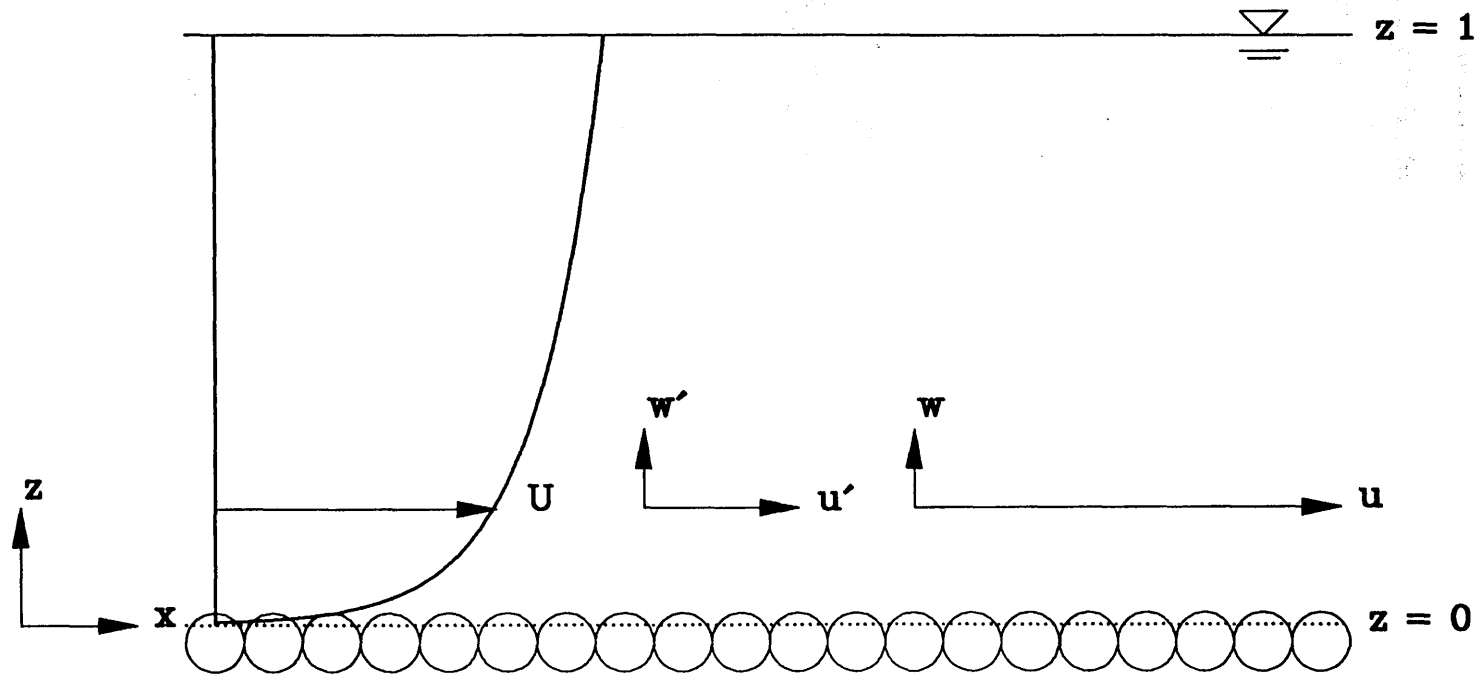

Figure 4.1 Components of flow

4.2.1 Mean flow component

In this model the mean flow component is calculated using the logarithmic velocity profile for turbulent flow over a rough boundary. The decision to use this description of the mean flow, rather than a more complicated description, is based on the available data and the types of data with which comparisons were being made. Flume data, with steady flows and little secondary flow effects show 2-dimensional flow with a logarithmic mean velocity profile to be a good approximation.

The model is only used to calculate the motion of individual particles of sediment, the relative densities of the particles is of order 1 and the extraction of momentum from the flow will be small, causing little modification of the velocity profile, therefore the use of a more complicated method of calculating the velocity profile, such as those of Ungar & Haff (1987) and Werner (1990) using a simplified Navier-Stokes equation with mixing length closure, is not necessary.

In calculations the non-dimensional form of the log law velocity profile equation used is

$$U = \frac{1}{\kappa} \ln \frac{z}{z_0}$$

where U is the mean velocity at height z, κ is von Karman's constant, taken to have a value of 0.4 and z_0 is the roughness length scale. Here it is assumed that

$$z_0 = \frac{k_s}{30}$$

where k_s is the Nikuradse roughness length scale. This is the appropriate form for fully turbulent flow over a rough bed (Young, 1989). Since the available data are for flows over beds of either a single size or single size range it is further assumed that

$$k_s = d$$

where d is the diameter representative of the bed material (Francis, 1973). The position for the zero height with respect to the particles forming the bed is harder to

fix; Einstein & El-Samni (1949) found that $0.2k_s$ below particle tops was appropriate for surfaces of spheres and gravel; Komar & Li (1988) used a value of $0.25k_s$; James (1990) found a quoted range from $0.15k_s$-$0.35k_s$ but in models for initial particle motion found a best fit with $0.5k_s$. The value used in these calculations was $0.2k_s$, this is within the range of values used and has been determined experimentally for similar surfaces to those described in the model by Einstein & El-Samni (1949). The logarithmic profile is assumed to hold down to the zero velocity height, measurements by Einstein (1950) show that the profile can hold down to $z = 3z_0$ and the extension to the zero velocity heights is used to simplify calculations as in Kirchner *et al.* (1990).

Since the flow system considered is steady uniform flow in 2 dimensions the mean vertical component of velocity, W, must be zero from continuity considerations.

4.2.2 Fluctuations in the flow

The fluctuations in the flow due to turbulence were modelled by tracking the paths of fluid particles, including variation in magnitude, correlation and the spatial and temporal scales of the turbulence. This section only describes the movement of fluid particles, the method by which the interactions of fluid and sediment particles are modelled is described in Section 4.3.4.

The description of the fluctuations of velocity and their effect on the movement of fluid particles is built up in stages. The magnitudes of the fluctuations, correlation between the fluctuations and finally a representation of the effects of coherent structures embedded in the turbulence will be described. These elements are introduced in such a way that the effects of increased complexity in the modelled fluctuations can be evaluated after each stage. These components describe the magnitude of the velocity fluctuations, but the spatial and temporal scales over which these fluctuations persist must also be modelled to describe correctly the movement of fluid particles

under the influence of turbulent velocity fluctuations. A model of these scales, completing the description of fluid particle movement, is described last.

The amount of statistical data reported in the literature describing the fluctuations in turbulent flow over a rough bed is not large. More data exist for turbulent flow over smooth beds and the measurements that have been made are often for regular roughness patterns and have been made to characterise turbulent stresses for turbulence modelling and not turbulent fluctuations for dispersion modelling, the type of data required here.

4.2.2.1 Magnitude and distribution of velocity fluctuations

The data used to describe the magnitude of the velocity fluctuations and their variation with depth is that of McQuivey (1973). This data set contains the results of measurements of horizontal and vertical fluctuations and their associated time and length scales from a variety of open channel flows, in flumes and conveyances. The variation of the velocity fluctuations as expressed by their standard deviations has been analysed by Naden (1987a), to give the following expressions:

$$\sigma_u = U \times 0.16 \times \left(\frac{z}{k_s}\right)^{-0.65}$$

$$\sigma_w = 0.77 \times \sigma_u$$

where σ_u and σ_w are the standard deviations of the downstream and vertical velocity fluctuations respectively.

More general expressions for turbulent flow over a rough boundary can be found in Perry *et al.* (1987), based on dimensional analysis (Perry *et al.*, 1986). The values of coefficients were measured in wind tunnels to give the following equations for the horizontal and vertical standard deviations of the velocity fluctuations, which in non-dimensionalised form are:

$$\sigma_u = \sqrt{2.01 - 1.26\ln(z) - \frac{7.50}{\sqrt{z_+}}}$$

$$\sigma_w = \sqrt{1.78 - \left(\frac{4}{3}\right)\frac{7.50}{\sqrt{z_+}}}$$

where

$$z_+ = \frac{U_* z}{\nu}$$

These expressions are shown plotted against a set of the observations of McQuivey (1973) in Figure 4.2. The horizontal fluctuations show a similar pattern though of different magnitude; the vertical fluctuations are of a similar magnitude though showing a different variation with height. The equations of Naden (1987a) would therefore seem a reasonable description to use in the present model.

Measurements of the horizontal, u', and vertical, w', velocity fluctuations in turbulent flows show probability density distributions that are close to Gaussian (Nakagawa & Nezu, 1977, open channel flow data , Heathershaw, 1979, marine data) the distribution of the fluctuations has therefore been assumed to be Gaussian.

4.2.2.2 Correlation of velocity fluctuations

Simultaneous measurements of horizontal and vertical velocity fluctuations have shown that the fluctuations are correlated (Heathershaw, 1979, Heslop *et al.*, 1993). These signals can be analysed to obtain a value for the correlation coefficient, r, between the streamwise and vertical velocity fluctuations.

$$r = \frac{\frac{1}{n}\sum^{n} uw}{\sigma_u \sigma_w}$$

While the velocity fluctuations show almost Gaussian distributions, the distribution of the product of the fluctuations, $u'w'$, is skewed. It has been found that a joint normal probability function for u' and w' can correctly predict the probability density function

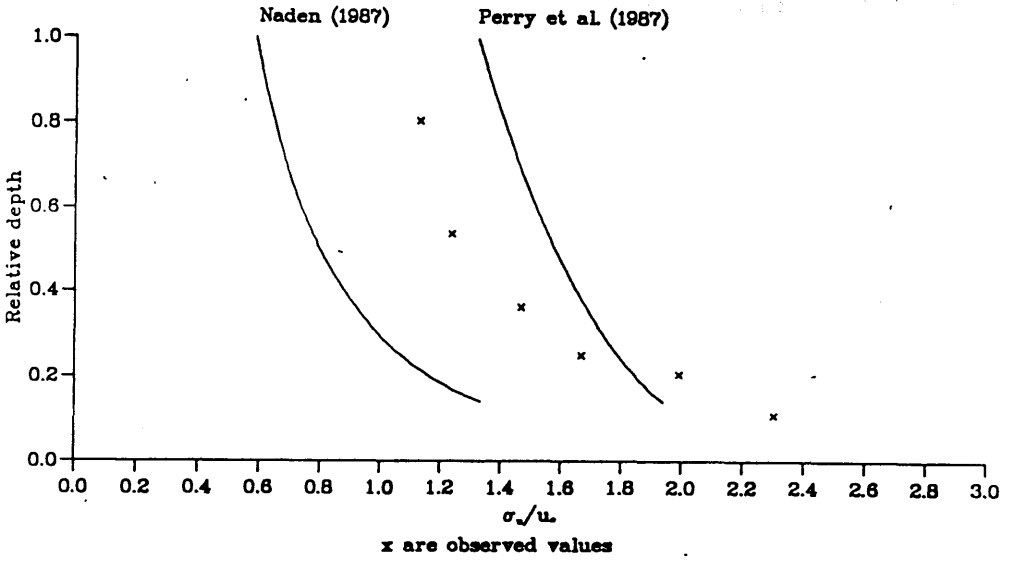

a) Variation of standard deviation of horizontal velocity fluctuations with depth

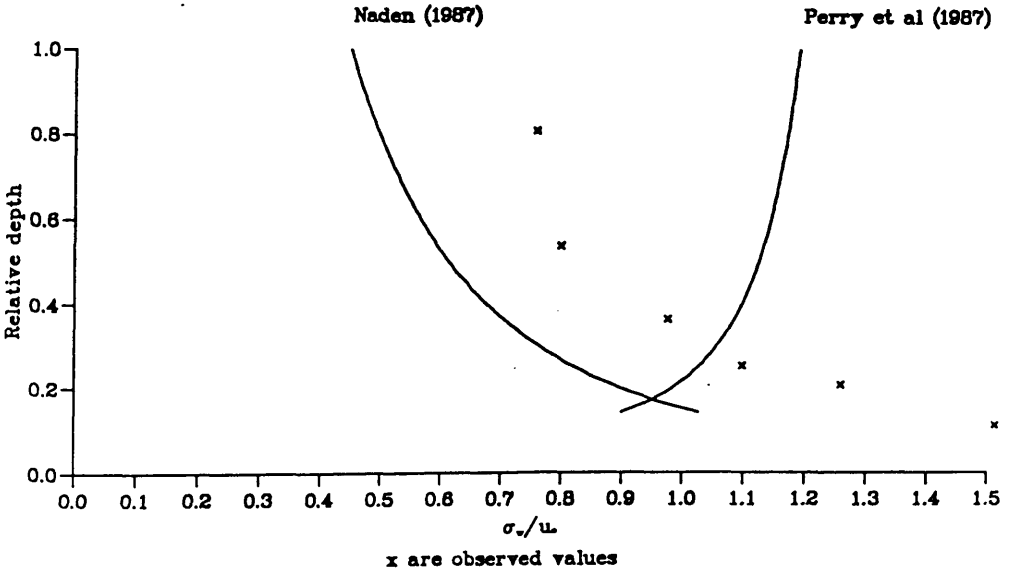

b) Variation of standard deviation of vertical velocity fluctuations with depth

Figure 4.2 Comparison of variation of standard deviations of velocity fluctuations with depth

Observations of McQuivey (1973), expressions of Naden (1987) and Perry et al. (1987)

for $u'w'$ (Antonia & Luxton, 1971, Heathershaw, 1979). This distribution was therefore used here to describe the correlation between the fluctuations of the horizontal and vertical velocity fluctuations. To calculate this a value for the horizontal velocity fluctuation, u', was selected from a Gaussian distribution, the corresponding values for the correlated mean and standard deviation of the vertical velocity fluctuations can then be calculated as;

$$\hat{W} = r\frac{\sigma_w}{\sigma_u}u'$$

$$\hat{\sigma}_w = \sqrt{1-r^2}\sigma_w$$

A value for the correlated vertical velocity fluctuation, $\hat{w}'$, can then be calculated from a Gaussian distribution with standard deviation, $\hat{\sigma}_w$, then added to the correlated vertical velocity,$\hat{W}$, to give the vertical velocity fluctuation, w', Figure 4.3.

Based on analysis of turbulence measurements made in the fluvial environment a correlation coefficient of -0.4 was used (Heslop *et al.*, 1993).

4.2.2.3 Structure in turbulent fluctuations

As was described in Chapter 2 turbulence near a boundary layer is not completely random but contains embedded coherent structures. These can cause significant variations in the shear stress at the boundary and the rate of sediment transport. The largest effects are due to sweeps, causing enhanced entrainment, and bursts, modifying saltations.

When records of turbulence are analysed, coherent structures show as highly correlated periods, with correspondingly high turbulent shear stress, amongst longer periods of relatively quiescent signals with low correlation. Soulsby (1983) described a method of analysis of turbulence records to calculate the contributions to shear stress from the different quadrants and hence different types of structure. The turbulence records were analysed to find the largest value of $|u'w'|$ in the series; the signal was

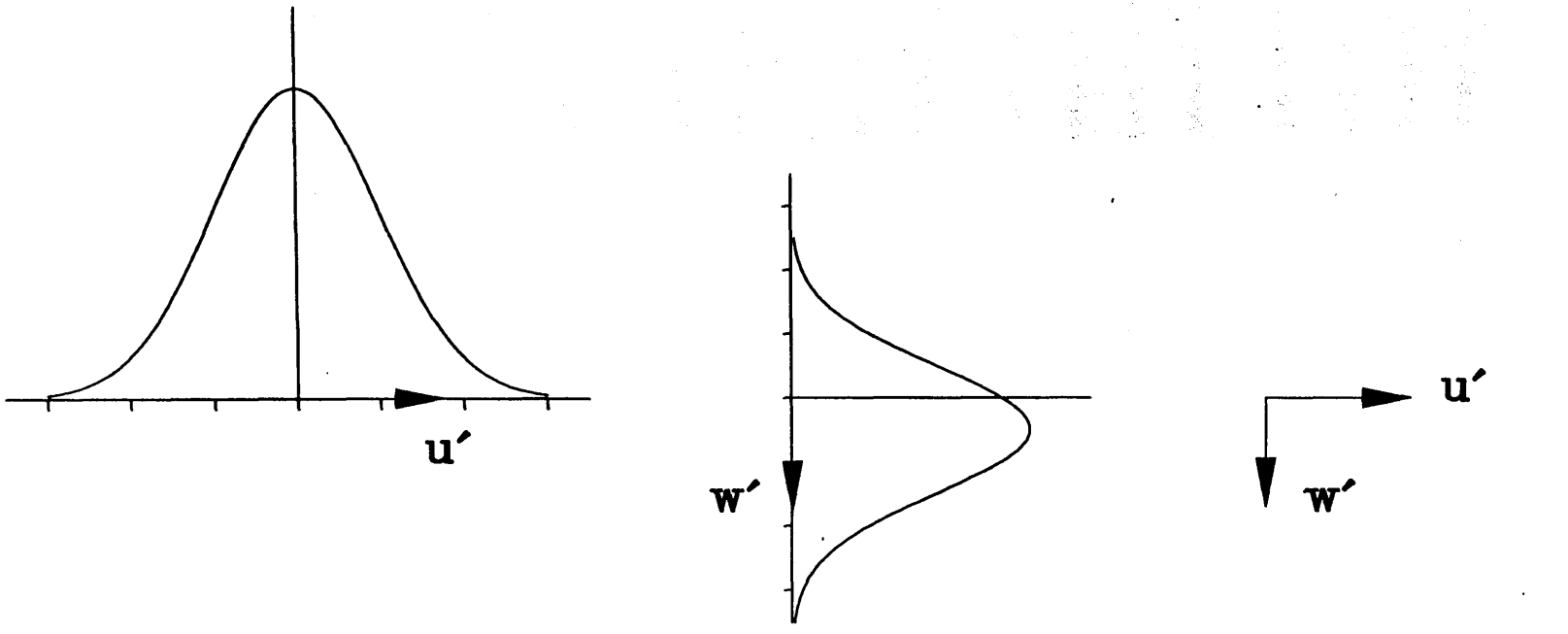

Figure 4.3 Correlated vertical velocity fluctuations

then followed backwards and forwards till $|u'w'|$ fell to 10% of its peak value. The contribution to the Reynolds stress due to this event was then calculated and recorded along with its duration and quadrant. This process was then repeated for the next largest value of $|u'w'|$ and so on until the cumulative Reynolds stress equalled 90% of the total value. This gave a record of the contribution of each quadrant to the Reynolds stress and the duration over which the contribution took place.

This method of analysis was applied to turbulence measurements made on the River Severn at the Leighton upstream site described in Heslop *et al.* (1993). Data from this particular site was chosen since it was a straight reach with the least 3-dimensional flow effects and therefore the most suitable data for use in this model.

The analysis of the turbulence records showed 89.9% of the turbulent shear stress occurred in 28.9% of the length of the record; the contributions by quadrant are shown in Table 2.1 (Holland, pers. comm.). The contributions can be described in three groups: that due to bursting and sweeping, quadrants 2 and 4, of which sweeps have been observed to have the most effect on sediment transport (Thorne *et al.*, 1990) and that due to inward and outward interactions, quadrant 1 and 3, of which outward interactions have been observed to cause significant sediment transport, though their shorter relative duration limits their overall significance (Thorne *et al.*, 1990). The remaining contributions take 71.1% of the length of the record but only contribute 10.1% of the turbulent shear stress, since it was the large contributions to shear stress of events that were of interest the quadrants in which these remaining contributions lay were not analysed.

To reproduce this type of behaviour three levels of correlation between horizontal and vertical velocity fluctuations were used: a large negative correlation for bursting and sweeping, r_1; a positive correlation for inward and outward interactions, r_2; and a small negative correlation for the remaining time, r_3. The correlation coefficients can be calculated from the contributions to stress over time as follows,

assuming that the standard deviations of the velocity fluctuations at a height remained constant.

The relative contribution of each of the types of behaviour to the total stress is known and can be written

$$\sum^{n_n} u'w' = a_n n r \sigma_u \sigma_w$$

so

$$\sum^{n_1} u'w' \quad : \quad \sum^{n_2} u'w' \quad : \quad \sum^{n_3} u'w'$$

$$a_1 = 0.968 \quad : \quad a_2 = -0.070 \quad : \quad a_3 = 0.101$$

likewise the relative durations are known $n_n = b_n n$,

$$n_1 \quad : \quad n_2 \quad : \quad n_3$$

$$b_1 = 0.260 \quad : \quad b_2 = 0.029 \quad : \quad b_3 = 0.711$$

hence

$$r_n = \frac{\frac{1}{n_n}\sum^{n_n} u'w'}{\sigma_u \sigma_w} = \frac{\frac{1}{b_n n} a_n n \sigma_u \sigma_w}{\sigma_u \sigma_w} = \frac{a_n}{b_n} r$$

This expression gives values for the correlation coefficients, r_1=3.729r, r_2=-2.414r and r_3=0.142r. The maximum value of the correlation coefficient, r is therefore limited to a value of -0.26, a value below the observed mean for the whole series, indicating that the assumption that the standard deviations have constant values is not true. In calculations the three correlation coefficients were used. Thus this method cannot reproduce a real turbulent signal but can produce high magnitude, short duration shear stress events which have been observed to be important in bedload transport.

4.2.2.4 Turbulence scales

The expressions given above can be used to describe the velocity fluctuations and their correlation. To describe the movement of fluid particles under such

fluctuations, the spatial and temporal scales over which these velocity fluctuations persist must be described. The appropriate scales to use when tracking fluid particles affected by turbulent velocity fluctuations are the Lagrangian integral scales of time and length. Measurement of Lagrangian data in open channel flows, at the scales necessary for this work, present a problem.

The number of measurements of Lagrangian data at an appropriate scale in open channel flows is small: McQuivey & Keefer (1971) for dispersion of surface floats, Sullivan (1971) for dispersion throughout the depth. In the absence of a set of field or laboratory measurements of open channel flow over a rough bed suitable for mapping Eulerian onto Lagrangian statistics the alternative approach of using Eulerian measurements in a pseudo-Lagrangian way, described in the previous chapter, is used.

The values of the velocity fluctuations are assumed to remain constant throughout each eddy in time and space. The size and duration of each eddy are assumed to be the calculated pseudo-Lagrangian time and Eulerian length scales, at the time and position when the eddy fluctuations are calculated. Thus when an eddy has been left the new values of the velocity fluctuations are only correlated with themselves and not with the fluctuations of the previous eddy. The eddies are assumed to be advected by the mean flow at the fluid particle position, unless the particle position is less than half the vertical length scale away from the boundary. When the particle is less than half the vertical length scale away from the boundary the mean velocity at this height is used to advect the fluid particle. This acts to speed up the advection of eddies close to the boundary.

The time scales used in the calculations were:

$$T_{Lx} = L_{Ex}/\sigma_u$$

$$T_{Lz} = L_{Ez}/\sigma_w$$

where T_{Lx}, T_{Lz} are the horizontal and vertical Lagrangian integral time scales, L_{Ex}, L_{Ez} are the Eulerian integral length scales and $\sigma_u(z)$, $\sigma_w(z)$ are the standard deviations of the velocity fluctuations at height z. The horizontal Eulerian length scales were calculated from the data of McQuivey (1973),

$$L_{Ex} = 2.676\exp\left(-5.020\frac{\sigma_u}{U}\right) \qquad (r\text{=-}0.744, n\text{=}60)$$

This data does not include values for vertical Eulerian integral length scales so, based on measurements from the River Severn (Holland, pers. comm.), the values of the vertical Eulerian length scale were calculated from

$$L_{Ez} = L_{Ex}/2$$

4.3 Sediment movement

The fluid forces due to rectilinear motion of the particles through the fluid are those of drag and lift (Figure 4.4, particle with negative vertical velocity), in non-dimensional form, for a sphere,

$$F_D = \frac{C_D}{2}\frac{\pi d^2}{4}\left((u-u_p)^2+(w-w_p)^2\right)$$

$$F_L = \frac{C_L}{2}\frac{\pi d^2}{4}\left((u-u_p)^2+(w-w_p)^2\right)$$

The magnitude of both these forces are set using experimentally determined coefficients. The lift force is expressed in this way rather than a more theoretical form due to the lack of analytical expressions for the lift forces other than for viscous motion (see Section 3.3.2.1). In addition to these forces there is the added mass force due to fluid acceleration, F_A, described in Section 2.3.2.1. In non-dimensional form, for a sphere,

$$F_{Ai} = \frac{\pi d^3}{6}(C_A+1)\frac{\mathrm{d}u_i}{\mathrm{d}t}$$

where

$$\frac{\mathrm{d}u_i}{\mathrm{d}t} = \frac{\partial u_i}{\partial t} + u_{pj}\frac{\partial u_i}{\partial x_j}$$

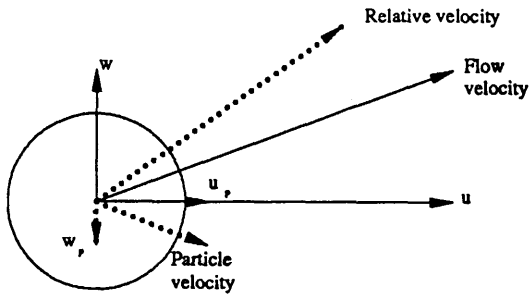

a) Flow and particle velocity components and resultants

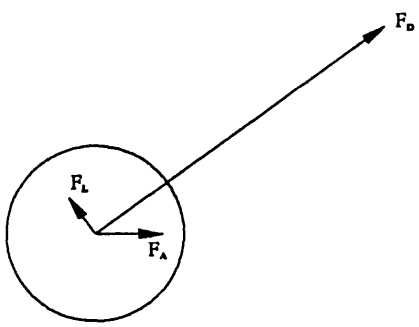

b) Forces due to flow and particle movement

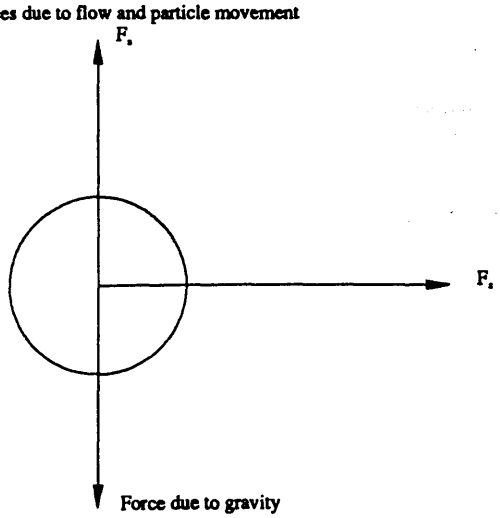

c) Forces acting on particle

Figure 4.4 Forces acting on particle in non-contact motion

If only mean flow components are considered, this reduces to

$$\frac{du}{dt} = w_p \frac{\partial U}{\partial z}$$

The component of force therefore becomes

$$F_{Ax} = \frac{\pi d^3}{6}(C_A + 1) w_p \frac{\partial U}{\partial z}$$

The effects of the velocity fluctuations on this term are not considered. The mean value of these terms is zero; further, the values are treated as constant for the life of an eddy with step changes between, rather than a gradual change with depth as occurs in the mean flow expression.

In the calculations of particle movement these are broken-down into horizontal and vertical components

$$F_x = F_D \frac{(u-u_p)}{\sqrt{(u-u_p)^2 + (w-w_p)^2}} - F_L \frac{(w-w_p)}{\sqrt{(u-u_p)^2 + (w-w_p)^2}} + F_{Ax}$$

$$F_z = F_L \frac{(w-w_p)}{\sqrt{(u-u_p)^2 + (w-w_p)^2}} + F_D \frac{(u-u_p)}{\sqrt{(u-u_p)^2 + (w-w_p)^2}}$$

All these forces are assumed to act in the same way throughout the flow, independent of the presence of the boundary.

4.3.1 Initiation of motion

The initiation of motion of particles is calculated using a force balance. The choice of initial motion calculation is in part determined by how the initial conditions for saltations are calculated, whether they are calculated or set empirically. If the initial conditions for saltations are set empirically then a calculation relating the effect of turbulent fluctuations on the shear stress and hence the Shields stress would be appropriate. When the initial saltation conditions are calculated some form of force balance must be performed in this calculation and is therefore also available to use in

an initial motion calculation. This has the advantage that different particle positions within the bed, the height and the position relative to neighbouring particles can influence whether the particle begins to move. The geometry and nomenclature used are shown in Figure 4.5. This gives an expression from the force balance, if movement is to occur, of

$$F_x \sin\theta + F_z \cos\theta > \frac{\pi d^3}{6}(\rho_s - 1)g\cos\theta$$

This differs from the force balance given in the previous chapter only in the use of θ, the angle above the horizontal rather than the use of the pivoting angle, θ_p. This terminology is used here because the force balance model is part of the rolling model, the force balance corresponds to the term in brackets in the rolling model (see Section 4.3.2.2)

For a particle initially at rest the subroutine to calculate rolling motion is called, fluid forces acting are calculated and the differential equation describing rolling motion is solved. If the particle remains at rest for the duration of an iteration then this process is repeated at the next iteration. If the particle starts to move then the calculation continues as a calculation of rolling motion. The fluid forces acting are calculated including the turbulent fluctuations in the velocity so the effects of turbulence and the persistence of fluctuations are included in the initial motion calculation.

The force balance calculation used is a very simple form, that is all the forces are assumed to act through the centre of mass of the particle, fluid forces are calculated for the total projected area of the particle and the particle is assumed to be spherical. For a particle resting on a bed of other particles the area exposed to the flow and hence the fluid forces acting and the position about which they act is influenced by the surrounding particles. The effects of this were included in the work of Kirchner *et al.* (1990), but are not included here because the simple model provides

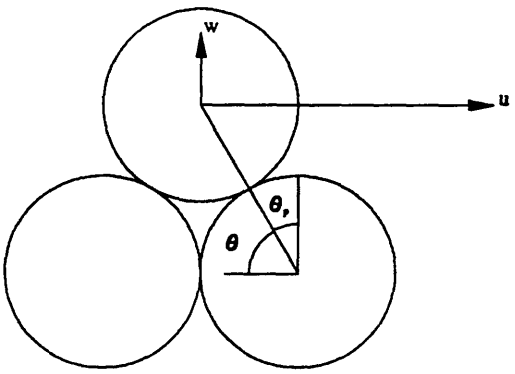

a) Fluid velocities

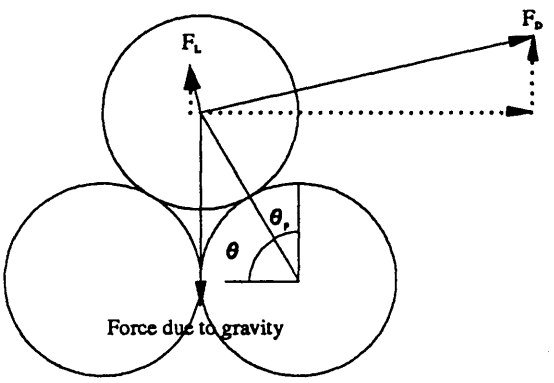

b) Forces acting (solid lines), horizontal & vertical components (dotted lines)

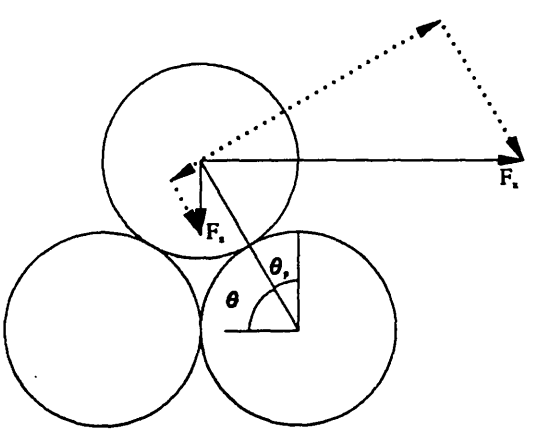

c) Forces resolved into i) Horizontal & Vertical components (solid lines)
ii) Normal & Tangential components (dotted lines)

Figure 4.5 Forces acting at initiation of motion

the correct qualitative responses to the flow without them. If such effects were included they would increase the computation time and the correct parameterisation of such models is difficult to achieve. Also the fixed beds with which initial comparisons were made form relatively simple geometries, without large protrusions or gaps, thus lessening the amount of particle hidden and therefore the importance of such effects. Such effects could be included at a later date.

The use of spheres rather than particles of more complex geometry has already been touched on in the introduction to this chapter. For the particular case of initial motion it would be possible to calculate the initial motion from the force balance using different particle geometries (Carling *et al.*, 1992). Once in motion, though, the interactions of a more complex geometry with the flow would be impossible to calculate and a sphere of equivalent volume would have to be used in such calculations. It is therefore simpler to use a sphere from the start, which also simplifies the related problem of how a different shape particle impacts with the bed at the end of a trajectory.

4.3.2 Movement

The model of particle movement includes two types of movement: contact movement and non-contact movement. The contact movement is modelled here as the rolling of one sphere over another without slipping. As described in Section 4.3.1 the rolling model provides the basis for the force balance for the initial motion criterion; distances travelled and time moving in rolling mode; the initial conditions for saltation; and the test for whether a particle is deposited after an impact.

4.3.2.1 Non-contact motion

The equation of particle motion used is a high Reynolds number approximation. In its non-dimensional form used here it can be written

$$\frac{\pi d^3}{6}(\rho_s + C_A)\frac{du_p}{dt} = F_x$$

$$\frac{\pi d^3}{6}(\rho_s + C_A)\frac{dw_p}{dt} = F_z - \frac{\pi d^3}{6}(\rho_s - 1)g$$

4.3.2.2 Contact motion

The contact model of particle motion is a rolling model without slip between the two particles, as described in Section 2.3.2.2. In its non-dimensional form this gives an equation

$$\frac{d\omega}{dt} = \frac{10}{7}\frac{\frac{\pi d^3}{6}\rho_s}{(d_{char} + d)}\left(-\frac{\pi d^3}{6}(\rho_s - 1)g\cos\theta + F_x \sin\theta + F_z \cos\theta \right)$$

where ω is the angular velocity of the particle and d_{char} is the diameter of the bed particles. The position at which the two particles lose contact can be found from the expression

$$\begin{aligned} N = & -\frac{\pi d^3}{6}\rho_s\left(\frac{d_{char} + d}{2}\right)\omega^2 \\ & + \frac{\pi d^3}{6}(\rho_s - 1)g\sin\theta \\ & + F_x\cos\theta \\ & - F_z\sin\theta \end{aligned}$$

when the value of N becomes positive the particles have lost contact. The derivation of these equations is given in Appendix 1.

4.3.3 Impact / Deposition

The position of particles on the bed is defined before calculations of particle movement start (see section 4.4). The possibility of impact is checked when the

vertical particle position is less than half the sum of the moving and bed particle diameters above the highest particle centre on the bed. The position and time of an impact are then calculated, along with the particle velocities immediately before impact.

The effects of this impact are calculated by splitting the particle velocity immediately before impact into components normal and tangential to the line between the particle centres, Figure 4.6,

$$u_{pN} = u_p \cos\theta - w_p \sin\theta$$
$$u_{pT} = u_p \sin\theta + w_p \cos\theta$$

where u_{pN} is the normal component of particle velocity and u_{pT} is the tangential component of particle velocity. Initially the fractions of momentum conserved were set to zero for the normal component and one for the tangential component, as suggested by the results of Gordon *et al.* (1972). The possibility of using other values of these coefficients to explore the effects this had on particle motion still remained.

Once the values of the particle velocities after impact had been calculated these values were used in the rolling model described in Section 4.3.2.2. This allowed three possible consequences of the impact: the particle rolling back to rest due to gravity, i.e. the deposition test used in Naden (1987b); the particle rolling forward for some period before starting to saltate; or an immediate rebound, starting a saltation with the conditions straight after impact.

4.3.4 Interaction of fluid and sediment particles

Two approaches to modelling the interaction of velocity fluctuations with sediment particles were described in Chapter 3. One approach was to use modified time scales, the other to track the movement of fluid and sediment particles to enable the interaction to be calculated. The latter approach was adopted in this model, thus

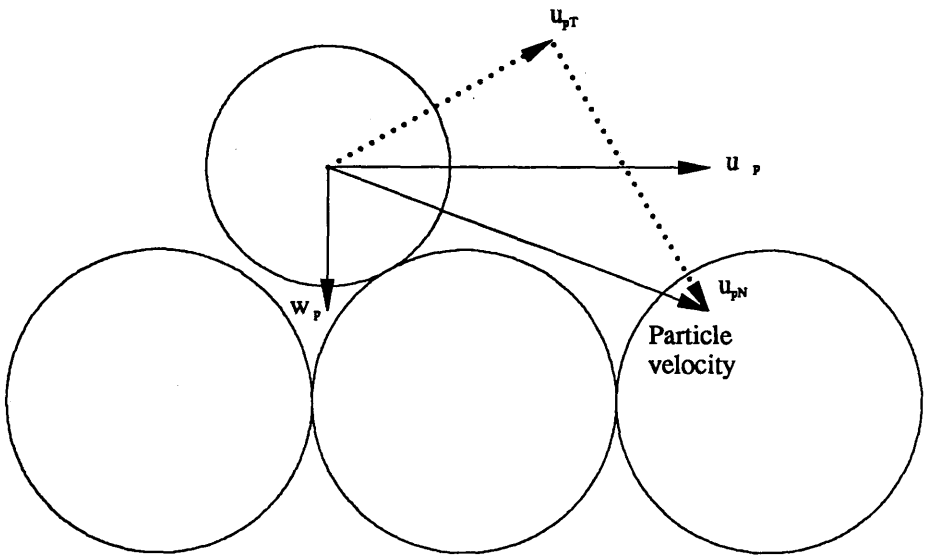

a) Particle velocity and components immediately before impact

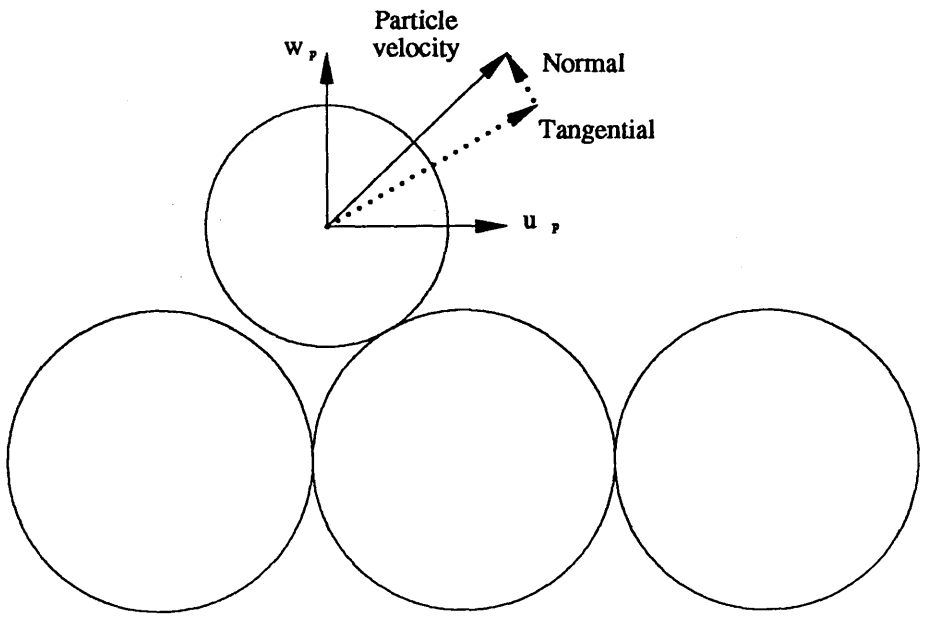

b) Particle velocity and components immediately after impact

Figure 4.6 Effects of impact on particle velocity

the inclusion of the interaction of fluid and sediment particles can be built directly on the existing descriptions of fluid and sediment particle movement.

The interactions are calculated by tracking fluid and sediment particles that are initially coincident over a number of iterations. The particles are tracked until either the divergence of fluid and particle or the time elapsed is too high for any correlation to remain, in which case the particle must have left the eddy represented by the fluid. Conditions for fluid coincident with the sediment particle are then calculated and the process is then repeated, as shown in Figure 4.7. This allows a representation of a turbulent eddy structure to be calculated based on the available data from measurement in open channel flow.

To calculate the movement of sediment particles the duration of the iterations must be smaller than either the time scales of the turbulent flow or the particle response time. The values of the turbulent time scales have already been described, the appropriate particle response time, t_r, to use is a high Reynolds number form. Hinze (1972) calculated the response time as the time taken for the particle relative velocity to fall to 50% of its initial value due to drag. This gives an expression

$$t_r = \frac{4d}{3C_D\sqrt{(u-u_p)^2+(w-w_p)^2}}(\rho_s + C_A)$$

where the relative particle velocity is the value at the start of an iteration.

These time scales, in particular the turbulent scales, give upper limits for the duration of an iteration, the choice of time interval at each iteration must therefore also be considered. In fact an appropriate fraction of these time scales to use will be less than these. In Anderson (1987) the value of Δt is set so that

$$\frac{\Delta t}{t_r} < 1$$

where Δt is the duration of an iteration; this ensures that the particle response time, t_r, is never exceeded. Zhuang *et al.* (1989) used a timestep

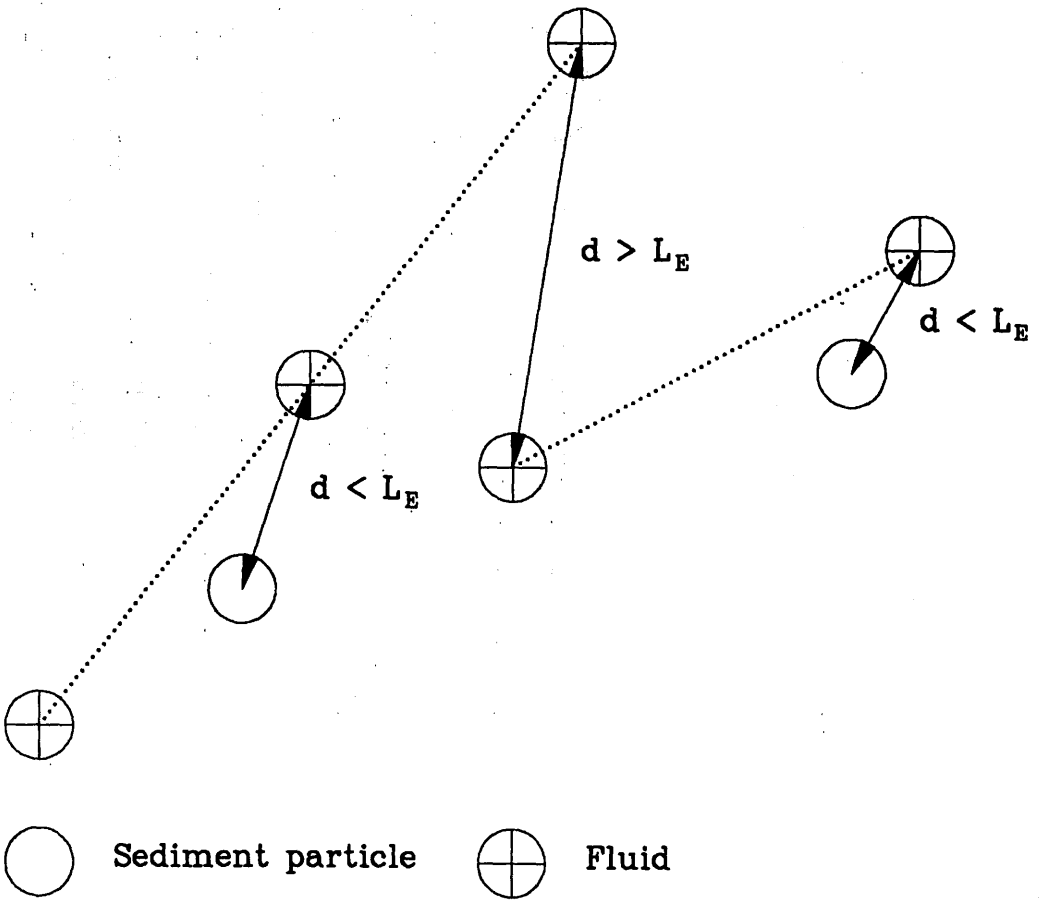

Figure 4.7 Tracking divergence of fluid and sediment particle

$$\Delta t = 0.1 \times \text{minimum}\,(T_L, t_r)$$

The choice of 0.1 as a multiplier came from previous work, Wilson & Zhuang (1989), calculating the restrictions on Δt in particle tracking dispersion models. It was found that using a value Δ=0.1 kept the difference between the solution using this value and smaller values to less than 2%, while larger values of Δ showed increasing percentage errors. In this work the expression of Zhuang *et al.* (1989) is used,

$$\Delta t = \Delta \times \text{minimum}\,(T_{Lx}, T_{Lz}, t_r)$$

this ensures that none of the time scales is exceeded during an iteration. An appropriate value for Δ for these calculations will be investigated by performing calculations over a range of values.

4.4 Bed

In this version of the model the bed has been reduced to a line of spheres, all with their centres at the same height, all touching one another. The use of different bed geometries to introduce a stochastic element in the calculations is not as important in this model as in those of Sekine & Kikkawa (1992) and Wiberg & Smith (1985), since the presence of turbulent fluctuations introduces a stochastic element. The bed is also a reasonable approximation of the surfaces used in the experiments with which the calculated movement of single particles will be compared. The diameter of the spheres is set from data after which appropriate roughness scales and position for the zero height can be calculated to supply the necessary values to the model of the logarithmic velocity profile as discussed in Section 4.2.1.

4.5 Implementation

The movements of particles were calculated iteratively, following the structure shown in Figure 4.8. Calculations were continued until either a set number of iterations had been performed or the particle had travelled a certain distance.

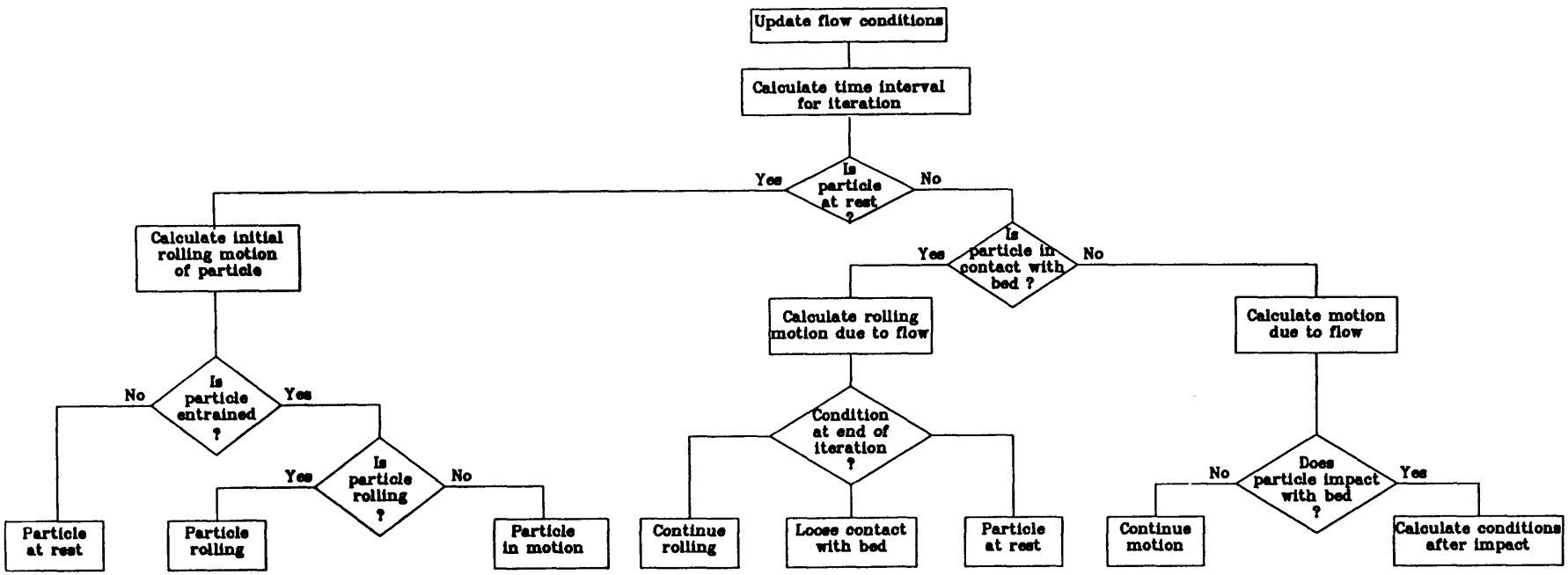

Figure 4.8 Structure of calculation of particle movement

The flow conditions for an iteration were determined as the sum of mean and fluctuating components, the mean streamwise component of velocity, U, at the position of the particle centre was changed throughout each iteration. The other velocity components were only changed when the particle was determined to have left an eddy.

The time interval to use for an iteration was determined at the start of the iteration, based on the flow and particle conditions at that time. The value was taken to be a fraction, Δ, of the minimum of the turbulent length scales and the particle response time. This ensured that neither particle response time nor turbulent time scales were exceeded. During iterations in which the particle either lost contact with or impacted with the bed the duration of the iteration was truncated at the time at which the change occurred. An appropriate value of Δ was determined from test calculations.

The other actions all depend on the processes already described, the rolling and non-contact particle motion are initial value problems, solved numerically using appropriate routines from the NAG Library. The solutions of both rolling and non-contact motion were continued until a set condition was reached. The rolling motion was continued until either the particle lost contact with the bed or the particle rolled to a halt. The non-contact motion calculation was continued until the particle came into contact with the bed at which point the resulting impact was calculated.

The model was coded in FORTRAN 77 and run on a Sequent Symmetry to produce single particle tracks and on a parallel Meiko Computing Surface, using up to 20 transputers to calculate multiple tracks and the statistics associated with them. When used on the Meiko the model was run in a Master-Slave configuration with a single master processor sending out conditions for calculations to slave processors, the number of slave processors used depending on availability and expected computation time. The calculation performed on each slave processor was that of a particle track

followed by calculation of statistics describing this track, particle velocity, saltation and suspension geometry. The values to be returned to the master process were therefore reduced to numbers describing the statistics of a track rather than the track itself, this reduced the quantity of data to be transferred between processors and reduced the time spent in communication between processors. This ensured that it was computation not communication that determined the time required for calculations and meant that the number of processors used in a calculation could be determined by availability.

To generate the sequences of pseudo-random numbers required to generate the turbulence two different random number generators were used. When calculations were performed on a single processor, either on the Symmetry or Meiko, the NAG routines, G05CAF and G05DDF were used for uniform and Gaussian distributions respectively, NAG (1991). When calculations were performed in parallel another algorithm due to Marsaglia *et al.* (1990), was used. By calling with different seeds this is said to produce up to 900 million independent sequences of pseudo-random numbers. The uniform output from this algorithm was converted to Gaussian distributions using RSS algorithm AS111, Beasley & Springer (1977).

4.5.1 Input data necessary to set model conditions

The data necessary to run the model are flow depth, h, bed roughness length, k_s, the size of particle in motion relative to this quantity, bed shear velocity, u_*, and particle density, ρ_s.. These values are input as a flow Reynolds number, Re_{*_k}, a particle Reynolds number, Re_{*_p}, non-dimensional specific particle weight, $g(\rho_s - \rho)h/\rho u_*^2$, and relative particle density, ρ_s/ρ. The other values input are a maximum number of iterations and the value of the fraction, Δ, to be used in calculating time intervals for iterations.

4.5.2 Parameters in model

In addition to the variables which need to be set for each calculation the value of parameters in the model must be set. The transport equations contain coefficients of drag, C_D, lift, C_L, and added mass, C_A. The impact model may also be modified by varying the fractions of normal and tangential momentum conserved.

The value of the coefficient of drag is calculated from the curve for an isolated sphere in steady motion, using a fit by Morsi & Alexander (1972), allowing the calculation of coefficient of drag over a range of particle Reynolds number. This ignores any effects due to the particle motion not being steady state, or any variation due to the proximity of a boundary, though measurements by Coleman (1972) and Bagnold (1974) show any variation in coefficient of drag due to the presence of a boundary to be small.

There is less information on the coefficient of lift, in particular about the variation of coefficient of lift with particle Reynolds number. In part this is due to the mechanisms generating forces normal to the direction of a flow. These are fluid shear and particle rotation, which can act at the same time for any particle Reynolds number. The presence of different mechanisms generating lift force means that measurement of one contribution to the lift force will often constrain the system in such a way that other contributions cannot be measured. The situation is further confused by the variation in lift observed approaching surfaces (Einstein & El-Samni, 1947; Bagnold, 1974; Sumer, 1984). The range of values of coefficient of lift obtained experimentally is partly due to measurements being of different contributions to the lift force, and partly due to the use of different definitions for the coefficient of lift. The contributions due to different mechanisms acting to generate lift on a particle close to a surface in turbulent flow are hard to determine, as is the variation in lift moving away from the surface. This makes parameterisation of these quantities difficult. In this

model the value for the coefficient of lift found by Einstein & El-Samni (1947) is used, with an inverse square reduction away from the wall.

In the presence of a fluid the effective mass of an accelerating particle is increased by an amount called the added mass. This extra inertia is due to the fluid accelerated with the particle; for an isolated sphere, assumed to be usable in these calculations, this added mass is equal to the mass of fluid that would occupy half the volume of the sphere (Milne-Thompson, 1968) , giving an added mass coefficient, C_A, of 1/2. The variation in the added mass coefficient observed by Odar & Hamilton (1964) was not included in the model.

4.6 Conclusions

The model described in this chapter consists of three parts, a flow, described by mean and fluctuating velocity components; a description of particle movement, in contact with the bed and away from the bed, including forces due to rectilinear motion and acceleration of fluid and particle, and a model of impact. All these occur over a fixed bed. The model therefore includes the components of particle movement and the flow causing the motion.

The use of a particle tracking method to describe the flow and its interaction with particles allows turbulent velocity fluctuations to be included in the model and the interaction is included in all the calculations of particle behaviour.

The model of particle movement in contact with the bed only includes rolling motion. Particle movement by sliding is not included because distances travelled and time spent in this type of motion would be small. The model of rolling is included because rolling is significant in terms of distance travelled and time spent in this type of motion. Rolling is also a significant process at the start of motion, forming the initial particle movement before saltation and providing the initial conditions at the start of the saltation, and any motion in contact with the bed between an impact and the next

saltation. The models of particle movement, both in contact with and away from the bed, include all the forces described in Section 2.3.2.1; the importance of these forces can be evaluated by performing calculation while varying parameters. The description of particle movement includes all the necessary components of particle movement and their interaction with the flow at all times.

The description of the bed as fixed is a function of the calculation being performed, movement of single particles cannot modify the bed. The description is also suitable for the data which is available to make comparisons between observed and calculated data.

Chapter 5

Calculations of movements of single particles

5.1 Introduction

The model of particle movement described in the previous chapter required calculations to be performed to determine the effects of different components within the model and to examine the results of varying parameters set in the model. The first calculations and their results, described in this chapter, were performed to examine the behaviour of the model. Once the form of the model derived from these calculations had been defined it was then used to calculate particle behaviour to compare with the observations of Fernandez-Luque & van Beek (1976) and Abbott & Francis (1977).

The calculations performed to determine the behaviour of the model were used to examine different components of the model. The first calculations examine the solution of the equations describing the movement of the particle, selecting suitable routines to solve the equations and appropriate timesteps over which to perform the solution. The other calculations determine the effects of different components of the model, the modelling of turbulent velocity fluctuations in the flow and the effects of fluid acceleration on the movement of the particle. The results of calculations of particle movements with different descriptions for the lift force acting on the particle due to the flow and conservation of momentum on impact were performed to examine the effect of varying these components due to the uncertainty in the exact description of these quantities.

5.2 Selection and testing of differential equation solver

The ordinary differential equations describing particle motion, contact and non-contact, were solved numerically. The routines used to calculate solutions to the

equations were taken from the NAG routine library. The routines used were those for initial value solutions to ordinary differential equations which are described in Chapter D02 (NAG, 1991). Routines based on three different methods of solving an initial value problem for a system of ordinary differential equations are available, these are based on the Runge-Kutta-Merson, Adams and backwards differentiation methods, of these the backward differentiation method is recommended for solution of stiff systems of equations. The routines available and the selection of an appropriate routine are described in Gladwell (1979) and NAG (1991).

For all of these methods the library consists of base routines which can be called from a number of different driver routines. The driver routine used in all the calculations described here integrates a system of equations until a function of the solution became zero. The interface to the driver routines are similar for each of the methods to enable the results of using the different methods to be tested for an application. In addition a routine to check whether a system of equations to be solved was stiff was available based on the Runge-Kutta -Merson method.

An initial calculation was made using the routine D02BDF to check whether a system of equations is stiff. The results of this calculation indicated that the system of equations was not stiff and that it was not necessary to use a backward difference scheme. The Runge-Kutta-Merson routine, D02CHF, and the Adams routine, D02EJF, were therefore investigated. The routines used both had a similar subroutine call, this varied only in the size of array passed to the subroutine as working space. In addition to these user supplied routines a variable, TOL, had to be set by the user to control the accuracy of the solution. The value of TOL is equivalent to the number of decimal places of accuracy required in the solution. The NAG documentation suggested that the accuracy of the solution calculated with this value of TOL can be checked by increasing the value of TOL by one and comparing the results of the different calculations. The value of TOL is also used as an indicator about the calculated results of a call to a routine. In normal use the value of TOL is returned

unchanged. If, however, the integration length, rather than TOL, controls the step length within a solution then at the end of a calculation the variable in TOL is returned with its value set to negative. For these conditions the accuracy of the solution could not be guaranteed and a call to the routine with a larger value of TOL was recommended.

The routines were called at each iteration to integrate particle movement over a timestep determined as described in Section 4.3.4. The integration of the solution required the derivatives to be calculated at a number of steps within the interval specified by the timestep. The derivatives of the equations describing the particle motion, contact and non-contact, were calculated from analytical expressions. The number of steps required for the solution at an iteration was determined within the chosen NAG routine, based on the specified required accuracy of the solution. The normal condition at the end of iteration, for both contact and non-contact motion, was for a particle to continue in the same type of motion. However the duration of an iteration was truncated if a particle either lost contact, when rolling, or came into contact, when in non-contact motion. The occurrence of these conditions during a particular iteration could not be predicted in advance, due to the stochastic elements in flow and bed. These conditions were therefore checked for during each iteration. The conditions determining when integration was truncated were set so that a function became zero when a moving particle lost contact with the bed, for contact motion, and for non-contact motion the function became zero when a moving particle came into contact with a bed particle. If the NAG routines were used in their simplest form hard error checking was in operation and the presence of any error conditions caused execution of the program to cease. The routines used here set an error condition if the integration proceeded to the end of the specified time interval, over which integration was to be performed, without the user specified function becoming zero. The functions used did not return a zero value during every iteration, since the normal condition was for a particle to continue in the type of motion that it started an

iteration. The routines therefore had to be called with soft error checking, this allowed the program to continue executing after an error condition had occurred. The flags for error conditions were trapped and checked on return from the subroutine. With the exception of cases where the value of the user specified function did not become zero, that is where particle movement continued as normal, errors were trapped and program execution stopped.

The differential equation routines were tested at three different transport stages, the values used are high though suitable for examination of saltation. The values of the stage used were some of those shown in Figure 2.4, from data of Abbott & Francis (1977). Each of the routines was used to calculate particle trajectories using the same random number sequence. The calculations performed and the durations of the calculations are shown in Table 5.1. The routines were initially called with a value of TOL equal to 6, that is an accuracy of 6 decimal places. For this condition the Runge-Kutta-Merson routine gave the fastest calculation times. However the variable TOL was returned with a negative sign. As noted above, this indicated that the accuracy of the solution could not be guaranteed. The calculations for the Runge-Kutta-Merson method were therefore performed with increasing values of TOL until it ceased to be returned with a negative value, this happened when the value of TOL was set to 11. The calculation times for the Runge-Kutta-Merson method were then slower than those for the Adams routine with a value of TOL equal to 6, for which the variable was returned with a positive value. The routine used in further calculations was therefore the Adams routine, with a value of TOL equal to 6, for which the value of TOL controlled the accuracy of the solution.

As described above the accuracy of the solution calculated with a value of TOL can be checked by performing a calculation with the value of TOL increased by one and comparing the results. A calculation performed with the value of TOL increased by one from, 6 to 7, gave calculated particle positions at each timestep that agreed for the first 7 decimal places. This behaviour continued until at least the first impact. The effect of the difference in the values in the calculated decimals below the 7th decimal

Transport stage	Runge-Kutta-Merson routine D02BHF	Adams routine D02CHF
1.521	12.1 seconds TOL = 6 67.2 seconds TOL = 11	32.2 seconds TOL = 6
1.900	9.6 seconds TOL = 6 31.4 seconds TOL = 11	32.2 seconds TOL = 6
2.506	10.9 seconds TOL = 6 58.3 seconds TOL = 11	32.5 seconds TOL = 6

Compiled with FORTRAN 77 compiler on Sequent Symmetry, using compilation flags, nfpa -O3.

Calculations were peformed for 5,000 iterations for a particle initially at rest.

Table 5.1 Comparison of calculation times using different methods of solution

place was then to give slightly different end conditions, position of impact and particle velocity at impact and hence slightly different initial conditions at the start of the next particle trajectory. The result was that the particles followed slightly different diverging trajectories until the next impact, which again differed in position and conditions. After a few impacts the initially similar trajectories had diverged completely, showing a sensitive dependence on initial conditions, a feature of non-linear dynamic systems. An increase in the number of decimal places required in the solution would only slow down, not eliminate, this effect, especially since even using double precision variables only 15 significant figures can be guaranteed in a calculation.

5.3 Sensitivity of results to selection of time intervals

Particle trajectories were calculated for a range of values of Δ, the fraction of the time scales to use for the duration of an iteration, to determine an appropriate value to use in calculations. The time scales used were the particle response time and the Lagrangian integral time scales, as described in Section 4.3.4. In deciding an appropriate value to use, the computation time required had to be balanced against the accuracy of the result, remembering that the model itself is only an approximation. Calculations were made for a single trajectory and for multiple trajectories.

The conditions used for the single trajectory were those of Figure 14 in Abbott & Francis (1977). Their figure shows an observed trajectory at 1/40 second intervals and it can therefore be used to set initial particle position and velocity. The single trajectory comparisons therefore only compare the effect of varying Δ on the non-contact motion of a particle. The calculations were only continued for one saltation since the variation in the trajectory after impact was a function of the impact as well as the particle motion as described at the end of the previous section. The calculations were performed without any turbulent fluctuations, since the turbulent fluctuations were stochastic and their effect would vary from calculation to calculation.

The effect of varying Δ on calculations of particle movement over longer distances, where calculations were continued after the first impact, was also examined. Calculations were performed for the three values of transport stage used to compare the different solution algorithms. Calculations for each set of conditions were performed 500 times, on the Meiko Computing Surface. Each calculation was performed for a particle initially in motion and continued until the particle had covered a fixed distance, which would contain a number of trajectories, saltating and suspended. Large numbers of calculations were performed since turbulent fluctuations were included in the calculation, introducing a stochastic element into the model.

5.3.1 Comparison of single saltation

To compare the effects of the range of values of Δ, calculated particle trajectories, Figure 5.1, and offsets, Figure 5.2, were plotted. The offsets were calculated for each value of Δ with respect to the track calculated with the smallest value of Δ, 0.01. The streamwise and vertical particle positions on the trajectory calculated with $\Delta = 0.01$ were calculated at the times for which solutions had been calculated for other values of Δ. The values were calculated using linear interpolation, the offsets were then calculated. The magnitudes of the offsets are shown as percentages of the saltation length.

The calculated particle trajectories, Figure 5.1, show that the basic form of the saltation was reproduced for all the values of Δ for which calculations were performed (0.01 to 0.5). The calculation with $\Delta = 0.5$ only took 5 steps to reproduce the experimental trajectory, for shorter and lower trajectories this number would be reduced, eventually falling to 2, one rising, one falling step. This would not be a good representation of a saltation and would be likely to give large errors over a number of saltations. The calculated offsets, expressed as a percentage of the length of the saltation, show the offset for $\Delta = 0.5$ rising to ~1.5%, though the final offset of the trajectory would be constrained by the bed form limiting the possible impact positions.

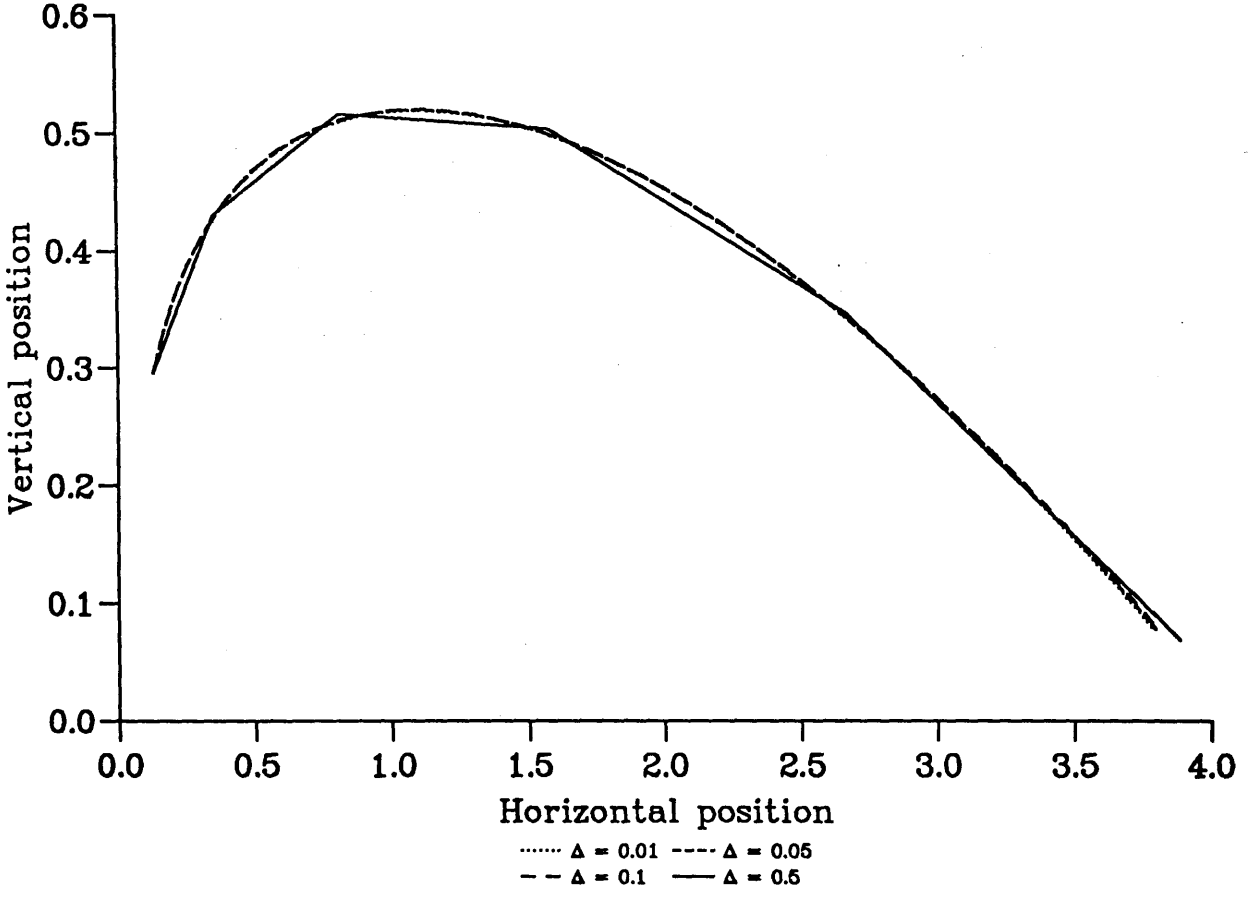

Figure 5.1 Calculated particle trajectories

Units non-dimensionalised with respect to flow depth

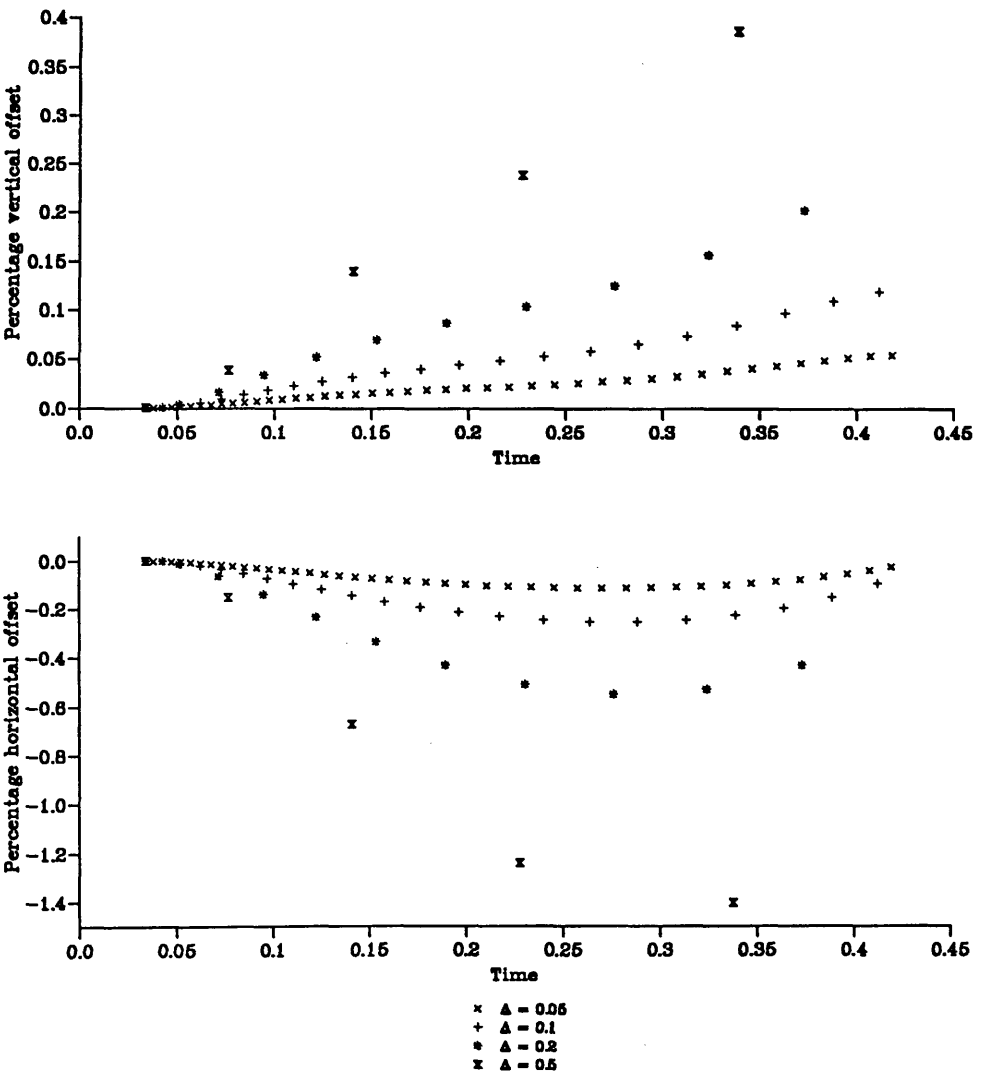

Figure 5.2 Percentage particle offsets

Offsets calculated with respect to particle positions for Δ = 0.01
Offsets calculated as percentages of saltation length
Units non-dimensionalised with respect to flow depth and mean bed shear velocity

Over a single saltation the offsets remain small, constrained by the initially specified conditions and the bed limiting possible impact positions. The effect of different values of Δ on calculated particle movements over longer distances, containing more than one trajectory, where errors due to failure to reproduce trajectories can increase is examined in the next section.

5.3.2 Comparison of particle tracks containing multiple saltations

The calculations of tracks containing multiple trajectories were performed for a similar range of values of Δ from 0.01 to 0.5. For each calculated particle track the means of the particle velocity, lengths and maximum height of saltations and suspensions were calculated. Though suspended particle movements occurred their incidence was low but the results are shown to compare with those of pure saltation. The mean values of the maximum heights and lengths of saltations and suspensions for each track are shown in Figure 5.3. The plot for the saltation values show a linear relation and therefore in other comparisons only the lengths are used. The plot for the suspended values shows a greater scatter, this is due to the low number of tracks containing suspensions. Both the number of tracks containing suspensions and the number of suspensions within those tracks that do was small, so that sufficient values to calculate a representative mean may not be available from a total of 500 calculated particle tracks.

The variation of the mean values of particle velocity and saltation length for all the calculated tracks are shown in Figure 5.4, a, b. The results at each transport stage for each calculated quantity are normalised by the value of that quantity calculated with Δ=0.01. These show that the values converge with decreasing Δ. Below Δ=0.1 the difference is less than 1% for both particle velocity and saltation length. The values for the suspended trajectory lengths and the number of suspensions occurring are shown in Figure 5.4, c, d. The length of the suspensions show a basically converging behaviour, the scatter, particularly for a transport stage of 1.5, being due to the number of values

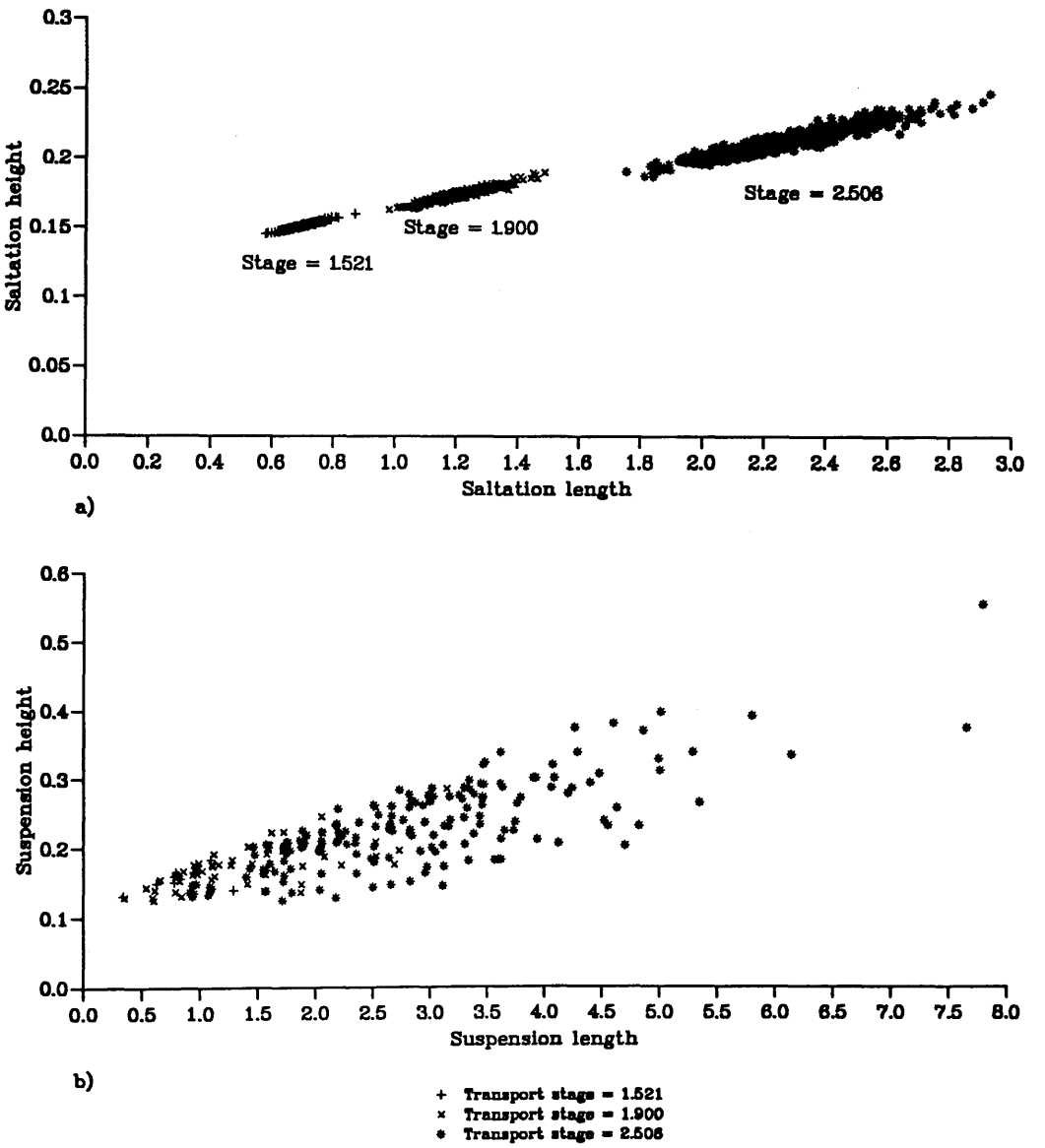

Figure 5.3 Trajectory heights vs. Trajectory lengths

Units non-dimensionalised with respect to flow depth

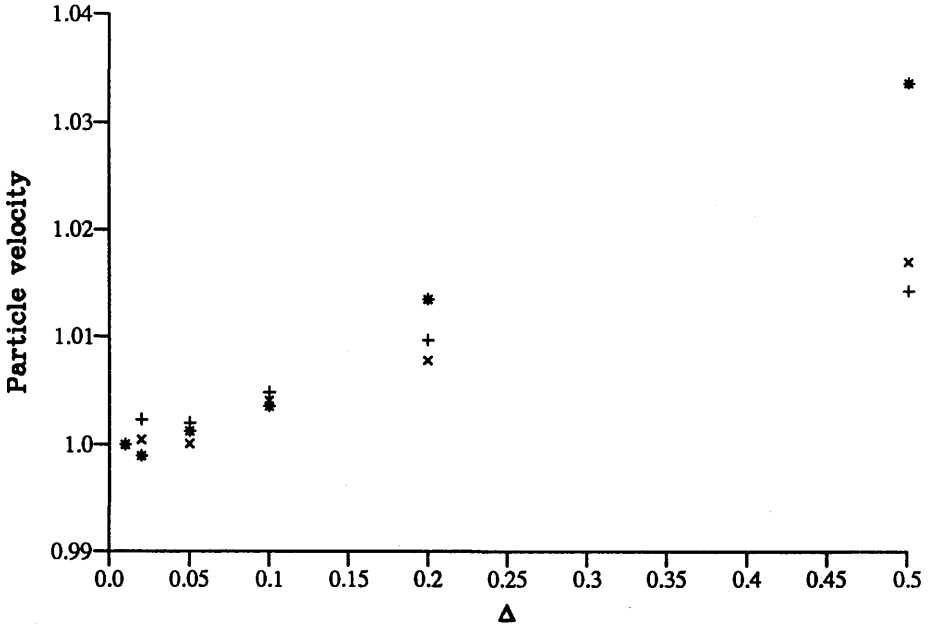

a) Particle velocity

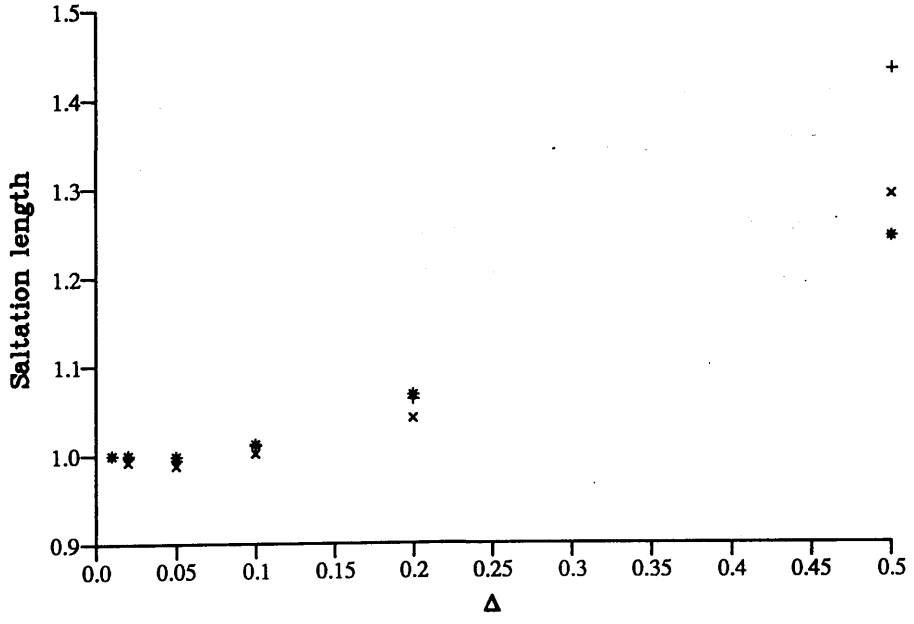

b) Saltation length

Stage = 1.521 +

Stage = 1.900 ×

Stage = 2.506 *

Figure 5.4 Effect of using different values of Δ in calculations
Quantities are normalised by calculated value for Δ = 0.01

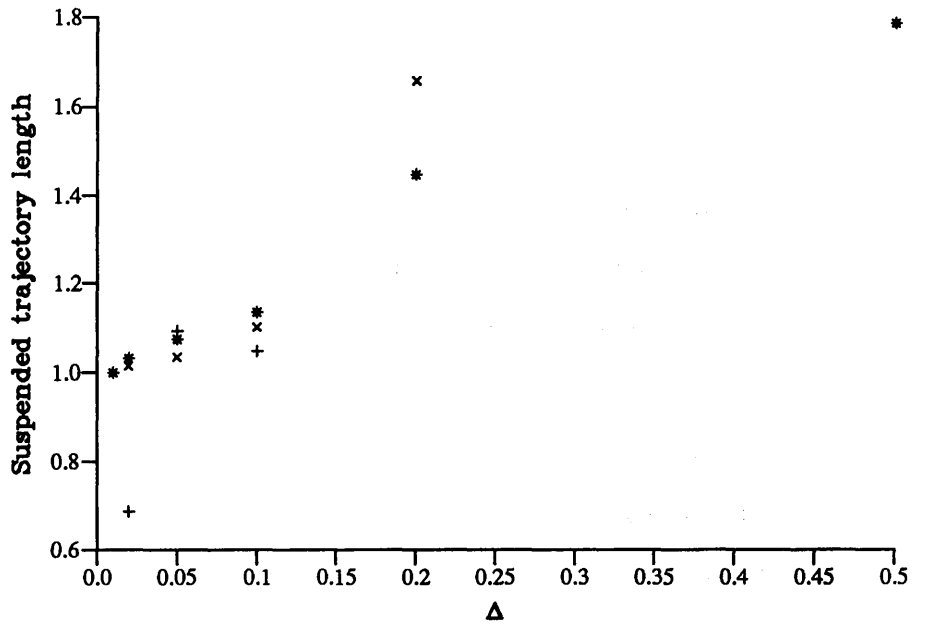

c) Suspended trajectory length

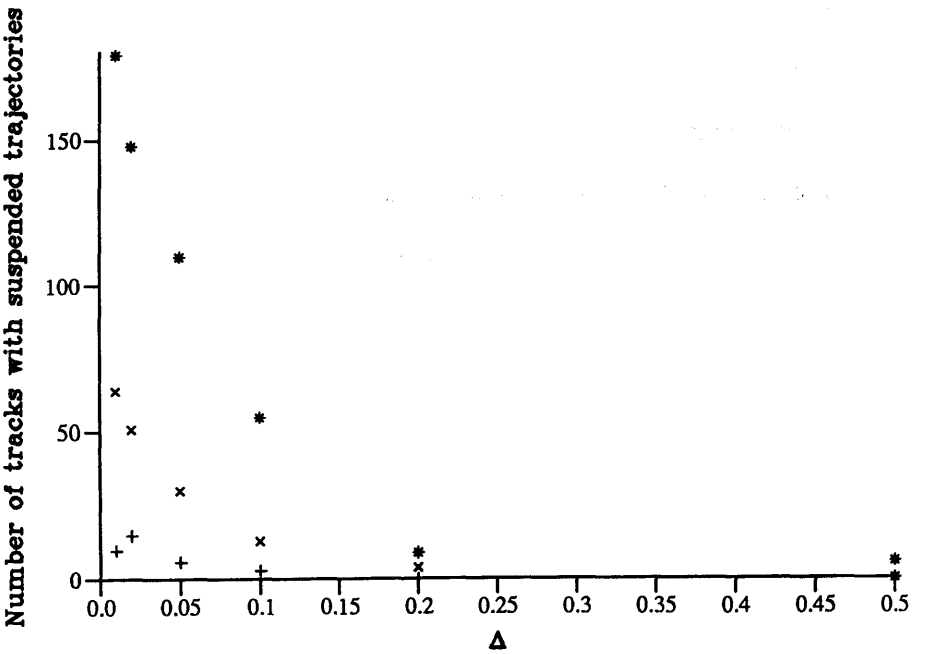

d) Number of tracks with suspensions

from which the mean was calculated. The number of suspensions shows an increasing trend with decreasing values of Δ, Figure 5.4d. This is a result of the duration of timesteps used in the calculations and the method of determining whether a particular trajectory was suspended. The definition of whether a trajectory was suspended was that it contained an upward vertical acceleration, after contact with the bed had been lost. Since the particles were in motion at the start of the distance over which their behaviour was analysed this excluded the possibility of any upward acceleration due to the initiation of motion being present. To allow comparison of the trajectories calculated using different values of Δ, and hence timesteps, all the calculations were compared to a reference time interval. The value of vertical acceleration used in this comparison at a time was the calculated average value for the timestep in which the comparison was made. Since the response to a change of conditions diminished with time the longer a timestep lasted the more likely the effect of gravity was to predominate giving an overall downward vertical acceleration. The result of this was that trajectories calculated with larger values of Δ were less likely to be suspended, giving the result shown in Figure 5.4d.

5.3.3 Values of Δ to use in calculations

Though the calculations of single trajectories showed small differences of ~1% even for a value of Δ of 0.5 the calculations for multiple trajectories showed large differences with increasing values of Δ. The use of a value of Δ of 0.1 in the calculations reduced any error due to the size of step used to ~1%, doubling this to a value of 0.2 would increase the error on saltation lengths to up to 5% for approximately half the computation time. The use of a value for Δ of 0.1 would therefore seem to be a reasonable compromise between accuracy and computation time.

5.4 Effect of different models of turbulence

The calculations described in the previous sections were all performed with uncorrelated random fluctuations in velocity in the vertical and horizontal direction, the simplest model including velocity fluctuations. In this section the results of calculations performed with no fluctuations are compared with the different levels of complexity in the velocity perturbation model described in Section 4.2.2. The calculations were performed for a particle initially in motion, for the same transport stages as used in previous calculations. At a transport stage of 1.5 the turbulent timescales were typically, horizontal 0.74 (0.8 seconds), vertical 0.48 (0.5 seconds) while the horizontal length scale was 1.07 (0.05m). At each transport stage four calculations were performed: no fluctuations, random fluctuations, correlated fluctuations and structured fluctuations. The values of the parameters used to described these different models are those of Section 4.2.2. The results of the calculations were analysed to produce the same variables as in the previous section. The results are plotted as absolute values in Figure 5.5 and normalised by the values from the calculations without fluctuations in Figure 5.6.

5.4.1 Comparison of different models of turbulence

The results in Figure 5.6 show an increase in the all the calculated quantities when the effects of turbulent fluctuations are included. As well as causing suspended trajectories the introduction of fluctuations also increased the lengths of saltations. The lengths of saltations were increased because of the definition used for suspended trajectories. A particle trajectory was defined as suspended if there was an upward vertical acceleration of the particle between contacts with the bed, the only mechanism that could cause this was turbulent fluctuations. It is possible for a particle to experience an upward vertical acceleration due to a turbulent fluctuation without the effect being sufficient to overcome the acceleration due to gravity, so the particle acceleration remains downward. The effect this has on the particle trajectory is to increase the length of the saltation without the particle ever experiencing an upward

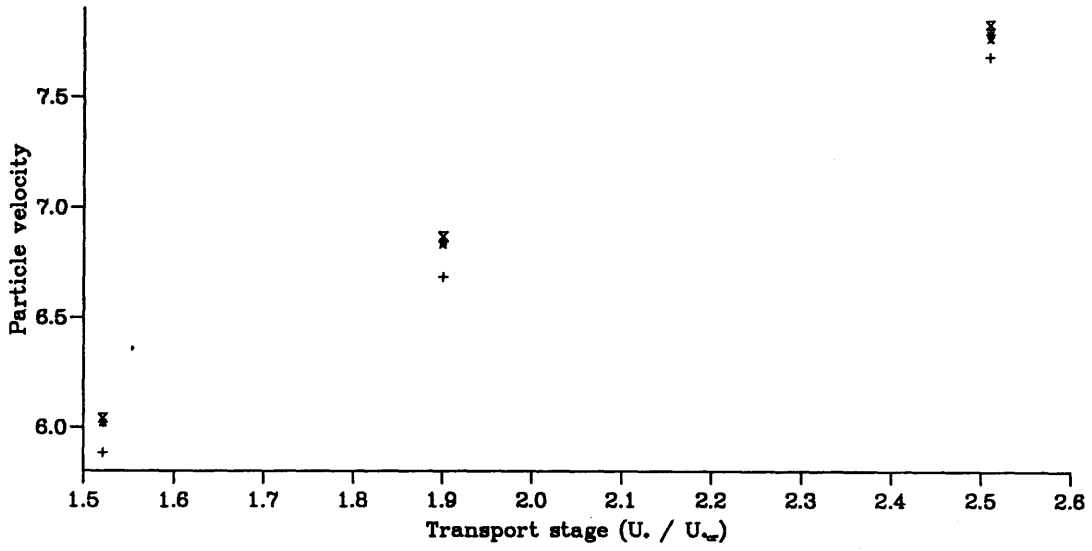

a) Mean particle velocity

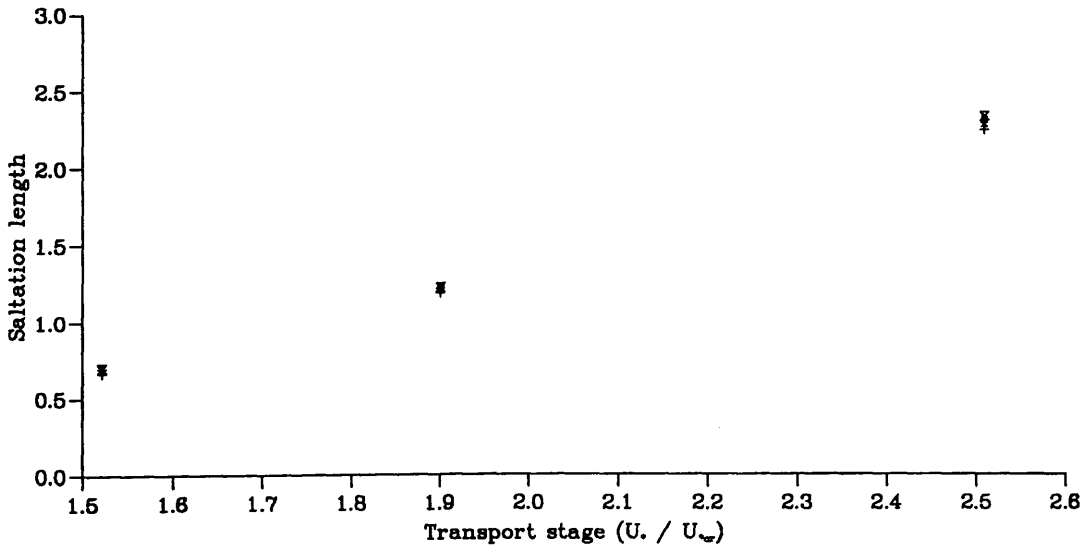

b) Saltation length

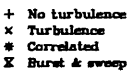

Figure 5.5 Comparison of different models of turbulence
Units non-dimensionalised with respect to flow depth and mean bed shear velocity

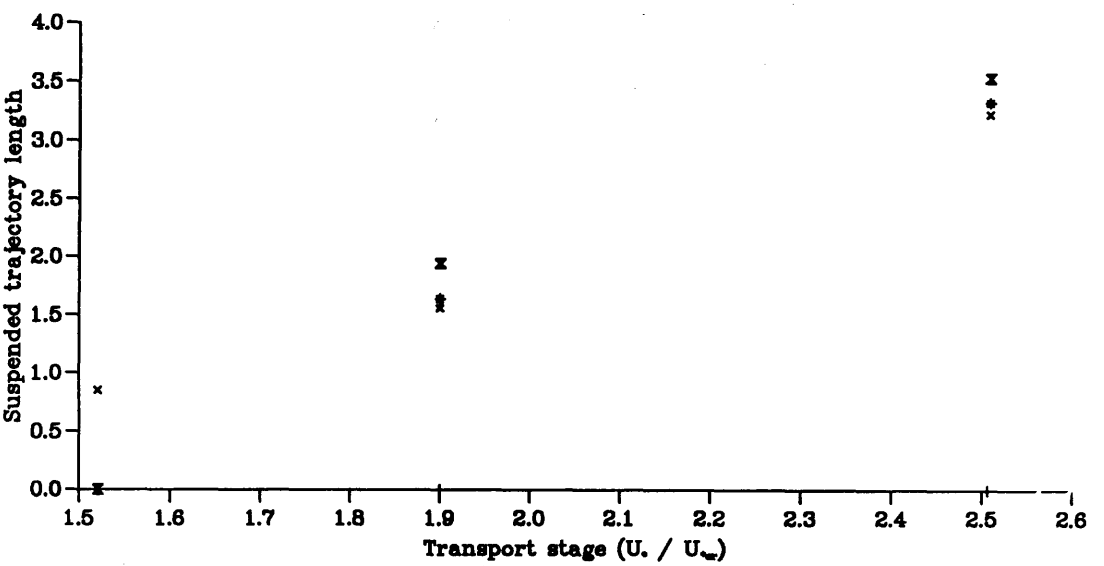

c) Suspended trajectory length

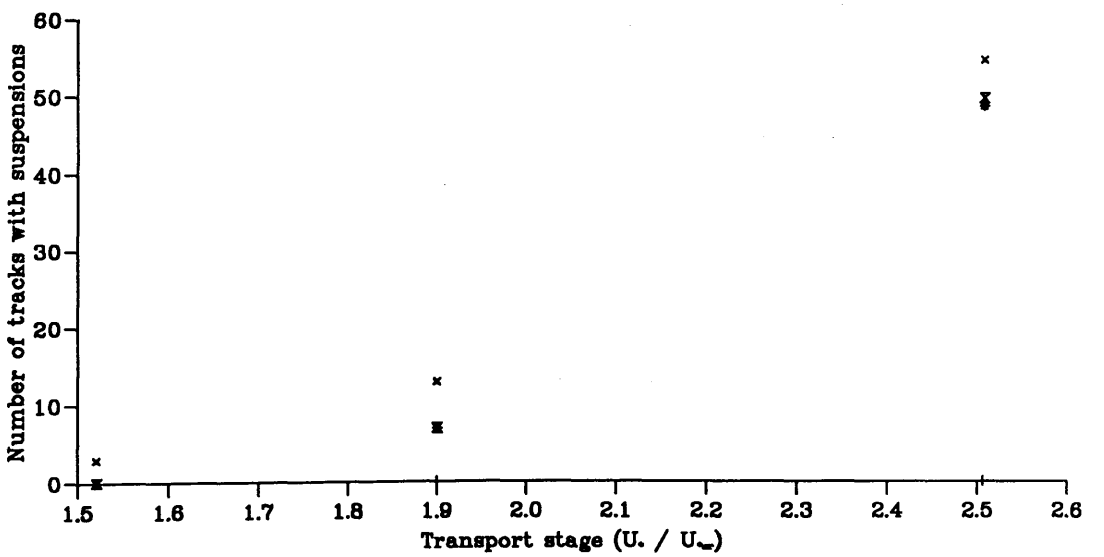

d) Number of tracks with suspensions

+ No turbulence
× Turbulence
✱ Correlated
⧗ Burst & sweep

Units non-dimensionalised with respect to flow depth

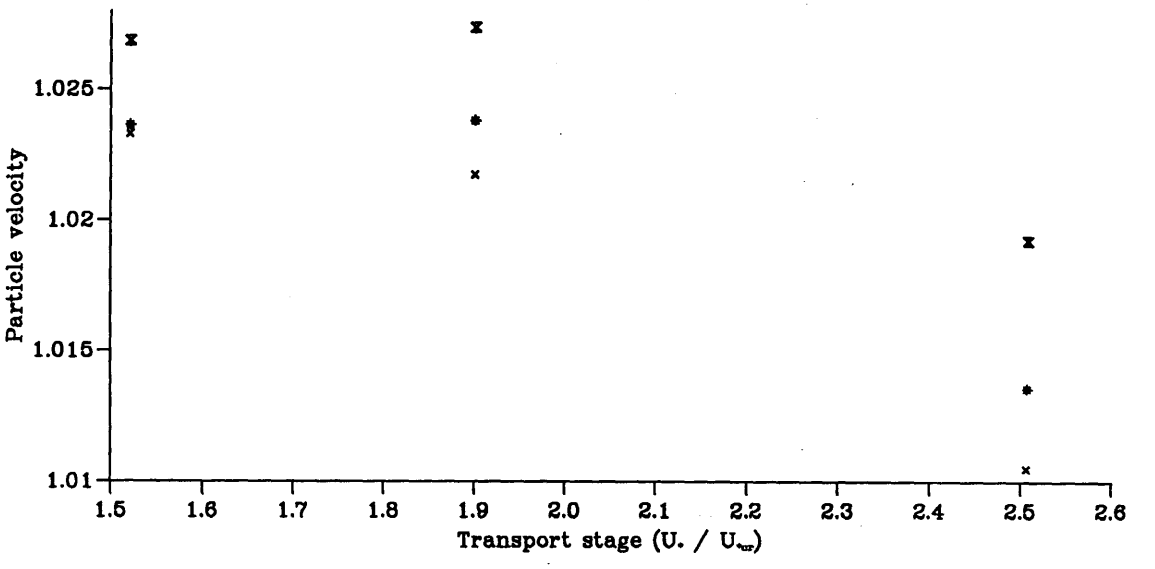

a) Mean particle velocity

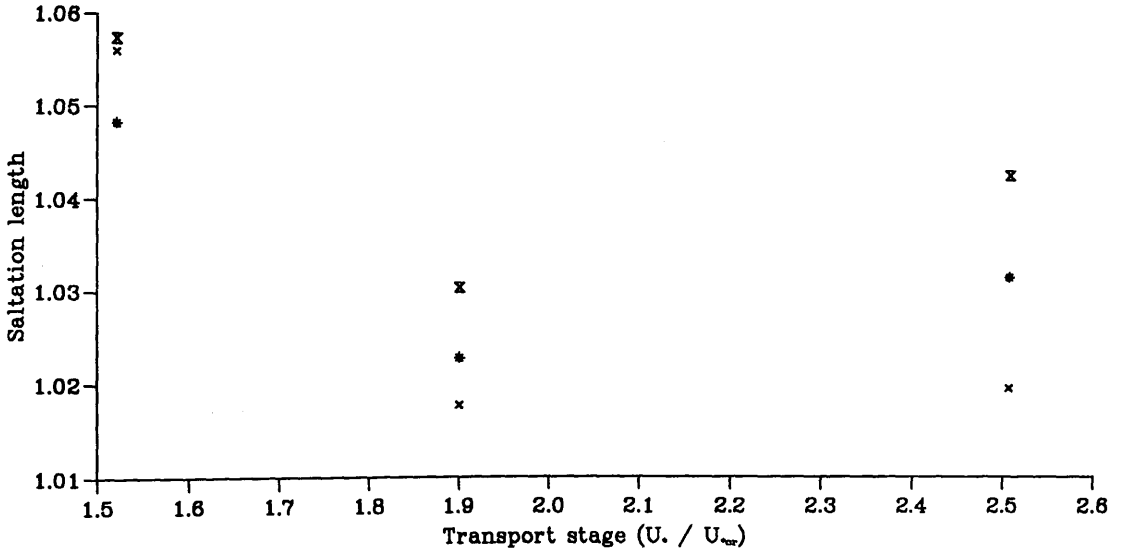

b) Saltation length

× Turbulence
✱ Correlated
⧗ Burst & sweep

Figure 5.6 Normalised comparison of different models of turbulence
Units normalised by value with no turbulence

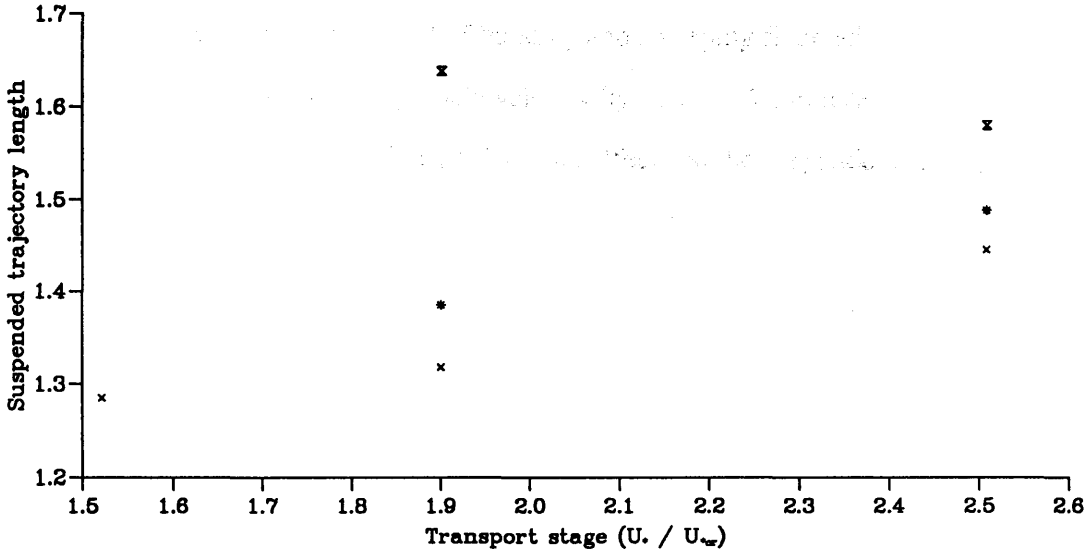

c) Suspended trajectory length

× Turbulence
* Correlated
⧗ Burst & sweep

Units normalised by value for saltations

vertical acceleration between impacts. The mean saltation length can therefore be larger for calculations including velocity fluctuations than for those that do not include velocity fluctuations.

The results show the model of bursting and sweeping fluctuations to have most effect on the values, increasing particle velocity by up to 2.5%, Figure 5.6a, and saltation length by up to 6%, Figure 5.6b. The effects on the suspended trajectories (normalised by the saltation length calculated with no fluctuations) increase by a maximum of 60%, Figure 5.6c. Though suspended trajectories did occur in tracks, Figure 5.5d, they did not occur in all tracks and the number of suspended trajectories in any track was low.

The inclusion of fluctuations in the model can be seen to affect the calculated behaviour of particles, particularly when a burst-sweep model of fluctuations is used, this model was therefore retained in other calculations.

5.4.2 Influence of fluctuations on particle tracks

The influence of turbulence on particle tracks, in particular the effect of moving from eddy to eddy can be seen if the vertical position of the particle is plotted against time, Figure 5.7. This shows one trajectory where the ascending limb of a trajectory is modified by an eddy and another where the descending limb of a saltation is interrupted by an eddy before the trajectory returns to the normal behaviour on the descending limb of a saltation, this type of behaviour for real particles can be seen in Figure 16 of Abbott & Francis (1977).

5.4.3 Influence of fluctuations on initiation of motion

Turbulent fluctuations can affect the initiation of motion of particles as well as the trajectory of particles once in motion. Since the previous calculations were performed for particles initially in motion any effects of turbulent fluctuations on initial

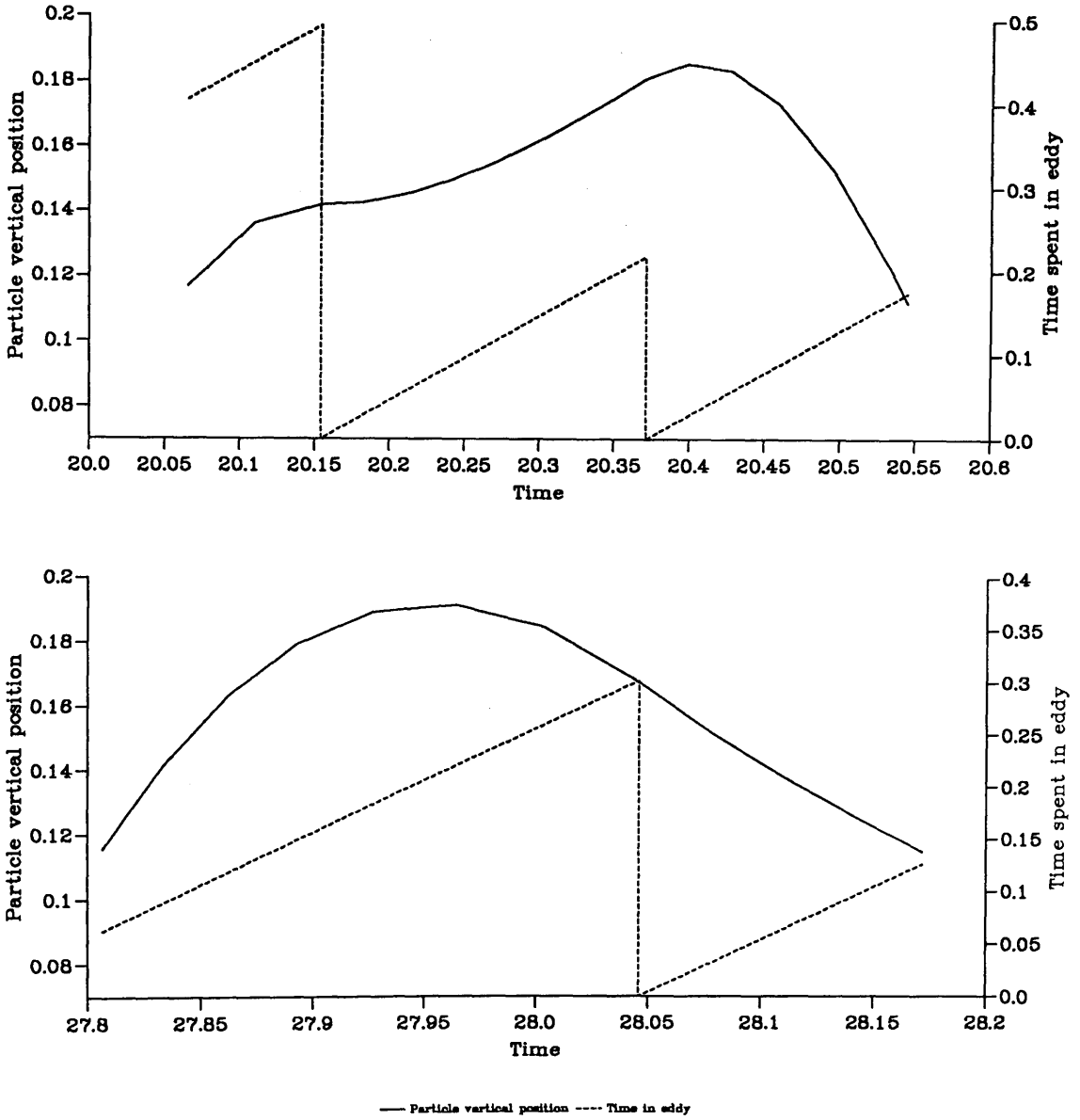

Figure 5.7 Vertical particle position through time for suspended trajectories
Transport stage = 2.742, particle density = 1.24

Units are non–dimensionalised with respect to flow depth, mean bed shear velocity and fluid density

motion were not included. To demonstrate the influence that turbulent fluctuations could have on the initiation of motion of particles the fractions of particles entrained after one iteration were calculated. The calculations were performed for a range of heights within the bed, using the burst-sweep model of turbulent fluctuations, at two different transport stages. The resulting distributions of fraction of particles entrained for four different heights within the bed are shown in Figure 5.8. The initial particle heights were uniformly distributed within these intervals.

The fraction of particles entrained with a flow including turbulent velocity fluctuations shows a gradual increase with increasing height; that without fluctuations a single step change from some particles entrained to all particles entrained, Figure 5.8. In these calculations a single size of sphere rested between two spheres of equal size, with their centres at the same height. For the calculations with no velocity fluctuations the only variable was the height of the particle, as this increased the mean flow velocity and fluid forces acting increased, until they were sufficient to entrain the particle. Above this height all the particles were entrained, below it none. For both transport stages this height was in the bottom height interval, though higher for a transport stage of one. With the calculations including turbulent velocity fluctuations the velocity at a height could vary. Thus, higher in the flow a particle might not be entrained immediately, while lower in the flow a particle might still be entrained when the mean velocity was below that for entrainment, as can be seen comparing the fraction entrained in the lowest height interval for a transport stage of one.

5.5 Effect of varying parameters and terms

For a number of the components of the model described in the previous chapter either their importance on the overall behaviour of the model was not obvious or they were identified as being ill defined. The results of leaving out a term completely was examined for the fluid acceleration term. The effect of varying the parameters used to define the lift force and impact process components are examined by calculations

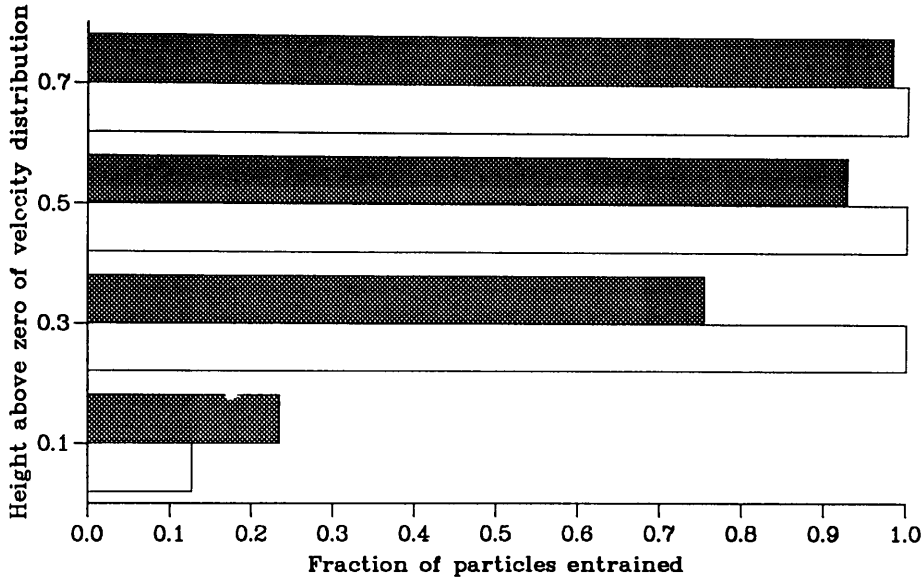

a) Transport stage (U_* / U_{*cr}) = 1.0

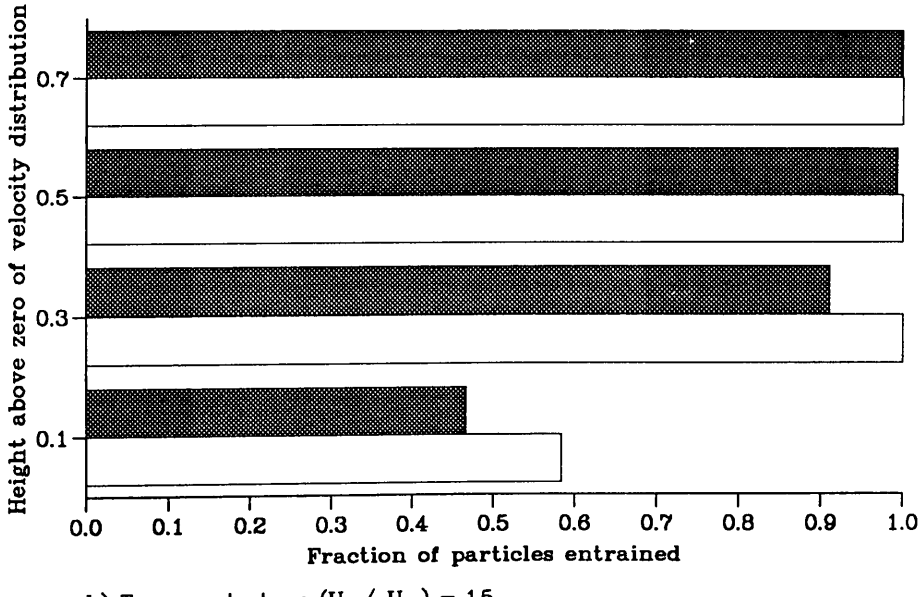

b) Transport stage (U_* / U_{*cr}) = 1.5

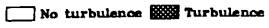

Figure 5.8 Effects of turbulent fluctuations on initial motion

Units non–dimensionalised with respect to bed particle diameter

across a range of parameter values. The final calculations examine the effects of varying the length scale of the turbulent fluctuations used in the model to see whether an improved fit between observed and calculated behaviour could be obtained.

5.5.1 Fluid acceleration term

The equations of particle motion include a number of different terms of which those due to fluid acceleration and the lift force have not been included in some calculations of particle movement, Sekine & Kikkawa (1992) determined by numerical experiment for their model that the combined effects of these terms were small, though neither the exact meaning of small or the values used for the coefficients of lift and added mass were stated. By contrast Wiberg & Smith (1985) preserved both lift force and added mass terms in their calculations. The decision as to whether to include these terms depends on the model and the values assigned to these forces. The results of calculations performed with and without the fluid acceleration term for the model used in this study are examined here, the effect of varying lift force in the next section. Calculations were performed with and without this term across a range of values of Δ. A range of values was used to ensure that the differences seen were not the result of different rates of convergence between calculations with and without the fluid acceleration term. The calculated values of particle velocity and saltation length are shown in Figure 5.9, normalised by the values calculated with the fluid acceleration term with Δ=0.01. These results show considerable differences if the term is included, up to 25% for the saltation length, the fluid acceleration term was therefore retained in further calculations.

5.5.2 Variation of lift and impact parameters

To perform a calculation all the parameters in the model had to be assigned values. Initial values for parameters were set based on data from the literature as described in Section 4.3.2. In two cases, lift force on a particle due to the flow and the

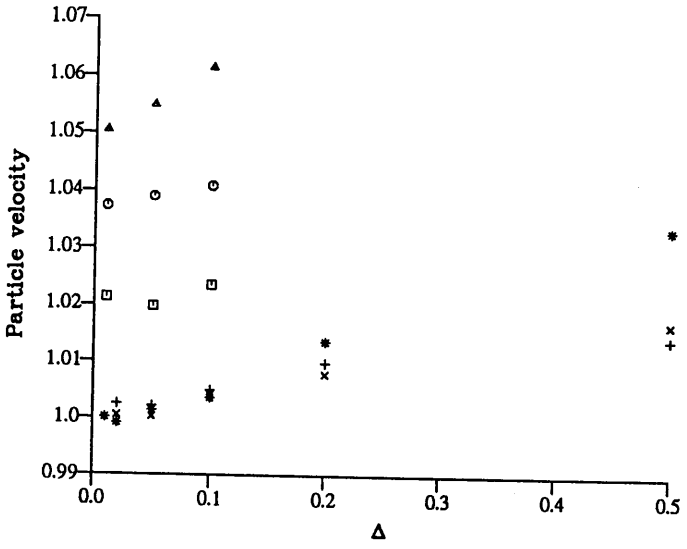

a) Particle velocity

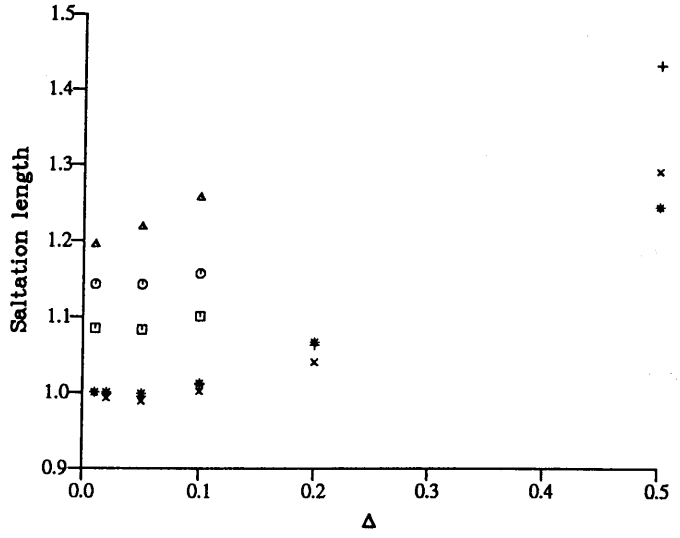

b) Saltation length

	With term	Without term
Stage = 1.521	+	□
Stage = 1.900	×	○
Stage = 2.506	✱	△

Figure 5.9 Effect of using different values of Δ in calculations
and of the inclusion of the force term due to fluid acceleration
Quantities are normalised by calculated value for Δ = 0.01 for the
calculation including fluid acceleration term

impact process, the process and the values of parameters describing the process are not well defined. The effect of this uncertainty in the models of these processes will be examined by performing calculations using a range of parameter values and examining the effect on the calculated results.

The effects of varying the lift force acting on particles was investigated by varying the coefficient of lift across the range of observed values. The variation in the lift force away from the wall was varied, using a parameter, n, in an expression:

$$C_L = C_{L0}\left(\frac{0.5}{z/d}\right)^n$$

The value C_{L0} is a value of the coefficient of lift set at a reference height. The ranges of values used are shown in Table 5.2. The calculations were performed both for particles initially at rest and particles initially in motion for each of the values of transport stage used in previous calculations.

The results of varying the impact process were investigated by varying the fractions of tangential (friction) and normal (restitution) velocity conserved after impact, across the ranges shown in Table 5.2. The fractions used were kept constant throughout the calculation of a particle track and were independent of the angle of impact. The calculations of impact were only performed for particles initially in motion, since the impact process is responsible for the continued motion of particles in the fluvial environment, not the initial motion.

The calculations of the effects of varying the lift force and impact process were performed independently. In each calculation the two parameters describing the process were varied, calculations were performed on a regular grid across the range of the parameters. The results were for the calculation of ten particle tracks using the values of the parameters at each grid point. Calculations were performed at each of the three transport stages used in the previous calculations described in this chapter.

Coefficient of lift	0.2 - 0.6
'n'	1.0 - 5.0
Coefficient of friction	0.0 - 1.0
Coefficient of restitution	0.0 - 1.0

Table 5.2 Ranges of parameters used to examine effect of varying parameters.

The aim of these calculations was to examine the effects of uncertainty in the values of the parameters used to describe the lift force and impact process; the results are also used to compare calculated results with observations and to determine appropriate values to use for the parameters. The results of each calculation are presented in contour plots, showing mean particle velocity, saltation length and height. The fluctuations on these plots are due to the sample size used. The quantity plotted has been normalised by the observed value for that quantity from the data of Figures 3, 4 and 12d of Abbott & Francis (1977). Contour plots have been produced for each of the three transport stages and for each set of conditions, that is varying lift force, with or without the particle initially in motion, and varying impact. The results for varying the lift force are shown in Figures 5.10-5.12, for calculations where the particle was initially in motion, and Figures 5.13-5.15, for calculations where the particle was initially at rest. The results for calculations where the parameters describing the impact process were varied are shown in Figures 5.16-5.18. The results for the quantities calculated for suspended trajectories are not plotted, since the model predicts a very low incidence of suspended trajectories and representative values for the mean cannot be calculated for the number of particle tracks calculated.

The effects of varying the lift forces show similar results for particles initially at rest, Figures 5.13-5.15, and for those initially in motion, Figures 5.10-5.12, the results of these calculations will therefore be considered together. The results at the different transport stages all show similar ranges of values with the exception of those for saltation length and height at a transport stage of 2.506, Figure 5.12b, c and Figure 5.15b, c. The results for these quantities at a stage of 2.506 show a much wider range of values and a better fit than those at lower stages. This is a result of the curves in Abbott & Francis (1977) from which the values were taken to normalise these calculated results. The observed behaviour shows a fall in the magnitude of saltation length and height above a transport stage of 2, the calculated results show a monotonic increase, the calculated and observed values are therefore closer together in this region

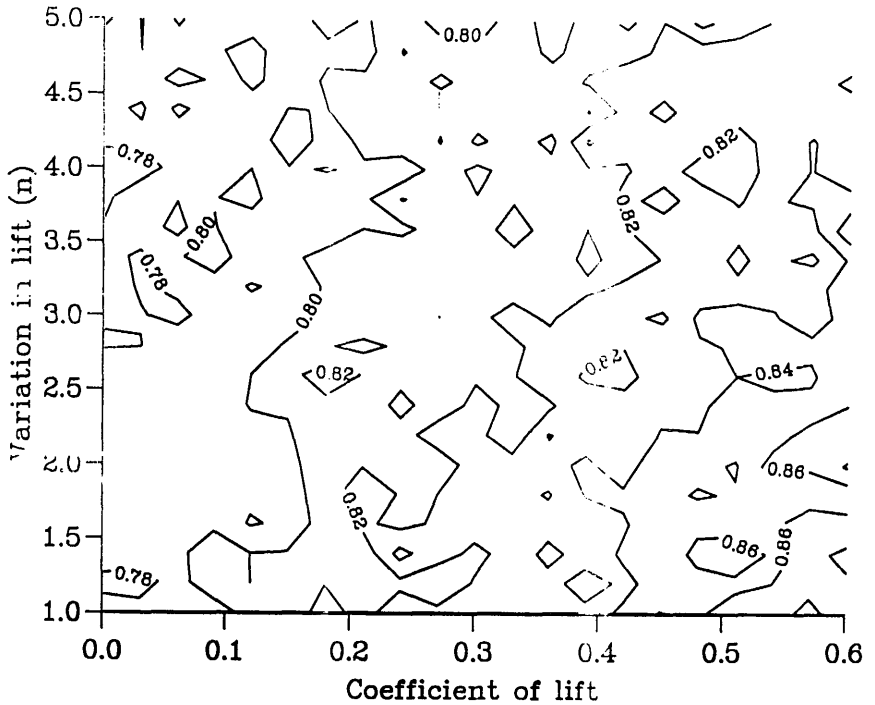

a) Mean particle velocity

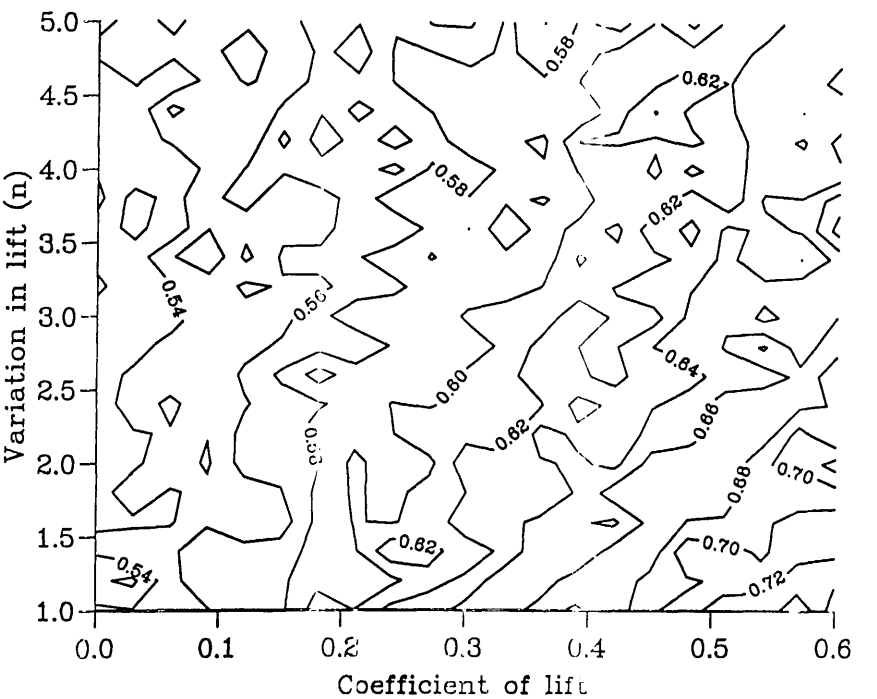

b) Mean saltation length

Figure 5.10 Effect of varying lift force for particle initially in motion, Transport stage = 1.521
Normalised with values from Abbott & Francis (1977)

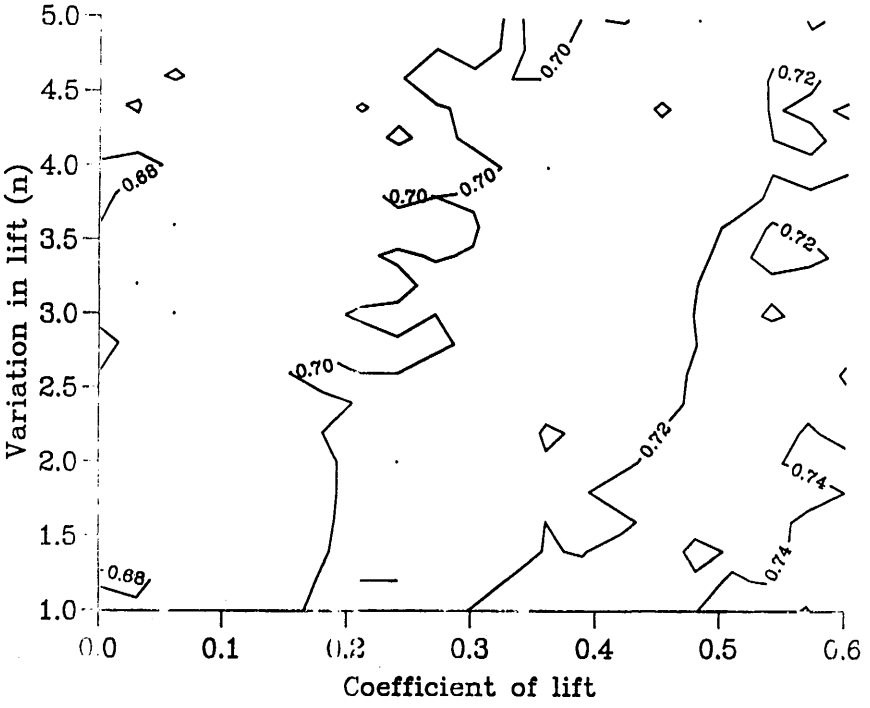

c) Mean maximum saltation height

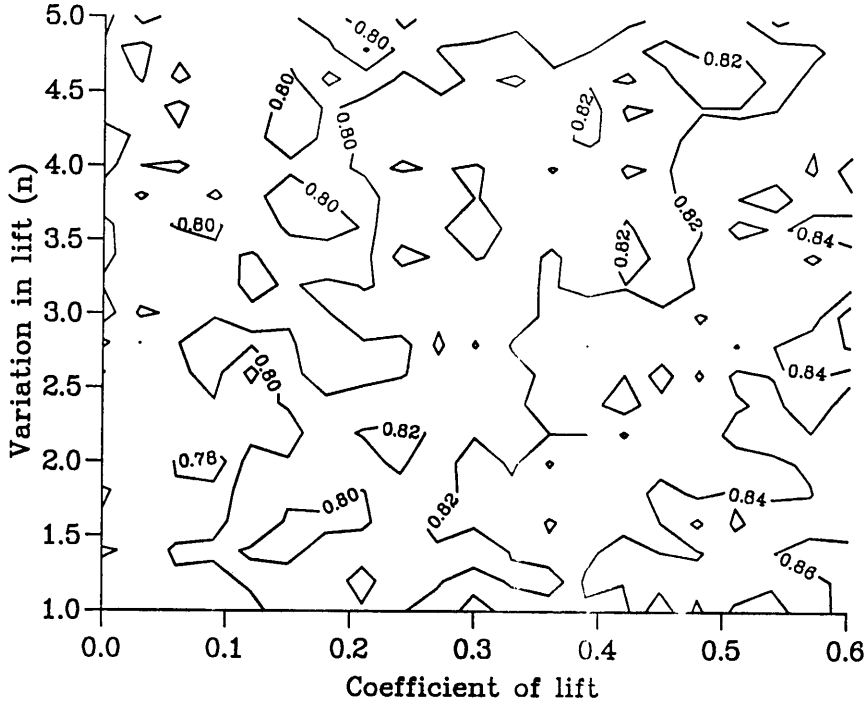

a) Mean particle velocity

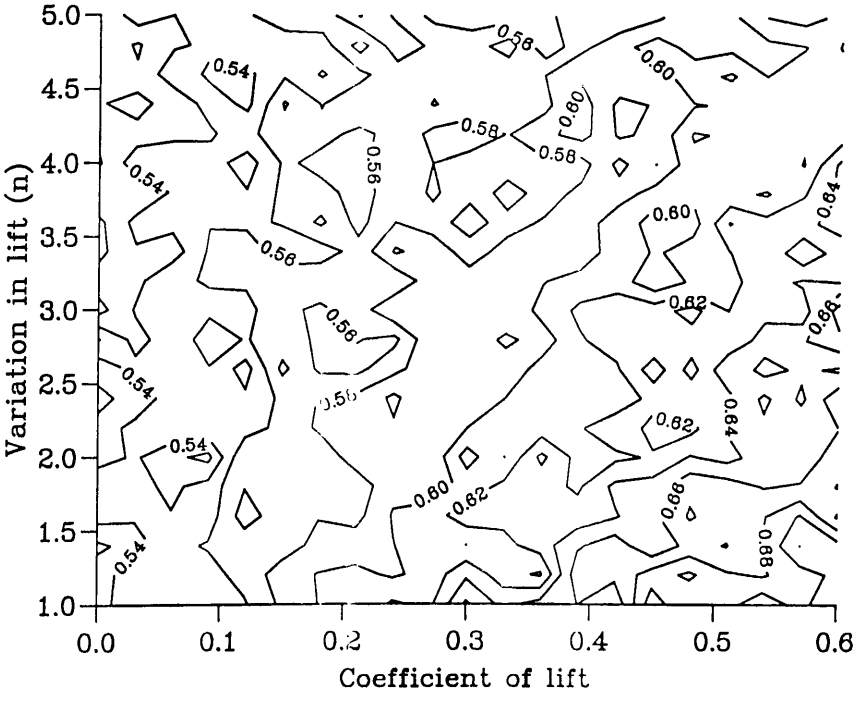

b) Mean saltation length

Figure 5.11 Effect of varying lift force for particle initially in motion, Transport stage = 1.900
Normalised with values from Abbott & Francis (1977)

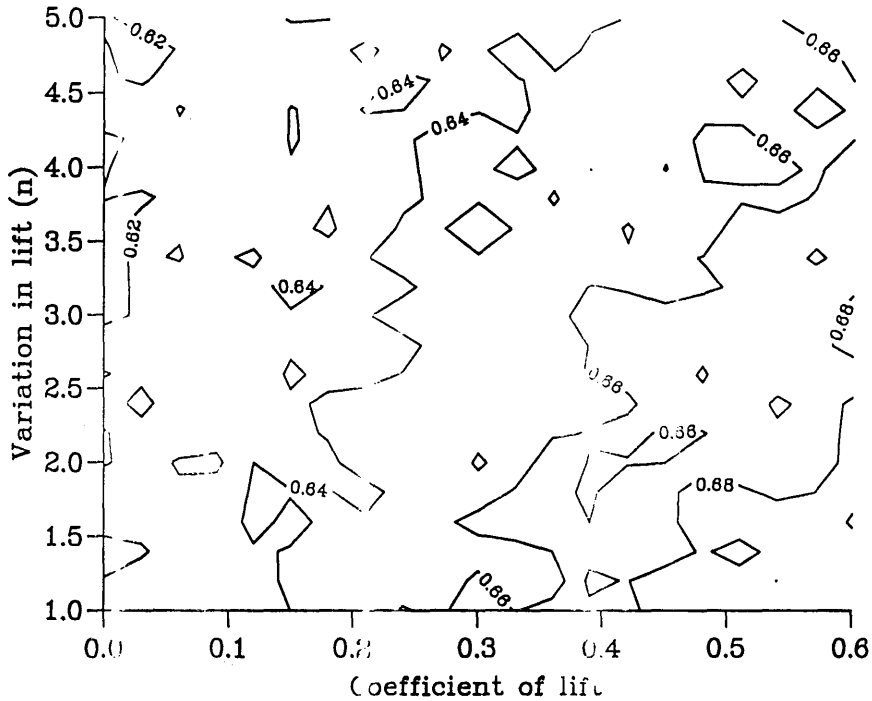

c) Mean maximum saltation height

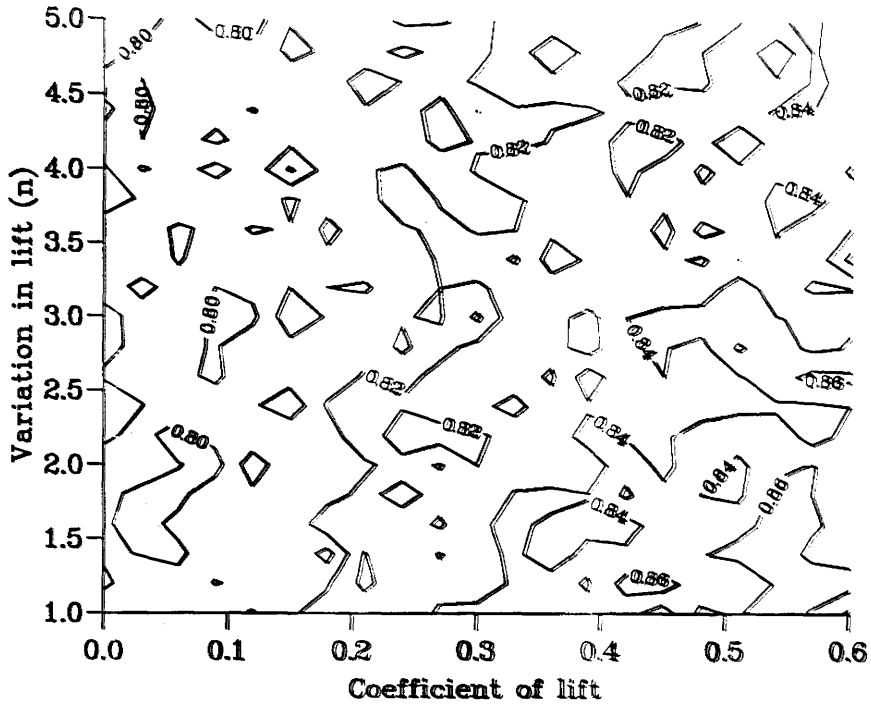

a) Mean particle velocity

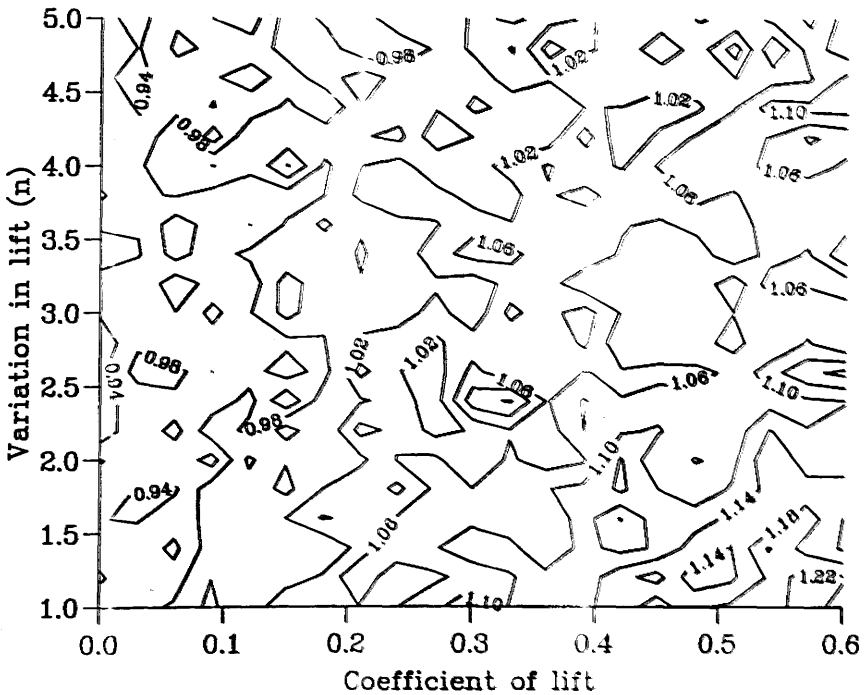

b) Mean saltation length

Figure 5.12 Effect of varying lift force for particle initially in motion. Transport stage = 2.506
Normalised with values from Abbott & Francis (1977)

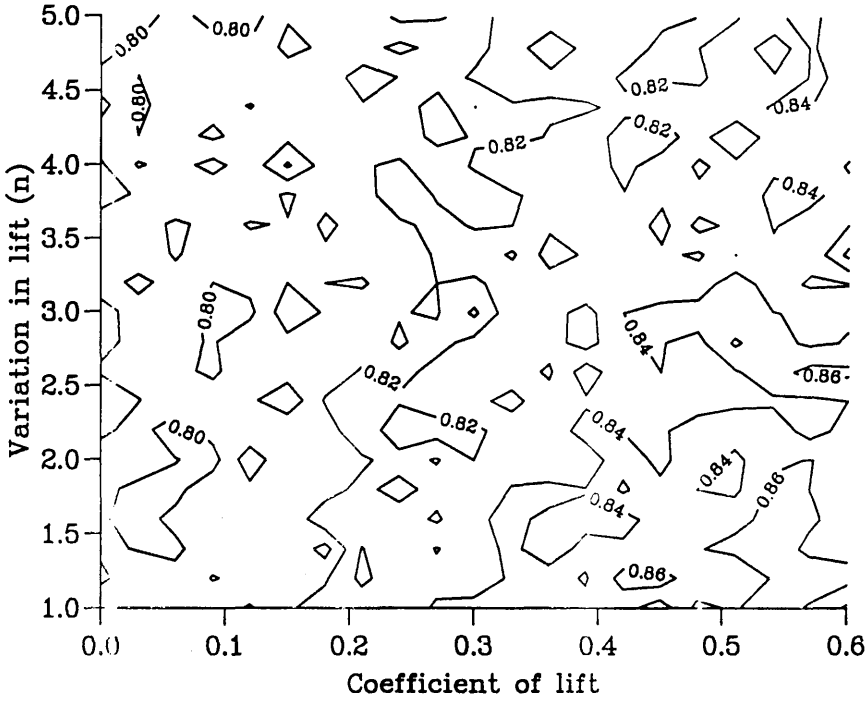

c) Mean maximum saltation height

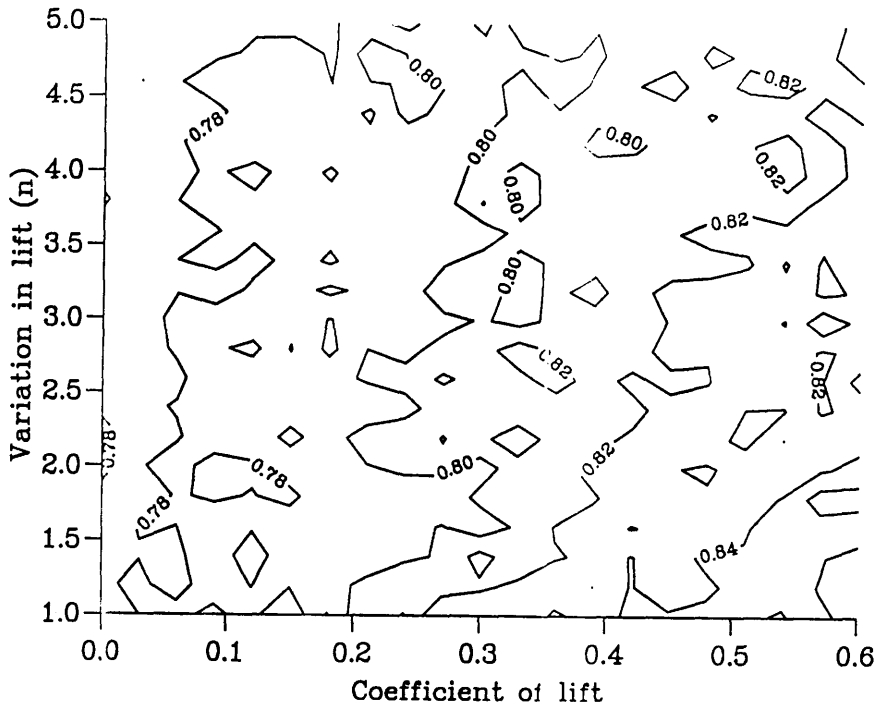

a) Mean particle velocity

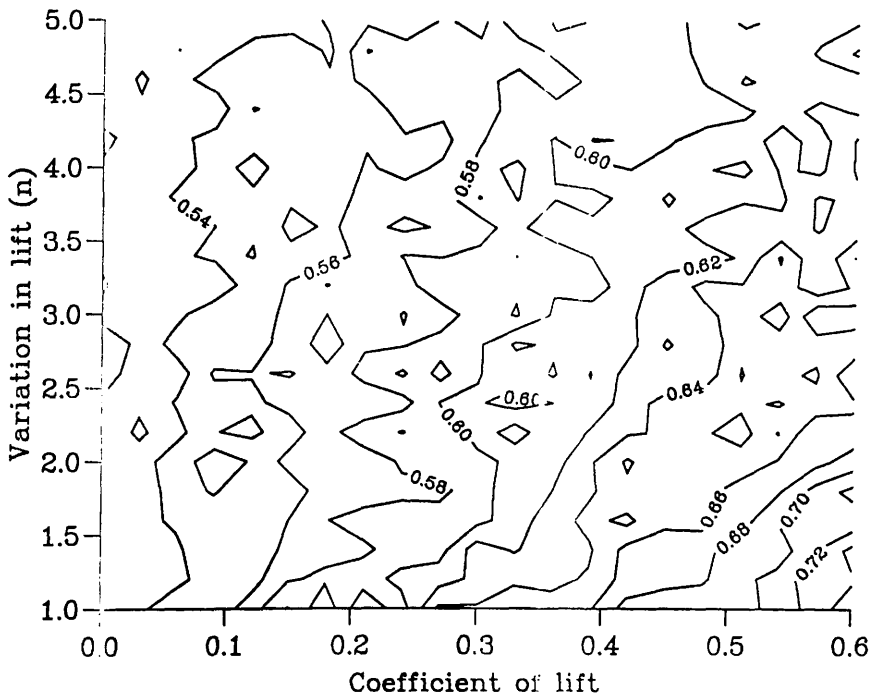

b) Mean saltation length

Figure 5.13 Effect of varying lift force for particle initially at rest. Transport stage = 1.521
Normalised with values from Abbott & Francis (1977)

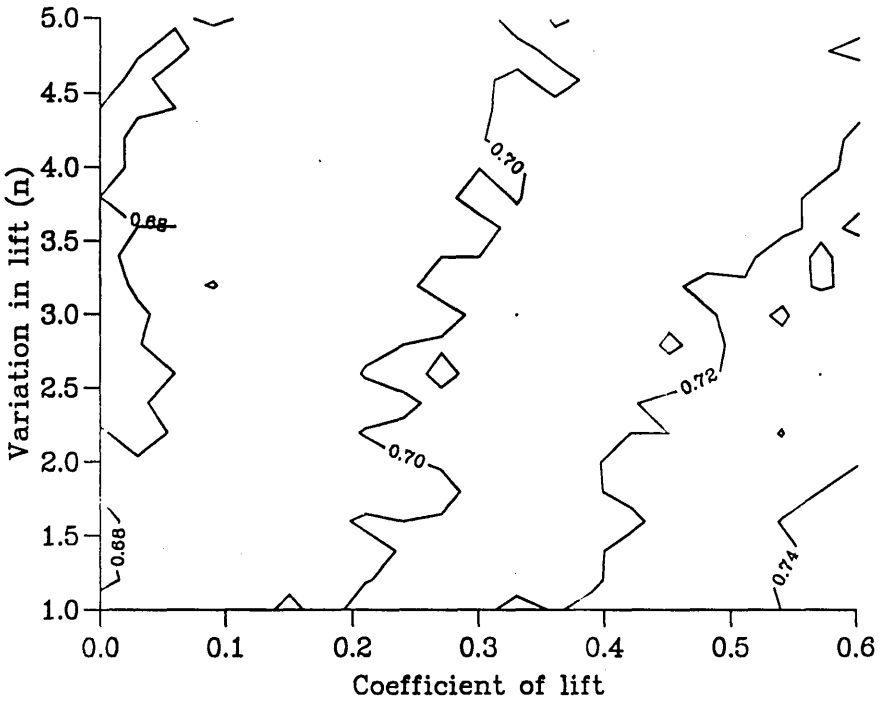

c) Mean maximum saltation height

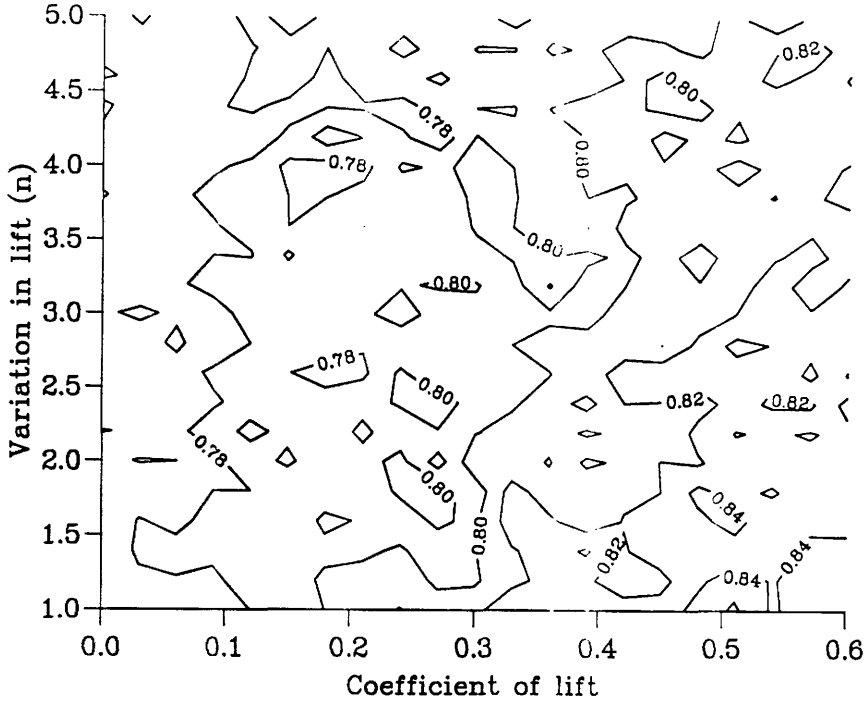

a) Mean particle velocity

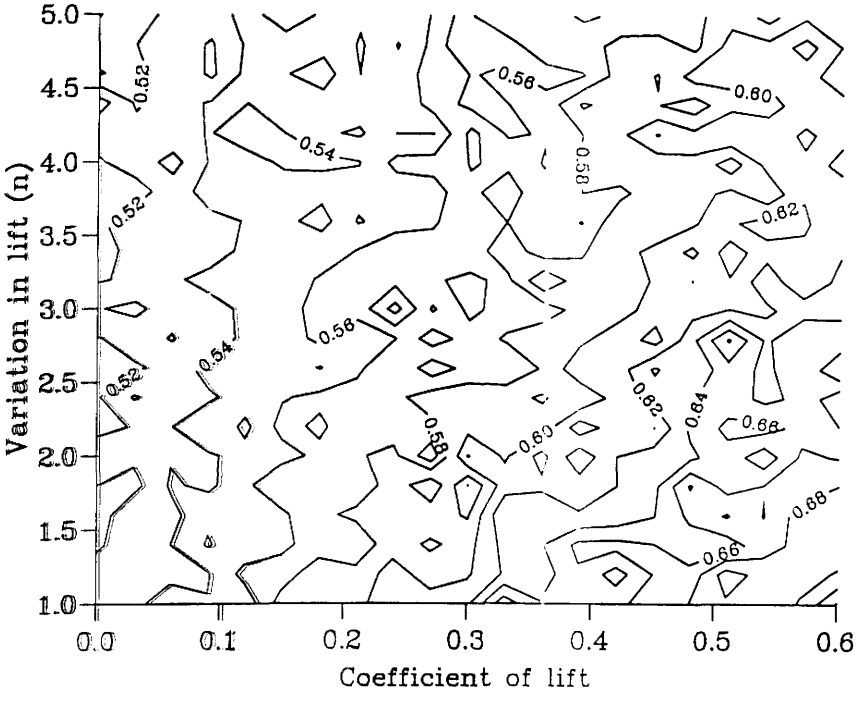

b) Mean saltation length

Figure 5.14 Effect of varying lift force for particle initially at rest. Transport stage = 1.900

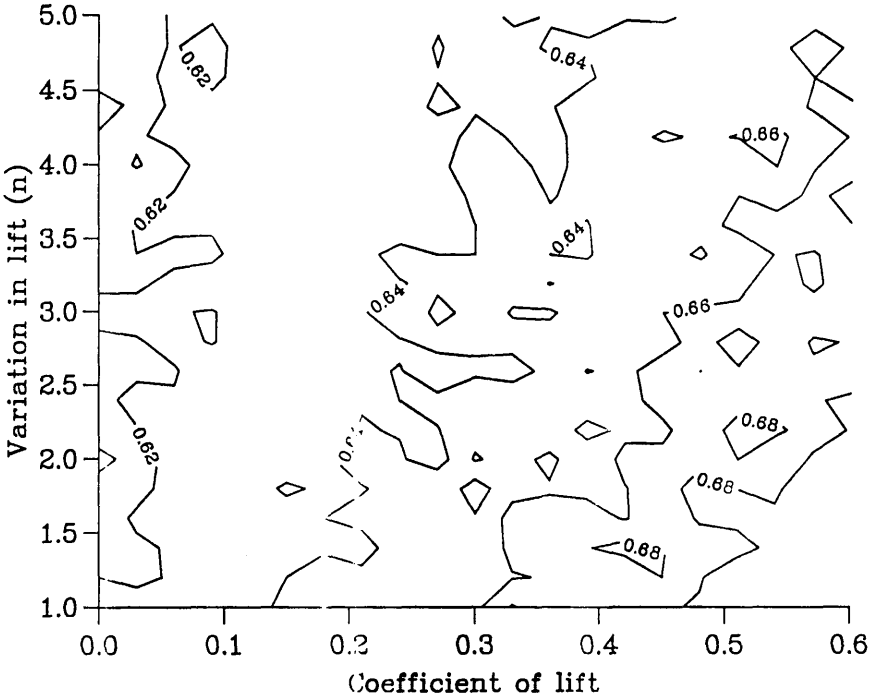

c) Mean maximum saltation height

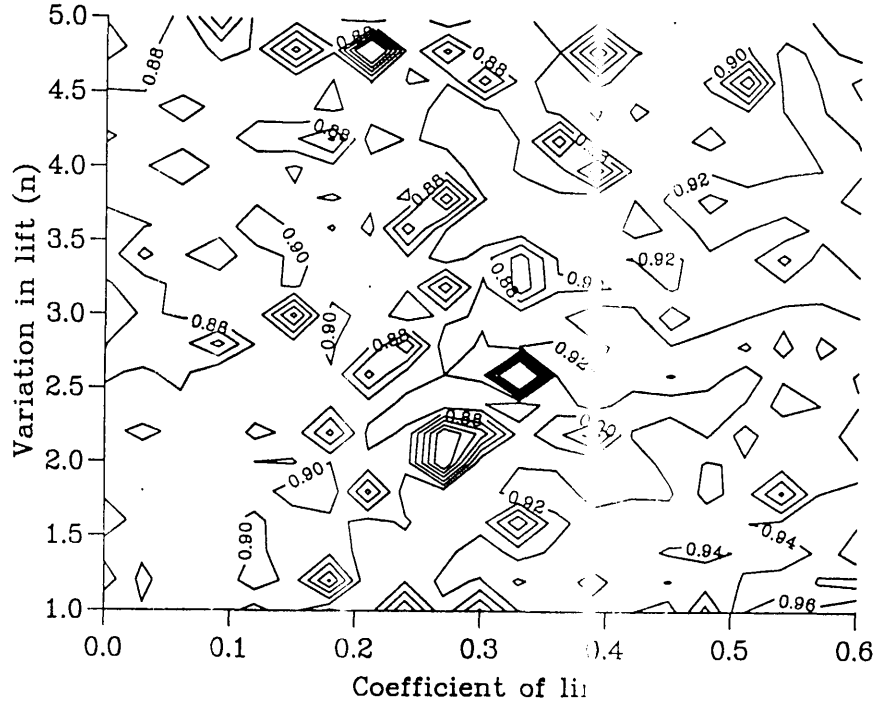

a) Mean particle velocity

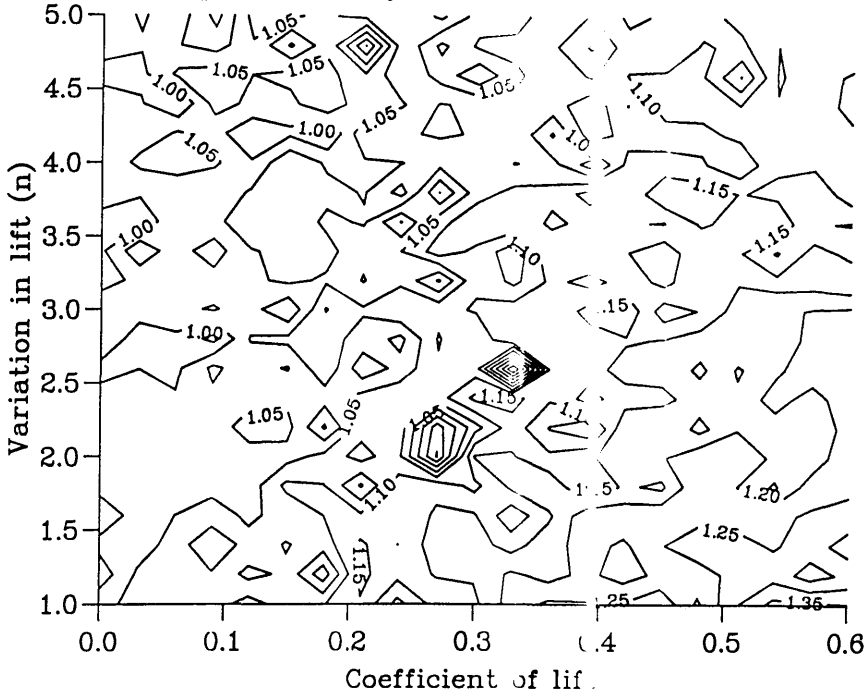

b) Mean saltation length

Figure 5.15 Effect of varying lift force for particle initially at rest, Transport stage = 2.506
Normalised with values from Abbott & Francis (1977)

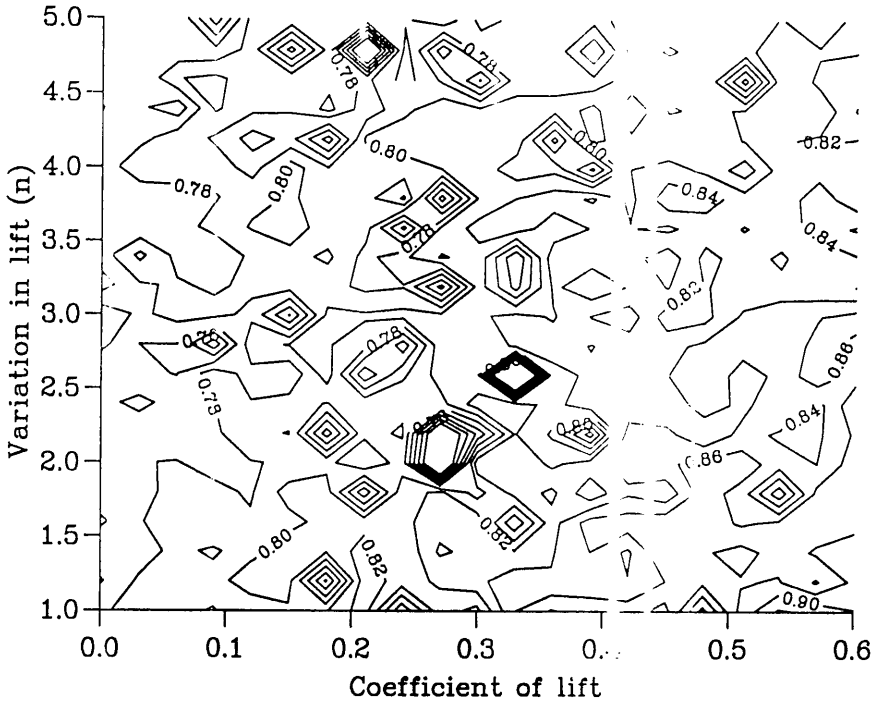

c) Mean maximum saltation height

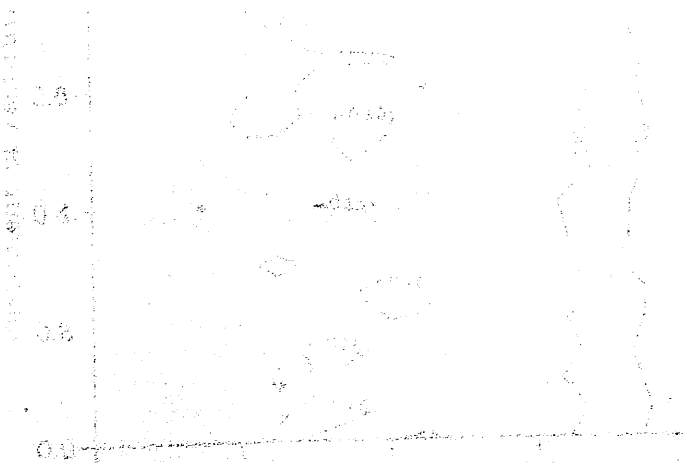

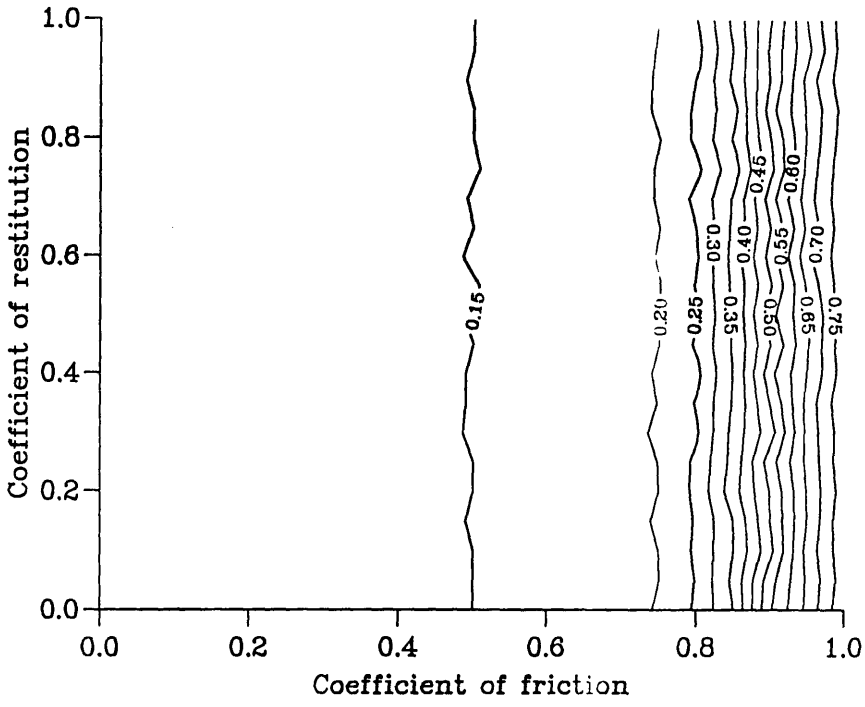

a) Mean particle velocity

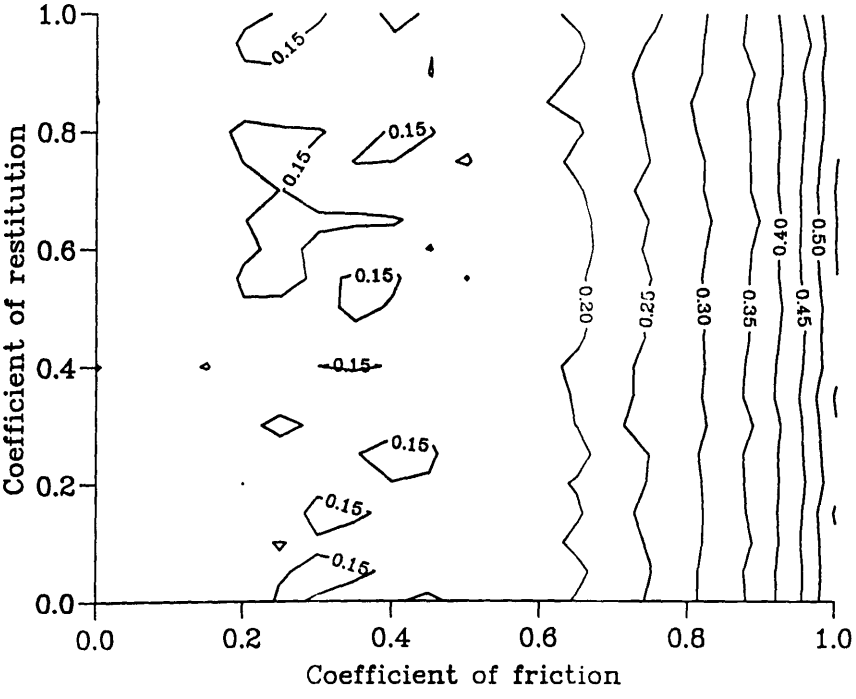

b) Mean saltation length

Figure 5.16 Effect of varying conservation of momentum on impact, Transport stage = 1.521
Normalised with values from Abbott & Francis (1977)

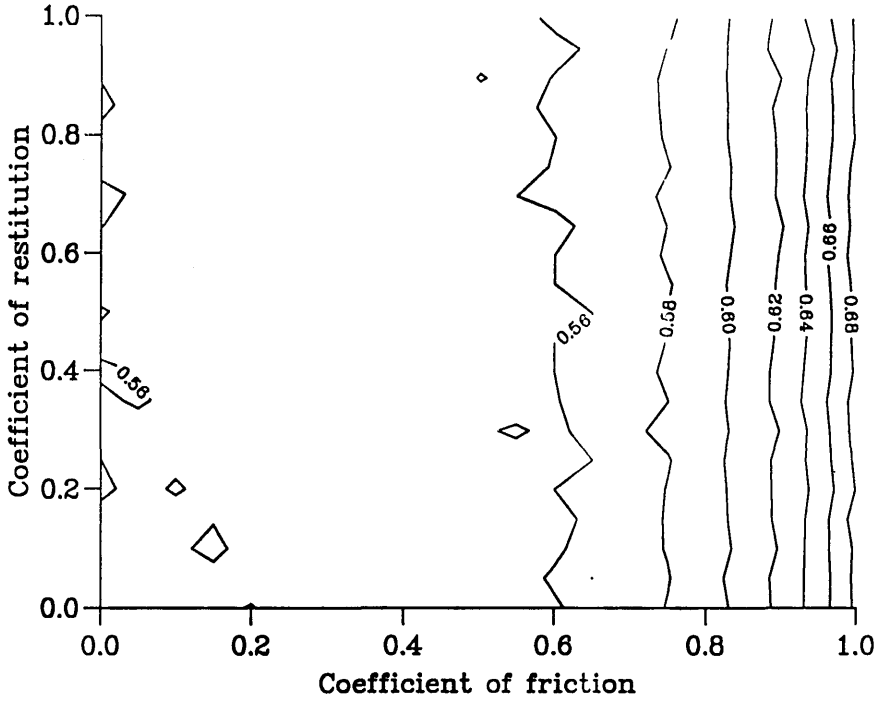

c) Mean maximum saltation height

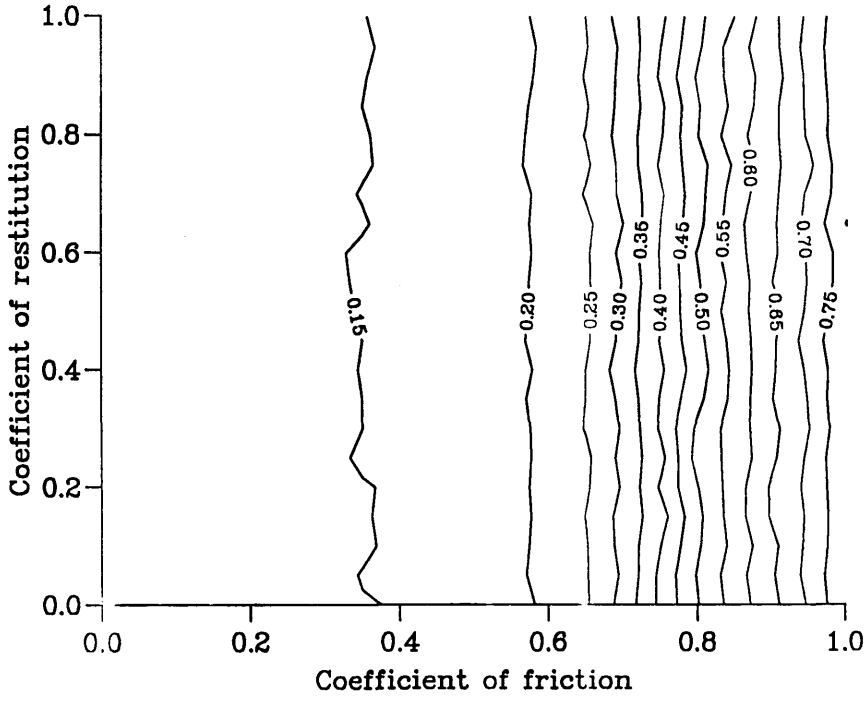

a) Mean particle velocity

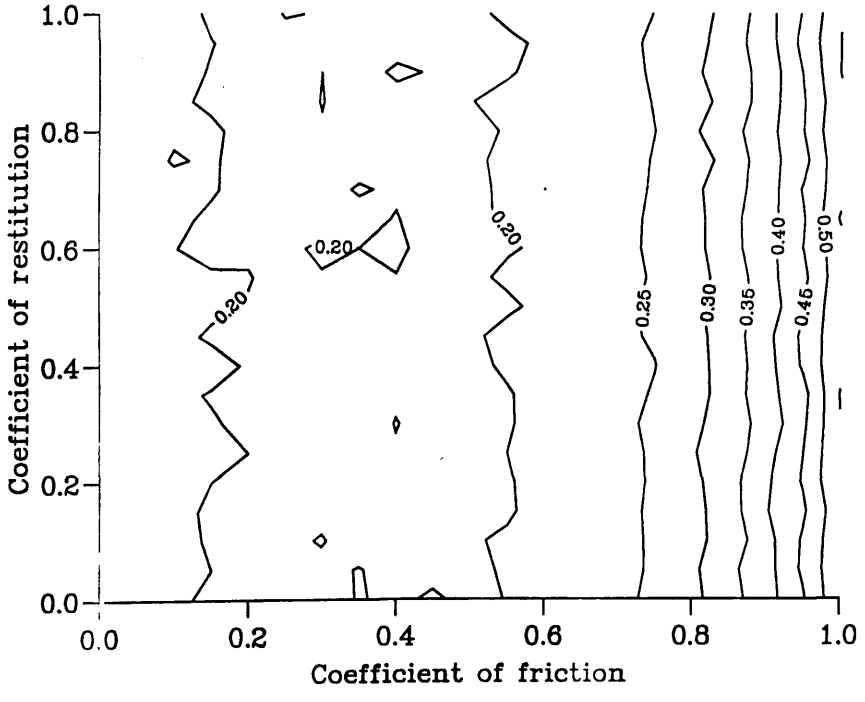

b) Mean saltation length

Figure 5.17 Effect of varying conservation of momentum on impact, Transport stage = 1.900
Normalised with values from Abbott & Francis (1977)

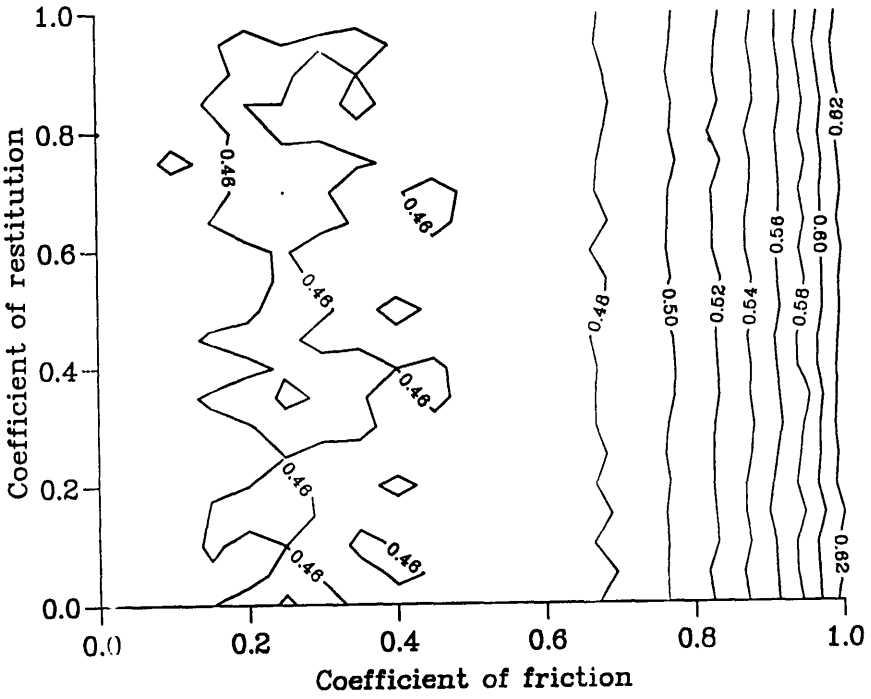

c) Mean maximum saltation height

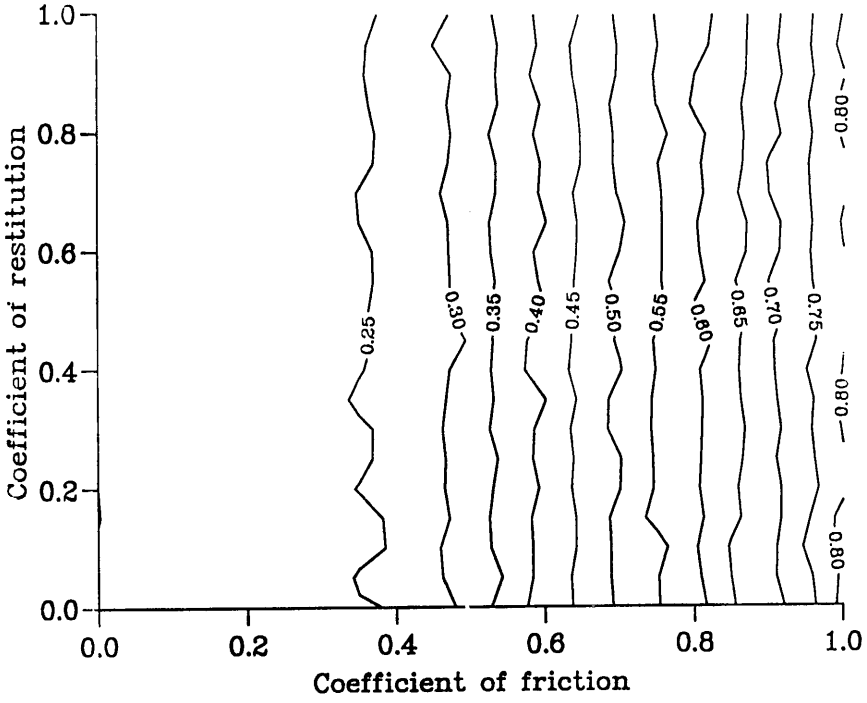

a) Mean particle velocity

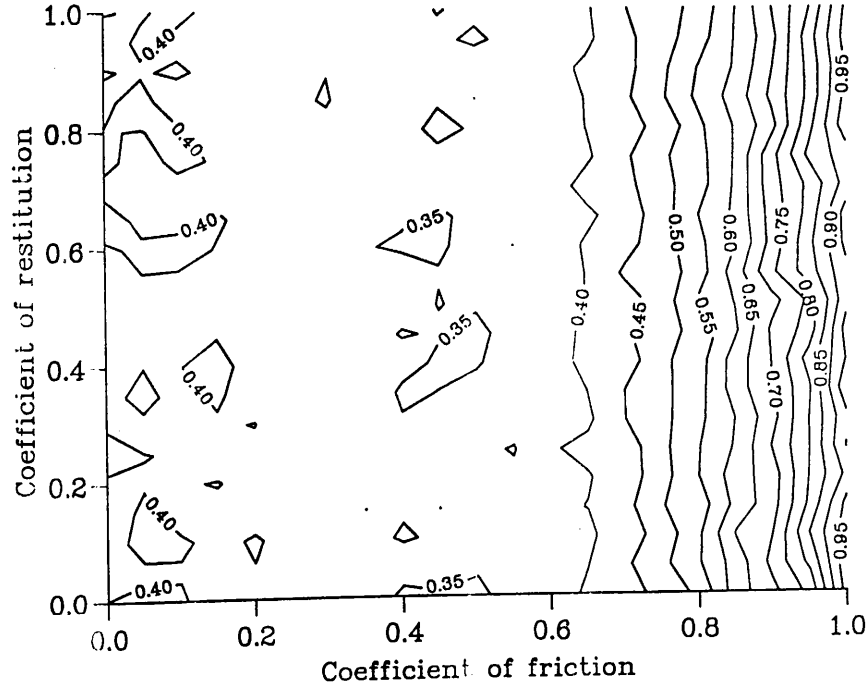

b) Mean saltation length

Figure 5.18 Effect of varying conservation of momentum on impact, Transport stage = 2.506
Normalised with values from Abbott & Francis (1977)

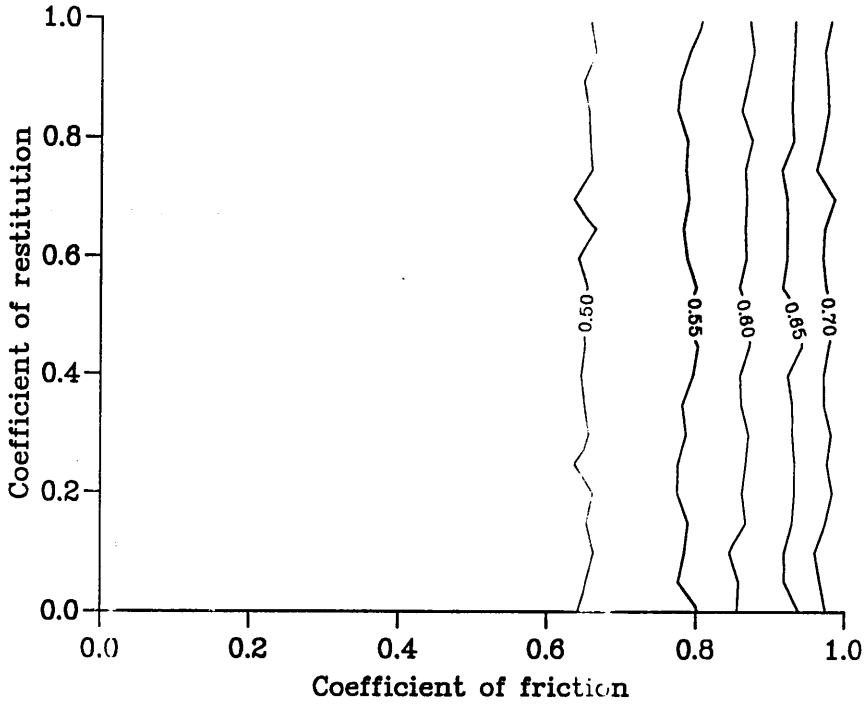

c) Mean maximum saltation height

than elsewhere. The difference is due to the fraction of trajectories observed to contain a suspension, the experimental results show a much higher fraction than the calculated results. For the experimental observations, as time in suspension increases the majority of long trajectories must contain a suspension, and therefore the average saltation length must fall. The smaller calculated time in suspension means that this effect does not modify the calculated saltation length. The mean particle velocity at a transport stage of 2.506, Figures 5.12a and 5.15a, which was not affected by the division of trajectories into saltation and suspension, shows a similar fit to the results for lower transport stages, Figures 5.10a, 5.11a, 5.13a, 5.14a.

The left hand axis of the contour plots of varying lift force represents a zero value of lift force for all values of 'n', since the coefficient of lift on this axis is zero. The result of this is that the values of any quantity on this axis should remain virtually constant, which the contour plots show, Figures 5.10-5.15. The rest of the region of the contour plots shows a better fit to the observations of Abbott & Francis (1977) with increasing effective lift force, that is towards the bottom right corner of the plots. The total range of the calculated values across the values of parameters used is only 6-8% of the observed values. The range is similar for each of the calculated transport stages though the position of the range of values changes. The calculated particle velocities are around 80% of the observed while the saltation length and height are around 60% of the observed. The calculated results are normally smaller than those observed, with the exception of the saltation geometry at a transport stage of 2.506, for reasons stated above. While variations in the lift force do affect the calculated results the variation is not of itself sufficient to match the calculated to the observed results.

The conservation of momentum on impact has a much greater effect on the range of calculated results. The velocity shows a range from 15% to 80% of the observed values of Abbott & Francis (1977), Figures 5.16a, 5.17a, 5.18a, while saltation length and height show a smaller range from 20% to 60%, Figures 5.16b, c,

5.17b, c, 5.18b, c. The calculations only show variation with changing fraction of the tangential component conserved, with the fraction of the normal component of momentum conserved having minimal effect on the results. The observations of Gordon *et al.* (1972) were explained as showing that the tangential component of momentum was conserved while the normal component of momentum was not conserved. The results calculated here give the best fit to observations when the tangential component of momentum is conserved, but show no dependence on the normal component of momentum. The other models of impact described in Section 3.3.3 used a single coefficient to represent the reduction in particle velocity, applying it to both normal and tangential components of velocity; this would not affect the results calculated here since the model is insensitive to the fraction of the normal component of velocity conserved.

5.5.3 Variation in turbulence scales

The calculated incidence of suspensions in particle tracks was much lower than would have been expected from observations. Many tracks showed no suspended trajectories, while in those that did only 1 or 2 saltations might be suspended out of a total of 40-50 trajectories, occupying a much lower percentage of the time than that observed. However the presence of some suspensions, Figure 5.7, and the variable time to initial motion, Figure 5.8, showed that velocity fluctuations could modify particle tracks, but that this did not occur very often. Examination of the calculated records of particle movements show that the number of times particles leave an eddy during a trajectory is low, which limits the possible number of suspended trajectories. To increase the possible number of suspensions the number of eddies that a particle moved through would have to be increased.

Particles might stay in eddies for too long for two reasons, the scale of the eddy was wrong, that is it was too large, or the speed with which the eddy was advected by

the flow was too low. The horizontal and vertical sizes of the eddies were taken to be the corresponding Eulerian length scales, described in Section 4.2.2.4. Measurements of the vertical length scale and its variation through depth are scarce and the value of this parameter was set using the best available data, that from the River Severn (Heslop *et al.*, 1993). More data would enable a better description of this parameter to be derived. The effect of varying this parameter can easily be examined by using a fraction of the original length scale in the calculations, as described below.

The speed with which eddies are advected by the flow might also be too low. Examination of the calculated records of particle movement also show that a particle most often moves from eddy to eddy while close to the bed. The effect of this is that one or more trajectories will occur within an eddy before the particle moves into another eddy, also when in contact with the bed. If this happens there is no mechanism for suspension of trajectories to occur. Another result of the particle moving from eddy to eddy close to the bed is that they are advected by relatively slow flows close to the bed, even if, as here, it is assumed that eddies less than half their vertical length scale from the bed are advected by the mean flow at half their vertical length scale from the bed. This is particularly significant when the importance of the burst-sweep cycle in the bedload transport of sediment is considered. In the burst-sweep cycle fluid is ejected from the region near the bed outward and sweeps in toward the bed from outer regions. The use of fluid initially coincident with the sediment particle in the region of the bed might stop these types of events occurring. Methods of altering the speed with which fluid and sediment particle diverge, in order to examine the effect this has on particle behaviour are less obvious, so no calculations trying to produce this effect were performed.

Calculations were performed with the horizontal length scale set at various fractions of the original value (see Section 4.2.2.4). This decreased the size of all the other turbulence scales. The results of these calculations are shown in Figure 5.19, in

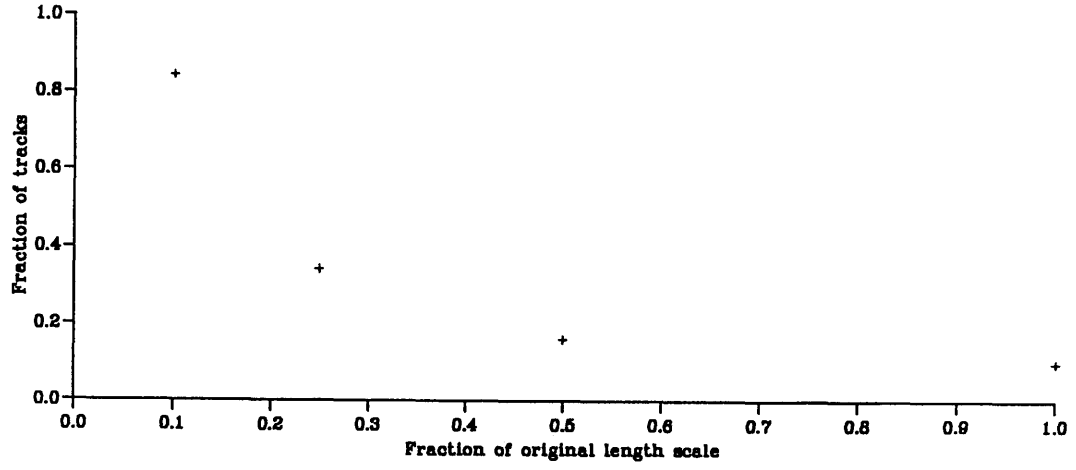

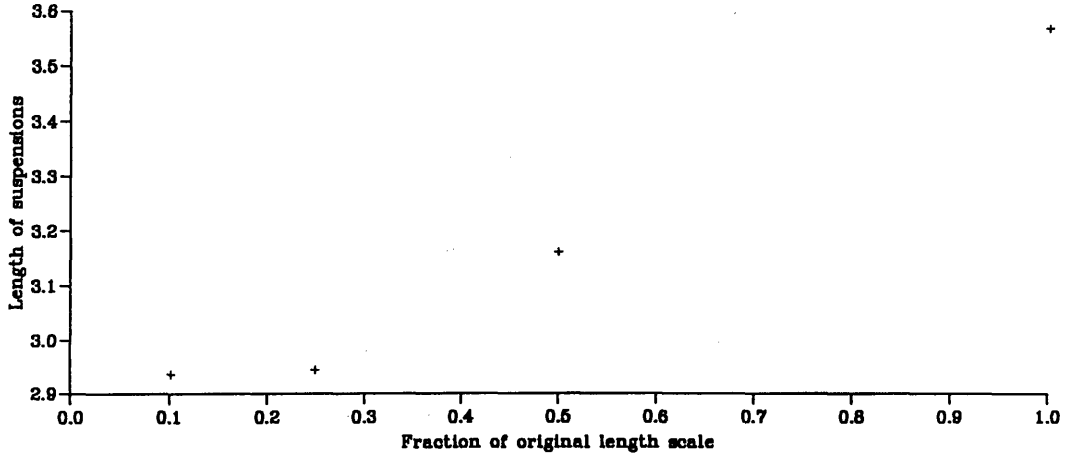

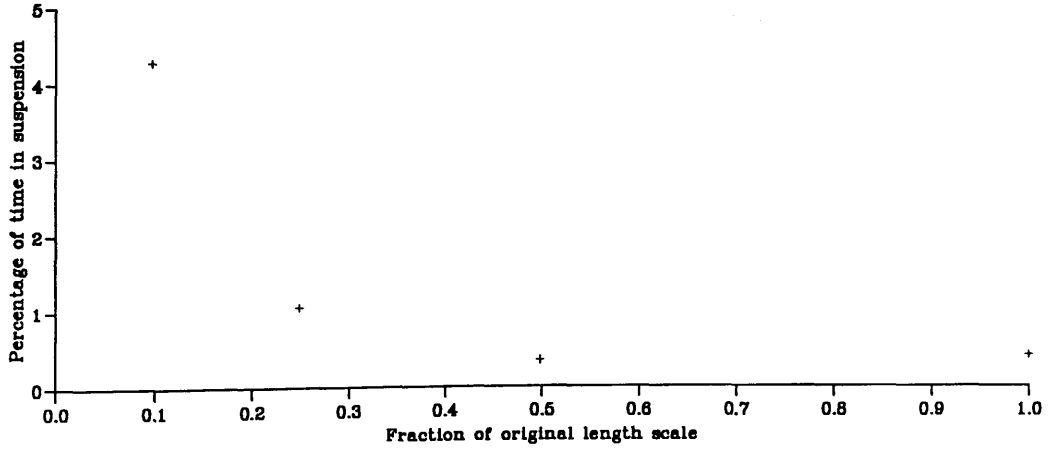

Figure 5.19 Effects of varying length scale of turbulence

terms of the fraction of tracks with suspensions, length of suspended trajectories and the percentage of time spent in suspension. The fraction of tracks containing suspended trajectories increased with decreasing length scales, that is as the eddies became smaller. The time in suspension increased with decreasing length scales and the length of suspended trajectories decreased as shorter trajectories began to contain suspensions.

Reducing the turbulent length scales, increased the number of eddies through which particles passed and increased the number of suspended trajectories. Whether the reason for the low number of suspended trajectories was incorrect length scales or problems related to using the particle tracking method close to boundaries, this shows that the technique can be modified to produce results closer to those observed.

5.6 Comparison of observed and calculated particle movement

5.6.1 Qualitative comparison of particle trajectory

The comparison made here is between the calculated particle trajectory and the observed particle trajectory shown in Figure 14 of Abbott & Francis (1977). As described earlier this shows observed particle positions at intervals of 1/40 second, enabling the initial particle position and particle velocity to be set to allow comparison of calculated and observed particle trajectories. Calculations of the particle trajectory were performed with flow velocity set at the mean values and with fluctuations of +/- σ_w. The calculated eddy size for these calculations was such that the particle remained in a single eddy for the duration of the calculation, so the use of a single value for the velocity fluctuation for the duration of the calculation is a reasonable approximation. The calculations were started from the second observed particle position, the first for which the particle velocities could be calculated.

The calculated particle trajectories, plotted with the observations, are shown in Figure 5.20. The plots show the mean flow calculation over-predicting the maximum

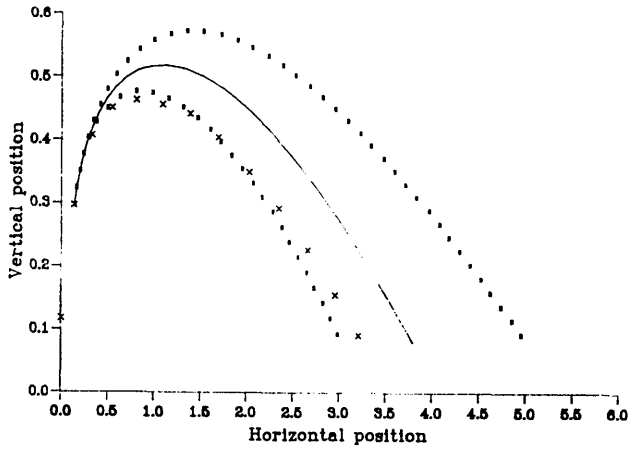

a) Particle trajectory

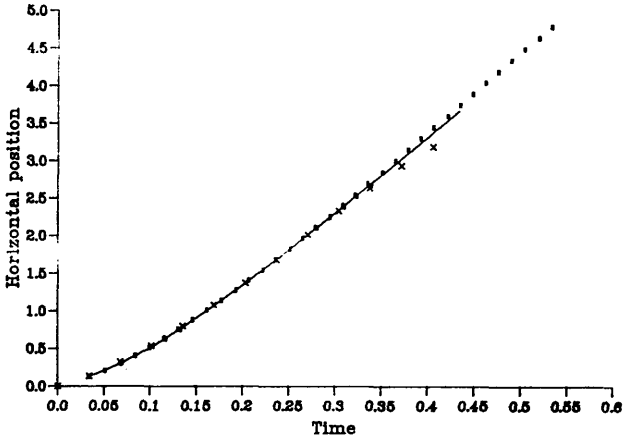

b) Horizontal position

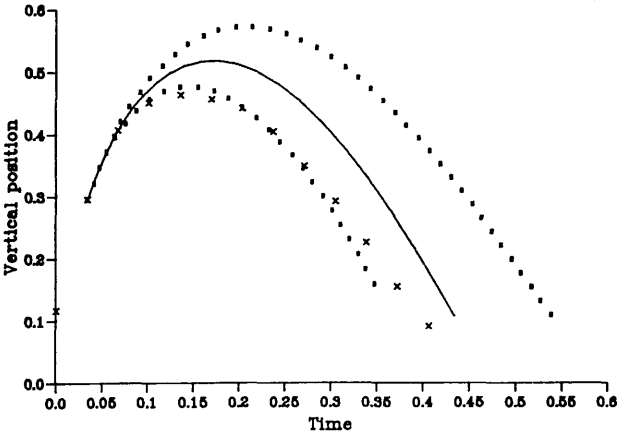

c) Vertical position

Figure 5.20 Comparison of observed and calculated particle trajectories
Observed particle positions are marked as crosses (x)
Solid lines are calculated particle positions for mean flow
Dotted lines are calculated particle positions for $+/-\sigma$.
Units are non-dimensionalised with respect to flow depth, h, and mean bed shear velocity, u_*

height and length of the saltation. The range covered by the +/- σ_w fluctuations is such that calculated trajectories could include the observed trajectory. The calculated trajectories including fluctuations also show the magnitude of the effect the velocity fluctuations can have, the saltation length with a negative velocity fluctuation being three times the flow depth, that with a positive velocity fluctuation five times the flow depth.

5.6.2 Quantitative comparison of particle movements

The quantitative comparison of calculated particle movements is made with the observations of Fernandez Luque & van Beek (1976) and Abbott & Francis (1977). The results of Fernandez Luque & van Beek (1976) were obtained from analysis of film of the movement of particles over a mobile bed formed of particles of the same size and type. The only results on particle movement from their analysis of this film were mean particle velocities; these were based on the analysis of the movements of single particles, though these particles were not moving in isolation. The results of Abbott & Francis were obtained from analysis of multi-exposure photographs of the movement of single particles over a fixed bed. These photographs were analysed to obtain horizontal and vertical particle positions at 1/40 second, this data could then be used to calculate particle velocities and accelerations. The data plotted from this analysis include mean lengths and heights of saltations and suspended trajectories, the percentage of time in different modes of transport and the mean particle velocity.

The calculations were performed using the model as described in Chapter 4, rather than with any of the values of parameters examined in the last section. The impact model described in the last chapter gave the best fit to the observations with which comparisons were made. Though the fit could be improved by increasing the lift force, the improvement was small and the parameter values would be extreme. The values for the quantities describing calculated particle trajectories were based on 20

calculations of particle tracks. The quantities were calculated for a particle initially in motion moving a fixed distance.

5.6.2.1 Results for data of Fernandez Luque & van Beek

The results of the calculations at conditions for which Fernandez Luque & van Beek (1976) made observations are shown in Figures 5.21 and 5.22. The calculations were performed for the conditions of the observations shown in Figure 6 of Fernandez Luque & van Beek (1976). The calculated and observed values are shown plotted against transport stage in Figure 5.21 and plotted against each other in Figure 5.22. The calculated mean particle velocities show a good fit to the observed values, particularly with increasing transport stage. Each of the particle sizes and densities appears to lie on a separate line with no correlation between density or particle size and goodness of fit.

5.6.2.2 Results for data of Abbott & Francis

The results of the calculations at conditions for which Abbott & Francis (1977) made observations are presented in Figures 5.23 - 5.26. The calculations were performed for the conditions of the observations shown in Figure 1 of Abbott & Francis (1977). All of the figures are plotted as a quantity against transport stage. In Figure 5.23 the percentage of time rolling and in suspension are plotted; Figures 5.24 and 5.25 show the lengths and maximum heights of trajectories in saltation and suspension and Figure 5.26 shows the mean particle velocity. On all these figures, observed and calculated values are plotted for each of the particle densities used by Abbott & Francis; data for four densities of particle are presented for all but the mean particle velocities, where observed data was only available for two densities. As has already being mentioned in Section 5.3.2 the number of tracks containing suspensions was small and the values of the suspended trajectory geometry are based on a small number of trajectories.

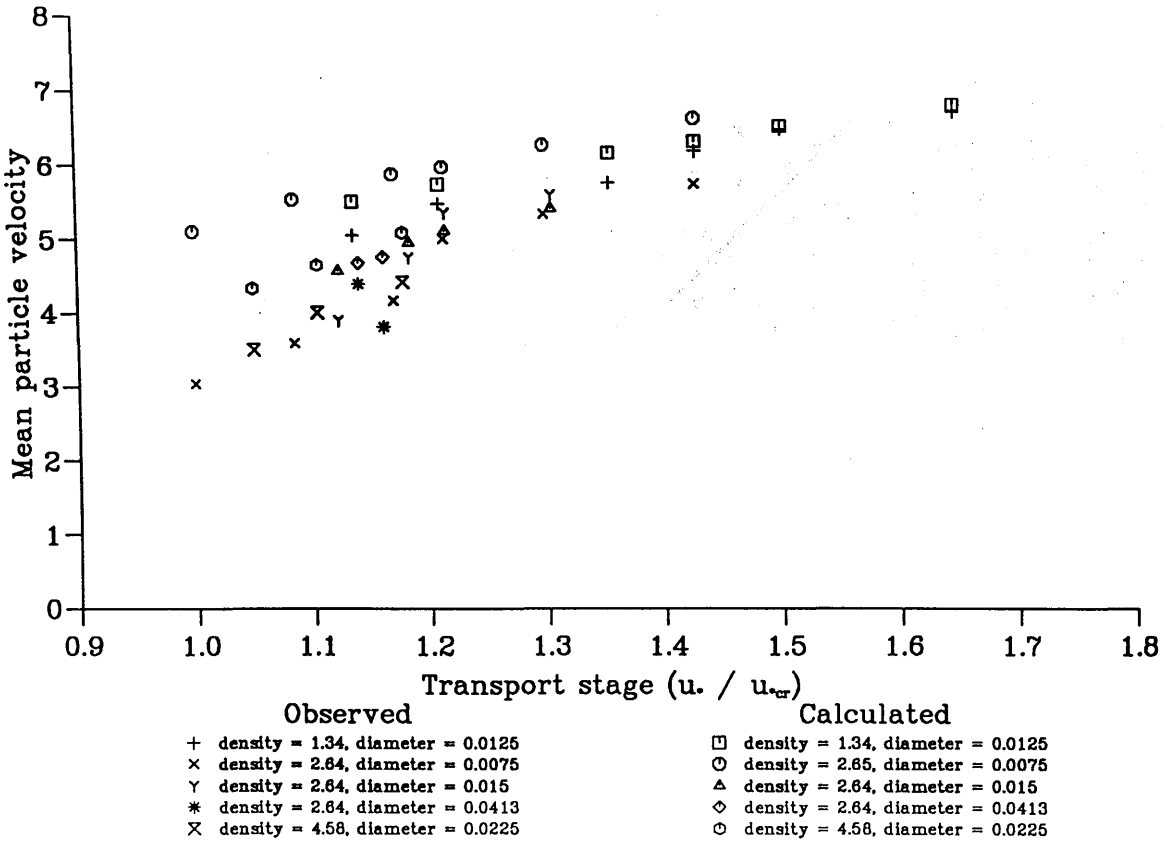

Figure 5.21 Observed & calculated mean particle velocitites against stage
Data of Fernandez Luque & van Beek (1976)

Units are non-dimensionalised with respect to mean bed shear velocity and fluid density

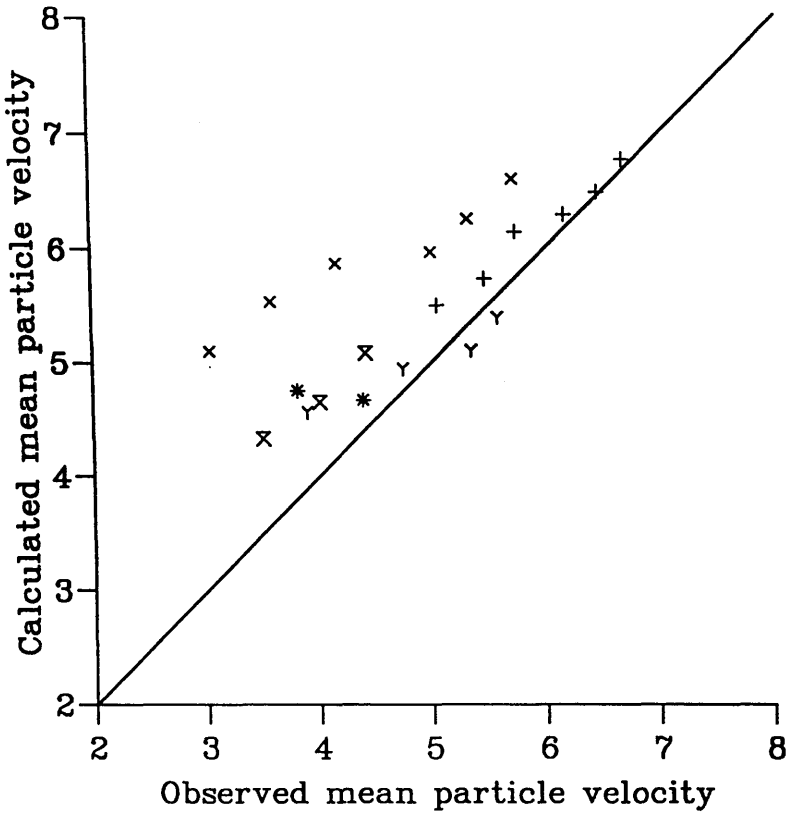

+ density = 1.34, diameter = 0.0125
× density = 2.64, diameter = 0.0075
Y density = 2.64, diameter = 0.015
✱ density = 2.64, diameter = 0.0413
X density = 4.58, diameter = 0.0225

Figure 5.22 Calculated against observed mean particle velocities Data of Fernandez Luque & van Beek (1976)

Units non–dimensionalised with respect to flow depth, mean bed shear velocity and fluid density

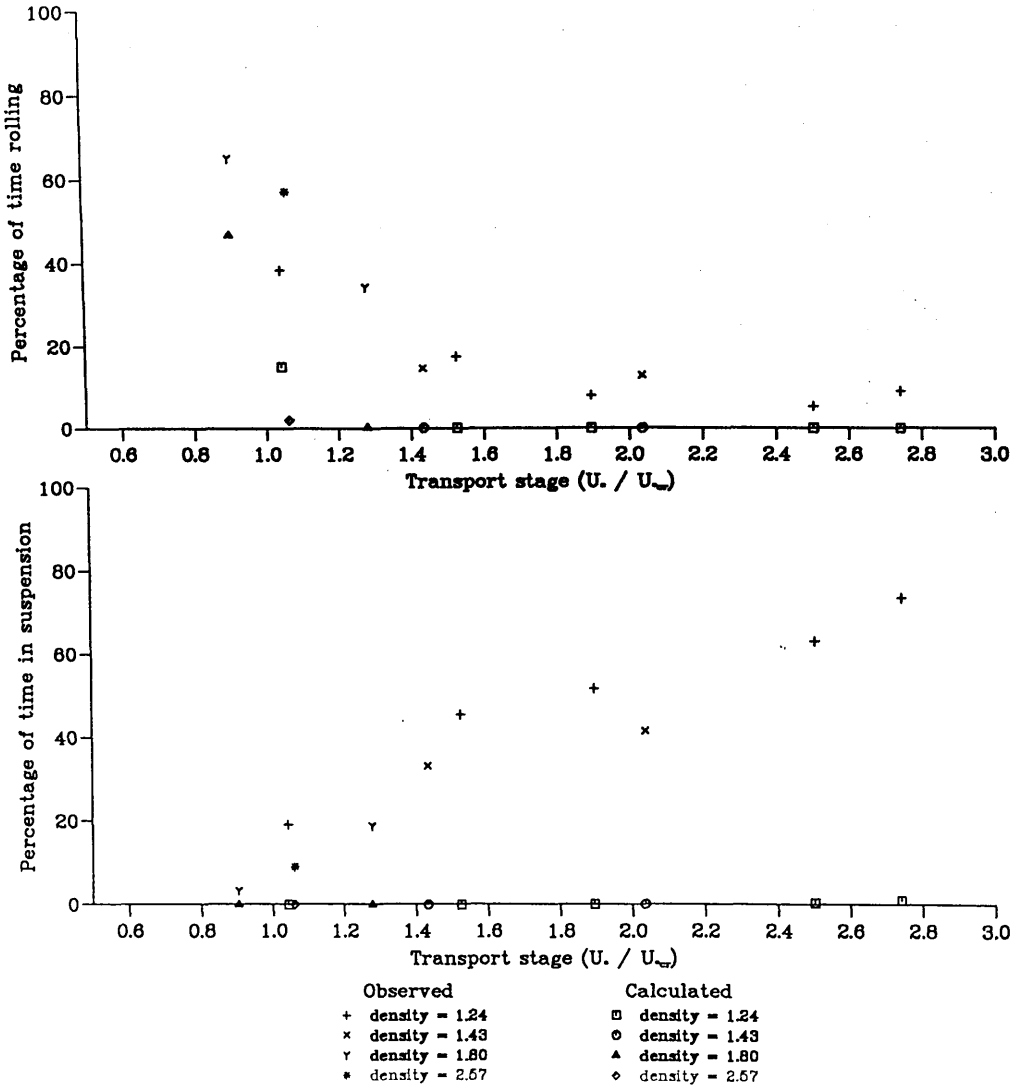

Figure 5.23 Variation of percentage time in mode of transport with stage
Data of Abbott & Francis (1977)
Units non-dimensionalised with respect to fluid density

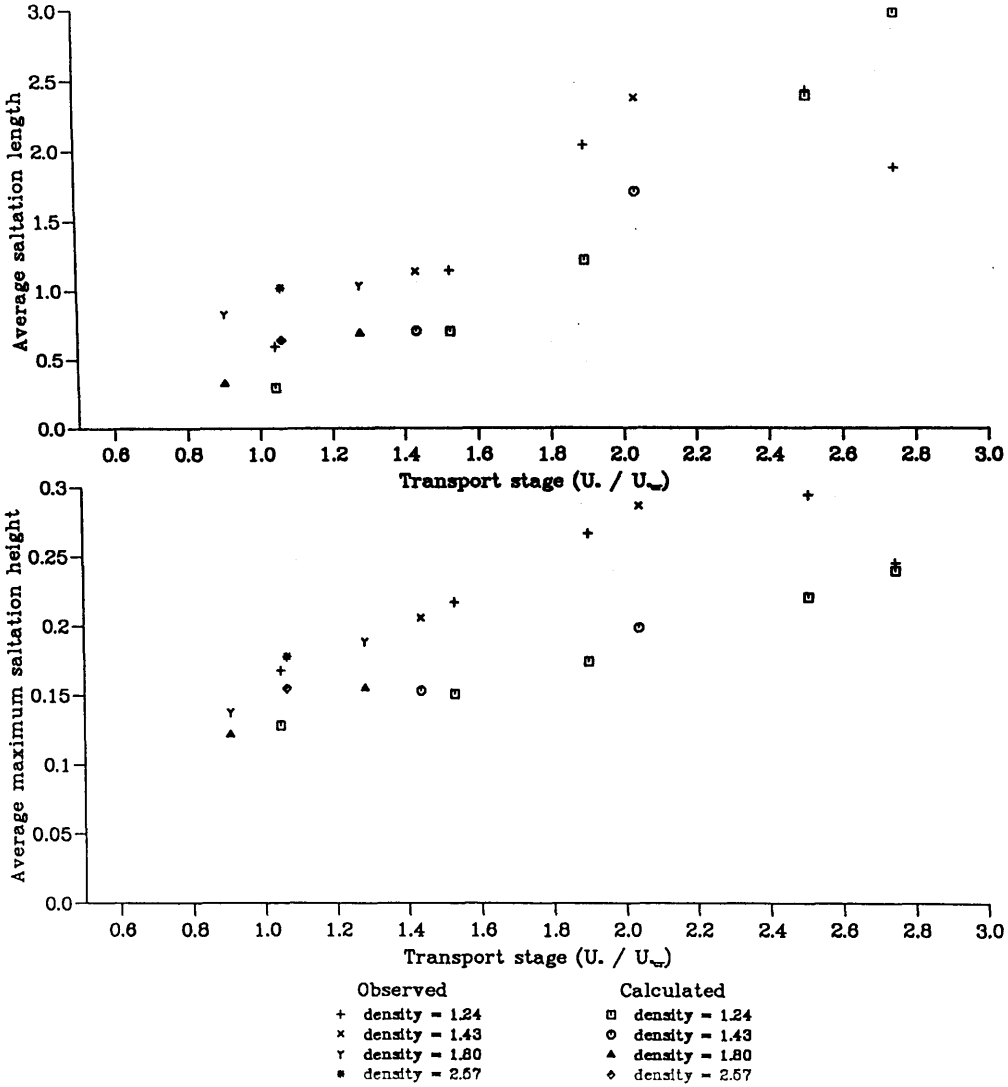

Figure 5.24 Variation of saltation geometry with stage
Data of Abbott & Francis (1977)

Units non-dimensionalised with respect to flow depth and fluid density

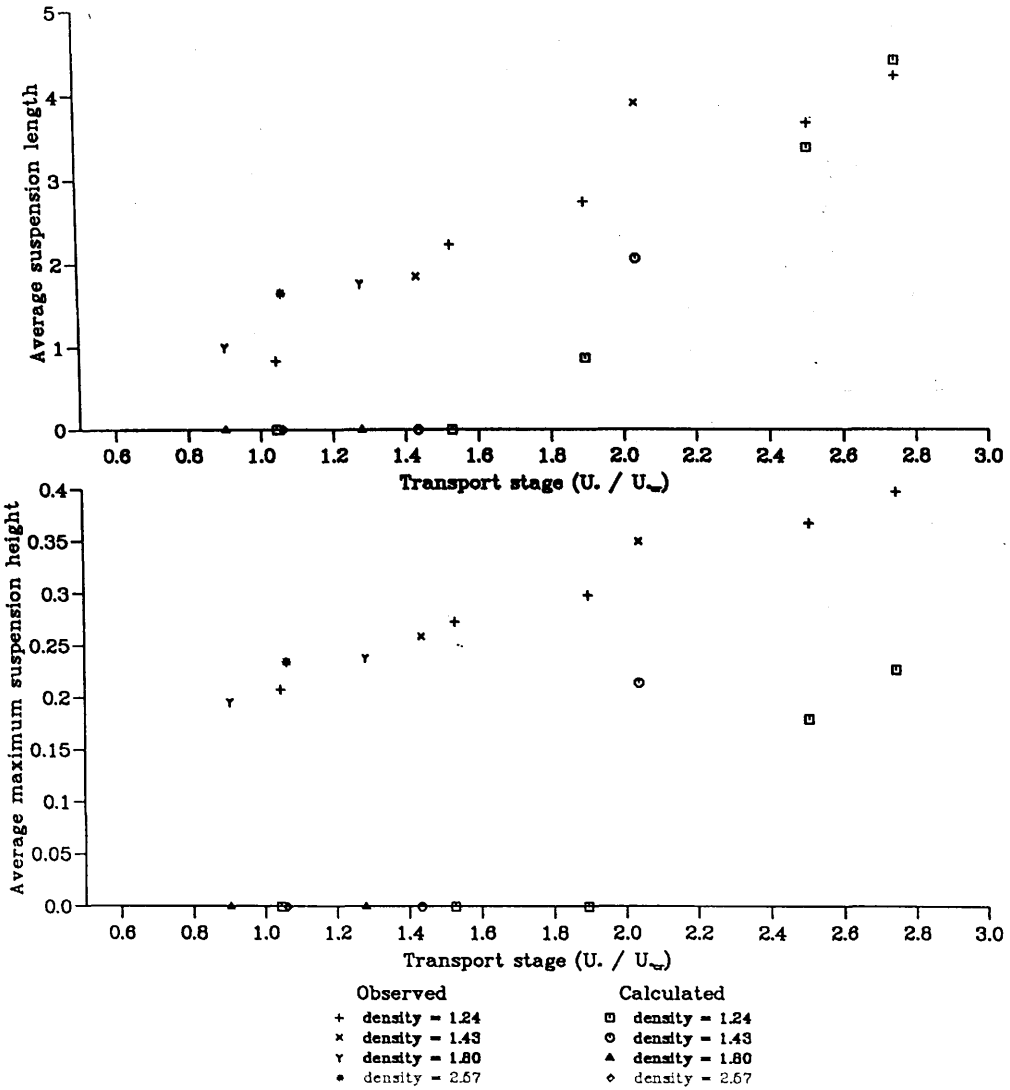

Figure 5.25 Variation of suspended trajectory geometry with stage
Data of Abbott & Francis (1977)

Units non-dimensionalised with respect to flow depth and fluid density

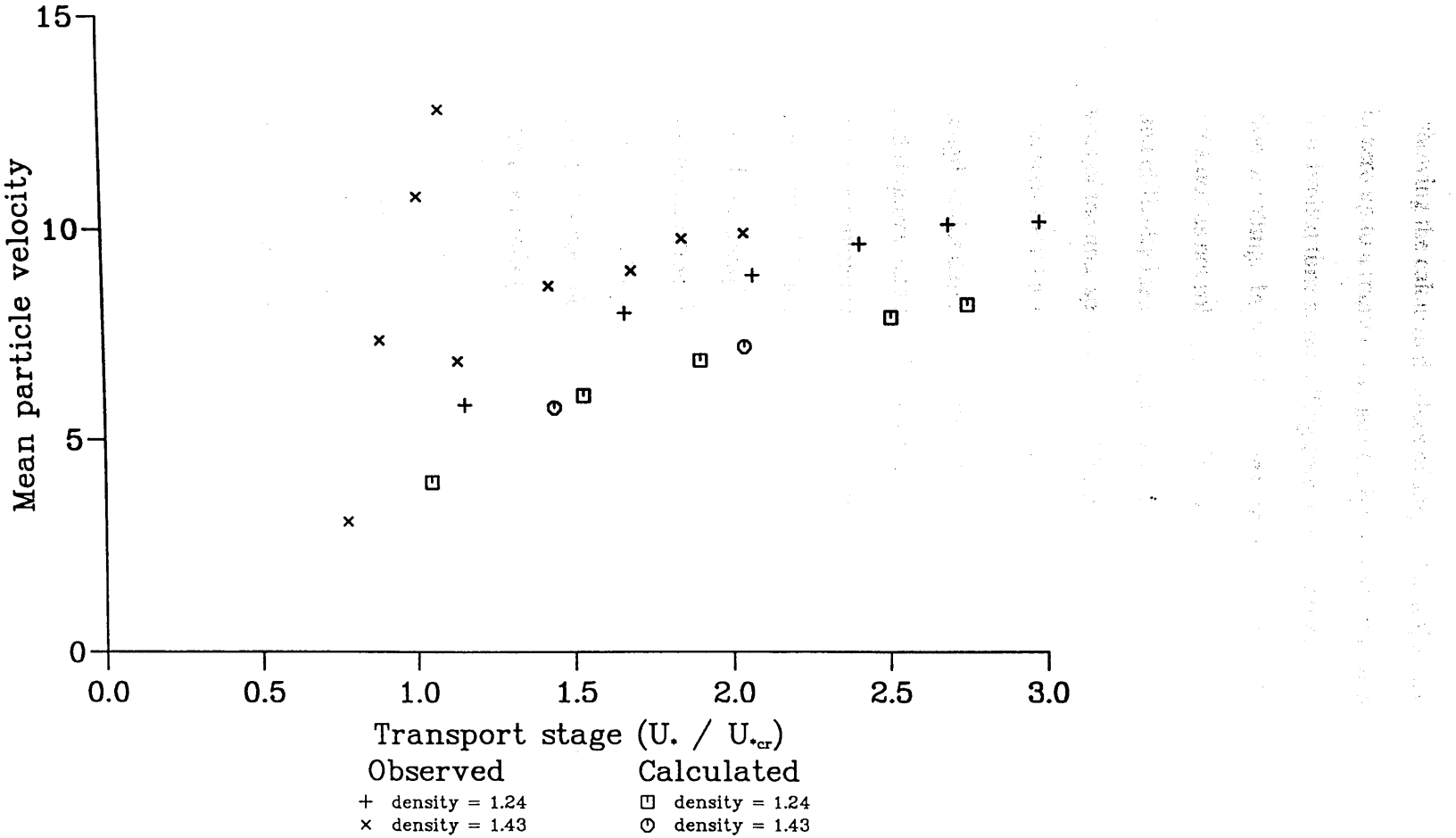

Figure 5.26 Observed and calculated mean particle velocity against stage
Data of Abbott & Francis (1977)
Units non-dimensionalised with respect to mean bed shear velocity and fluid density

The percentage of time rolling and in suspension were both underestimated (Figure 5.23). The effect of the time in suspension being so small can also be seen in Figure 5.25, showing the calculated values of suspended trajectory length and height. These remain zero up to a transport stage of 1.8 because no trajectories become suspended. The limited time spent rolling compared to observation could well be due to the definition of rolling. In the calculations, once contact has been lost with the bed, a particle is regarded as not rolling; in the observations a particle would still be rotating at this point and difficulty identifying the precise time contact was lost might well lead to overestimates of the time spent rolling. The underestimation of time in suspension and possible reasons for it have already being discussed in Section 5.5.3.

The length scales describing particle trajectories, saltating and suspended, are underestimated (Figures 5.24 and 5.25) for all but the highest transport stage for saltations, for reasons already described in Section 5.5.2. Since higher trajectories are likely also to be longer it is not surprising that both trajectory dimensions are underestimated. Even though the calculated values of these dimensions are underestimates the variation with stage and particle density does follow that of the observed points for the saltations (Figure 5.24). The variation of the dimensions of the suspended trajectories does not follow those of the observation (Figure 5.25) but that is a result of the low number of suspended trajectories calculated.

The calculated values of mean particle velocity underestimate observed values (Figure 5.26). The calculated points also seem to lie on a single curve for the different particle densities, as do the observed values, with the exception of the lowest transport stage. This point is the transport stage and particles density for which the highest percentage of time rolling was calculated, which may indicate that the simple rolling model used is incorrect.

5.7 Conclusions

The model of particle movement described in Chapter 4 and tested in this chapter is capable of reproducing initial motion of particles and particle trajectories including the effects of turbulent velocity fluctuations in the flow on particle movements. The particle tracking method of including the effects of turbulent velocity fluctuations, where positions of fluid and sediment particles are calculated independently and the effects of the fluid velocity on the particle movement calculated, is able to reproduce the effects of velocity fluctuations on particle movements. This can be seen in calculated particle trajectories (Figure 5.7) and behaviour at initiation of motion (Figure 5.8).

The initial tests of routines to solve the ordinary differential equations describing particle motion and to test for an appropriate choice of timestep, described in Sections 5.2 and 5.3, showed it was possible to calculate the movement of particles influenced by velocity fluctuations without having to use so small a timestep that the calculations became unusable due to execution time.

Though the effects of turbulence are included and can be seen in both particle trajectories (Figure 5.7) and statistics describing them (Figures 5.23, 5.25) the calculated number of suspended trajectories was lower than observed. Possible reasons for this discrepancy were presented in Section 5.5.3, along with calculations showing that the number of suspended trajectories could be increased. The possibility that the length scales used and their variation with depth did not apply to the flows in the calculations performed can only be tested by measurements of turbulence above rough beds. The effects of the boundary on movement of particles have been seen in calculations including a viscous sub-layer (Allen, 1982), where particles entering this layer tended to remain in it for long periods of time. Problems with the tracking of fluid particles close to the bed requires further examination of calculated behaviour of fluid and particles and perhaps new approaches to the description of eddies. The

effects of using different models to describe the turbulent velocity fluctuations, Section 5.4, showed that the burst-sweep model of the velocity fluctuations had the most effect on the calculated quantities used to describe particle movement. Though this model reproduces the effects of the burst-sweep cycle, that is high shear stress events, it does not reproduce the structure of these events. The description of eddies used, eddies the size of the length scale and constant values of velocity fluctuations in time and space for the duration of the eddy was the simplest description possible. In Zhuang *et al.* (1989) the same model is used but with the introduction of correlated velocity fluctuations within an eddy, along with uncorrelated velocity fluctuations between eddies. This model was not used here because it did not seem appropriate for the quantity of data available to set parameter values. If such a model were to be used it would introduce the possibility of fluctuations occurring within an eddy, resulting in a greater tendency for particles to become suspended.

The effects of the added mass terms and variation in lift force and conservation of momentum on impact showed that the most significant of these terms was the conservation of momentum on impact. The calculations with different values of lift force showed that while this did affect the results the range of such effects was only ~8% of observed values. By contrast the effect of varying the conservation of momentum on impact gave a range of calculated values an order of magnitude larger. Studies of the impact process in the aeolian environment have been performed because the process is important in both continuing saltation and initiation of motion; impact in fluvial environments has been studied much less. The range of the results obtained by varying the impact process make this an important process for further studies, experimental and numerical.

The actual model of impact used here, similar to that of Rumpel (1985), is one extreme of the possible range of effects of impact. This model made better predictions of the results of Fernandez Luque & van Beek (1976) than those of Abbott & Francis(1977). This may be due to the assumptions of the impact model, which are

those of a non-mobile, non-rigid bed. For this type of bed, particles are free to move due to impact without leaving the bed, which conserves tangential momentum and dissipates normal momentum. This description is closer to the bed used in Fernandez Luque & van Beek (1976) than that of Abbott & Francis (1977), where the bed was fixed and rigid. However the results may also be due to the fact that the results of Fernandez Luque & van Beek (1976) were for particles moving in a group, for which Francis (1973) observed a reduction in mean grain velocity, compared to the movement of individual grains. Particles moving a part of a group see lower flow velocities due to momentum extracted from the flow, hence the observed reduction in mean grain velocity. The better fit for the observations of Fernandez Luque & van Beek (1976) could be because the calculated momentum transfer from the flow was low for a particle moving in isolation and closer to that for a particle moving in a group.

Though the calculated results of particle movement presented here are not a perfect fit to observations they reproduce the behaviour of particles. The different degree of fit with different data implies that the model is not taking into account all possible variables. The differences in the bed, described above, might be one such effect. However it would seem worthwhile to examine scaling of calculation from single particle to mass transport using this model. This possibility is examined in Part II of this thesis.

Part II

Transport of sediment

Chapter 6

Particle based approaches to sediment transport

6.1 Introduction

The movement of individual sediment particles in turbulent flow over a rough boundary was described and modelled in Part I of this thesis. Such single particle models can be used to model experimental data and examine particle behaviour using different models and mechanisms for the component processes, however they cannot be used directly to calculate sediment transport and its effects. In this part of the thesis the problem of calculation of sediment transport and the associated development of bedforms based on particle calculations, either directly, or using such calculations to supply coefficients describing processes, will be considered. The change of scale in moving from single particle calculations to calculations of sediment transport affects the physical processes being described and the scale over which they act.

The model of particle movement described in Part I of this thesis included a stochastic element by modelling the effects of turbulence on particle movement, affecting the entrainment and motion of particles. When scaling from single particle movement to sediment transport it would be easy to lose such stochastic effects in the calculation of quantities to represent particle movements at the new scale. The approach to calculating sediment transport and its effects developed will attempt to include the effects of this stochastic element at the larger scale for which calculations are performed. The change in scale also affects appropriate descriptions for the components of the model, such as the flow, and the appropriate methods by which the calculations can be performed. The change from calculation of single particle movements to mass transport of sediments increases the effect of momentum extraction from the flow, which was previously ignored, and introduces the possibility of interaction of particles in motion, which was previously not allowed. The

appropriate methods for performing calculations of sediment transport are related to the computing power available and how it can best be utilised in the solution of the problem.

The first chapter of this part of the thesis, Chapter 6, examines approaches to the calculation of sediment transport based on a particle as opposed to a continuum description of the problem. Particle based calculations have been made for fluvial and aeolian environments, the main emphasis here will be on those for the fluvial environment. The information calculated using these models has been used in the calculation of sediment transport rates and to calculate bedform development. Observations of sediment particle movements made in the field, the data obtained and the analysis of results from this data will also be examined.

The second and third chapters of this part of the thesis describe work based on the single particle model from Part I of the thesis. The second chapter, Chapter 7, describes the use of the single particle model to calculate information about particle movements suitable for use in the calculation of sediment transport. The final chapter, Chapter 8, describes the use of the calculated data on particle movement to calculate sediment transport rate and describes possible approaches to using such information in the calculation of the effects of sediment transport on bedform development.

6.2 Particle based calculations

The particle based models of sediment transport described here can be considered as extensions of models of single particle movement. The descriptions in the sections on particle based calculations will concentrate on the differences between single particle calculations and the calculation of the mass transport of sediment. The sections describing the modifications to the single particle calculations will be considered under the headings of flow, sediment transport, particle interactions and bed. Of these components the most significant differences relative to the single particle

model occur in the section on particle interactions as the calculation of the effects of the presence of multiple particles reintroduces the possibilities of feedback between the components of the model.

6.2.1 Flow

Any model used to calculate flow over a mobile bed must be able to calculate the effects on the flow due to modification of the bed topography and composition by sediment transport. The flow is also modified by momentum extracted from the flow by the movement of sediment. In a particle based model this momentum extraction from the flow, and its effects, are often calculated explicitly and used to determine transport rates, rather than using empirical expressions for the quantity of sediment in motion. In this section the modelling of flow and how the variation in bed topography and composition have been included in models will be described. The effects of momentum extraction from the flow will be considered in Section 6.2.3. As with all the other components in the simulation of the sediment transport process the description of flow used depends on the uses for which the simulation is being designed and the scale at which it will be used.

The extensions of the single particle models of van Rijn (1984), Wiberg & Smith (1989) and Sekine & Kikkawa (1992) were intended to form expressions for the rate of sediment transport based on theoretical analysis and deterministic expressions rather than empirical relationships (although the expression developed by van Rijn (1984) contains empirical and theoretically based terms). The expressions derived for the rate of sediment transport were all functions of the shear stress, τ, exerted by the flow on the bed, which can be calculated as:

$$\tau = \rho g h S$$

where ρ is the fluid density, g the acceleration due to gravity, h the flow depth (in a 2-dimensional flow) and S is the water surface slope. The calculation of the rate of sediment transport does not of itself require the calculation of the effect of modified

bed topography on flow and in none of these models was the calculation of rate of sediment transport used in a model of bed movement and development.

The models of fluvial sediment transport described in Naden (1987b) and Jiang & Haff (1993) were used to simulate bedform development and therefore required a flow calculation that could allow for the effects of modified bed topography due to movement of sediment.

The model of Jiang & Haff (1993) used a different approach from any of the other fluvial particle based methods described here. The calculations were performed at different scales, spatial and temporal, to the other models. The length scale considered in the simulations was much smaller and the duration the calculation represented much shorter than in any other. The type of calculations performed were based on particle dynamic methods; in this method the forces acting on each particle due to the flow and other particles are modelled explicitly. The technique has also been used in models of aeolian sediment transport, Haff & Anderson (1993). This approach imposes limitations on the calculation due to available computing resources and speed of computation. The calculations were based on the behaviour of approximately 100 particles. At the start of the calculation these particles formed the bed, they were then driven by the flow to be transported. The bed was formed with periodic boundary conditions, particles moving out of the area of calculation downstream being reinserted upstream. The duration of simulations was short, typically 2 seconds in the time of the system. The model of flow used in these calculations was the simplest possible, a slab of fluid moving parallel to the bed, the bottom of the slab overlapping the top particles forming the bed, its top surface being driven by a shear force.

Though this is a greatly simplified model of the near bed flow, with no vertical structure to the velocity, it is appropriate to the type of calculation performed and can be related to the ideas of Owen (1964), discussed further in section 6.2.3. If the thickness of the slab is equated with the bedload layer as described in Owen (1964)

then the velocity profile outside this region is the logarithmic law velocity profile with the bedload layer forming a layer of enhanced roughness, with which the logarithmic profile scales. The structure of the flow in the bedload layer is influenced by the movement of particles within this layer and probably not strongly height dependent. In such circumstances the use of the slab model rather than any other velocity profile is a reasonable approximation.

The final description of flow in a fluvial particle based model is that used in Naden (1987b), the aim of which was to examine bedform development, though at a larger scale and over longer durations. The model of particle movement in Naden (1987b) was much simpler than that of Jiang & Haff (1993) with the descriptions of particle movement being calculated from empirical expressions for mean values of saltation height and length, the values being calculated from the transport stage at a point. The flow through the reach was calculated using the gradually varied flow equations for steady flow. Once the velocity and energy slope through a section were known the shear velocity and hence transport stage could be calculated, assuming a logarithmic velocity profile. To recreate the effect of a hydrograph the model was run using different flow rates, increasing and decreasing in steps. The flow and sediment calculations were uncoupled, the conditions calculated from the gradually varied flow equations were kept constant until 10% of the bed had changed, the gradually varied flow equations were then solved again and the results used until a further 10% of the bed had changed.

6.2.2 Sediment transport

The increase in scale from single particle movements to sediment transport has the least effect on the description of sediment movement used in the different models. Of the particle based models of sediment movement three have been used to estimate coefficients for the rate of sediment transport based on the behaviour of single particles (van Rijn, 1984, Wiberg & Smith, 1989, Sekine & Kikkawa, 1992). These will not be

considered in this section since there was no extension of the model of particle movement over that already described in the single particle model. The models of Naden (1987b) and Jiang & Haff (1993) were models of sediment transport over mobile beds. The model of Naden (1987b) used a treatment of particle movement based on the movement of single particles. In Jiang & Haff (1993) the interactions between all particles were calculated at each iteration giving a complete description of the behaviour of all the particles. The calculation of the rate of sediment transport in particle based methods was based on the interaction of sediment and flow and will be discussed in the next section.

6.2.3 Particle interactions

The movement of many sediment particles at once introduces the possibility of moving particles interacting with each other as well as the bed. The possible effects on the flow of the extraction of momentum from the flow due to particle movements, ignored in the single particle calculations must also be reconsidered.

Of the models already mentioned only in the model of Jiang & Haff (1993) were the effects of these terms calculated directly, as part of the calculation of the movement of all the particles in the simulation. Collisions between particles, both those in motion and forming the bed were calculated directly, while momentum extracted from the flow was calculated from the drag force experienced by particles, acting to resist the shear force due to fluid. The collisions between particles were split into two components

$$F = F_N + F_T$$

where F_N is the normal component of force at the impact and F_T is the tangential component of force at the impact. The normal component was modelled as a stiff, damped spring

$$F_N = -k\delta - b\frac{\mathrm{d}\delta}{\mathrm{d}t}$$

where k is a spring constant and b is a damping coefficient, which determines the coefficient of restitution, δ is the overlap of the particles during the collision. The tangential force F_T was described using a friction model with a coefficient of friction μ. The values for all these coefficients were chosen to match the behaviour of observed systems.

The balance of shear force and drag force was simplified to some extent by the use of a slab model of flow, the near bed fluid being modelled as a single slab moving with a velocity determined by the balance between the shear force acting on the top of the layer and the drag force of particle opposing this motion. The drag force on each grain was calculated

$$F_D = \rho \frac{C_D}{2} \frac{\pi d^2}{4} \left|(u - u_p)\right| (u - u_p)$$

each grain being treated as if it was moving in isolation in a flow. The balance of forces acting on the slab was then written

$$\tau A_{slab} - \sum F_D = m_{slab} \frac{\mathrm{d}^2 x_{slab}}{\mathrm{d}t^2}$$

i.e. the force due to shear force, τ, acting on the top layer of the slab of area, A_{slab}, is opposed by the total drag force acting on particles within the slab. Any difference between the applied force due to the shear and that due to drag on the particles accelerates the slab, mass m_{slab}, at a rate of acceleration of $\mathrm{d}^2 x_{slab} / \mathrm{d}t^2$. The possibility of interactions between all particles must be checked at each iteration and the effects of interactions calculated, where appropriate, the drag force due to each particle in the slab must also be calculated at each iteration.

In the other models described here the possible effects of the interactions between particles and between particles and the flow were considered but not necessarily included as part of the final model. The effects of the interactions of moving particles were not included in any of the other models, the limits for which it could be assumed that moving particle interactions were not significant being

determined from experimental data. In Leeder (1979) the concentrations at which particle-particle interactions were likely to occur were derived from a consideration of grain concentration and hence the mean free path of grains. The data used in this analysis were derived from the sediment transport tests of Williams (1970) and the particle trajectory data of Francis (1973) and Abbott & Francis (1977). Based on his analysis Leeder concluded that bedload transport occurring above a transport stage of two would contain a significant proportion of particle-particle collisions acting to modify the transport behaviour.

In Sekine & Kikkawa (1992) analysis of roughness length from observations of sediment transport carried out in a flume diverge from roughness lengths calculated from those from a model based on calculated data from their single particle model, above a non-dimensional shear stress of 0.10. This divergence was thought to be due to the influence of collisions present in the flume data whose presence wasn't included in the simple model based on results from the single particle model. The value of critical Shields stress that has been used in this study is 0.06, this gives a transport stage at which the effects of collision become important of 1.3, rather lower than that calculated by Leeder. If calculations of mass movement of sediment are performed with regard to the limitations on transport stage above which particle-particle interactions become important then data from single particle models can be used to model mass movement of sediment particles.

The interaction of particle and flow due to particles extracting momentum from the flow was included in the models of Wiberg & Smith (1989) and Sekine & Kikkawa (1992) but not in that of Naden (1987b), where the number of particle in motion was assumed to be small enough not to affect the flow, or that of van Rijn (1984), where the sediment concentration was set empirically. The basis of the model of momentum extraction from the flow in both models was the work of Owen (1964). The aim of this work was to examine the effect of saltation on the flow away from the bed and the mechanism by which the near bed sediment concentration was limited. Saltation was

assumed to be confined to a layer close to the bed, within this layer the shear stress, τ, would be partitioned between fluid, τ_f, and grain, τ_g,

$$\tau = \tau_f + \tau_g$$

The magnitude of the fluid shear stress falling as the bed was approached until at the bed it fell to a value equal to the critical shear stress for motion, τ_{cr}, for the bed material. This splitting of shear stress and limiting condition at the bed leads to a feedback controlling the concentration of grains near the bed. If grain concentration falls the fluid shear stress at the bed rises above the critical value for particles to be entrained, more grains are entrained and the fluid shear stress falls back to the critical shear stress for entrainment of particles. Likewise if the grain concentration rises the fluid shear stress falls below the critical value for initiation of particle motion, less grains are entrained and the particle concentration falls until the fluid shear stress rises again to the critical value for initiation of motion. If the saltation layer is thin in comparison with the depth of fluid in which the transport is occurring then the shear stress acting at the top of the saltation layer can be assumed to be that due to the complete depth of fluid, the balance between grain and fluid shear stress then sums to this value down to the bed, where the fluid shear stress falls to the critical value for entrainment of particles, Figure 7.1.

Though the calculations of Wiberg & Smith (1989) and Sekine & Kikkawa (1992) are both based on Owen's model the component of shear carried by the grains was calculated differently. In Wiberg & Smith (1989), as in Jiang & Haff (1993) the momentum transfer was calculated from the drag force acting on particles, the sediment stress being set equal to the drag force per unit area. The drag force was calculated as in the model of Jiang & Haff (1993), the shear stress carried by the grain was regarded as the downstream component of drag force per unit area. The average fluid volume between two grains can be calculated from

$$V/c_s$$

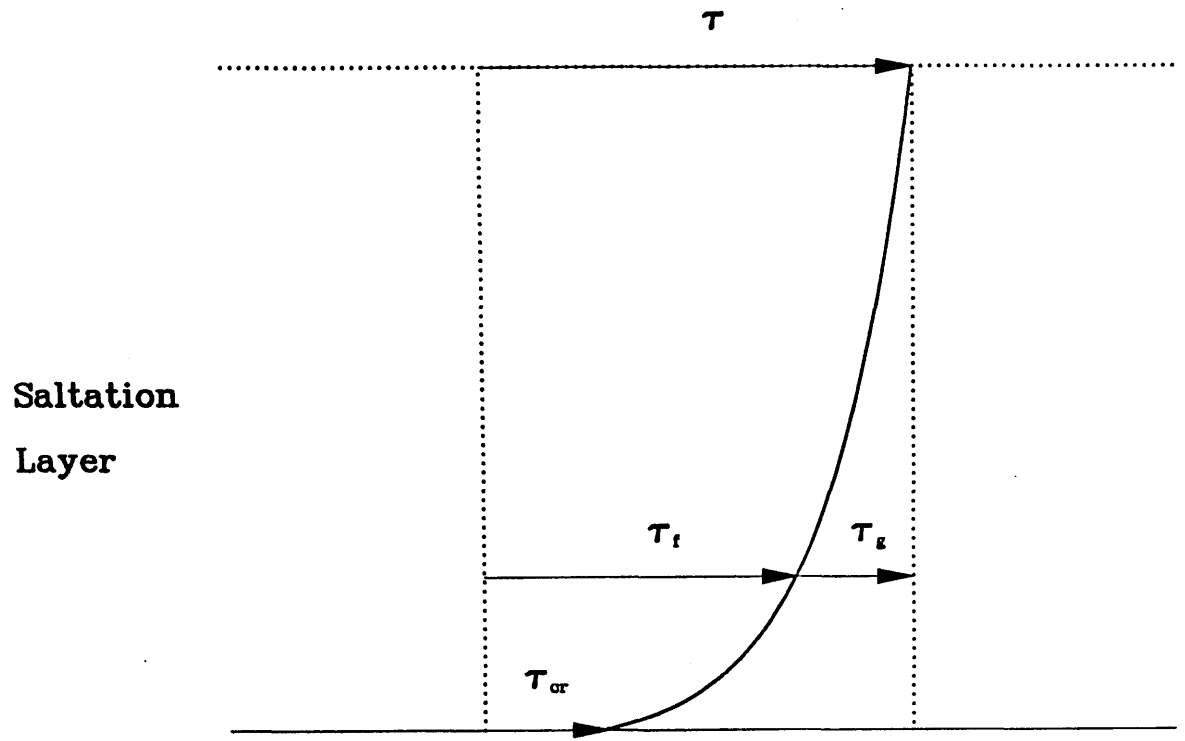

Figure 6.1 Variation in shear stress through the saltation layer

where V is the volume of a grain and c_s is the concentration of sediment. The average distance between two grains in the downstream was calculated from

$$l(z) = \frac{V}{d^2 c_s(z)}$$

so that

$$\tau_g(z) = \frac{F_D(z)}{l(z)d} = \frac{F_D d}{V} c_s(z)$$

this can be rewritten

$$\frac{F_D/A}{V/dA} c_s(z) = \frac{F_D \alpha}{A} \langle c_s \rangle c_*(z)$$

where c_* is the normalised concentration profile, summing to unity over the height of the bedload layer, $\langle c_s \rangle$ is the vertically averaged sediment concentration, A is the projected area of the particle and α is a shape factor. At the bed height, z_b, the shear carried by the fluid was assumed to be the critical shear stress for entrainment of sediment, τ_{cr}, after the argument of Owen (1964). This gives an expression

$$\tau_{gb} = \tau - \tau_{cr} = \frac{F_D \alpha}{A} c_*(z_b) \langle c_s \rangle$$

from which the average sediment concentration can be calculated.

An alternative approach is used in Sekine & Kikkawa (1992), momentum is transferred to the bed by the collision of particles, the grain shear stress at the bed, τ_{gb}, corresponds to the rate of transfer of streamwise momentum to the bed per unit area. This can be calculated from

$$\Delta M_{bx} = \rho_s V \Delta u_{pc}$$

where ΔM_{bx} is the change in particle momentum in the streamwise direction at the bed in an impact where the change in particle velocity in the streamwise direction is given by

$$\Delta u_{pc} = u_{p\text{after}} - u_{p\text{before}}$$

where $u_{pbefore}$ and u_{pafter} are the streamwise particle velocities immediately before and after impact with the bed respectively. The mean duration of a saltation can be calculated as

$$t_s = \frac{L_s}{U_p}$$

where L_s is the mean saltation length and U_p is the mean particle velocity. The grain bed shear stress can be calculated as:

$$\tau_{gb} = n_{pA} \frac{\Delta M_{bx}}{t_s}$$

where n_{pA} is the number of particles per unit area.

The grain shear stress was then used to calculate the dynamic coefficient of Coulomb friction as defined by Ashida & Michiue (1972)

$$\mu_d = \frac{\tau_{gb}}{(\rho_s - \rho) g V_s}$$

where V_s is the volume of sediment per unit area, with the usual assumption about shear stress at the bed

$$\frac{V_s}{d} = \frac{1}{\mu_d}(\tau_* - \tau_{*_{cr}})$$

which can be used in an expression for volume streamwise bedload transport per unit width

$$q = V_s U_p$$

As with the expression of Wiberg & Smith (1989) the necessary values can be obtained from the particle model.

6.2.4 Bed

The bed description in a mobile-bed model affects what the model can be used to simulate, erosion only, or erosion and deposition. The modification of the bed by

the flow can affect both the height of the bed and its composition and hence the roughness experienced by the flow.

Only the models of Naden (1987b) and Jiang & Haff (1993) include any bed description. The bed in Naden (1987b) was a 2 dimensional grid; there are therefore no lateral processes. The grid was 1,000 grains long by 50 grains high, overlying bedrock. The size of the grid was determined by the diameter of the sediment particles. The calculations were performed using grains of two diameters, 1 grid space and 2 grid spaces. The initial bed topography was flat with random perturbations of +/- one grain diameter. The calculation at each iteration consisted of calculating the movement, or otherwise, of each surface grain in turn, at the end of this calculation the surface was checked to determine whether to recalculate the flow before the next iteration.

The bed described in Jiang & Haff (1993) was also 2 dimensional, the bed consisted of 100 grains and a periodic boundary condition was applied. Particles leaving the downstream end were reintroduced at the upstream end. The bed was formed by dropping grains onto a solid base. The grains fell under the influence of gravity, their kinetic energy was then dissipated by friction and inelasticity, bringing the grains to rest. The grains forming the bed were drawn from a range of sizes to ensure that the packing produced was random, rather than a regular pattern. During a calculation the surface grains were driven by the slab model of flow already described. The base of the slab was set so that the centres of 30% of the surface particles lay within the slab. This was an arbitrary setting, a compromise between slowly shearing a large number of bed particles and imposing no drag on particles protruding from the surface. The interactions between particles affected by the flow and the rest of the bed, due to normal and tangential components of force, were then calculated to observe the effects on the bed.

6.2.5 Results of particle based models

The models of rate of sediment transport of Wiberg & Smith (1989) and Sekine & Kikkawa (1992) both produces good fits of calculated to observed rates of sediment transport. The single particle models were capable of producing appropriate values to describe the mass movement of sediment particles provided the calculation was not for a transport stage where particle-particle interactions were significant. The ideas described in Owen (1964), used in both these rate models also seem to provide a good fit between observed and calculated behaviour.

The model described in Naden (1987b) was able to generate a variable bed topography which contained small scale structures of wavelength 5-10 grains, superimposed on longer structures with wavelengths of 30-40 grains. The model also showed a response to changing hydrographs and exhibited pulsing behaviour in the rate of transport of material, due to movement of a single large grain allowing surrounding material to be entrained. All these showed that the model was qualitatively capable of reproducing observed behaviour. At a much smaller scale the model of Jiang & Haff (1992) demonstrated that calculations involving the interaction of all particles can be performed, but only at small length scales and for short durations, even though the system had been simplified to perform these calculations.

6.3.1 Observations of particle movements

The movements of sediment particles in rivers have been tracked using a variety of techniques. The simplest technique used has been to paint or dye sediment particles, either individually (Carling, 1989, Ashworth & Ferguson, 1989), or in bulk (Emmett & Myrick, 1985). The sediment particles once marked were replaced either onto or into the bed, the latter in an attempt to reproduce the entrainment behaviour of undisturbed particles already forming the bed. The position of particles were then recorded after events, either from observations of individual particles, or from

concentrations in samples for the bulk measurements. The greatest drawback with this technique is that only the positions of particles which are exposed at the surface can be recorded after an event, therefore for any individual event the fraction of particles whose position can be recorded is low.

A number of other techniques have been used which allow the tracking of particles when not directly exposed. The distribution of bulk samples have been tracked by using irradiated sand as a tracer, in the laboratory (Crickmore & Lean, 1962) and in the field (Hubbell & Sayre, 1964). More recently a variety of different techniques have been used to track larger sediment particles. Particles have been tagged with iron cores (Schmidt & Ergenzinger, 1992), magnets (Hassan *et al.*, 1991, Schmidt & Ergenzinger, 1992) and radio transmitters (Chacho *et al.*, 1989, Schmidt & Ergenzinger, 1992). All of these techniques require sediment particles of sufficient size that the form of tag in use can be embedded within the particle, for example the smallest value for the b-axis used with the radio transmitter system described in Schmidt & Ergenzinger (1992) is 60mm. The advantage of all these tagging techniques over simply colouring particles is that retrieval rates are enhanced since particles that aren't left exposed on the surface at the end of an event can still be detected. For all but the radio transmitter tagged sediment particles the techniques are limited to recording the movement of particles over the duration of an event, that is from a recorded position prior to an event to the rest position of a particle after an event. The movement of particles containing radio transmitters can be detected during an event, allowing the duration of rest periods and periods of movement and the distances travelled during the periods of movement to be measured (Schmidt & Ergenzinger, 1992).

6.3.2 Analysis of observed particle movements

The data obtained from observations of sediment particles were distances of particle movement and in some cases time in motion. In Einstein (1937) observations

of particle movements in flumes were described, these showed similar size particles moving very different distances under the influence of the same flow, while the shape of the distributions of particle movement remained constant over a number of experiments. The description of the movement of sediment as a probabilistic problem was therefore adopted by Einstein. In trying to produce a description of the distribution of particle movements he broke the movement down into two components, periods of rest and instantaneous movements. The distribution of the distances of particle movement and the durations of the periods of rest were both assumed to be negative exponential curves, which were characterised by the mean distance of travel in a movement and the mean duration of rest periods.

These assumptions were used to produce probability distributions for the positions of particles,

$$f_t(x) = k_1 e^{-(k_1 x + k_2 t)} \sum_{n=1}^{\infty} \frac{(k_1 x)^{n-1}}{\Gamma(n)} \frac{(k_2 t)^n}{n!}$$

which is the density function for x at time t, where k_1 is the reciprocal of mean step length, k_2 is the reciprocal of the mean rest period and n is the number of rest periods and movements. The results of observations were used to fit these distributions, giving values for the mean quantities of the distributions. The mean values for the quantities were derived from the distribution rather than being directly observed. The resulting fits were reasonable, showing that the ideas of the basic distributions could be used to explain the observed behaviour of sediment particles. The experiments on which this work was based were mainly performed using uniform sizes of sediment, the different particles, though of the same size, were identified as being either spherical or flat. The analysis of the distributions of particle movement found that particles of each type had the same mean step length and all particles had the same mean rest duration, these differences affected the speed of travel of the different types of particles.

The work described in Hubbell & Sayre (1964) also used the idea of exponential distributions for step length and rest period duration, with individual steps and rests independent of particle position and time, leading to the same distribution derived by Einstein (1937). The work described analysed the distribution of radioactive sand and the distribution of particles was converted into a tracer distribution, based on weight of tracer and area through which the tracer was moving. An expression for sediment transport was also derived based on the mean distance travelled by the tracer in a time and the depth of bed through which this transport was occurring. The data for this calculation and the parameters for the distribution were derived from the observations, giving values for the mean step length, mean duration of rest period and the mean velocity. Once these values had been calculated the curves calculated from the distribution functions could be calculated and compared with the observed distribution of tracer, once again showing a reasonable fit.

The experiments of Crickmore & Lean (1962), used radioactive sand as a tracer and were used to calculate transport rate but mean particle velocity was calculated directly from observed distribution curves. Attempts were made to fit distributions based on an equal probability of each particle moving a constant distance in a time interval. This gave a Poisson distribution when the probability of movement was small and the number of movements large, with further increase in the number of movements the distribution tended to a Gaussian distribution. The distribution shows similarities to observed behaviour. The major difference was in the amount of tracer remaining at the origin. The calculations assumed an equal probability of movement for all particles, observations showed that some particles lower in the bed were not exposed to the flow for long periods of time and remained at rest for long periods of time. The assumption of equal probability of movement was too simple. Extension of the model to a two-layer model improved the fit of the model. The probability of movement in the two layers represented the passage of shallow and deep ripples, with a greater probability of movement from the shallow layer.

All of the work described to this point was performed in very steady, homogeneous systems, either laboratory flumes or rivers with very steady flow regimes. When tracers are used in more usual river regimes the movement over an event will be due to a range of flows occurring during a hydrograph, the bedform can also significantly affect particle behaviour. The rest of the work described here attempts to analyse the behaviour of particles moving in such systems.

Data on particle movement from a number of different sources were analysed in Hassan *et al.* (1991) and Hassan & Church (1992). The data were fitted with the distributions developed in Einstein (1937) and Hubbell & Sayre (1964) and also with a two parameter gamma distribution. The gamma distribution was used as an alternative description since the homogeneity condition that the earlier distributions were based on was not met. The gamma distribution was used with the mean step length used as one parameter, the other parameter, corresponding to the number of movements made, n, was then used to fit the curve to the observed distribution, giving a density function

$$f_t(X) = \frac{(k_1 X)^{n-1} k_1 e^{-k_1}}{\Gamma(n)}$$

where $X = L/\langle L \rangle$, the step length over the mean step length, $k_1 = 1/L_0$ and $L_0 = \sigma_L{}^2/2\langle L \rangle$, where σ_L is the standard deviation of the step length. The assumption behind the use of the number of movements made in this distribution was that all the particles would move approximately the same number of times during an event. The two parameter gamma distribution gave a similar level of fit as the earlier distribution.

The fitting of gamma distributions to observed distributions of particle movements was also performed by Kirkby (1991). The first distribution Kirkby fitted to data of particle movement was a negative exponential distribution defined

$$n_p = n_{0p} e^{-(k_1 x)}$$

where n_{0p} is the number of particles initially in motion, n_p is the number of particles travelling a distance greater than x and k_1 is the reciprocal of the mean step length, $\langle L \rangle$.

This was found to give a reasonable fit to observed behaviour of particles over an event. This distribution was then generalised from that for a single movement to a form for n hops, which gave a Gamma function of order n, with a mean travel distance $n\langle L\rangle$,

$$f_n(x) = \frac{x^{n-1}}{L^n n!}$$

the density function for a particle travelling a distance x in n hops. This gave a slower drop away from 100% of particles remaining in motion to the extent that the simple negative exponential curve gave a better fit to observations. However the mean travel distance increased with the number of events, a feature present in observations.

As a result the fit of a mixed gamma model to the data was examined, in which a proportion, p of stones moved at each event and $\langle L\rangle$ was the mean travel length. Examination of this distribution showed that for a low value of p the curves matched the original negative exponential curves, with increasing values of p the mean distance travelled increased with the number of hops, though still taking an exponential form, higher still and the curve showed the initial flattened behaviour of the gamma distribution. The mixed gamma distribution with a value of p=0.5 gave the best fit showing the observed initial slow decay of the exponential curve. Since the number of hops is usually unknown an alternative form of p was also used

$$p^* = 1-(1-p)^n$$

to represent the total probability of motion for an event. The distributions from this function were relatively insensitive to n until p^* tended to 1. The fitting of such distributions to observations showed that they were capable of explaining a large part of the distribution. The final conclusion of Kirkby suggested that the negative exponential curve was appropriate where some particles remained in their original positions. Where all particles moved gamma distributions, whose derivation was based on the same assumptions as the negative exponential were suggested, the order of distribution being chosen as that giving the best fit.

6.3.3 Results of observations of particle movements

Observations of particle movement showed that the distances of movement of particles were best described by distributions rather than mean values. The fitting of probability curves to observed distributions of particle movement show that these distributions can be described using simple distribution curves, such as negative exponential or gamma distributions. These have been fitted to data collected under steady conditions and for movements of particles occurring over hydrographs. The exact terms used within the distributions varies, those for steady conditions were based on distributions of time and distance travelled in single movements, those for movements over hydrographs substituting a distribution of movement during the hydrograph and the number of movements making up the total distance travelled. Observations of particle movements for a range of particle sizes and shapes (Schmidt & Ergenzinger, 1992) showed that negative exponential and gamma distributions fitted observed particle movements but that the distributions varied with particle size, weight and shape, the flow and the bed.

6.4 Conclusions

The results of calculations of particle motion show that models based on particle calculations can be used to describe both sediment transport and its effect on bedform development with some success. However the calculations of bedform development of Naden (1987b) and Jiang & Haff (1993) are limited since in both cases the movements of individual particles are described, requiring significant amounts of both computing power and memory.

The results from observations of particle movement show that rather than using single mean values for quantities like distance travelled by particles, as in Naden (1987b) the movements of sediment particles are better described by distributions. Analysis of the results of particle movement shows that some form of Gamma (or

negative exponential) distribution are capable of providing good fits to the observed movement of particles, for homogeneous and heterogeneous systems. The results described in Schmidt & Ergenzinger (1992) show that the parameters of distribution curves vary with flow, grain size, grain shape and also bed profile.

Direct calculation of movement of sediment particles will always be computationally intensive, but observations show that fairly simple distributions can be used to describe the movement of particles while retaining stochastic effects on the distribution of particle movements. Observations also show that the parameters describing such distributions vary with a number of variables. While difficult to collect data on this variation in the field, distributions of particle movement can easily be calculated across ranges of parameters. Calculation of such distributions is described in the next chapter, their application to modelling sediment transport in the one after.

Chapter 7

Distributions of particle movement

7.1 Introduction

The models reviewed in the previous chapter were of two types, those based on numerical models of particle motion, which were deterministic in nature, and those based on analysis of observations of particle movement, which were stochastic in nature. In the deterministic models the movements of particles were considered as a series of saltations. In the stochastic models the movements of particles were considered as a series of movements. The models of rate of transport of sediment of van Rijn (1984), Wiberg & Smith (1987) and Sekine & Kikkawa (1992) analysed saltations to calculate quantities describing the mean characteristics of saltations, length, height and the variation in time spent at heights by particles, these quantities were then used in the analysis describing the rate of transport of sediment. The models of particle movement based on the analysis of particle movements from tracer experiments, either laboratory or field experiments attempted to describe the distribution of particle movements and the rest periods between them, either for steady flow conditions (Einstein, 1937, Crickmore & Lean, 1962, Hubbell & Sayre, 1964), or over the duration of an event (Hassan *et al.*, 1991, Kirkby, 1991).

Another use for particle based models is to examine the development of bedforms, the ultimate aim of this work. Of the particle models described in the previous chapter only two calculated the effects of the motion of particles on the development of bedform, Naden (1987b) and Jiang & Haff (1993).

The use of deterministic models to derive expressions for rate of sediment transport does not provide a direct route to the calculation of bedform development. The direct calculation of the movements of individual particles is limited in its

application by the availability of computing resources, an alternative approach to describing particle movements in sediment transport is therefore required. In this work an approach based on the use of distributions of particle movement is examined, this would allow the results from the calculated motion of large numbers of particles to be used in calculations of sediment transport and its effects, while avoiding the need to calculate all these movements at the time the sediment transport calculation is performed.

The observations of particle movements from field observations show a wide range of values for distance travelled and therefore the use of distributions rather than mean values to represent particle movements will enable the movements to be represented more realistically. The reasons for these distributions of particle motion can be seen in the stochastic nature of the bed and the turbulent flow over it. The bed gives a range of initial particle heights and a range of positions at which particles can impact and be deposited. The turbulent flow can influence initial particle motion and particle movement. The size and shape of particles can also influence the conditions under which a particle moves. The number of particles used to calculate the distributions of particle movement from field observations were limited by the ability to retrieve particles and by the time required to track each particle. The calculation of distributions of particle movement using a model of particle movement do not suffer from this problem, can include many of the effects influencing the distribution of particle movement described above, and can be made using a modified version of the model described in Part I of this thesis. The calculation of such distributions is described in this chapter, their possible use in modelling sediment transport and bedform development is considered in the next.

The work described in this chapter consists of the modifications to the single particle model necessary to calculate distributions of particle movement and how these calculations were performed. The range of calculations performed and the results obtained will then be described.

7.2 Modelling particle movement

The model used to calculate particle movement for the distributions is based on the single particle model described in Part I modified so that calculations are performed for particles initially at rest and continued until particle motion ceases, rather than calculating the properties of particle motion, over a fixed distance, for a particle initially in motion. The single particle model already contains descriptions of particle entrainment and deposition. The effects of turbulent fluctuations on entrainment are described in Section 5.4.3. The second modification to the model was in the description of the bed and the effects that this had on the other components of the model. The model of the bed used in the previous calculations of particle motion is greatly simplified, being reduced to a row of touching spheres, the diameter of the spheres being equivalent to the roughness length scale used in the experiments with which comparisons were being made.

7.2.1 Description of bed

The description of the bed used here is based on that of Sekine & Kikkawa (1992). Their model calculated the effects of impacts in 3 dimensions, the bed description therefore had to include both a streamwise and transverse component. In plan view the bed of their model consisted of a series of rows spheres of identical diameter, with their centres a diameter apart in the streamwise and transverse directions. The heights of the particle centres were selected from a truncated Gaussian distribution, formed about a mean position with a standard deviation of $d/3$, where d, was the diameter of the bed particles. The distribution was truncated at +/- 3 standard deviations. This description was obtained from analysis of video of the bed surface when saltation was occurring. The only other condition imposed on the bed was that the vertical separation between adjacent particle centres was always kept below that which would exceed the angle of repose. The height of the bed at the upstream end of

the calculation was defined from the rest height of the moving particle, the choice of the value for this is described in section 7.2.2.2.

In this model only 2 dimensions are considered, the particle centre heights are calculated from a truncated Gaussian distribution as described above and checked for the angle between centres. If it is below the angle of repose the value is accepted, but if above the angle of repose a new value for the particle centre height is selected from the distribution, Figure 7.1a.

7.2.2 Effects of bed description on model

The bed description affects other components of the model, not changing the nature of the components but modifying coefficients.

7.2.2.1 Flow

The effects of the model of the bed on the description of the flow are seen in the decisions as to how to define an appropriate roughness length scale, k_s, and where to set the zero height of the velocity distribution with respect to the position of the heights of the particle centres forming the bed. The roughness length scale k_s is set equal to the diameter of the particles forming the bed, d. Sekine & Kikkawa (1992) found k_s to increase slightly with transport stage, however, at low values of transport stage the approximation of k_s to d seems reasonable. It is assumed that the zero height of the velocity distribution would be at a height of $0.2k_s$ below the top of particles with their centres on the mean centreline height of the distribution. The calculation of the mean velocity profile and fluctuating components of velocity with respect to this position used the burst/sweep model described in Part I.

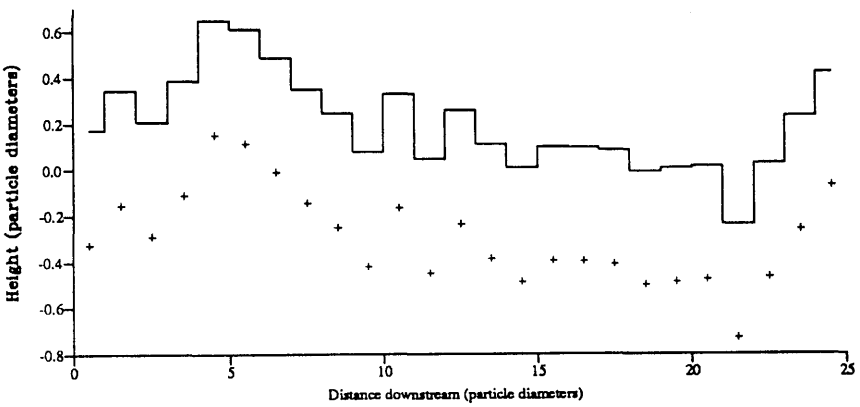

+ particle centre heights
solid line shows position of particle top

a) Particle centres and height of particle tops in bed

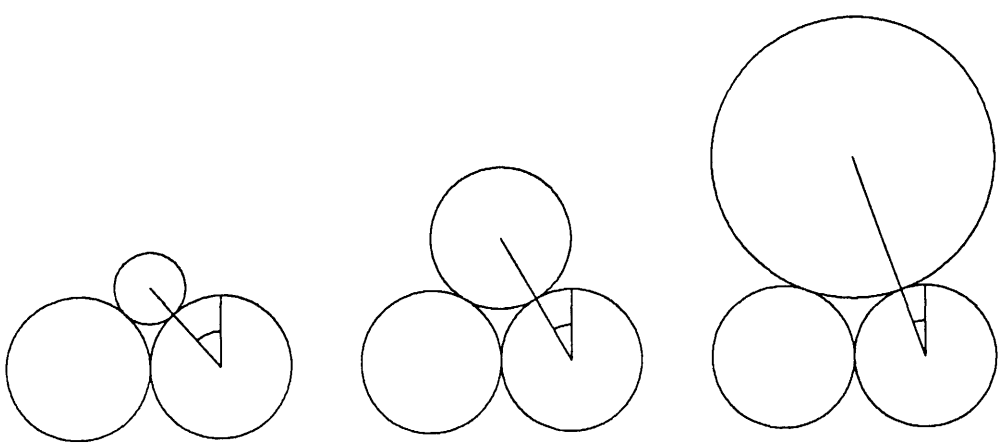

b) Initial particle positions

Figure 7.1 Geometry of bed

7.2.2.2 Sediment movement

The description of sediment movement is not affected by the different description of the bed. The descriptions of particle entrainment and deposition are affected, but only insofar as the new bed geometry and the change to calculation of distributions of movements affected them, not in the description of the process.

The bed description used in Part I has only one rest height whereas the truncated Gaussian, used to described the distribution of particle centre heights here, has a range of possible rest heights. Of the possible rest heights a certain range results in the centre of the particle to be entrained lying below the zero velocity height, allowing no mechanism for the particle to be entrained in this model. The rest of the possible centre heights are discretised into 4 sections, $0.2k_s$ in height. This discretisation is performed to enable a discrete description of the bed for use in models of bed development, it also allows comparison of entrainment rates from the different levels.

The moving particle centre heights are uniformly distributed within each of the levels. The height of the moving particle's centre is used to calculate the centre height of the particles forming the bed, assuming the two particles supporting the moving particle are touching each other and have their centres at the same height, Figure 7.1b. The use of the moving rather than the bed particle to define the bed particle heights means that the full range of bed particle centre heights will not be used.

The deposition process was modified so that in addition to particles being deposited when they rolled or fell back after an impact, particles are also considered to be deposited when the position of the particle centre was calculated to be below the zero velocity height of the flow. By definition there is no mean flow velocity below this height and the magnitude of the standard deviations of the velocity fluctuations are scaled from the mean flow velocity. It was therefore assumed that any particle falling below this height would lose too much momentum to rebound into the flow.

7.2.3 Calculation of distributions

The distributions of particle movements were calculated on the Meiko Computing Surface at Lancaster University, using Inmos T800 transputers. The calculations were performed using a master-slave configuration of processors, in most cases using 5 slave processors, though the number of slave processors could be modified depending on the loading of the system.

The master process was used to send initial conditions for calculations and receive the results from slave processes and to output these results to file. No computation of particle movement, or analysis of results were performed in the master process. The slave processes were used to calculate groups of particle tracks for specified flow and initial particle conditions. For any particular combination of moving particle size, initial height and bed particle size 1,000 particle tracks were calculated. The calculations on the slave processors were performed in groups of 50, between receiving initial and boundary conditions and returning results to the master. The calculations were performed in this way to spread the calculation load evenly between processors, it meant that the maximum number of particle tracks any processor would have to calculate when all the other processors had finished was 50. All the particle tracks for a flow condition were calculated at the same time. The calculations typically took 12 hours when 5 slave processors were used.

7.2.4 Calculations performed

The particles whose movements were calculated were of a relative density of 1.24, this is a low density suitable for comparison with the data of Abbott l& Francis (1977). For gravel a relative density of 2.65 would be more appropriate. All the calculations were performed for a flow depth of 9.6cm over a bed formed of particles of diameter 0.828cm. The distributions of particle movements were calculated for particles of size $d/2$, d, and $2d$, where d was the diameter of the bed particles.

Distributions were calculated for transport stages from 0.1 to 1.9, for different sizes of particles moving over a bed formed of a single size of particles for a range of initial particle heights. The values of shear velocity, calculated from the transport stage used to define the flow conditions, were those for a particle of diameter *d*. For each combination of variables the tracks of 1,000 particles were calculated enabling a distribution of particle movements to be described. Each particle track was calculated over a different bed surface, the initial particle height was used to set the height of the first bed particle as already described, the rest of the bed was then calculated from the truncated Gaussian distribution described.

Calculations were performed for a range of initial particle heights. The range of heights of particle centres in the bed were considered to be split into 11 segments for the purposes of describing the bed. Of these segments 4 were above the zero height of the velocity distribution so entrainment was only considered from these segments. Within each of these segments the initial particle heights were selected from a uniform random distribution. This is equivalent to a uniform distribution of initial particle heights above the zero velocity height. The distribution of initial particle heights was only split into segments to allow comparisons of entrainment rates and particle movements for particles initially at rest at different heights within the bed.

Each calculation of particle movement was calculated for a particle initially at rest until it came to rest again. The variation in initial particle height and fluctuations in the flow meant that particles were not always entrained into the flow immediately. The data output to describe these movements was time in motion, distance travelled and the total difference in particle velocity at impact over the movement. This last was calculated by summing the change in horizontal particle velocity at each impact with the bed. This was used to calculate the momentum extracted from the flow.

7.3 Results

The results describing each calculated particle track were output from the program non-dimensionalised with respect to the conditions for the particle of diameter d for the transport stage at which they were calculated. To allow comparison of results at different transport stages they were all then non-dimensionalised using the conditions at a transport stage of 1.5. The transport stage referred to in all figures and the text are those for a particle of diameter d, unless otherwise stated. The results output from the calculations were analysed to give descriptions of entrainment, movement and momentum extraction and deposition.

7.3.1 Entrainment

The results for each set of 1,000 particle tracks were analysed to find the number of particles entrained and the number remaining at rest. The results are plotted here as fractions of the total number of particle tracks analysed.

The fraction of the particles remaining at rest for a specified time are shown in Figure 7.2 and 7.3. Figure 7.2 shows the fraction of particles remaining at rest for a particle of diameter d across a range of transport stages, Figure 7.3 shows the same information for a transport stage of 1.0 for all three sizes for which calculations were performed. The curves for each of the conditions show an initial decay curve which is truncated, followed by a second decay curve following the first. These results represent two different types of behaviour by particles. The first is due to a particle rolling back instead of forward at the start of the calculation. During the calculation of rolling motion the only condition checked for is whether a particle looses contact with the bed. The position is only checked for at the end of an iteration. If as would be found for a particle rolling back from rest, the particle is below the bed the motion is stopped, particle motion therefore ceases after one iteration with the particle at its initial rest position. This type of behaviour accounts for the first part of the decay

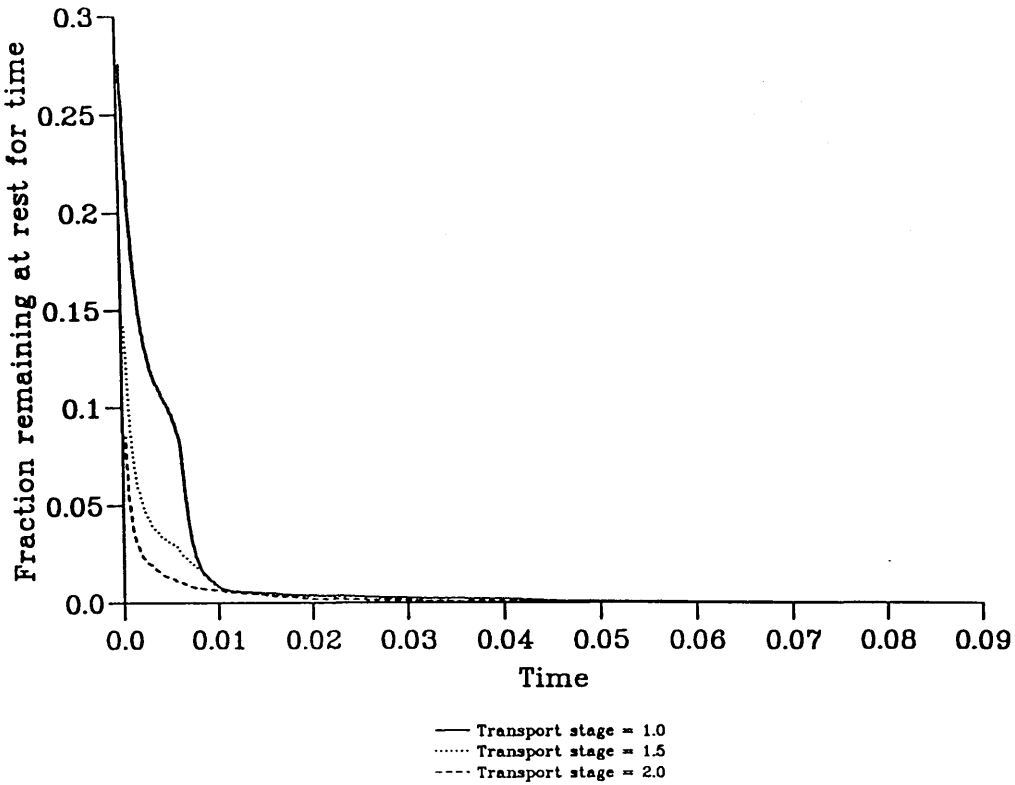

Figure 7.2 Fraction of particles remaining at rest for specified time, variation with transport stage

Units non-dimensionalised with respect to flow depth and mean bed shear velocity

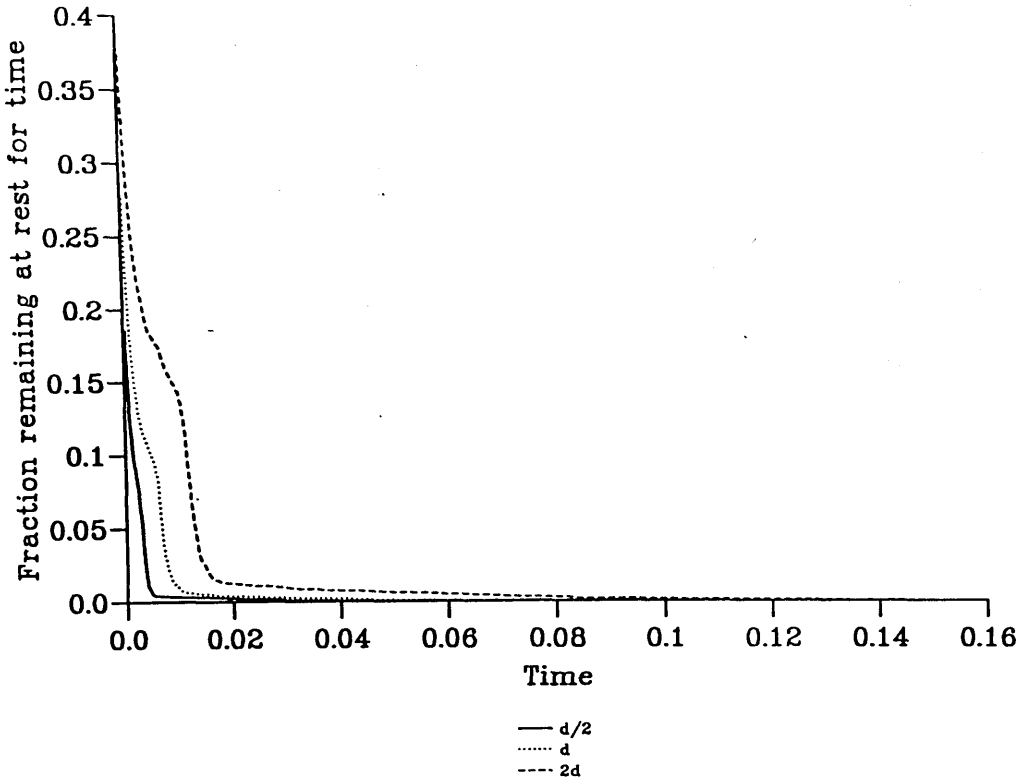

Figure 7.3 Fraction of particles remaining at rest for specified time, variation with particle size

Units non-dimensionalised with respect to flow depth and mean bed shear velocity

curve, this curve is truncated at the limit of the duration of an iteration. The variation in iteration duration, giving rise to this curve, occurs because the durations of iterations are calculated as fractions of the particle response time and the fluid integral length scales. These time scales are functions of height and for the particle response time the initial flow velocities, so the iteration duration varies with initial particle height and initial flow velocities. The second type of behaviour, accounting for the long tail of the curve is due to particles which start rolling forward in the initial turbulent eddy but do not either loose contact with the bed or reach the top of the first bed particle before moving into another eddy which is incapable of continuing to move the particle forward, the particle then rolls back to rest at its initial position. The fraction of particles exhibiting the first type of behaviour diminishes with increasing transport stage as the flow becomes competent to entrain a particle for a greater proportion of the time, Figure 7.2. The fraction of particles exhibiting the first type of behaviour also diminishes with decreasing particle size. Since each set of calculations were performed at a constant shear velocity this equates to an increase in transport stage with decreasing size and so the behaviour is as described above for variation with transport stage.

Though the information on fraction of particles remaining at rest at a time can be used to indicate what fraction of particles are entrained immediately it does not give a full distribution of time to entrainment. To produce a full distribution of time to entrainment the calculation would have to be continued until the particle came to rest having moved from its initial position.

The variation in the fraction of particles entrained at the different initial particle heights are shown for a single transport stage in Figure 7.4. As would be expected there is a trend of increasing numbers of particle entrained with increasing initial particle height and decreasing particle size. The variation due to initial particle height occurs because particle centres lower in the flow experience lower flow velocities and are therefore less likely to be entrained. The variation due to particle size occurs

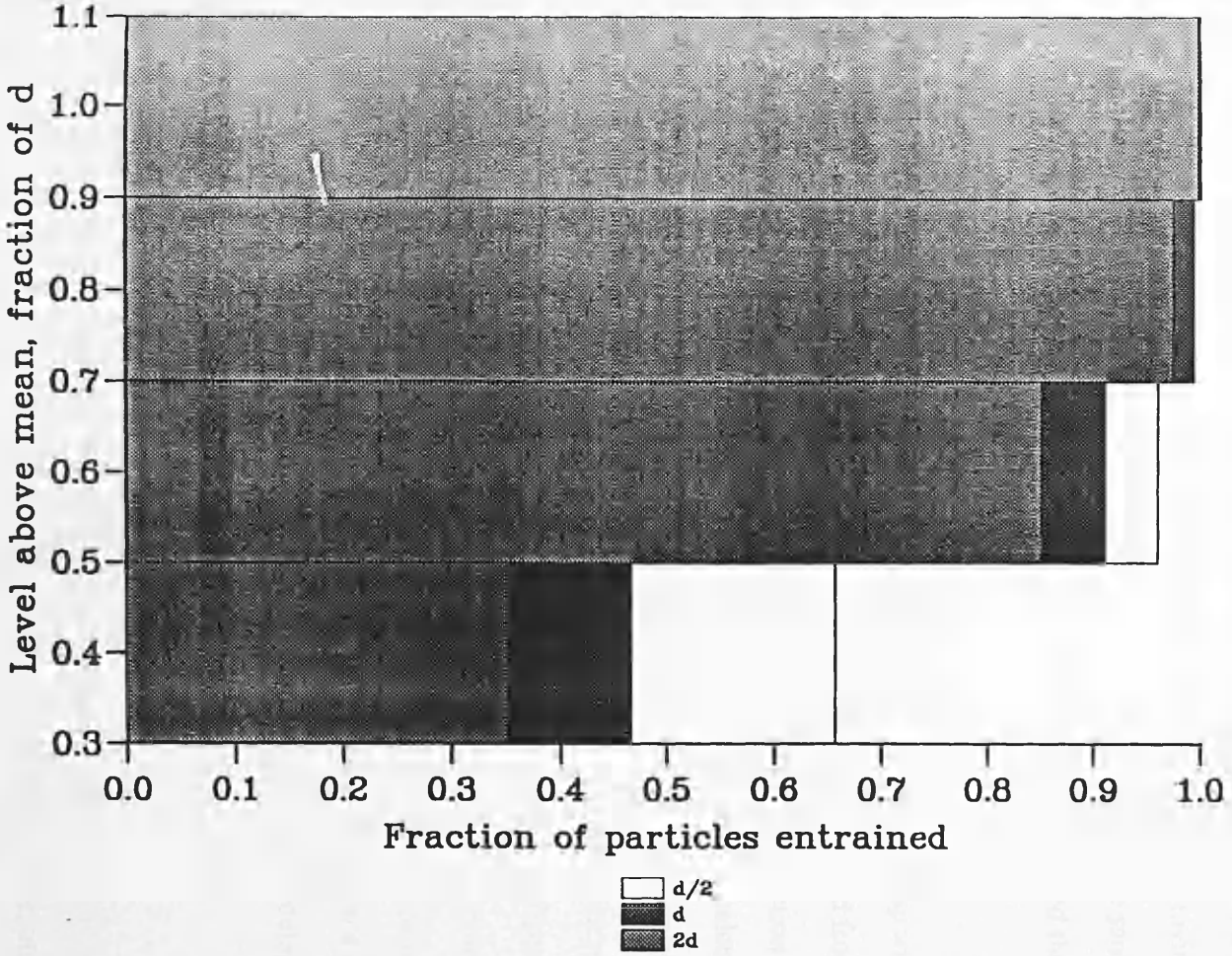

Figure 7.4 Fraction of particles entrained, variation with initial particle height and particle size

because the smaller particles require smaller forces to initiate particle movement though for the initial particle configuration used here must pivot through a greater entrainment angle, Figure 7.1b. If a Shields stress criterion was used to describe the critical shear stress for initial particle motion the critical shear stress would be directly proportional to the diameter of the particle. The pivoting analysis used here including relative sizes of moving and bed particles and the height of the moving particle in the flow modifies the entrainment condition for a particle but for the same particle centre height a particle of diameter $d/2$ is still more likely to be entrained than one of diameter d.

The fraction of particles entrained across a range of transport stages can also be examined and are shown in Figure 7.5. As would be expected from the description of the variation of entrainment with initial particle height the fraction entrained increases with increasing particle height. The transport stage is calculated as U_*/U_{*cr}, where U_{*cr} is calculated assuming a Shields stress of 0.06 for a particle of size d. The use of a single value critical Shields stress ignores the fact that different rest geometries change the value of critical Shields stress. The inclusion of the effects of turbulence in the model varies the value of shear stress acting about the mean value, enabling entrainment to occur when the mean shear stress is below that required for entrainment. These factors explain why entrainment occurs below a transport stage of 1.0, even for a particle of size d, on which the transport stage calculations were based.

7.3.2 Movement of particles

The movements of particles were described by time in motion and distance travelled; the variation of these values with respect to particle size, initial particle position and transport stage will be considered. This section will mainly consider the movement of particles, deposition rates will be considered in the next section, except where necessary to describe the particle movements.

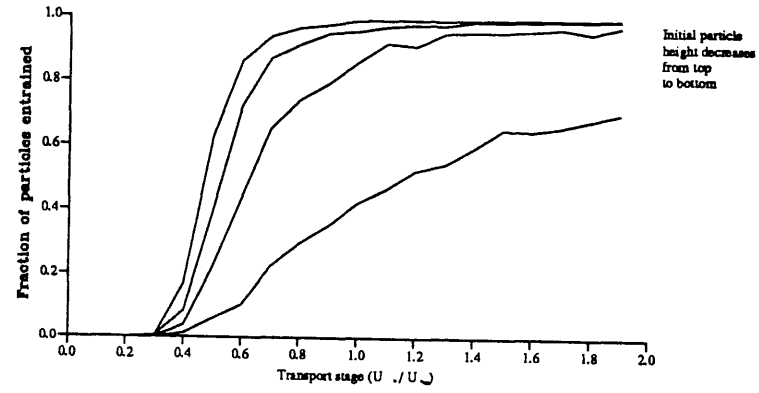

a) Particle diameter = d/2

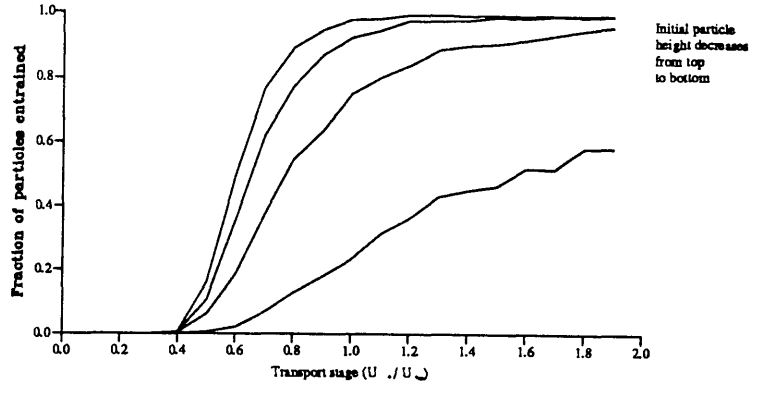

b) Particle diameter = d

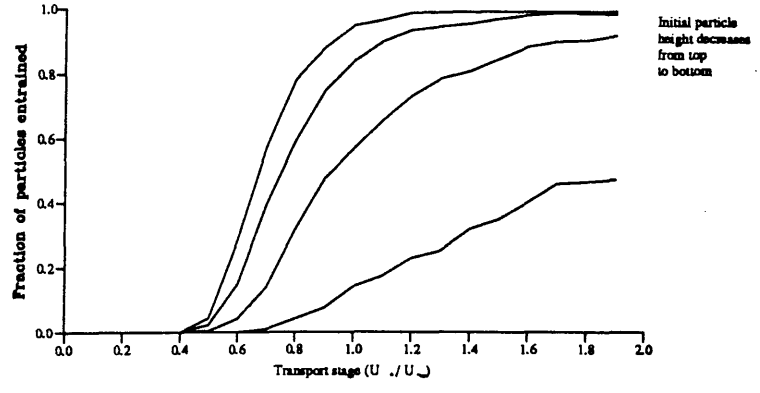

c) Particle diameter = 2d

Figure 7.5 Variation in fraction of particles entrained with transport stage and height

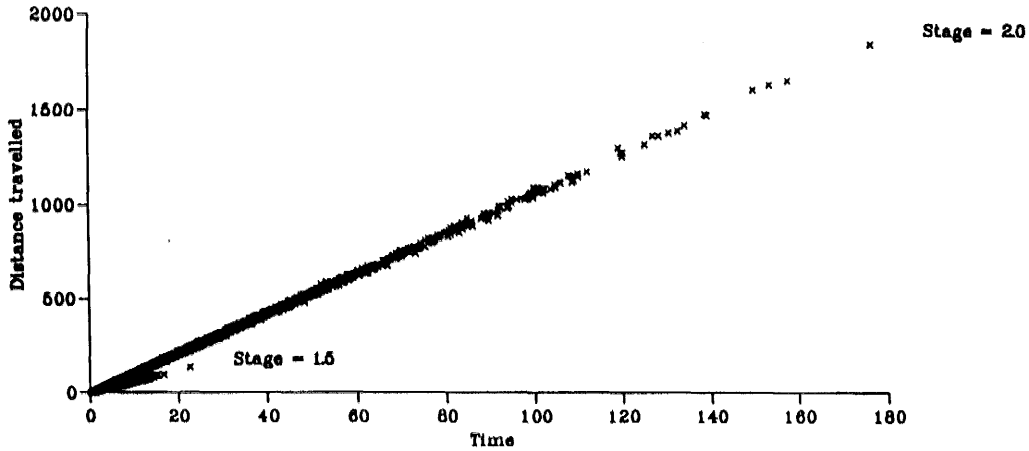

a) Full scale

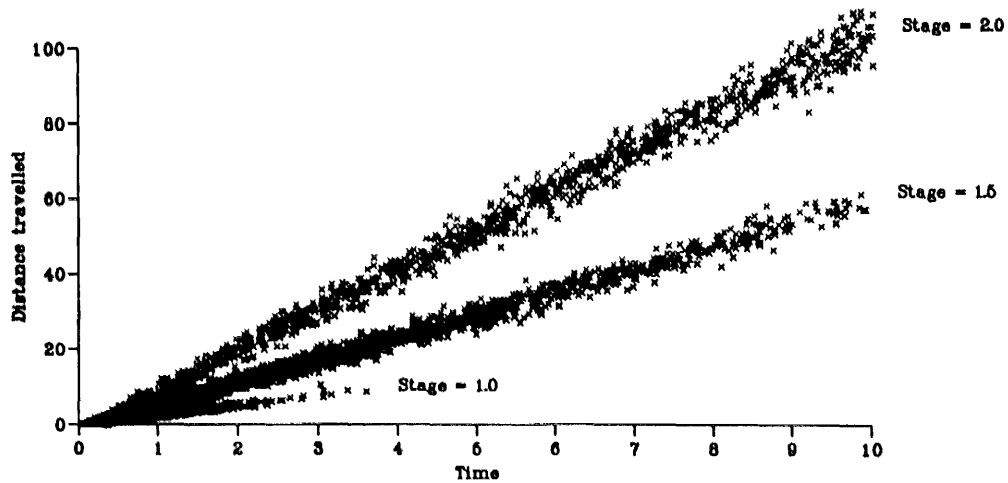

b) Detail

Figure 7.6 Distance travelled against time in motion

Units non-dimensionalised with respect to flow depth and mean bed shear velocity

A plot of distance travelled against time in motion is shown in Figure 7.6, for a single particle size at a number of transport stages. The plot shows all the calculated particle movements at each transport stage, that is the particle movements from each of the initial heights are plotted together. The graph in Figure 7.6a is scaled to show all the particle movements including the largest movement at the highest transport stage, in Figure 7.6b the same data is shown rescaled to show the particle movements at the lower transport stages while truncating the larger movements. At these scales the relation between distance travelled and time in motion appears to be linear at each of the transport stages, with a limited amount of scatter about a linear fit. This means that the calculated particle velocity for a single particle size over the range of movements remains constant.

Since the relation between distance travelled and time in motion appears to be linear the data points were fitted using a least squares fit using the Nag routine G02CAF (NAG, 1991). The values of the slope obtained from this fit, that is the particle velocity across the calculated range of transport stages are shown for each particle size in Figure 7.7. The graph shows that all particle sizes are calculated to move at similar velocities for the same shear velocity. The break in curve at the start of each of the curves indicates where the majority of particles start to move in saltation, which can be described using the linear fit. Below this stage the particle move by rolling and the linear fit does not adequately describe the behaviour of the particles. This condition will be described further later in the chapter.

The effect of varying initial particle height on the movement of particles is shown in Figure 7.8 for each of the three particle sizes at a transport stage of 1.5. The curves show similar distributions for particle diameters of $d/2$ and d, but that for $2d$ shows a different distribution. The initial particle height does not affect particle movement for the particles of diameter $d/2$ and d at this transport stage. The cause of the different distribution with height for the particle of diameter $2d$ is that the transport

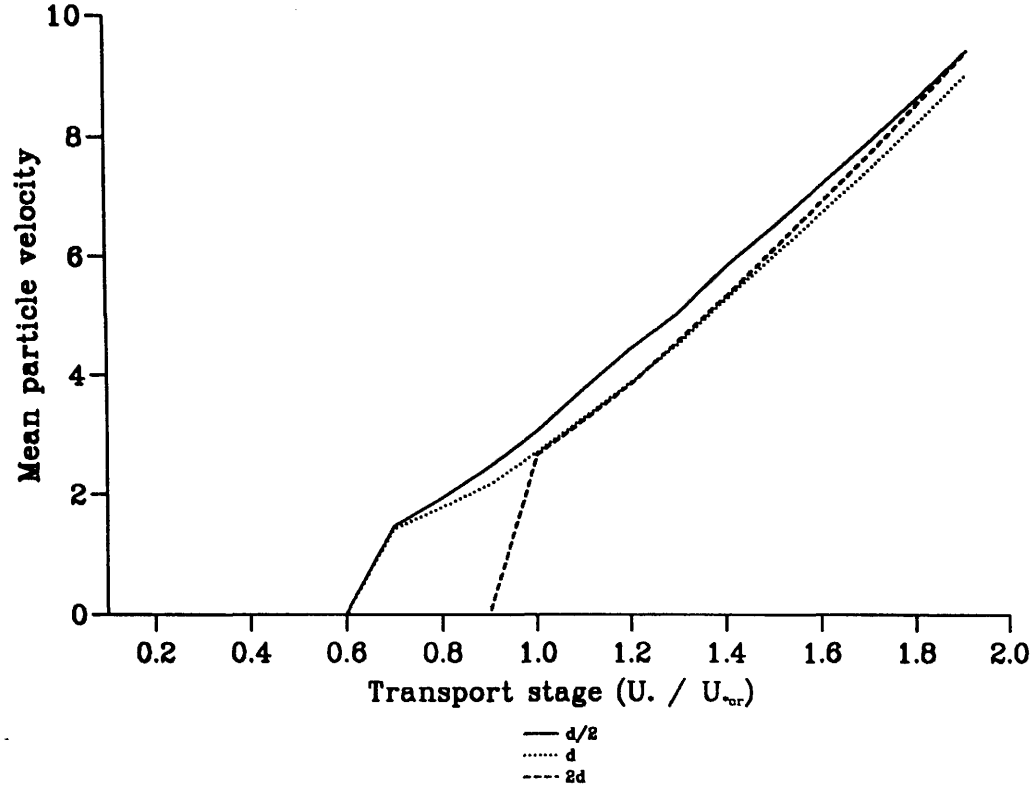

Figure 7.7 Variation in mean particle velocity with transport stage

Units non-dimensionalised with respect to flow depth and mean bed shear velocity

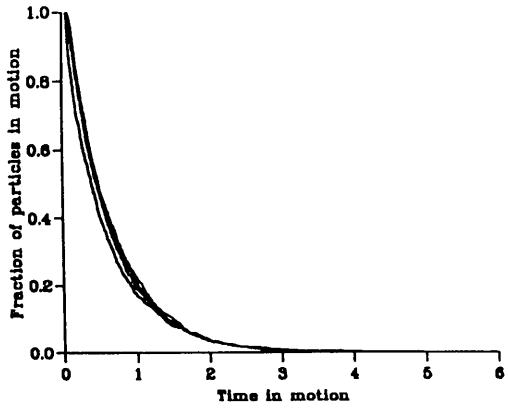

a) Particle diameter = d/2

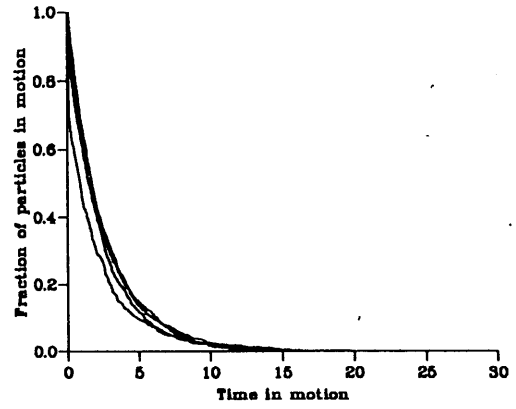

b) Particle diameter = d

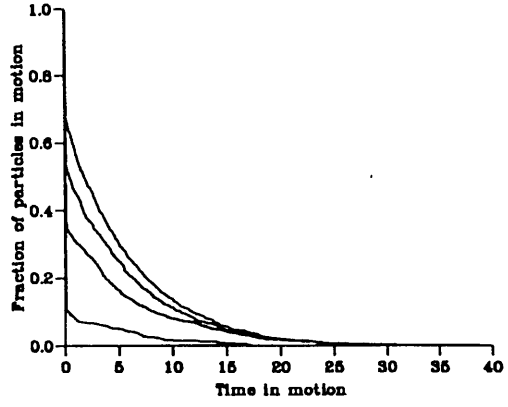

c) Particle diameter = 2d

Figure 7.8 Effect of initial particle height on time in motion
Units non–dimensionalised with respect to flow depth and mean bed shear velocity

stage is close to the entrainment condition and many particles are only moving one or two particle diameters, those lower in the flow never move high enough into the flow to speed up and so only move the one particle diameter before coming to rest, those higher in the flow can be entrained into longer distances of movement, higher curves are higher initial heights.

The effect of particles only moving a short distance, one or two particle diameters is present at all stages, the importance of this effect on the distribution increases as the transport stage approaches the critical stage for motion for a given size of particles when increasing numbers of particles in the distribution of motion move in this fashion. The distribution of particle movements in time and space can be seen in Figure 7.9, the graph plotted in Figure 7.9b is an enlargement of the region near the origin of that shown in Figure 7.9a. The cluster of points near to the origin are those where the particle moves from its initial position to the next rest position between particles. The scatter in distance travelled being due to the range of different bed geometries used in the calculations giving a scatter of rest positions.

7.3.3 Deposition of particles

The other information describing particle motion is time or distance to deposition. The section on movement of particles shows that the linear relationship between distance travelled and time in motion breaks down where the particle only moves a short distance, one or two particle diameters. However plotting time in motion gives a good indication of particle behaviour. In Figure 7.10 the fraction of particles remaining in motion after a time are shown for each particle size. The effects of only moving one or two diameters can be seen in the rapid drop in the fraction remaining in motion for the particles of diameter $2d$ and to a lesser extent the particle of diameter d. The other obvious feature is that once in motion the larger particles tend to stay in motion longer. These effects are both due to the greater mass of the larger particles, larger particles require a greater transfer of momentum from the flow to be entrained into the flow, but once in motion move with a greater momentum

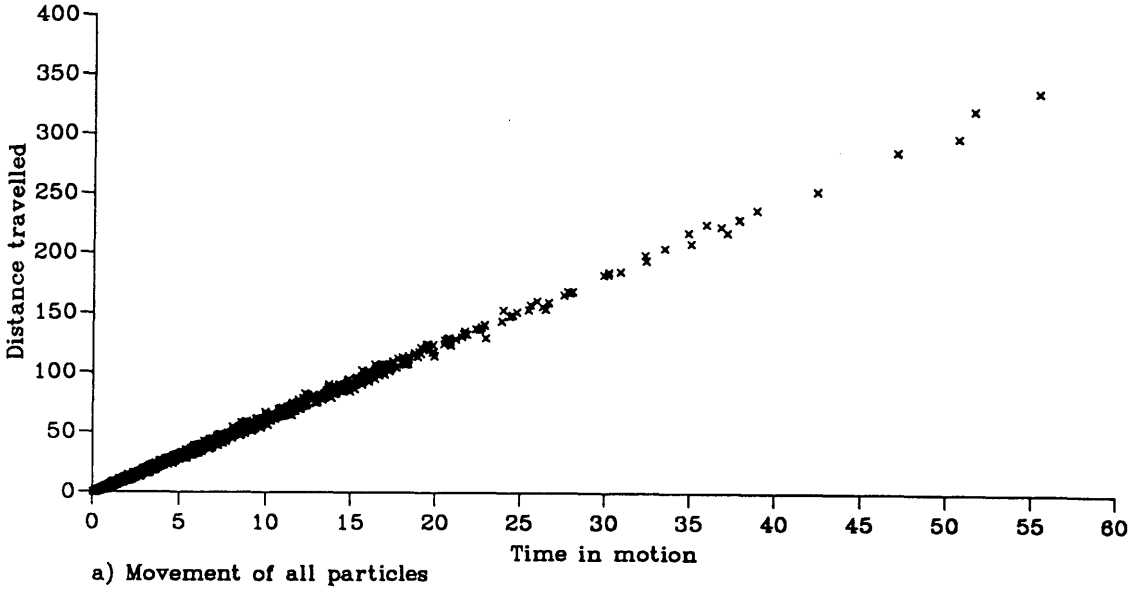

a) Movement of all particles

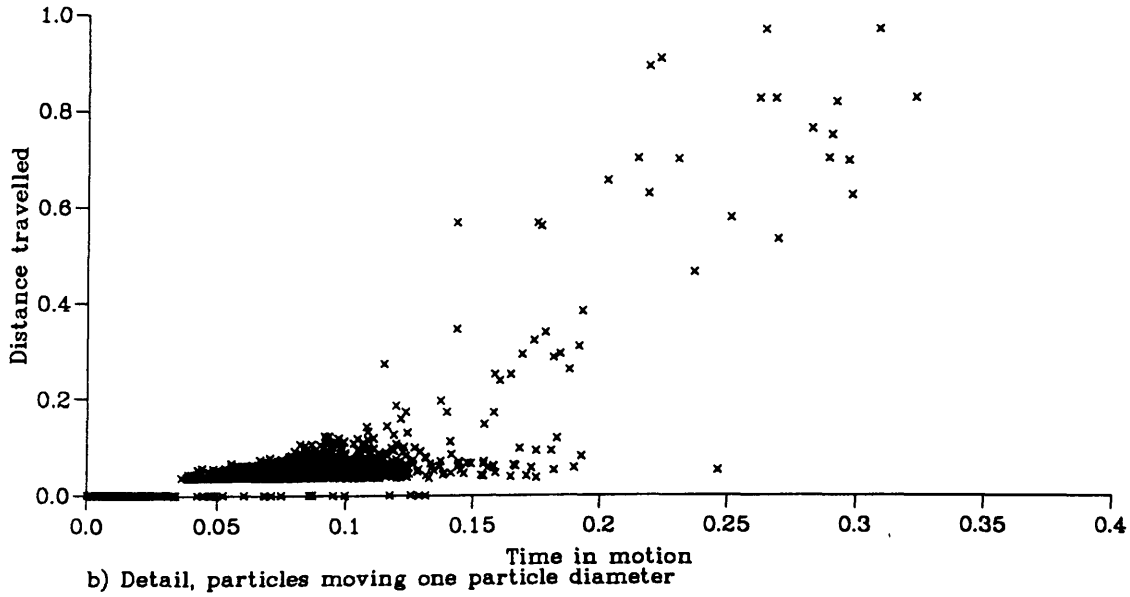

b) Detail, particles moving one particle diameter

Figure 7.9 Comparison of particle movement types

Units non-dimensionalised with respect to flow depth and mean bed shear velocity

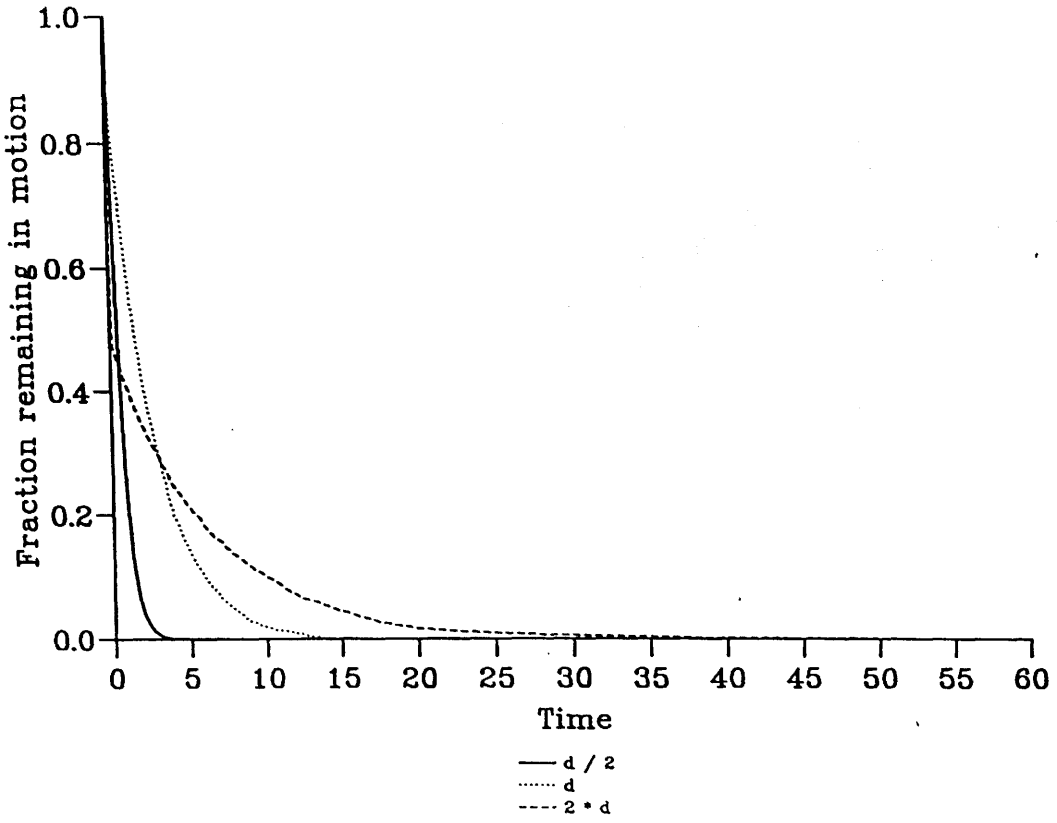

Figure 7.10 Fraction of particles remaining in motion for time, variation with particle size

Units non-dimensionalised with respect to flow depth and mean bed shear velocity

allowing movement to continue after impact, also the larger particles cannot fall into holes in the bed in which smaller particles can be trapped. This distribution of time in motion shows that though different size particles are calculated to move with a similar velocity at the same shear velocity, large particles will move further in a single movement at higher transport stages.

The mean values of the distance travelled of each distribution are plotted in Figure 7.11a, the transport stage in this figure is that for the bed particle size. This shows smaller particles moving further at lower transport stages, though only up to mean distances of travel of 1 or 2 particle diameters, beyond this distance the importance of the bed in trapping particles begins to influence the distribution of distance of movement of particles and the larger particles begin to show larger distances of travel. The results show a much wider distribution of mean distances travelled by particles than the simple 100 times the particle diameter suggested in Einstein (1950). The mean values of distance travelled are compared with an expression fitted by Sekine & Kikkawa (1992) to the results of their calculations of particle movement; only the data for the particle of diameter d is plotted (Figure 7.11b). Though the curves are different the scatter observed by Sekine & Kikkawa (1992) when comparing their curve with observations was between 0.5 and 2.0 times the calculated value, the curve based on calculations performed here lies within that region.

7.3.4 Interaction of sediment and flow

The final information output about the movement of particles was a value of the change in streamwise particle velocity at impact, summed across all the impacts that occurred during a particle movement. This represents the transfer of momentum from the flow to the bed (Sekine & Kikkawa, 1992). The cumulative change in particle velocity for a track was converted into a change in momentum over the whole track

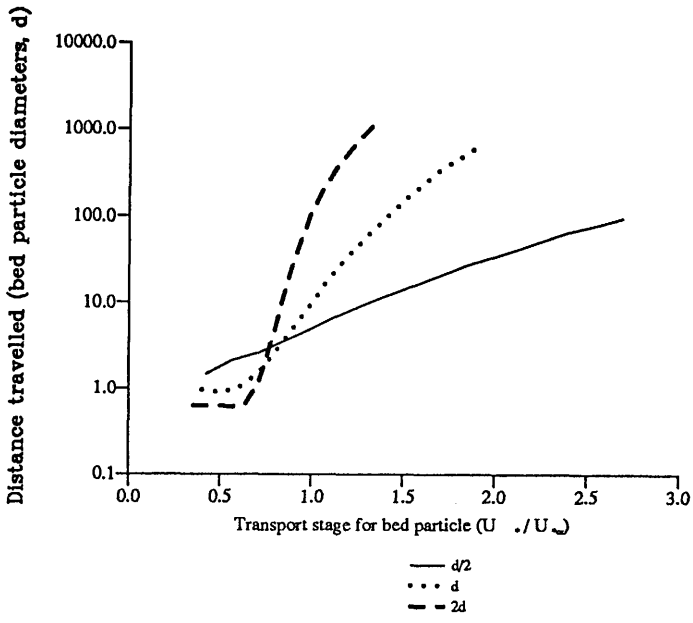

a) Distance travelled against transport stage of each particle

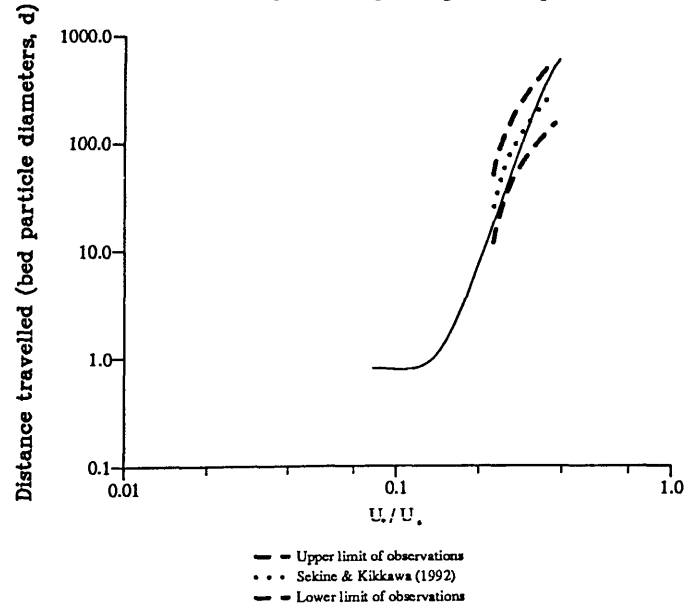

b) Comparison with expression of Sekine & Kikkawa (1992)

Figure 7.11 Mean distances travelled by particles

$$\sum \Delta M = \rho_s \frac{\pi d^3}{6} \sum \Delta u_{pi}$$

where Δu_{pi} is the change in the streamwise component of particle velocity at impact, ρ_s is the particle density and d is the diameter of the particle being considered. When this information is plotted as a curve of momentum extracted against time in motion, (Figure 7.12). The curve shows the change in momentum for all the particle tracks, added together and divided by the number of tracks. The much larger extraction of momentum from the flow caused by a large particle compared with that due to a small particle can be seen.

7.4 Discussion of distributions

Though the aim of this work was to use calculated distributions of particle movement to calculate sediment transport and bedform development, comparison of calculated distributions with observed distributions of particle movement provides a basis for consideration of the calculated distributions.

There are differences between what was observed in experiments on particle movement and what has been calculated here. The recent work on calculation of distributions of particle movement has been based on particles which are sufficiently large to be tagged in some way (see Table 1, Church & Hassan, 1992). However previous work has been performed using smaller particles, Sayre & Hubbell (1964), for example, used radioactive sand as a tracer. The ideas behind the stochastic distributions used have been successfully applied at both these scales and in between and so should be applicable here. Another important difference is that with the exception of the work described in Schmidt & Ergenzinger (1992) all the records of particle movement have been for the duration of an event, including an unknown number of periods of rest between particle movements of unknown individual lengths. This is in comparison with the single particle movements calculated here.

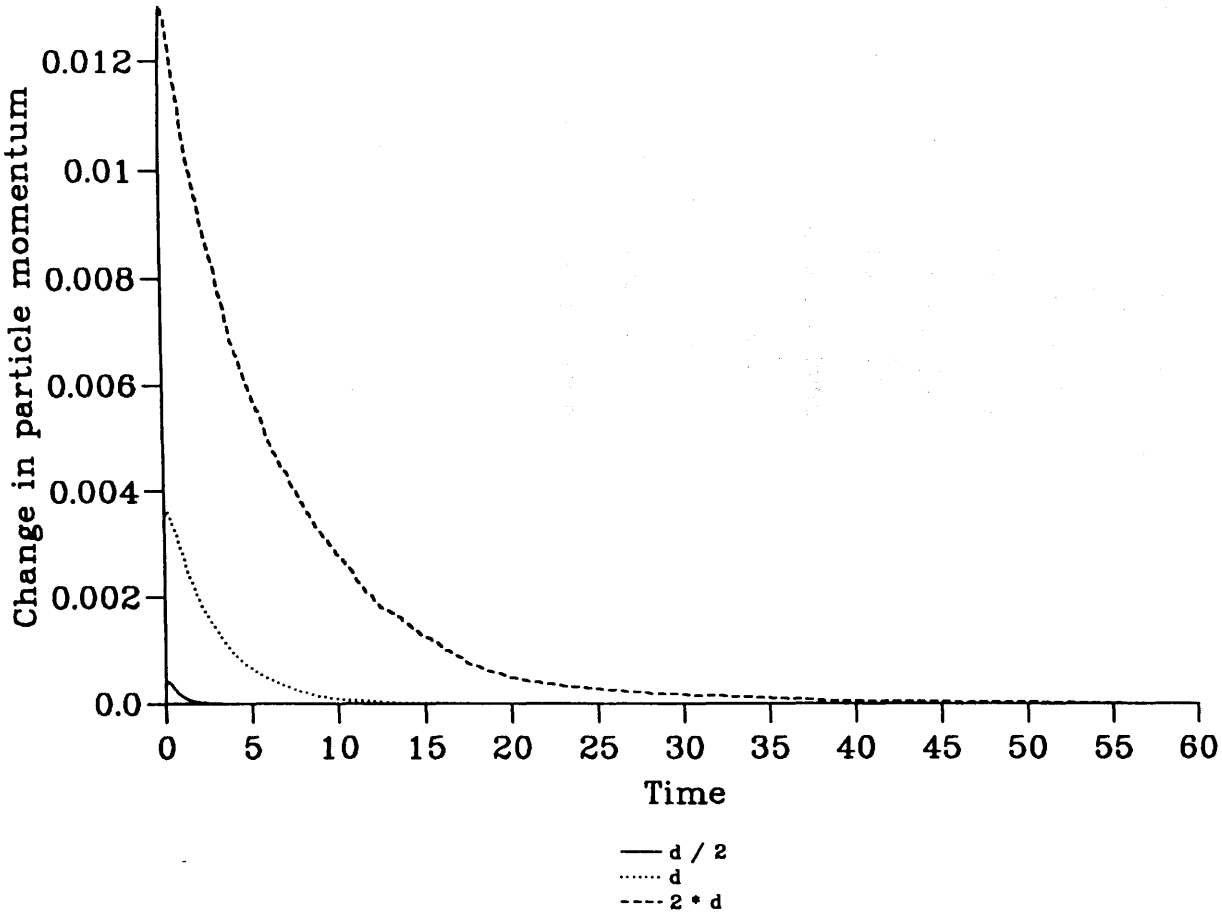

Figure 7.12 Distribution of change in particle momentum
Units non–dimensionalised with respect to flow depth, fluid density and mean bed shear velocity

Kirkby (1991) found that, though more complicated distributions could be used to describe the distribution of particle movements, a negative exponential curve gave a good fit to the fraction of particles moving beyond a distance for the particles which moved, when some of the particles remained at their initial positions. The distribution was defined by

$$\text{fraction in motion} = \exp\left(-\frac{\text{distance travelled}}{\text{mean distance of distribution}}\right)$$

comparing the curve calculated using this expression with the distributions calculated here the results are shown in Figure 7.13. For a particle of diameter $d/2$ the results show a good fit to the negative exponential curve until the tail of the distribution is reached. In the tail of the distribution the position of one particle can have a large effect on the fit of the distribution but the overall fit is acceptable. The results for the other two sizes of particles are not so good, but examination of the fitted curves and calculated points show a large discrepancy at the axis showing the fraction of particles in motion, that is in the number of particles moving only a short distance. This discrepancy corresponds to the movement of particles which only move over one or two bed particles before coming to rest, in comparison with the mean distance travelled these are very small movements and could be regarded as zero movements. If these particles are removed from the distributions and the mean distance travelled is recalculated the fit of curve to calculated distances of travel is much better, as shown in Figure 7.14. The calculated distributions of particle movement do show the negative exponential curve which has been observed for the distribution of particle movements.

A number of the assumptions made either in the version of the model described in Part I or among the modifications to use the model in calculating distributions of particle movement may over-simplify the system and modify the results obtained. In particular these simplifications occur in the modelling of impact and deposition. The logarithmic law velocity profile has a zero velocity height which is here treated as a

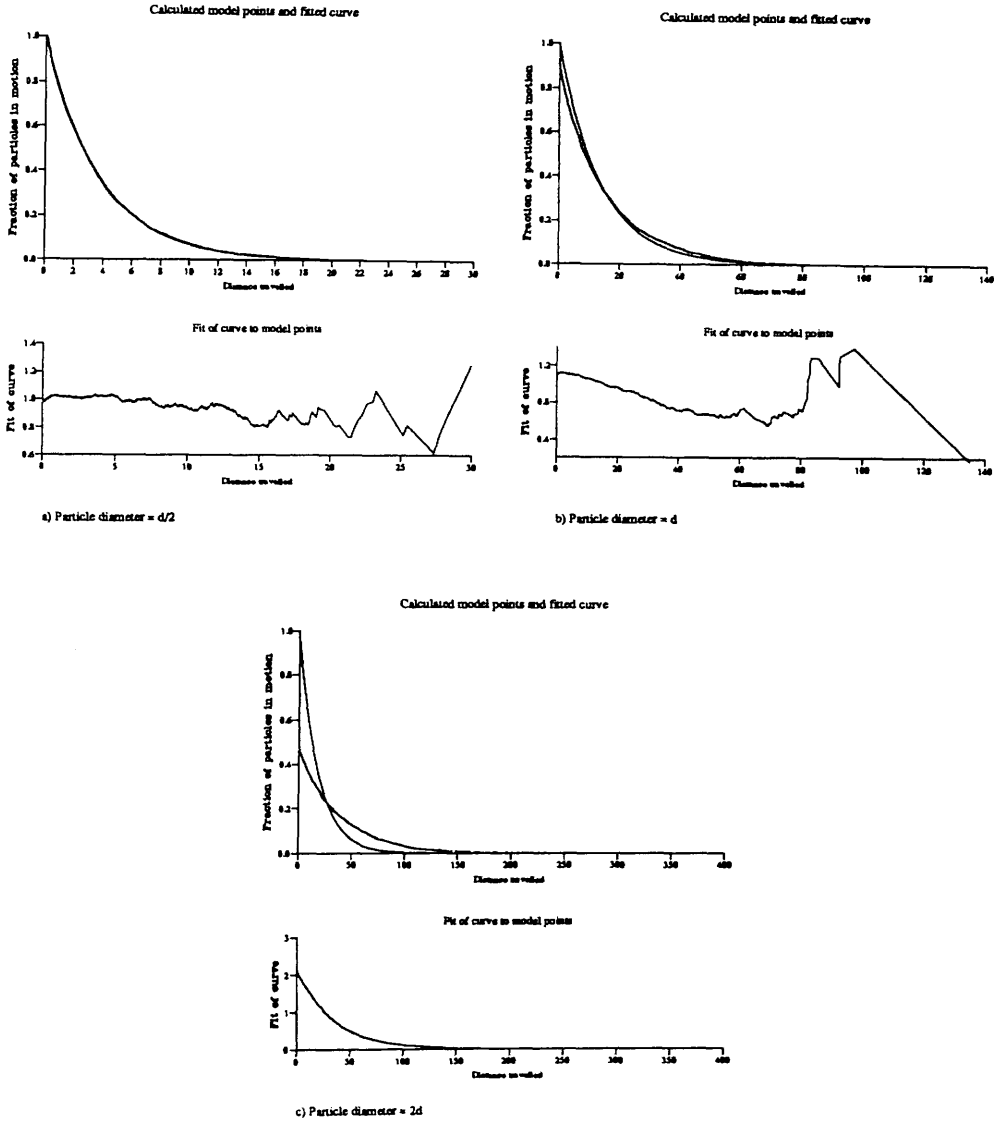

Figure 7.13 Comparison of distribution of distance travelled
Calculated distances from model and fitted exponential curve
Fit uses all distances travelled greater than zero

Units non-dimensionalised with respect to flow depth

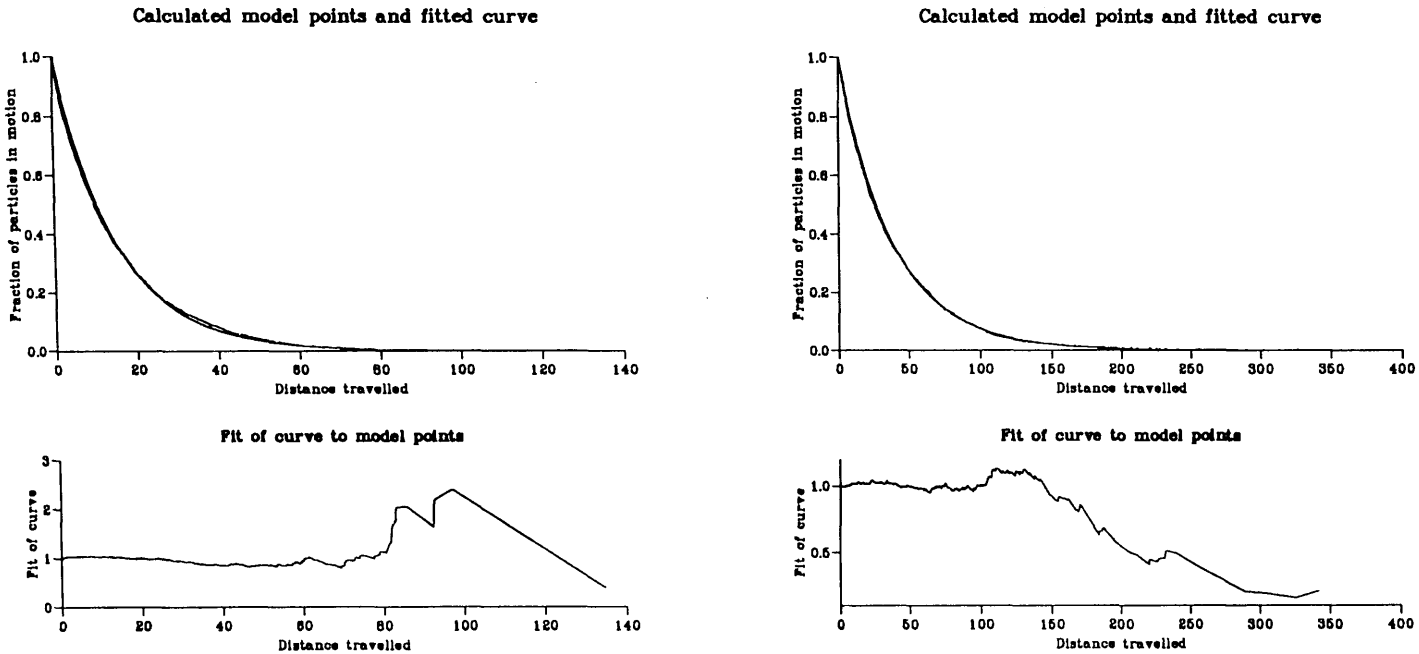

Figure 7.14 Comparison of modified distributions of distance travelled
Calculated distances from model and fitted exponential curve
Fit uses all distances greater than one or two particle diameters

Units non-dimensionalised with respect to flow depth

lower height for movement, if a particle centre is below this height it is regarded as deposited, regardless of turbulent fluctuations, especially burst-sweep features. An alternative treatment would be to set the mean velocity component to zero below this height and allow the particle movement to continue to be calculated. In the modelling of impact and deposition particles falling back are always set to rest, since the exact time intervals between impacts are calculated the calculation could be continued until the particle came to rest or had insufficient energy to leave the bed without distorting the calculated time in motion for the particle. The treatment of impact and deposition used here affects the transfer of momentum from moving particles to the bed, changing to more realistic descriptions would change the calculated values of this quantity. These alterations might affect the fit of the calculated particle movements to observations.

7.5 Conclusions

Distributions of particle movement have been calculated showing similar behaviour to observations made of particle behaviour. The distributions can easily be calculated for large numbers of particles with no losses of particles occurring. The calculations of distributions performed here were for 1,000 particles, Hassan *et al.* (1992) suggest that of the order of 10^3 particles are required to calculate distributions of movement accurately from field observations. While the largest number of particles used in any study they describe is 564, the model calculations can easily be performed for this number of particles.

The calculations performed were of the independent movement of single particles. Such calculations are easy to implement on parallel processing computers, making the calculation of large number of movements relatively cheap and able to be carried out in short periods of time, in comparison with performing the same calculations on a sequential computers. The disadvantage of using such a model is that

the effects of interactions of multiple particles on the flow and each other are not explicitly calculated, unlike the calculations of Jiang & Haff (1993).

In the next chapter the application of distributions of particle movements to the problem of sediment transport and bedform development will be considered.

Chapter 8

Towards a model of sediment transport and bedform development

8.1 Introduction

The distributions calculated using data from the single particle model described in Chapter 7 described movement of sediment in time and space. In Chapter 6 approaches to calculating sediment transport based on descriptions of particle movement were reviewed and some of the problems associated with such a model described. In this chapter the use of distributions of particle movement to model first the rate of sediment transport and then the more general problem of bedform development will be examined.

The calculation of the equilibrium rate of sediment transport using data from calculations of particle movement was described in Wiberg & Smith (1989) and Sekine & Kikkawa (1992), both models being based on the ideas described in Owen (1964). A similar approach to the calculation of an equilibrium rate of sediment transport will be taken here, allowing for the differences due to the use of distributions of particle movements in the calculation.

The problem of the calculation of the effects of sediment transport on the bed over which the transport occurs has been addressed for continuum models, but only to a much lesser extent for particle based models, the work of Naden (1987b) and Jiang & Haff (1993) being for special cases, low intensity and very small scale respectively. Other than the direct interaction of sediment particles and flow, considered in the calculation of the equilibrium rate of sediment transport , the problems relating to a mobile bed are the calculation of flow over a surface changing in height and roughness in time and space and how to describe this change in height and composition. These

problems also occur in continuum models and the approaches used in these will be reviewed. Based on these and the descriptions used in calculating distributions of particle movement appropriate models of flow and the bed will be developed. The use of these descriptions in a model of sediment transport and bedform development will be described and the results of trial calculations presented

8.2 Equilibrium rate of transport

The rate of sediment transport calculated by Wiberg & Smith (1989) and Sekine & Kikkawa (1992) was the quantity of sediment in motion at an instant such that the momentum extracted from the flow reduces the fluid shear stress at the bed, τ_{fb}, to the critical shear stress required to initiate particle motion, τ_{cr}. The same idea, based on that of Owen (1964), is used here, that is the shear stress is considered to be partitioned between grains and fluid in the saltation layer. However the model used to calculate the distributions and the use of the distributions themselves in the rate calculation make some alterations to the calculation and its interpretation necessary.

The model of particle movement used to calculate particle movements for the distributions included stochastic elements representing turbulent fluctuations in the flow and the variability of the bed. The result of these stochastic elements is that, for a single size of particle, entrainment occurs over a range of conditions, including conditions where the mean shear stress is below that capable of entraining the particle. The single value of critical shear stress at the bed, used as the control on entrainment, must therefore be regarded as representing a mean condition for entrainment, with the number of particles entrained at mean shear stresses below this value assumed to be balanced by the number of particles remaining at rest at mean shear stresses in excess of this value.

The turbulence within the saltation layer was assumed by Owen (1964) to be dominated by eddy shedding from particles moving in the layer. The flow outside the

saltation layer follows a logarithmic velocity profile, with the surface over which saltation was occurring acting as a surface of greater roughness length than would be expected from the sizes of particles forming the surface. By contrast the turbulent fluctuations in the calculations of particle movement already described were assumed to be those of the flow and to act down to the level of the bed. Observations in the fluvial (Drake *et al.*, 1988) and the marine (Williams, 1990) environments show a pattern of transport dominated by sweeping events due to structures in the flow. The bulk of the sediment transport occurs during these events which are isolated in space and time. The description of turbulence used in calculating the movement of particles includes these events in the model. Though there are differences between the underlying assumptions of the different models the idea of shear stress dropping to a critical value for the motion of particles at the bed was still adopted since it had proved capable of accurate predictions in the models of Wiberg & Smith (1989) and Sekine & Kikkawa (1992).

The distributions of particle movement described in the last chapter represent the fraction of the entrained particles which are still in motion at a specified time, Figure 7.10. Due to the linear relation between distance travelled and duration of motion, Figure 7.6, these can be converted into a distance travelled, by multiplying the time in motion by the particle velocity. The distributions of momentum extracted from the flow represent the momentum being extracted from the flow due to particles entrained at an earlier time, that is the distribution is related to the number of particles initially entrained, not the number still in motion, Figure 7.12. The use of distributions in the calculation carries the implication that the behaviour of a particle is dependent on the conditions when the movement started and that this dependence remains throughout the period of movement without being modified by conditions at any later time or position.

8.2.1 Calculation of equilibrium transport rate

The calculation of the rate of transport was based on a summation of the momentum extracted and the fraction of particles in motion derived from a discretisation of the distribution curves of Chapter 7. To use distribution curves in calculations they had to be described, one approach would be to fit functions, as was done to curves of distance travelled, Figure 7.13, Figure 7.14, another would be to discretise the curves. The latter approach to describing the curves was used here, to calculate equilibrium transport rates and in the model of sediment transport over a mobile bed. For the model of sediment transport the use of discretised distributions meant that the calculations of movement and deposition only required simple arithmetic rather than the evaluation of functions. These calculations were performed inside loops and reducing the computation required for each iteration made the calculations more efficient. The use of discretised curves in the calculation of equilibrium transport rate allowed the effects of using different levels of discretisation in calculations to be evaluated. The discretisation intervals used were simple fractions of the longest time in motion for the highest transport stage for which calculations were performed. The same time interval was used for each transport stage for which distributions had been calculated. When the sediment transport is in equilibrium the number of particles entrained during any time interval is constant. The total momentum extracted from the flow at a transport stage can therefore be calculated as:

$$M = n_p \sum_{1}^{\text{no. of time intervals}} (\Delta M \times \Delta t)$$

where n_p is the equilibrium number of particles entrained at each time interval per unit area, ΔM is the momentum transferred to the bed at the time interval, the value is taken from the discretised form of the momentum transfer curve, Figure 7.12, and Δt is the time interval used to discretise the curve. The total momentum that must be extracted

from the flow to reduce the fluid shear stress at the bed to the critical value for the entrainment of particles, can be found for a stated transport stage from:

$$\tau_g = \tau - \tau_{cr}$$

Shear stress can be expressed as a force acting over an area, and force is rate of change of momentum, the grain shear stress, τ_g, can be written

$$\tau_g = \frac{F}{A}$$

where $F = M/\Delta t$, for unit area this gives an expression

$$\tau_g = \frac{M}{\Delta t}$$

$$\tau_g = \frac{n_p \sum_{1}^{\text{no. of time intervals}} (\Delta M \times \Delta t)}{\Delta t}$$

the number of particles entrained at each time interval per unit area, n_p, can therefore be calculated as:

$$n_p = \frac{\tau_g \Delta t}{\sum_{1}^{\text{no. of time intervals}} (\Delta M \times \Delta t)}$$

The total momentum at each of the transport stages for which distributions were calculated in Chapter 7 can be calculated, giving a curve, Figure 8.1.

Once the number of particles entrained during each time interval has being calculated the total number of particles in motion above a unit area can be calculated. This is done by calculating the total fraction of particles remaining in motion for each of the transport stages of Chapter 7, Figure 8.2. The total number of particles per unit area at a transport stage can be calculated

$$n_{total} = n_p \sum_{1}^{\text{no. of time intervals}} \text{fraction of particles in motion}$$

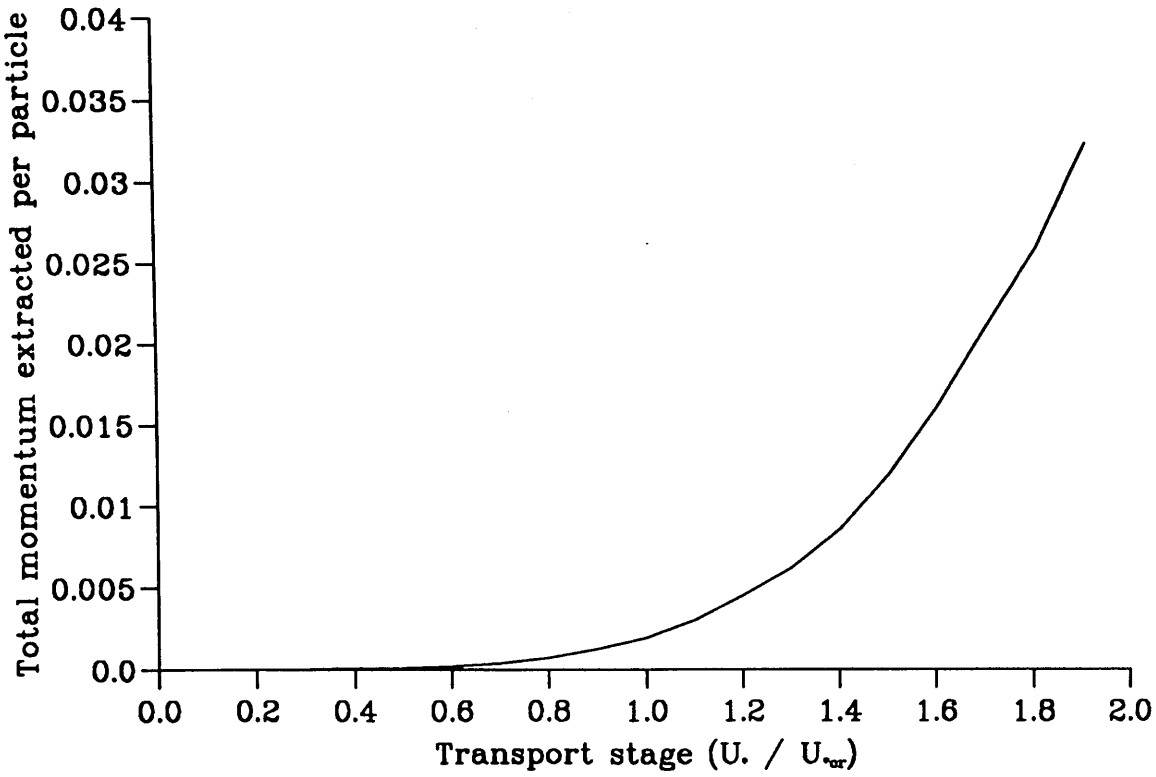

Figure 8.1 Variation in momentum extracted from flow with stage Units non-dimensionalised with respect to flow depth, fluid density and mean bed shear velocity

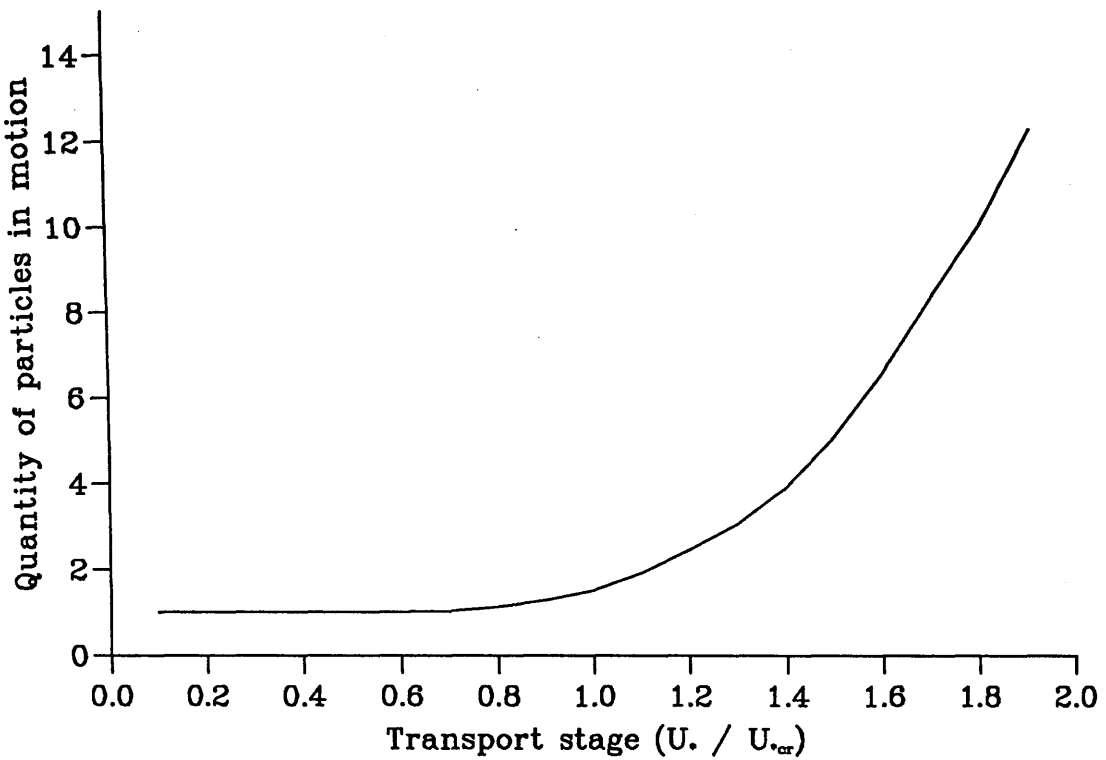

Figure 8.2 Total fraction of entrained particles in motion for equilibrium transport

Quantity in motion in units of particles entrained during a time interval

for the value of shear stress, where the fraction of particles in motion is the value from the discretised curve of Figure 7.10 at each time interval. The rate of transport can then be calculated

$U_p n_{total}$

where U_p is the mean particle velocity at the value of the shear stress, which can also be calculated from the data described in Chapter 7.

8.2.2 Equilibrium calculations performed

Calculations of equilibrium transport rate were performed across a range of transport stages from 1.1 to 1.9 at intervals of 0.1. The calculations were performed using different levels of discretisation of the distributions. The distributions were discretised as fractions of the longest duration of motion determined from the distribution for a transport stage of 1.9. The fractions used were 0.01, 0.005, 0.0025 and 0.00125, giving distributions of 100, 200, 400 and 800 intervals, single values of time interval were used at all transport stages, the values were 0.58, 0.29, 0.145 and 0.073 respectively. All the time and momentum terms were non-dimensionalised with respect to the conditions at a transport stage of 1.5.

8.2.3 Results of equilibrium calculation

The total equilibrium quantity of particles in motion is calculated as being almost identical with each of the levels of discretisation used, Figure 8.3. Though the range of results remains approximately constant for all the calculated flow transport stages the range as a fraction of the values is larger at the lower flow transport stages. This is due to the way in which the distributions of particles in motion were discretised. In the discrete distributions of particles in motion a particle was counted in an interval if it was in motion for any part of a time interval. This meant that at low transport stages and large time intervals the total fraction of particles in motion was overestimated, Figure 8.4. The equilibrium transport rate is shown in Figure 8.5.

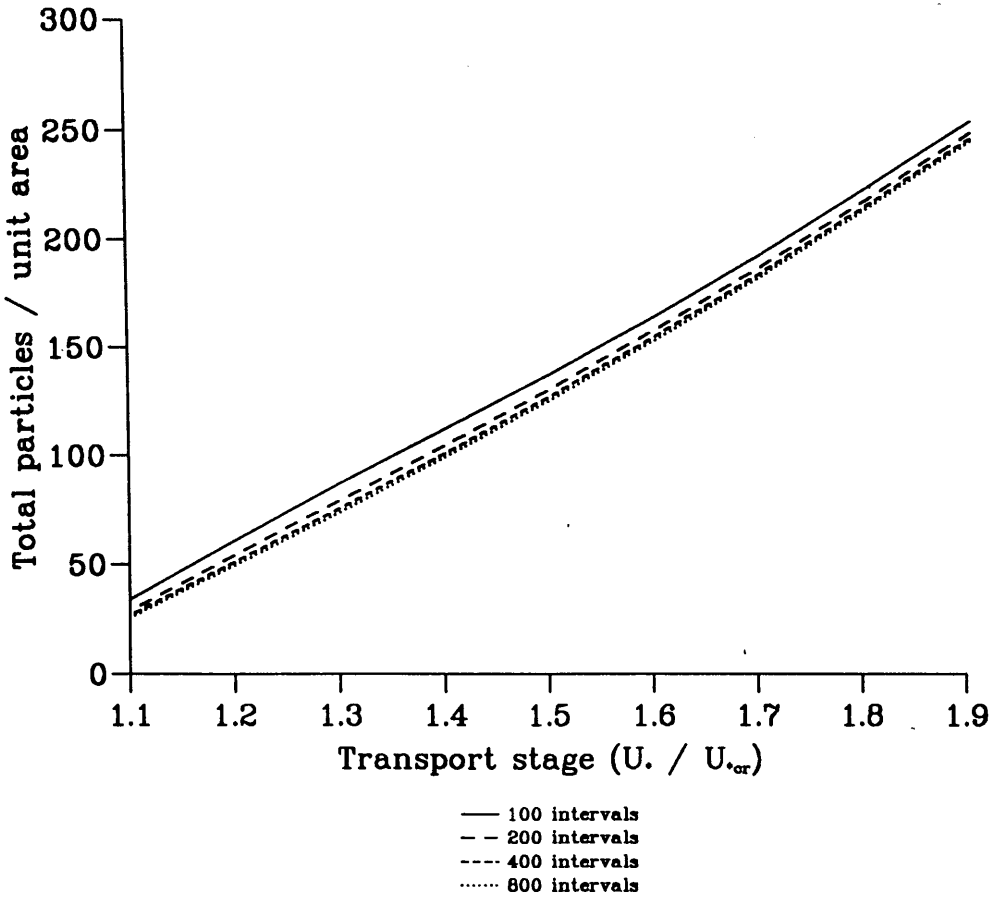

Figure 8.3 Equilibrium number of particles

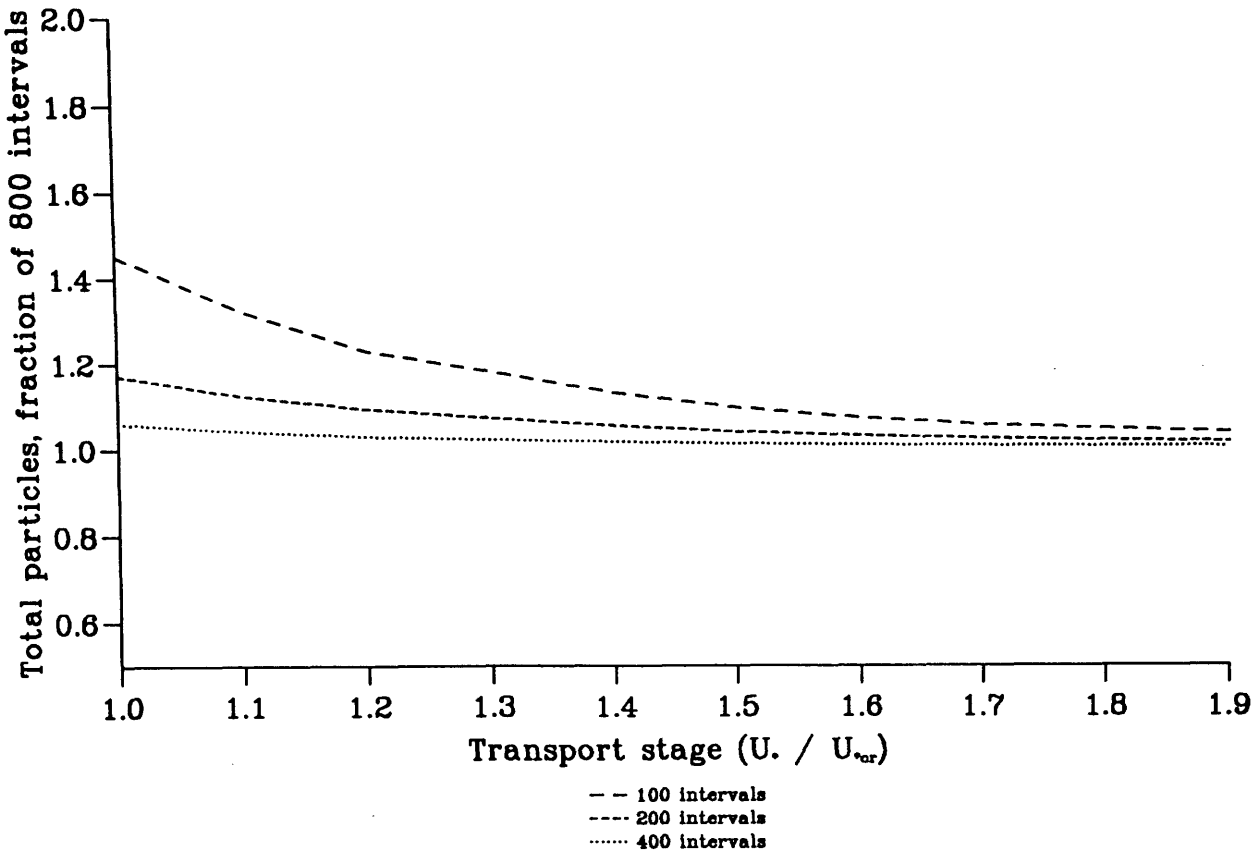

Figure 8.4 Total number of particles in motion as fraction of value with 800 intervals

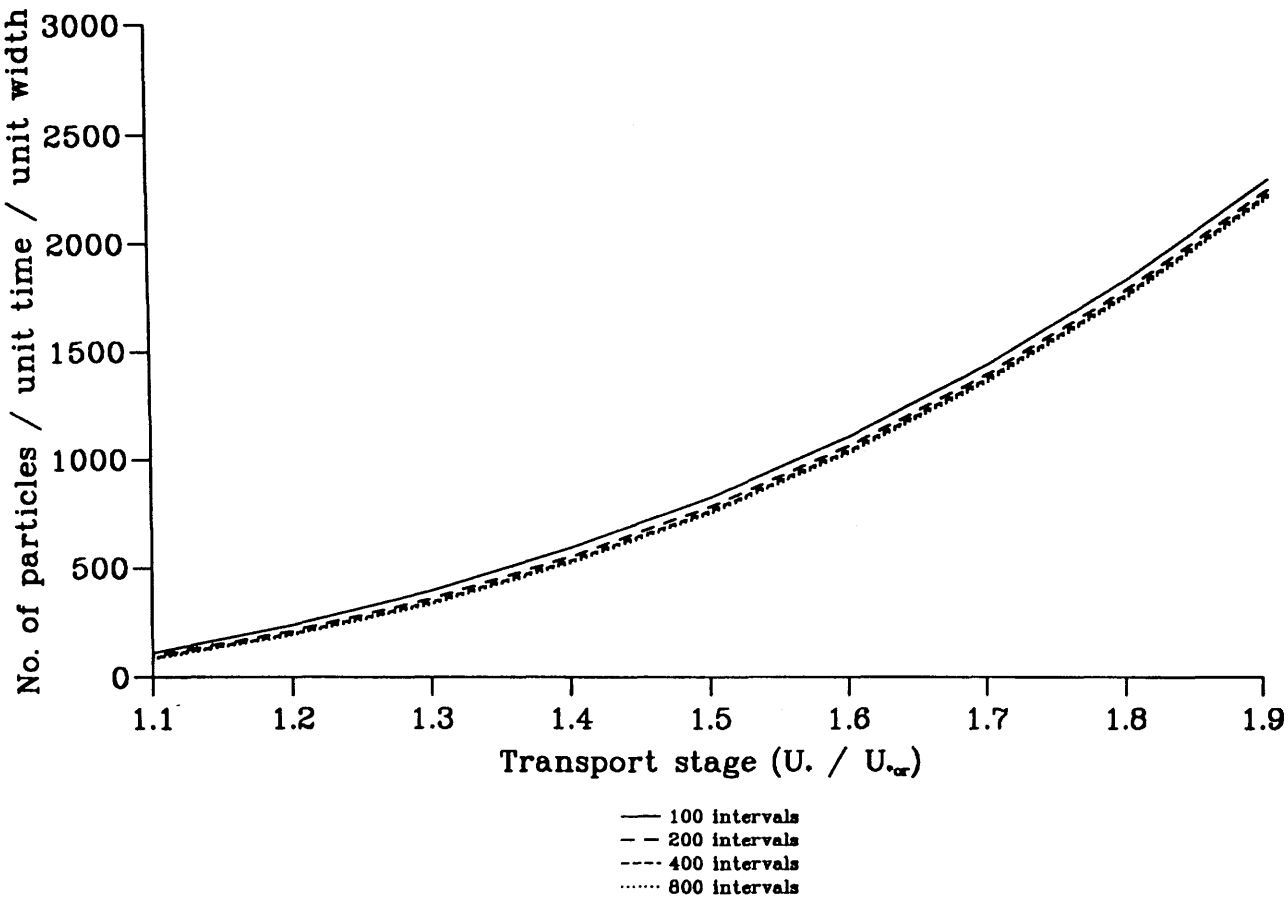

Figure 8.5 Variation in equilibrium transport rate with stage

The results for equilibrium quantity of material in motion, Figure 8.3, and rate of transport, Figure 8.5, show that a range of discretisation intervals can be used to describe the movements of particles producing similar results. However the results show a poor fit with those of Sekine & Kikkawa (1992), Figure 8.6, which show a good fit with observations. Each particle in the calculations of Sekine & Kikkawa (1992) must be transferring momentum to the bed at a faster rate than in these calculations. This along with the comparison of step length in Figure 7.11b imply that the model of impact and deposition needs to be examined, to alter the rate of momentum transfer. The present model of impact and deposition is simplistic and could be improved, particularly by allowing particle movement to continue when the particle centre is below the zero velocity height. Another possible source of the difference is the low density used in these calculations, though the expression plotted is non-dimensional any density dependency would affect results, this could be checked by further calculations with a higher density.

8.3 Mobile bed modelling

The mobile bed models reviewed here are continuum models where the sediment transport is calculated from rate equations. The calculation of sediment transport in these mobile bed models is different from that of distribution based calculations. However the modification of flow, by changes in bed height and composition, and how these changes in the bed are modelled, are relevant to the calculation of sediment transport and its effects based on distributions of particle movements.

8.3.1 Flow

Any model used to calculate flow over a mobile bed must be able to calculate the effects on the flow due to modification of the bed topography and composition by sediment transport.

The descriptions of flow in mobile bed models are of two types: coupled solutions, where the effects of changes in bed topography are explicitly included in the

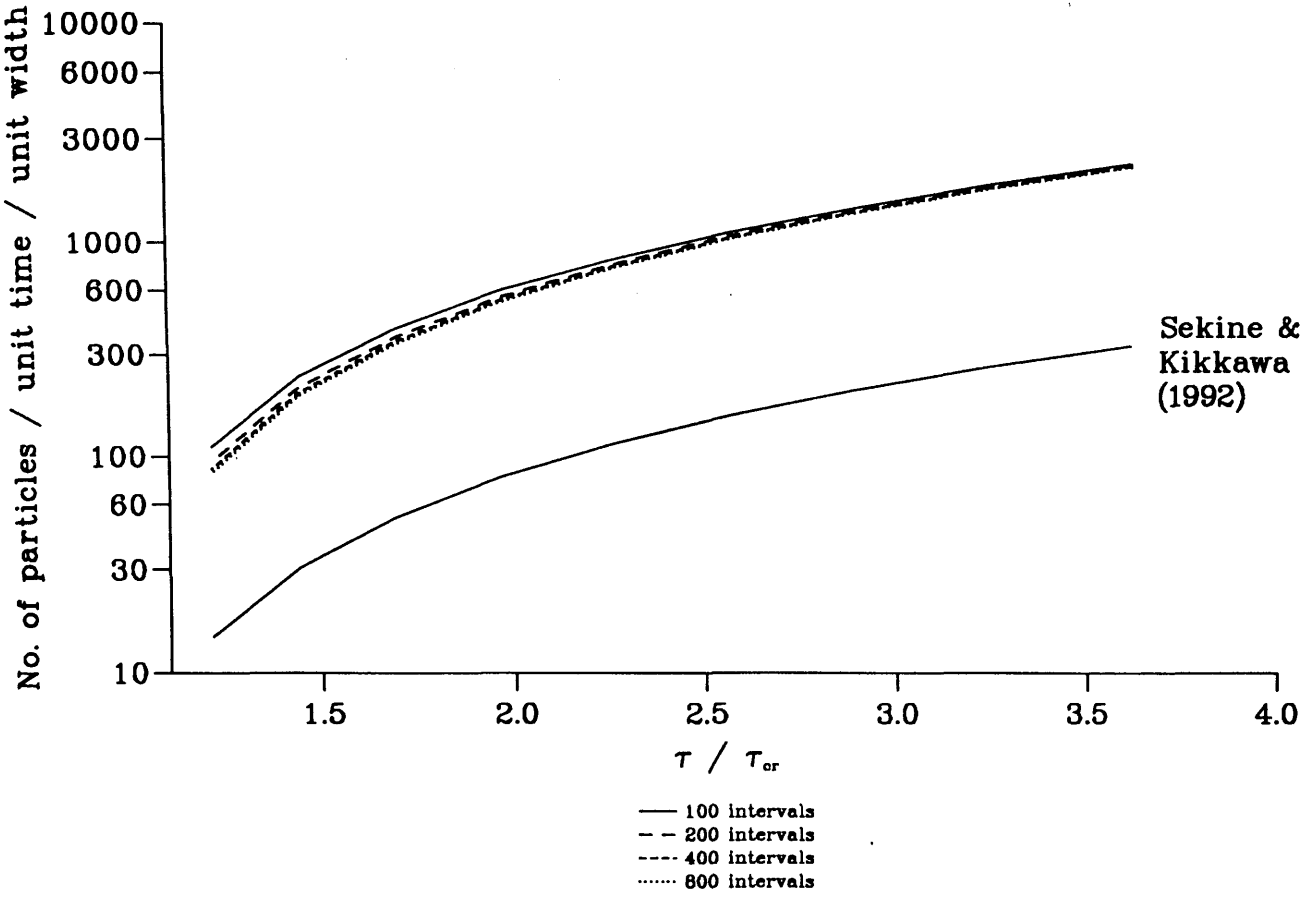

Figure 8.6 Comparison of calculated transport rate and expression of Sekine & Kikkawa (1992)

equations describing the flow (Holly & Rahuel, 1990; Correia *et al.*, 1992); and uncoupled solutions. In uncoupled solutions the flow over an immobile bed is calculated, the results are used to calculate sediment transport rates and their effects on the bed, a flow solution is then calculated over the new immobile bed topography (van Niekerk *et al.*, 1992; Vogel *et al.*, 1992; Willetts *et al.*, 1987). The uncoupled solutions typically used gradually varied flow solutions, with flow conditions kept constant for the duration of an iteration, after which sediment movement is calculated. The coupled solutions use the de St. Venants equations to calculate flow coupled with sediment transport and its effects. Uncoupled solutions make the assumption that the flow will not be affected by changes in the bed, caused by sediment transport, during an iteration, and that the material available for transport during an iteration can be specified at the start of the iteration. If the first of these conditions is not true the duration of iterations must be reduced, if the second is not true a different model of material available for transport must be used. Coupled solutions avoid both these problems at the expense of using a more complex system of equations.

8.3.2 Sediment transport

The calculated flow conditions are used to calculate the rate of sediment transport. The rates of sediment transport are then used in equations of sediment continuity to determine the effects of the transport. For a 1 dimensional model the change in bed height, z, with time, can be calculated as:

$$\frac{\partial z}{\partial t} = \frac{1}{p}\frac{\partial q}{\partial x}$$

where p is the bed porosity and q is the volumetric transport rate. For known transport rates and time intervals the change in bed heights can then be calculated. The rates of entrainment and deposition of sediment are not calculated explicitly in any of the mobile bed models.

8.3.3 Bed

The bed description in a mobile-bed model affects what the model can be used to simulate, erosion only, or erosion and deposition. The modification of the bed by the flow can affect the height of the bed, its composition and the roughness experienced by the flow. The variation in bed height is calculated from the consideration of sediment continuity, as described above.

In all the models the description of the bed is based on the fraction of each size of bed material present, rather than the numbers and positions of particles, used in the particle based models of Naden (1987b) and Jiang & Haff (1993). The bed models are used in two types of calculations: armouring models, where only degradation occurs; and models where both agradation and degradation occur. The latter models are more complex to account for storage of deposited material. The models of Park & Jain (1987) and Willetts *et al.* (1987) represent models of armouring, those of Bennet & Nordin (1977), Borah *et al.* (1982), Rahuel *et al.* (1989) and van Niekerk *et al.* (1992) agradation and degradation.

8.3.3.1 Description of bed layers

All of the models represent the bed by layers, an active layer, a mixing layer and a layer formed of undisturbed bed material, Figure 8.7. The active layer can exchange material with the flow during an iteration. The limitation of material available for sediment transport to that in the active layer introduces the possibility of the rate of sediment transport being limited by availability, where all the material of a size fraction is entrained, or capability where the flow cannot transport all the available material of a size fraction. The mixing layer is the layer through which bedforms migrate, that is dunes and ripples. The material within this layer is mixed by these movements and can be expected to be exposed to the flow. The undisturbed bed material lies below the mixing layer. If no net erosion of material occurs this material

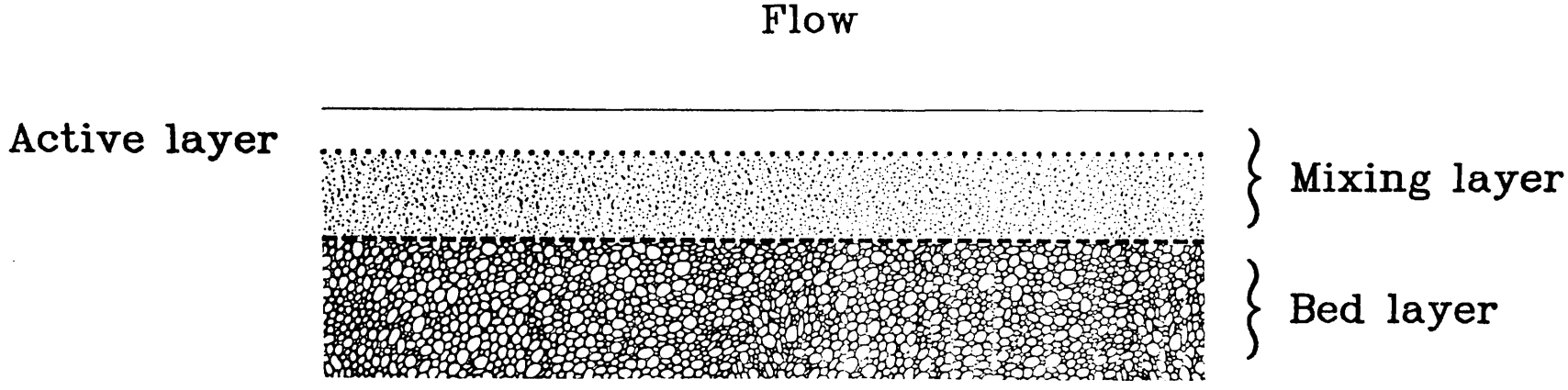

Figure 8.7 Layers in bed models

remains undisturbed by the flow. In all of the models the composition of the material within each layer is assumed to be homogeneous, with the exception of the mixing layer of Borah *et al.* (1987).

The active layer and mixing layer are related spatially and temporally, the definition of the active layer thickness depends on the time interval under consideration (Rahuel *et al.*, 1989). For short time intervals the active layer consists of the thin layer of particles on the surface susceptible to entrainment. Over larger intervals of time, of the order of the time taken for bedforms, ripples or dunes, to move their own wavelength, the active layer occupies the vertical space through which the bedforms move, and is equivalent to the mixing layer. For longer time intervals the active layer can also include the effects of changes in bed elevation due to erosion or deposition.

8.4 A particle distribution based model of sediment transport over a mobile bed

The model of flow over a mobile bed, with its associated sediment transport, described here uses the distributions calculated in Chapter 7 and discretised in the calculation of equilibrium transport rate at the start of this chapter.

The review of continuum models of sediment transport over mobile beds of the previous section revealed problems common to all such models, variation in flow due to changes in bed height and composition. The approaches to these problems used in this model will be described here In addition the interaction between sediment and flow, which replaces the rate equations used in the previous section will be described. The models of the bed described in the previous section included effects of erosion and deposition. However the underlying bed material composition was always kept constant. A possible way of examining changes to the composition of this material is also described. The components and interactions of a model of sediment transport over a mobile bed will be described, followed by calculations testing aspects of the model. Though the model described could be used for calculations involving multiple

size fractions of sediment the calculations performed here will only be for a single size fraction.

8.4.1 Components of model

The model described allows variation in bed height and flow depth in the downstream direction, calculations are performed over a series of elements of length $\Delta x_{element}$, in the downstream direction, and unit width, Figure 8.8. Entrainment, deposition and modification of the bed composition and height are calculated for each of these elements. As before in the description of single particle movements the model can be considered as consisting of components of flow, sediment transport and the bed. The relation of these components to the downstream length elements are described in the sections below. The quantities used in the model were all non-dimensionalised with respect to the fluid density, ρ, flow depth, h, and shear velocity U_*. The same time interval was used to describe all distributions and iterations of the calculation, simplifying the structure of the model. The disadvantage of using a single time interval, already mentioned in section 8.2.3, is that since the time interval is based on the distribution of the highest transport stage the discretisation at lower transport stages becomes progressively coarser.

8.4.1.1 Flow

The review of mobile bed models emphasised the need to calculate flow solutions in which the effects of variation in bed height and composition could be included. The descriptions of flow and their solutions were either coupled, with the changes in bed height included in the solution of the flow, or uncoupled, where flow solutions and changes in bed height were calculated independently. The approach used here was to use an uncoupled solution, with flow solutions calculated assuming steady gradually varied flow over an immobile bed, before calculating sediment transport and its effects independently. This solution was used for a number of reasons: solution of

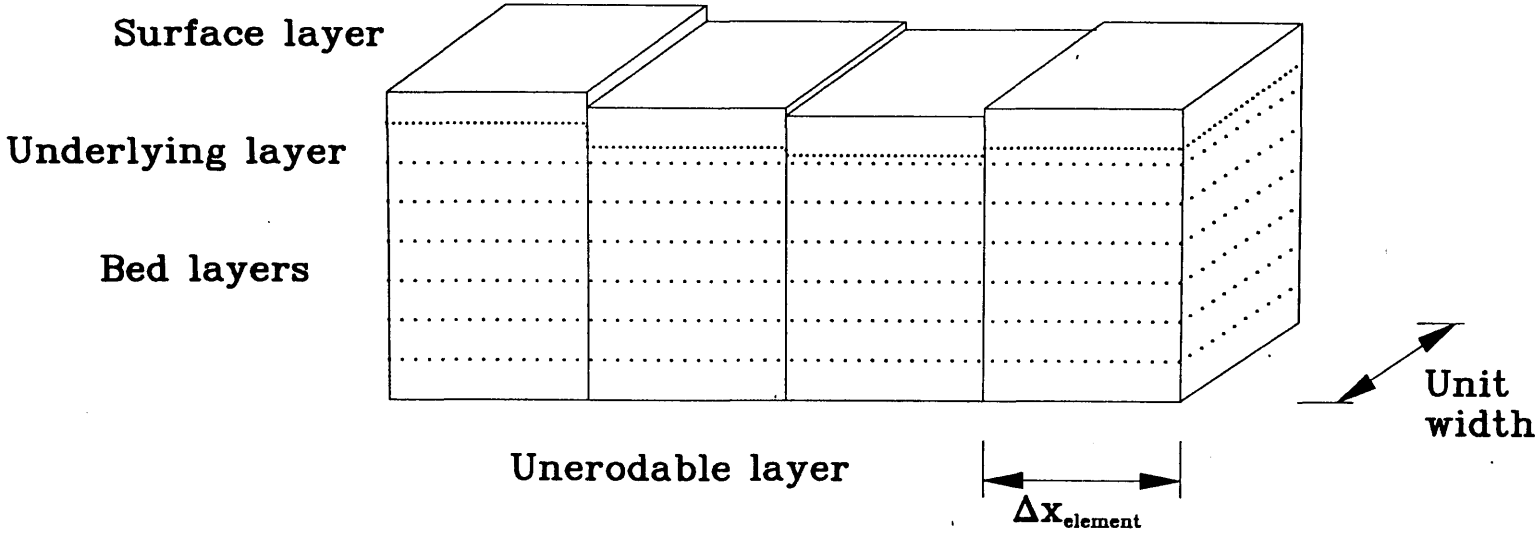

Figure 8.8 Elements of bed

steady gradually varied flow was simple to implement and the results described in Vogel *et al.* (1992) showed a solution of this type could match observed behaviour. The time intervals used in these calculations, determined by the distributions of particle movements, were short in comparison with those used for the coupled solutions (Correia *et al.*, 1992), and the change in bed height during such time intervals would therefore be limited, making the use of an uncoupled solution a reasonable approximation.

The gradually varied flow was solved using Newton's iteration technique as described by Fread & Harbaugh (1971). In a calculation of gradually varied sub-critical flow the calculation proceeds from the downstream end to the upstream end, to ensure an accurate solution. The method required a value for the energy slope, S_f; in Fread & Harbaugh (1971) this was supplied by use of the Manning formula, here a calculation based on bed grain size was used. Assuming that a logarithmic velocity profile is an appropriate description of the flow the mean flow velocity can be calculated from

$$\frac{\overline{U}}{U_*} = \frac{1}{\kappa} \ln\left(\frac{11h}{k_s}\right)$$

where $\overline{U}$ is the depth mean velocity of the flow, U_* is the mean bed shear velocity, κ is von Karman's constant, h is the flow depth and k_s is a roughness length scale, for a single size of particle

$k_s = D$

for calculations involving more than one size of particle this expression could be replaced (Hey, 1979)

$k_s = 3.5 D_{84}$

the value of D_{84} could be calculated from the bed composition at the iteration for which the calculation was being performed. The shear velocity can be calculated from

$$U_* = \frac{\overline{U}}{\left(\frac{1}{\kappa}\ln\left(\frac{11h}{k_s}\right)\right)}$$

and hence for a two dimensional flow the friction slope is given by

$$S_f = \frac{U_*^2}{gh}$$

In the calculations performed here the gradually varied flow was initially recalculated at each iteration. The effect of recalculating the flow only when the bed height at an element had changed by some fraction was also examined. The boundary conditions used in calculations were flow rate and downstream water surface height.

8.4.1.2 Entrainment

The quantity of material entrained from an element at an iteration was a function of transport stage and the bed surface composition and height distribution. The shear stress , τ, due to the flow was calculated from the solution to the gradually varied flow. This shear stress was considered to be partitioned between fluid, τ_f, and that extracted from the flow by movement of sediment, τ_s, (Owen, 1964)

$\tau = \tau_f + \tau_s$

The calculation of the value of the shear stress due to sediment movement is shown in Section 8.4.1.5.

The shear velocity of the flow, U_{*f}, can be calculated from the shear stress of the flow,

$U_{*f} = \sqrt{\tau_f}$

was that available to entrain material. It was this value that was used to calculate the entrainment fractions for each particle size and height from distributions of the type shown in Figure 7.4. The values for these fractions were calculated using linear

interpolation between the 2 nearest values of transport stage for which distributions had been calculated.

The number of particles of each size of material entrained from the surface for the calculated shear velocity could be calculated from

$$ne_d = \sum_{h=-\text{no. of heights}}^{h=\text{no. of heights}} nb_{hd} \times f_{eh}$$

where ne_d is the number of particles of size d entrained, nb_{hd} is the number of bed particles of size d at level h in the bed and fe_{hd} is the fraction of particles of size d entrained from level h. The range from a negative number of heights to a positive number of heights represents the number of levels used to describe the surface of the bed, which is described in Section 8.4.1.6 and Figure 8.10.

8.4.1.3 Transport

Once material was entrained the conditions at entrainment were used to calculate the movement of particles until deposition occurred. For any given set of conditions particle velocity was shown earlier to be almost constant and independent of the distance travelled, Figure 7.6. Constant duration iterations were used throughout a calculation, the speed of movement of particles could therefore be expressed as the distance a particle would travel during an iteration,

$$\Delta x_{transport} = \Delta t \times U_{U_{*f}}$$

where Δt is the duration of a time interval and $U_{U_{*f}}$ is the mean particle velocity at the transport stage at which entrainment occurred. The mean particle velocity was calculated by linear interpolation between the 2 nearest stages for which distributions had been calculated.

The position of material in motion had to be known to calculate where material was deposited during an iteration, Section 8.4.1.4, and where momentum was extracted from the flow by particle movement, Section 8.4.1.5. The description of

where material was at an iteration consisted of a position and a range. The shortest distance travelled by material deposited during an iteration was if it was deposited at the start of an iteration. This gives a minimum distance of travel for material n iterations after it was entrained,

$$x_{deposition} = (n-1) \times \Delta x_{transport}$$

All the material entrained from an element at an iteration moved with the same velocity and could be deposited at any time during an iteration. The range over which deposition could occur during an iteration was therefore

$$\Delta x_{deposition} = \Delta x_{element} + \Delta x_{transport}$$

where $\Delta x_{element}$ is the length of an element and $\Delta x_{deposition}$ is the distance over which deposition occurs at an iteration.

Material, both that remaining in motion after n iterations and that being deposited during the iteration was considered to be between $x_{deposition}$ and $x_{deposition} + \Delta x_{deposition}$. The quantity of material in motion was calculated from the discretised curve of fraction of material deposited. The curve was of the cumulative fraction of material deposited, the material remaining in motion was therefore

$$nm_d = ne_{dn} \times (1 - f_{dn})$$

where ne_{dn} was the quantity of material of size d entrained n iterations before and f_{dn} was the fraction of material of size d deposited in n iterations, for the transport stage at which the material was entrained. Once the position of material in motion at an iteration was known it was mapped onto the position of bed elements for the calculation of momentum extraction from the flow and hence the fluid shear stress and fluid shear velocity available to cause entrainment at an iteration.

The above describes the calculation of movement for a single size of particle entrained at an iteration. To calculate the total amount of material in motion the same calculation must be performed for each downstream element, particle size and position in the distribution of particle movement, Figure 8.9.

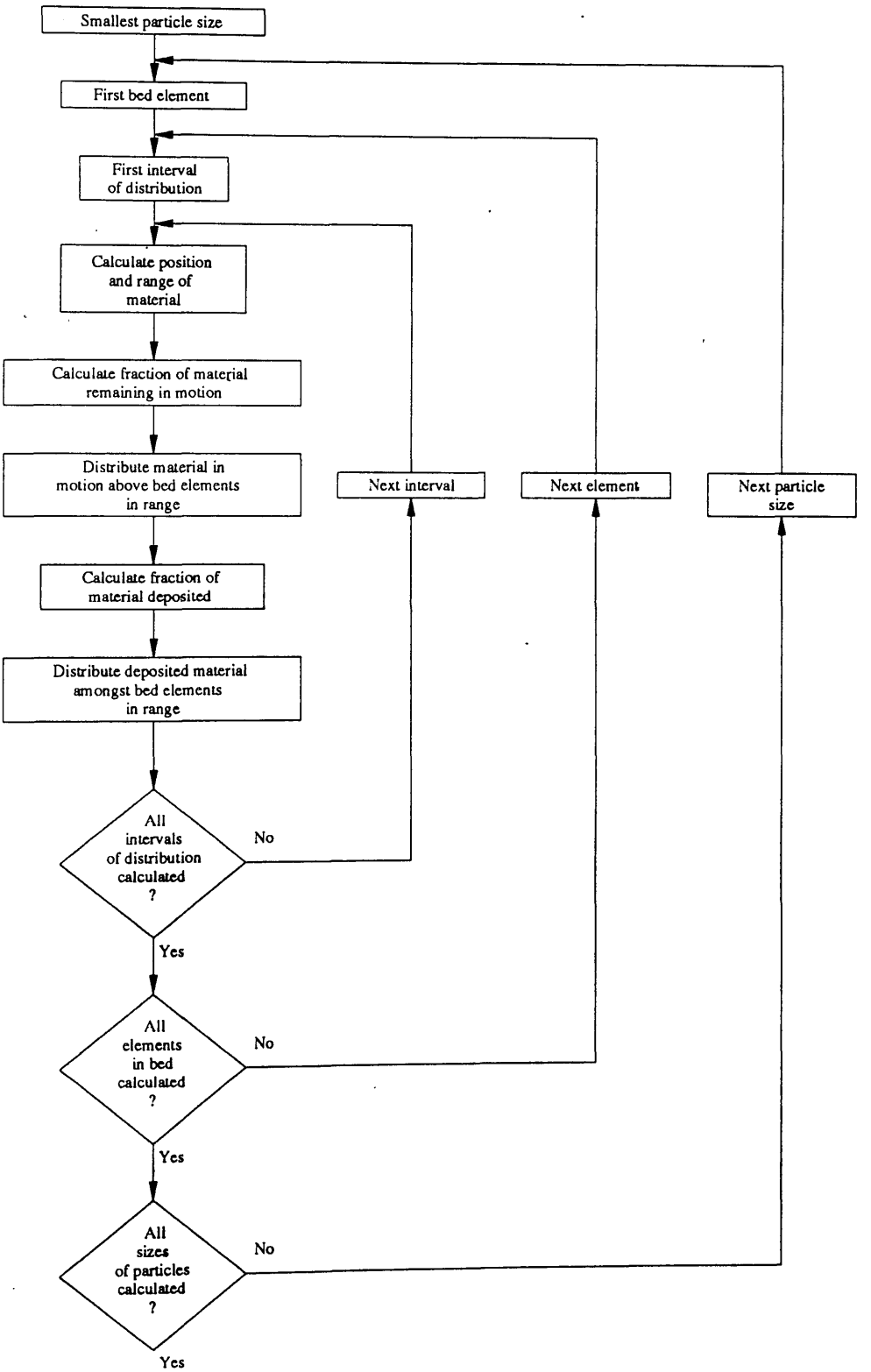

Figure 8.9 Transport of sediment

Material calculated to travel beyond the downstream element of the simulation, either still in motion or deposited there, was trapped, this allowed the total quantity of material to be checked, to ensure that continuity of bed material was being preserved. The trapping of material also allowed for the possibility of recirculating material to the upstream element of the simulation, to examine the effects of sediment feed on calculations.

8.4.1.4 Deposition

The calculation of the position of deposition of material entrained at n iterations is described in the section on transport of material. The quantity of material deposited is calculated from

$$nd_d = ne_{dn} \times (f_{dn} - f_{dn-1})$$

where nd_d is the fraction of material of size d deposited n iterations after it was entrained and f_{dn} and f_{dn-1} are the fractions deposited n and n-1 iterations after material was entrained. As with the calculation of the total quantity of material still in motion the total quantity of material deposited required the calculation to be performed inside the loop shown in Figure 8.9.

8.4.1.5 Interaction

The interaction of sediment being transported and the flow due to the momentum extracted from the flow by the particles, reducing the fluid shear stress τ_f is calculated from the distributions of momentum extracted. As with the equilibrium calculations the momentum of the flow over an element during an iteration could be calculated as

$$\Delta M_f = \tau \Delta t A_E$$

where Δt was the duration of an iteration and A_E was the area of an element. The momentum extracted from the flow due to ne_d particles of size d entrained n iterations before can be calculated

$$\Delta M_g = ne_d \times \Delta M_n$$

where ΔM_n is the momentum extracted from the flow due to a particle entrained n iterations before for the flow conditions at the entrainment of the particle. The position where this momentum is extracted was described in Section 8.4.1.3. The total momentum extracted over each element at an iteration can be calculated then used to calculate the residual fluid shear stress

$$\tau_f = \frac{\Delta M_f - \sum \Delta M_{ge}}{\Delta t \, A_E}$$

where ΔM_{ge} is the momentum extracted over an element, which must be summed for all the material in motion over an element. This value can then be used in the calculation of the entrainment of particles, described in section 8.4.1.2.

8.4.1.6 Bed

The description of the bed used in the model must be made in a way that is compatible with the calculations of particle movements used to form the distributions which are then used to calculate the sediment transport in these calculations. The bed description must also provide the values necessary for the flow calculations.

The bed was modelled as a series of elements of unit width and of length $\Delta x_{element}$. The effects of varying the length of elements was determined by calculations using elements of different length. Each element had a surface layer, corresponding with the active layer of the mobile bed models, which could contribute material to the sediment in motion during an iteration, and a number of underlying layers, which could either empty or fill, depending whether material was deposited on, or eroded from, the surface layer. The total number of layers of the bed was limited, if the final layer was eroded then a non-erodable layer was reached.

The quantity of material in the surface layer was determined as the quantity of particles required to cover the surface of an element in a square packing geometry.

The amount of material in the surface layer was always kept at that necessary to cover the area of the element. If erosion occurred material was transferred from lower layers, if deposition occurred material was transferred to lower layers. The initial surface composition was calculated from the initial composition of the bed material. The quantity and composition are functions of particle size and bed material composition, the surface layer is also described by a distribution through height. The distribution through height used is the truncated Gaussian used in the calculation of distributions of particle movements, discretised into 11 levels. Each particle size used was assumed to have the same truncated Gaussian distribution of particle centre heights, giving initial distributions of particles by number shown in Figure 8.10. The top 4 sections of this distribution correspond with the sections for which the fraction of particles entrained were calculated from the distributions of particle movement in Figure 7.4.

The quantity of material in each of the sub-surface layers was also that required to cover the area of an element on a square packing geometry, as with the surface layer the initial composition was determined by that composition of the bed material giving an initially identical composition. The composition of sub-surface layers was modified by interchange with the surface layer, due to either deposition on, or erosion of the surface layer. The quantity of material in the sub-surface layers varied between nothing and that required to completely cover the area of the element. When a layer became full a new layer was started and it was between this new layer and the surface that interchange of material occurred, when a layer was emptied, interchange between the surface and sub-surface occurred with the next layer down.

Erosion and deposition of material can alter the height of the bed, change the surface composition and its distribution through height and modify the composition of the sub-surface layer. The model of the bed had to be able to reproduce all these effects so that bed development due to sediment transport and the effects this had on the flow could be calculated.

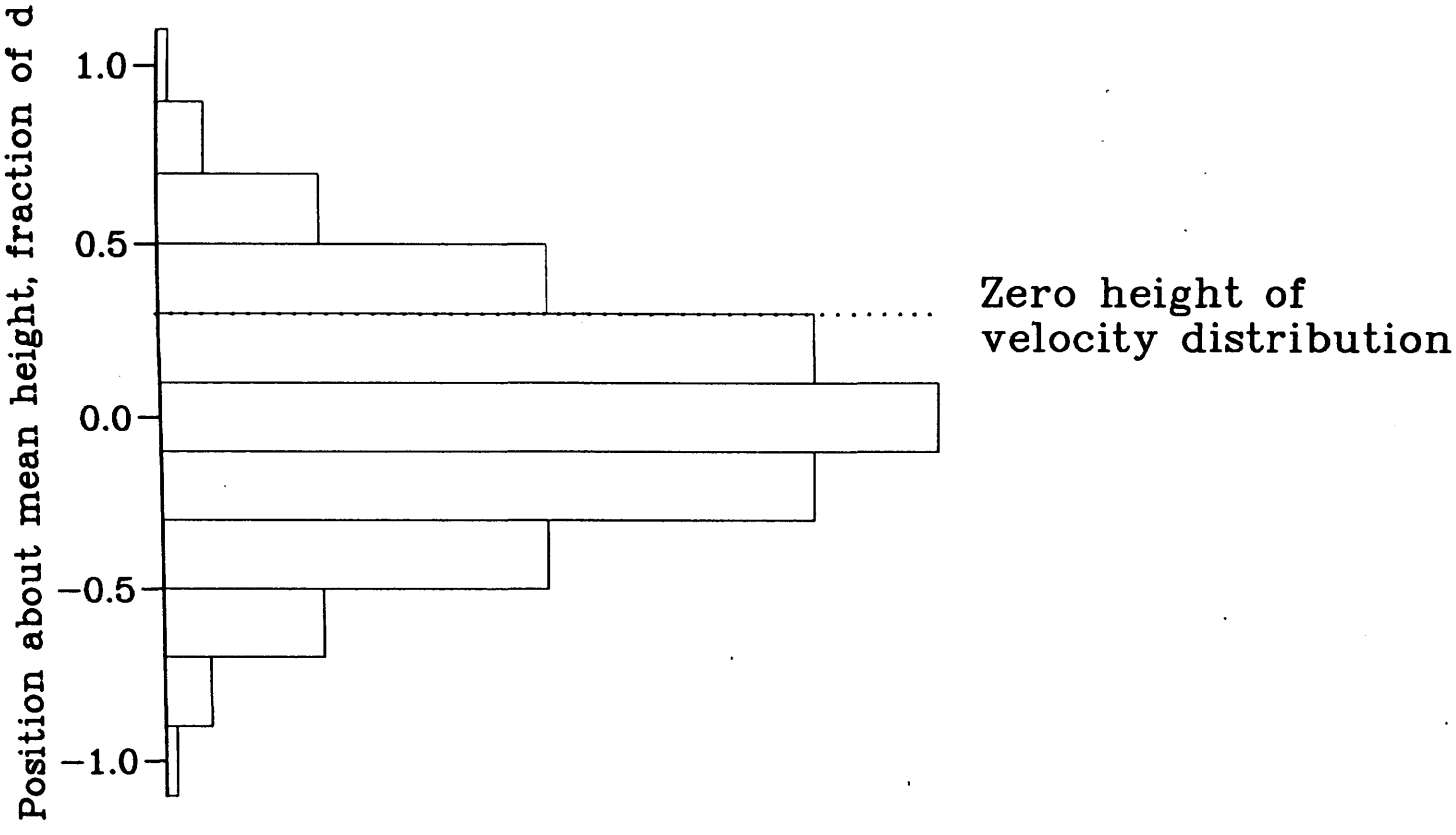

Figure 8.10 Initial distribution of particles on surface

The change in height due to material flux at the bed surface in a cell was calculated

$$\Delta z = \frac{\sum^{sizes}(\text{no of particles} \times \text{volume of particle})}{\text{area of element}}$$

where the sign of Δz could be either positive or negative depending on whether material was being eroded or deposited. The change in bed height was used to calculate the change in slope in the calculation of flow.

The effects of erosion and deposition of material on surface composition, distribution with height and sub-surface composition were calculated in a similar manner, though the exact order in which operations were performed varied, see Figure 8.11, for entrainment, Figure 8.12, for deposition.

When the composition of the surface layer was changed due to either entrainment or deposition the ratio of the particle sizes in the material added to the surface layer was the same as that of the complete mixture, the content of the sub-surface layer for entrainment, the material being deposited on the element for deposition. The fraction of the area of the element covered by material with particle centres in a level of the surface was used to determine the fraction of material deposited on that level, this preserved the range of surface heights independent of the area which the deposited material covered. The replacement of entrained material from the sub-surface layer filled the area exposed.

The surface of the bed was described by the number of particles of each size in each of the 11 levels. The height at which particles were added to this distribution from above or below was determined by the bed particle centre height and the sum of the radii of the bed particle and new particle. When material was being deposited the bed particle was that on which a particle was being deposited, when eroded the bed particle was that eroded, exposing the underlying material.

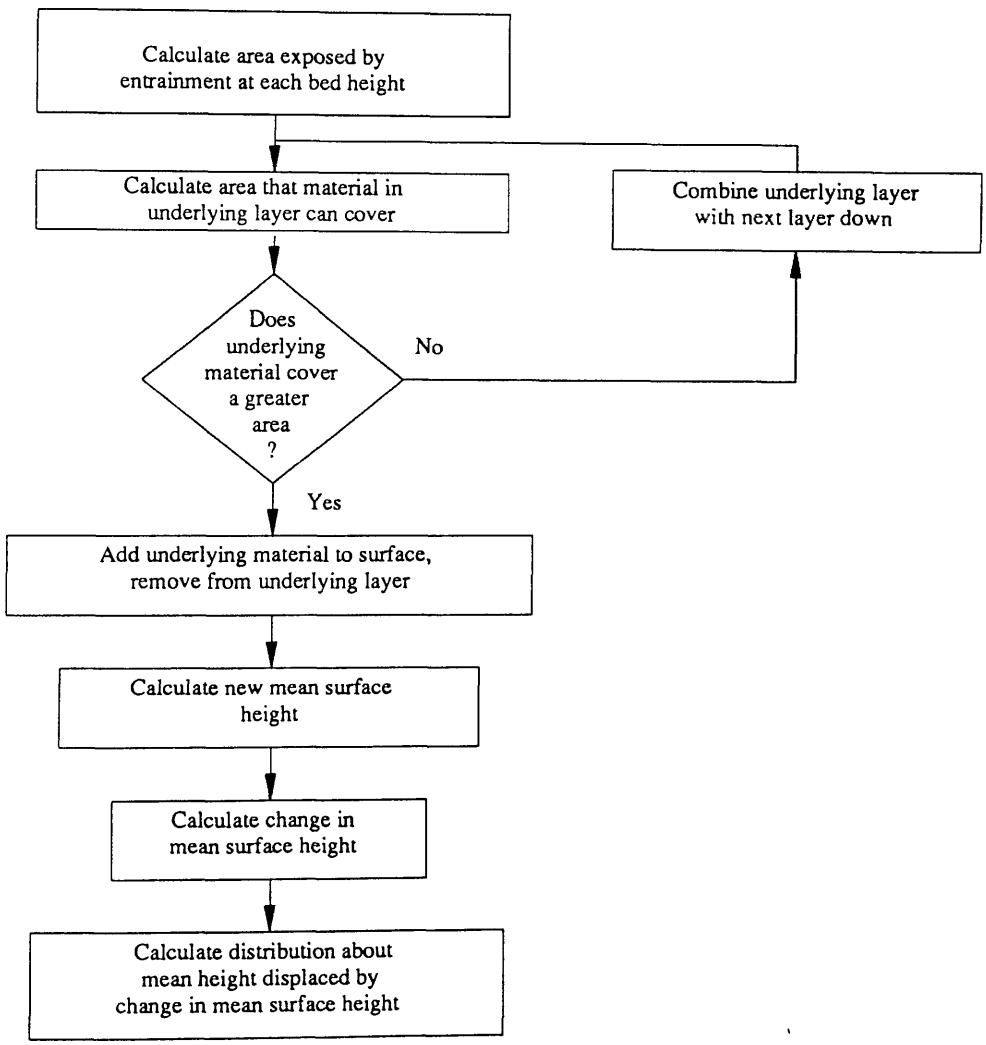

Figure 8.11 Calculation of effects of entrainment on bed

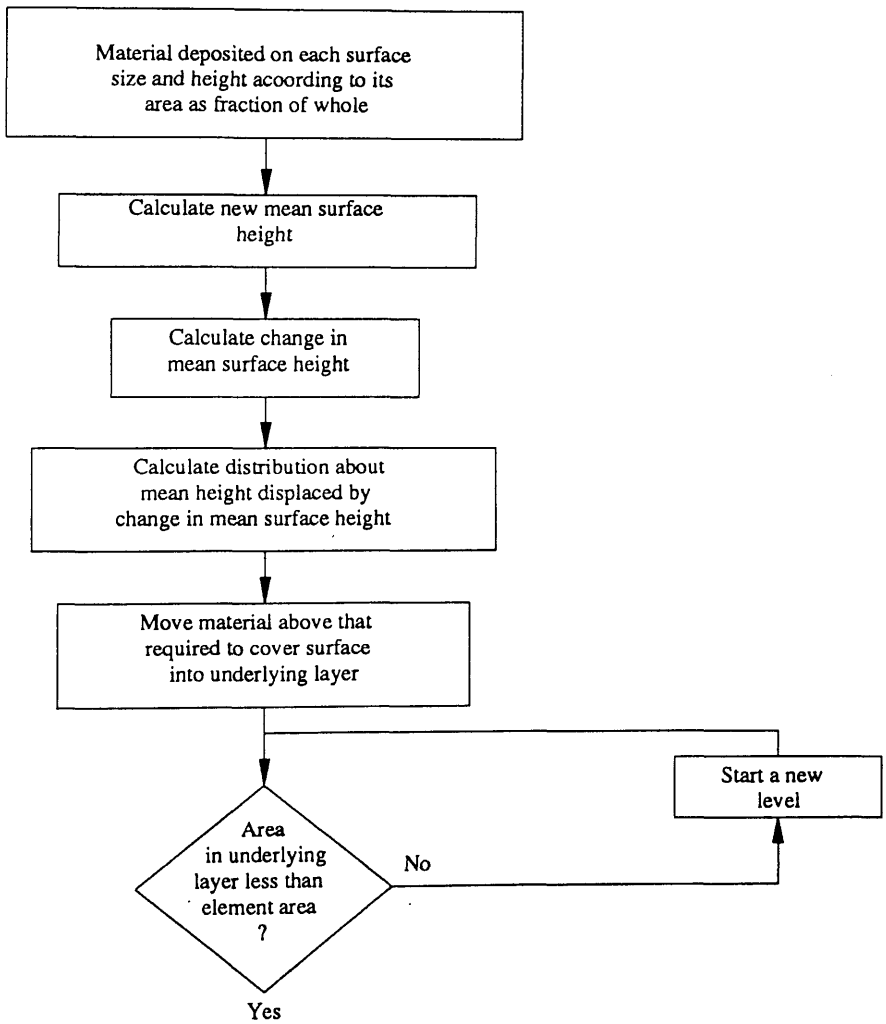

Figure 8.12 Calculation of effects of deposition on bed

The content of the sub-surface layers could also be affected by entrainment and deposition at the surface. When material was moved between sub-surface layers the ratio between sizes in the layer was preserved.

The modification of the surface layer by sediment transport affected the flow by the change in surface height and by changes in surface roughness due to changing composition. The surface roughness had to be described in a way that could be used in the calculation of flow, here the value of D_{84} was used to indicate the surface roughness. The value of D_{84} was calculated from the cumulative mass of each size of particle present, being the particle size for which 84% of the bed material by mass was smaller.

8.4.2 Calculations

The model described was coded in FORTRAN 77 and run on Intel i860 processors using a Transtech system hosted by a Sun server. The code optimisations available using the Portland Group FORTRAN 77 compiler were tested giving the range of results shown in Table 9.1 to determine the compilation options to give the fastest execution time for the code. The code was compiled and run using double precision floating point variables. The code was run on individual i860 processors, each of which had 16Mb memory. For the distributions and number of elements the array describing the distribution of particle motion and momentum extraction for input and the arrays describing the material in motion and material composing the bed could be stored in memory, without use of virtual memory which would have required swapping to disk, slowing down the calculations.

To describe the results of calculations a number of different sets of data were output from the model. The sum of the quantity of sediment in the bed, in motion and trapped at the downstream end of the simulation was output at each iteration to ensure that continuity of the sediment was being obeyed. The quantity of sediment

Compiler flags	Duration of calculation seconds
no optimisations	543.33
-Mbeta -Mvect	224.22
-Mbeta -O2	214.55
-Mbeta -O3	214.37
-Mbeta -O4	214.36
-Mbeta -Mvect -O4	223.38
-Mvect -O4	223.39

All compilations were performed using the Portland Group FORTRAN 77 compiler for i860's (pgf77), all had the compiler flag -Mr8 set to convert single to double precision.

Calculations were performed for 100 iterations.

Timings were obtained using the time860 command.

Table 8.1 Comparison of effect of different optimisation options on model runtime

transported out of the downstream end of the simulation during each iteration was recorded each iteration. The composition and height of the bed at each element were output every 100 iterations, likewise the flow depth, transport stage and Froude number of the flow at each element were output every 100 iterations.

The calculations performed were for a single particle size and for all the calculations the initial flow conditions were those for a steady uniform flow of transport stage 1.5. Previous calculations used the value of shear velocity for the transport stage at which the calculations were performed, here the value of the shear velocity for a transport stage of 1.5,

$U_* = 1.5U_{*_{cr}}$

was used to non-dimensionalise all relevant quantities. The results are presented in terms of the transport stage, rather than in terms of a fraction of a transport stage of 1.5. Each calculation was performed for a flow over a mobile bed with no recirculation or feed of sediment, and since only a single size of sediment was used no armouring could occur. The length over which the calculations were performed was set at 150 units (14.4m), this length was discretised into between 30 and 120 elements, depending on the calculation being performed and the distribution used.

8.4.3 Results

The calculations performed were for a steady flow rate, with the downstream surface height kept constant throughout calculations. The sediment transported during the calculation was that available from the bed, there was no feed of sediment at the upstream end of the calculation.

The continuity of sediment present, either in the bed, in motion or trapped at the downstream end was preserved in all the calculations performed. The variation in bed height and flow depth along the elements are shown in Figure 8.13, the variation of transport stage along the elements are shown in Figure 8.14. The graphs of Figure 8.13a and 8.14a show the results after 100 iterations, a non-dimensional time of 58.02,

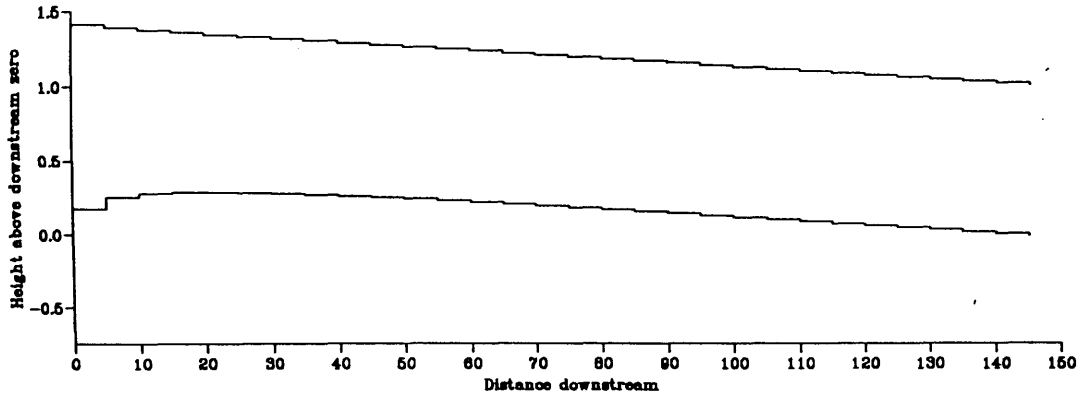

a) Time = 58.02

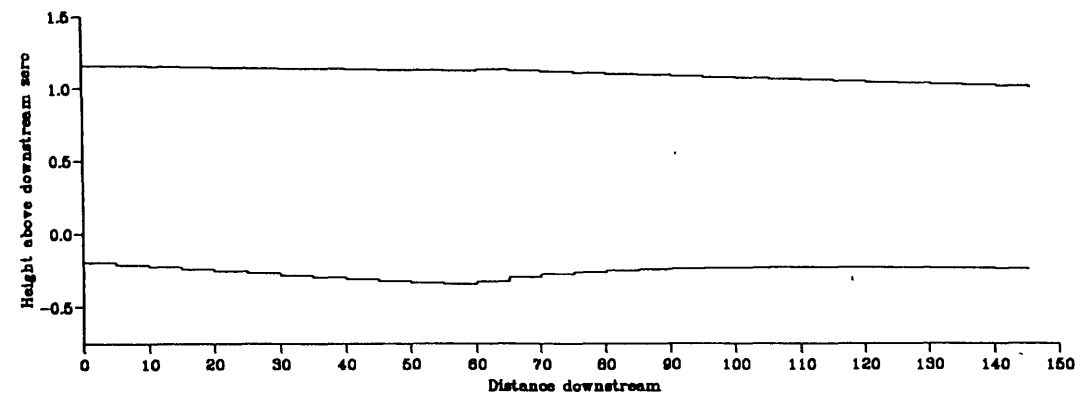

b) Time = 2901.0

Figure 8.13 Change in flow depth and bed height with time

Units non-dimensionalised with respect to downstream initial flow depth and mean bed shear velocity for a transport stage of 1.5

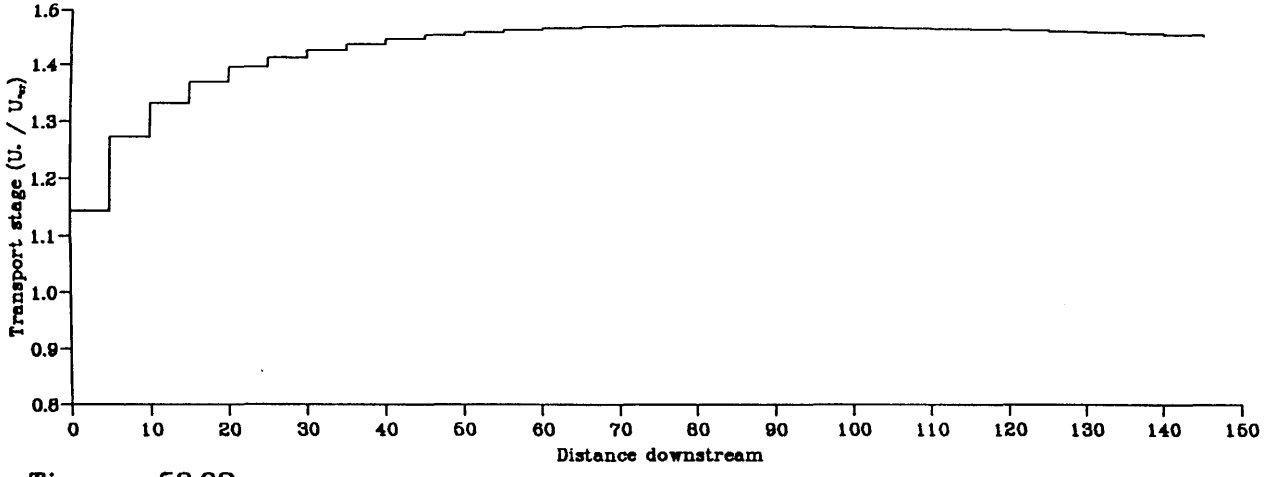

Time = 58.02

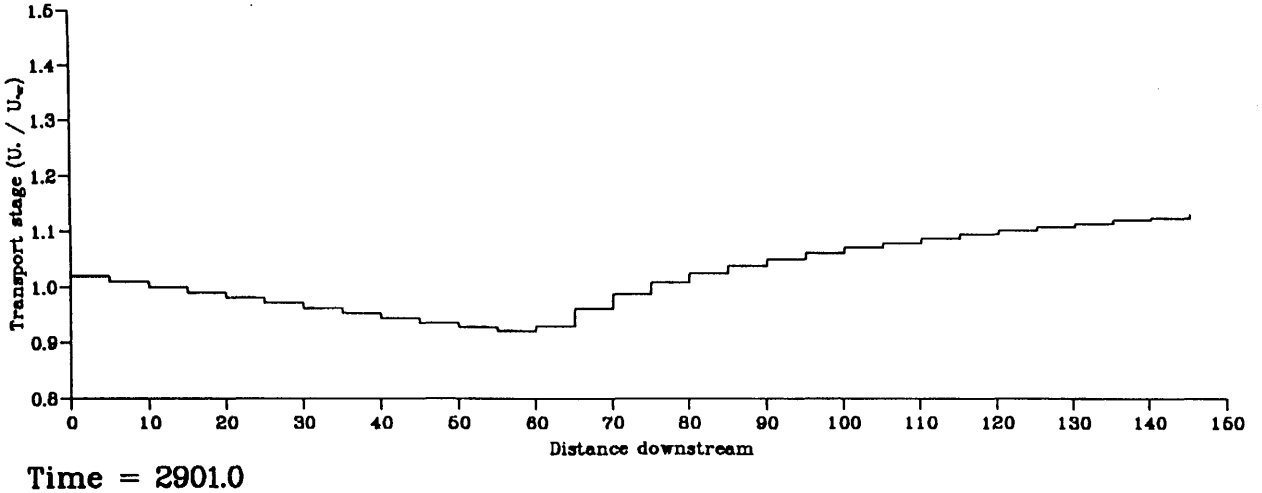

Time = 2901.0

Figure 8.14 Comparison of transport stage at different times

Units non-dimensionalised with respect to downstream initial flow depth and mean bed shear velocity for a transport stage of 1.6

an actual time of 108.6 seconds, while those in Figure 8.13b and 8.14b are the results after a non-dimensional time of 2901, an actual time of 5428.7 seconds. The curves show a reduction in surface slope combined with erosion of the bed to give a reduced transport stage upstream where the bed has been eroded to the base layer. Further downstream and at the interface between non-erodable and erodable material the water surface slope remains high and the transport stage is such that available material continues to erode. When the calculation is continued until all the available material has been removed the flow depth is greater than the original depth throughout. The downstream flow height is fixed and since the bed slope does not match the water surface slope for the downstream depth the result is a steady gradually varied flow through the length of the simulation. The flow increases in depth moving downstream, the flow rate is kept constant and therefore the mean flow velocity and transport stage drop moving downstream.

The effects of using different sizes of element was examined by performing calculations with elements of 2.5, 5 and 10 unit lengths, equivalent to 60, 30 and 15 elements respectively. Each calculation was continued for 15,000 iterations of duration 0.5802, sufficient for the mobile bed material to have been transported from the reach. The results of the calculations are shown in Figure 8.15, represented by the transport rate of material out of the downstream end of the calculation. The transport rate was used since it integrates the behaviour over the reach and over a number of time intervals. The results show that with the exception of the initial iterations the calculation was not sensitive to size of element used.

The effect of varying the condition for which the flow was recalculated are shown in Figure 8.16. The transport rate is plotted in Figure 8.16a, the difference in calculated transport rate between the most frequent recalculations and the others are plotted in Figure 8.16b. The condition used to cause recalculation to occur was determined by change in bed height. When this had changed by more than the fraction indicated for the curve the flow was recalculated. The results show that the simulation

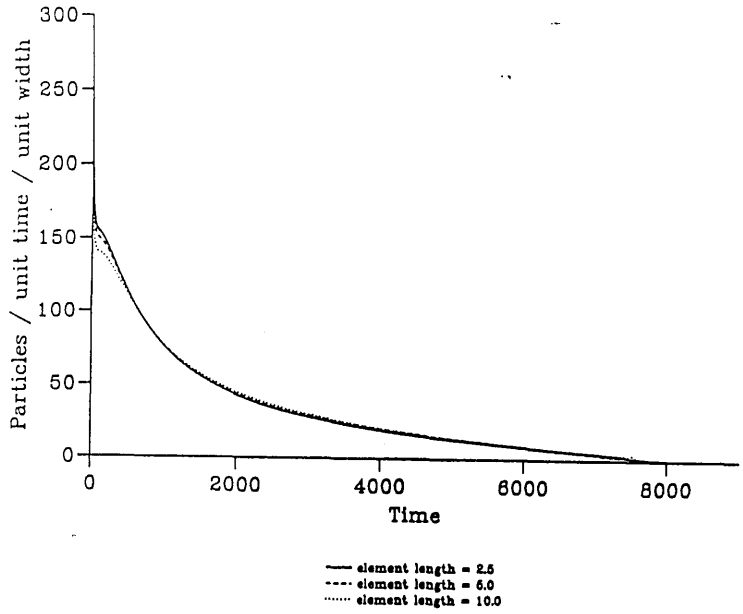

a) Linear time axis

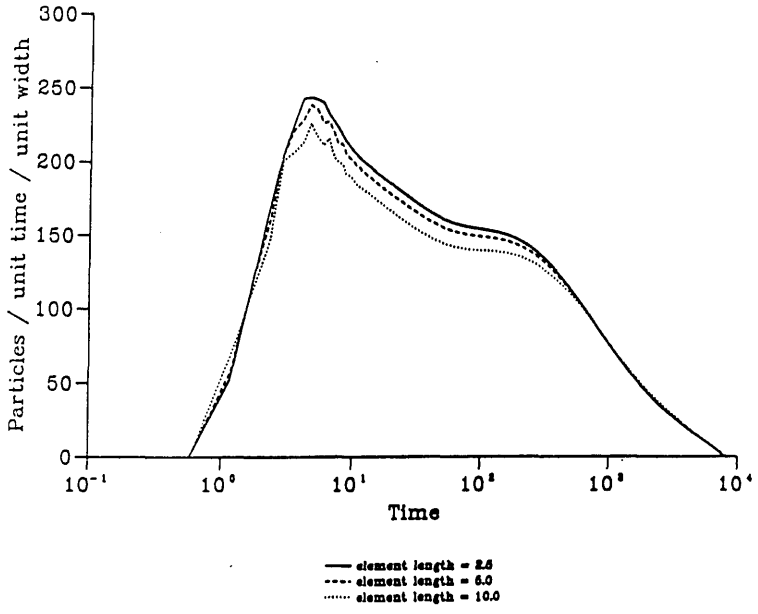

b) Logarithmic time axis

Figure 8.15 Effect of varying element length on transport rate at downstream boundary

Units non-dimensionalised with respect to initial downstream flow depth and initial mean bed shear velocity

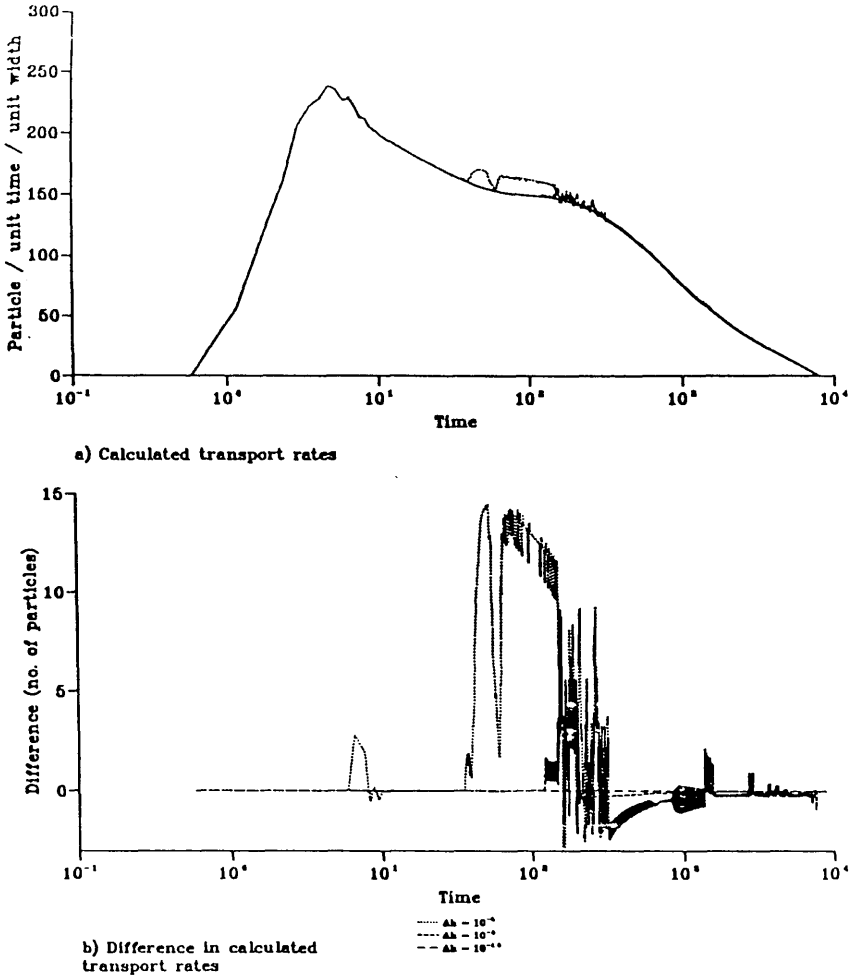

Figure 8.16 Effect of changing condition for recalculating flow on transport rate at downstream boundary

Units non-dimensionalised with respect to initial downstream flow depth and initial mean bed shear velocity

is relatively insensitive to the fraction used to cause the flow to be recalculated. The curves of Figure 8.16b show that the differences in calculated numbers of particles transported remains small even when differences start to occur. The obvious reason for wishing to reduce the number of recalculations of the flow would be to increase the speed of calculation, the results showed that the difference in calculation times was less than 5%, therefore recalculations of the flow were continued at each iteration.

The effects of varying the time interval used in the discretisation of the distributions and hence the duration of iterations in the calculations is shown in Figure 8.17, showing the transport rate out of the downstream end of the calculation, plotted on linear (a) and logarithmic axes (b). The curves show a higher initial rate of transport and faster completion of the transport of the erodable material for smaller time intervals. The total quantity of material transported out of the downstream end of the calculation was the same for each of the calculations. The rate of transport from these calculations never reaches the calculated equilibrium value shown in Figure 8.4, the calculated residual fluid transport stages confirm this, Figure 8.18. The residual fluid transport stage is above the critical stage for entrainment for almost the whole of the reach and certainly for the downstream end of the reach, close to where the transport rate is calculated. The transport rate in these calculations is therefore supply limited, either by the time interval used, the bed model used, the model of interaction between flow and sediment or some combination of these.

The calculated quantities of sediment in motion at equilibrium, Figure 8.3, show only a small range between values calculated using distributions with 800 intervals and those calculated using only 100 intervals, the time interval alone is therefore unlikely to be the cause of the different transport rates calculated here. For the size of particle used arranged in a square packing there are 134 particles per unit area, of these only those in the top four levels are available for transport during an iteration. The required rate of entrainment for the calculations performed using the distribution with 100 intervals is greater than the number of particles available from the

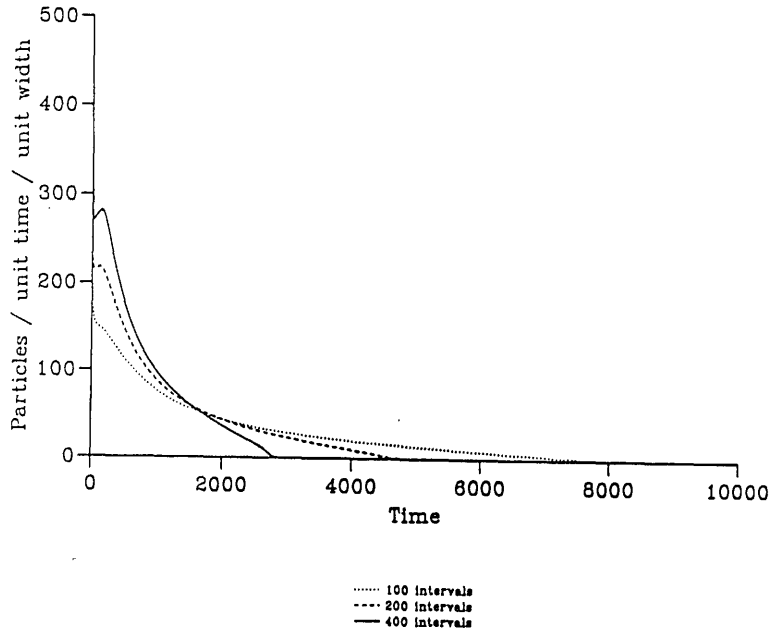

a) Linear time axis

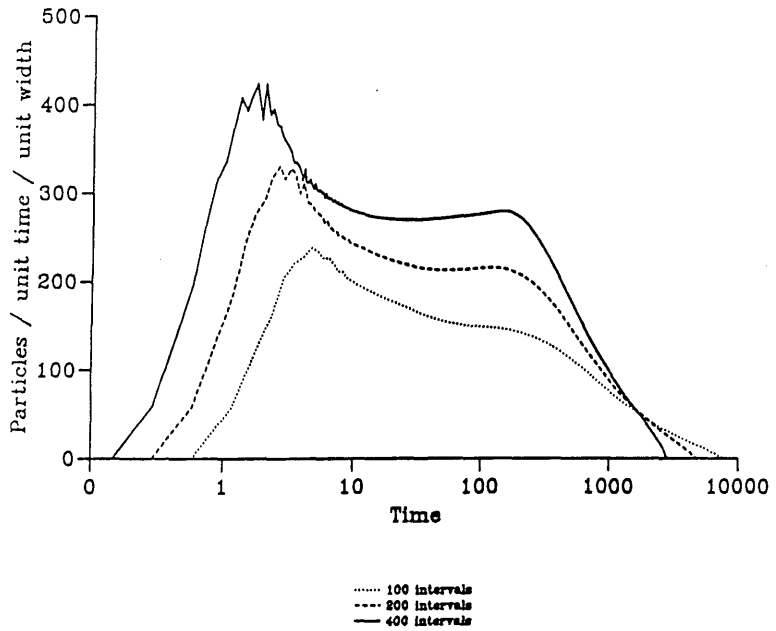

b) Logarithmic time axis

Figure 8.17 Effect of varying time interval to discretise distribution curves on transport rate at downstream boundary

Units non-dimensionalised with respect to initial downstream flow depth and initial mean bed shear velocity

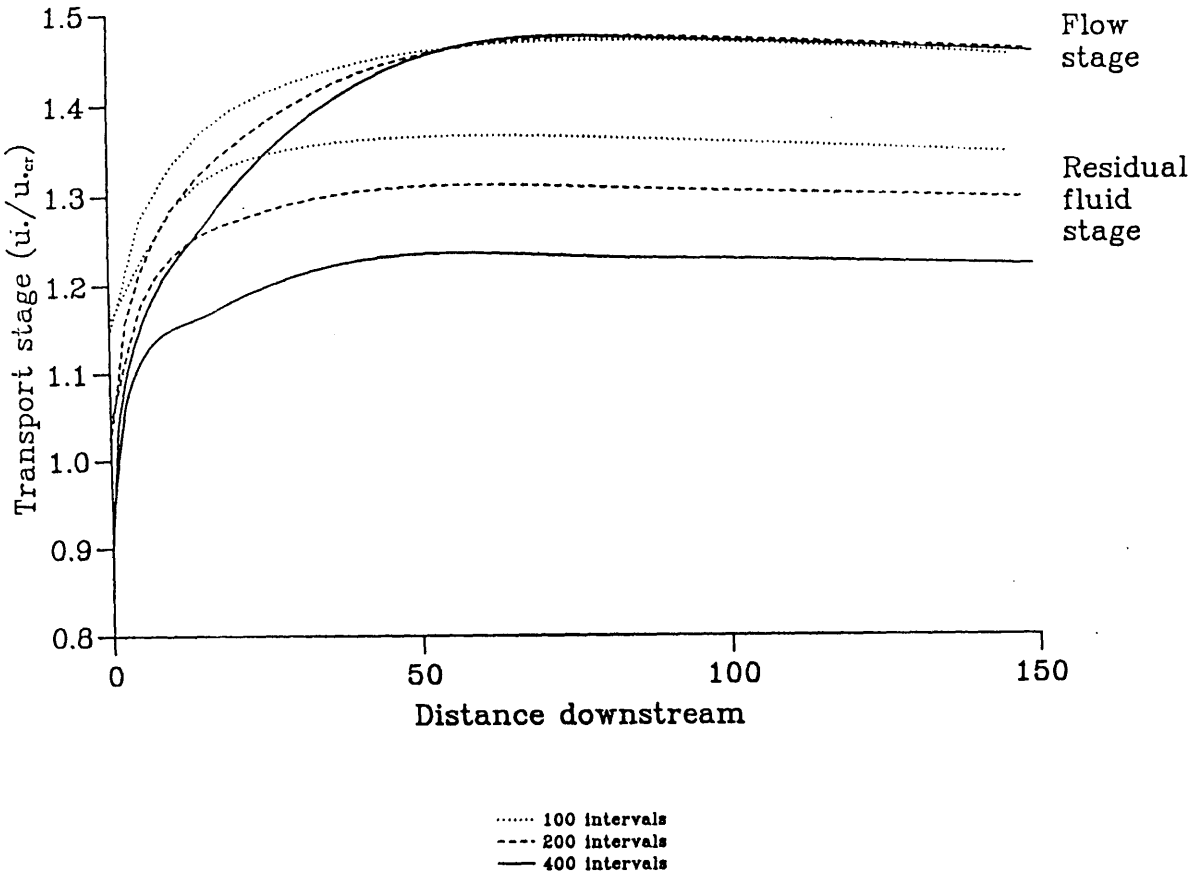

Figure 8.18 Calculated flow stage and residual fluid stage at bed

Units non-dimensionalised with respect to initial downstream flow depth

top four levels of the distribution. Therefore for this bed model and time interval the equilibrium transport rate cannot be reached. As the time interval decreases the number of particles required to be entrained for the equilibrium transport rate decreases and the calculated transport rate is able to approach the equilibrium rate. The present bed model takes no account of the duration of time interval in the quantity of material available for entrainment and for the calculations performed short time intervals are needed for the calculation to reach equilibrium. For the calculations performed a combination of bed and time interval limited the transport rate, however the calculated equilibrium transport rate might be high, Figure 8.6, and so the assumptions used in the interaction of sediment and flow might also be affecting the results.

8.5 Conclusions

The calculations of equilibrium transport rates show that distributions of particle movement can be used to calculate a consistent transport rate when a range of time intervals are used to discretise calculated distributions. Since larger time intervals give similar results to those calculated with smaller time intervals they can be used to represent distributions, reducing memory and computational power required for calculations involving the discretised distributions.

The results calculated for the equilibrium transport rate did not match the expression derived by Sekine & Kikkawa (1992), based on calculations and experiment. This could be due to the particular conditions used in the calculations and this possibility needs to be examined by performing further calculations.

The model of sediment transport over a mobile bed shows that distributions could be used to calculate the movement of sediment, though the description of the bed used here needs to be modified. The calculations described here only examine the behaviour of the model for a single size of particle. However the model was

programmed in such a way that calculations involving multiple size fractions could easily be performed once the appropriate distributions had been calculated.

The distributions used in the calculations of equilibrium transport rate and sediment transport over a mobile bed were produced from multiple calculations performed on a parallel processing computer. The use of distributions to represent particle behaviour allowed stochastic effects due to turbulence and the random nature of the bed to influence mass transport of sediment at a larger scale. The calculation of the distributions by the performance of repeated calculations on a parallel processing computer made efficient use of such a resource. The use of distributions to represent the movement of sediment in a calculation of mass movement of sediment allowed the results from previously performed calculation of the movement of thousands of particles to be used without the computational overhead of computing their movements at the time the transport calculation was performed. The use of a discretised distribution rather than a fitted function took advantage of increasing availability of memory and further simplified computation at the time calculations were performed by removing the need to repeatedly evaluate a function describing a distribution curve.

Chapter 9

Conclusions

9.1 Conclusions

Models of fluvial bedload transport at two scales have been developed. The first model, described in Part I of this thesis, is of the movement of individual sediment particles under the stochastic influences of turbulent velocity fluctuations in the flow. The second, described in Part II, is at the scale of mass transport of sediment particles, based on calculations from the single particle model and including the stochastic influences in that model.

9.1.1 Single Particles

At the scale of individual particle movements the stochastic nature of the process is due to turbulent velocity fluctuations of the flow and the structure of the bed. Turbulent velocity fluctuations affect initiation of particle movement and the trajectories of particles once in motion. The structure of the bed affects initiation of motion, due to the influence of bed geometry on particle position and the flow, and the impact of particles with the bed, due to the range of heights and angles at which an impact can occur. Existing deterministic models of the movement of sediment particles as bedload, such as those of Wiberg & Smith (1985) and Sekine & Kikkawa (1992), include a stochastic element in the model, due to the impact of particles with the bed, but do not include the influence of turbulent velocity fluctuations on particle movement. The model of particle movement developed here includes stochastic influences on particle movement due to the flow as well as the bed.

The model of the movement of single particles produced qualitative and quantitative agreement with observations of initiation of particle motion and particle

movements. The qualitative agreement included prediction of entrainment for a range of mean flow conditions. The movements of particles were also modified by velocity fluctuations. The method of including the effects of velocity fluctuations on particle movements, independent tracking of sediment particles and the fluid affecting the sediment particle, was therefore capable of introducing the effects of velocity fluctuations, on particles at rest and in motion.

Quantitative agreement with observations was reasonable but not perfect. Calculated quantities describing particle movement were consistently underestimated for the data of Abbott & Francis (1977), while for the data of Fernandez Luque & van Beek (1976) the predictions were better, if anything slightly over-predicting mean particle velocity. The results of Abbott & Francis (1977) were for the movements of single particles over a fixed bed, those of Fernandez Luque & van Beek (1976) for particles moving with other particles over a mobile bed. Particle movement extracts momentum from the flow and a particle moving with other particles would see lower flow velocities than a single particle. The fact that the calculated behaviour for the data of Fernandez Luque & van Beek (1976) was a better fit than that for Abbott & Francis (1977) could be because calculated momentum transfer from the flow was less than actual momentum transfer for a single particle. The treatment of impact at the bed in the model might also be more appropriate for a mobile than a fixed bed. The data of Abbott & Francis (1977) contained data describing saltations and suspended trajectories. The model of particle movement predicted suspended trajectories, but the number calculated was much lower than observed, a result of this is that no suspensions were predicted below a transport stage of 1.8.

9.1.2 Mass movement of sediment

The work on mass movement of sediment was based on the single particle model of particle movement. The reason for basing the calculations of mass movement of sediment on the single particle model was to include the stochastic influences of the

single particle movements in the calculated mass transport. Observations of particle movements, in flumes (Einstein, 1937), and in rivers (Hassan et al., 1991, Schmidt & Ergenzinger, 1992), show that particle movements are best described by distributions.

The obvious approach to scaling from single particle movements to mass transport of sediment would be to calculate the movement of all particles involved in the mass movement. To perform this calculation directly would involve calculating the movement of a very large number of particles. This approach has been used (Jiang & Haff, 1993), but is limited in the number of particles whose movements can be calculated by available computing resources. Here an alternative approach was developed.

The approach used was to calculate distributions of particle movements for a range of transport stages, combinations of particle size and initial particle height. Multiple calculations of single particle movements were performed for each set of conditions to generate the distributions. The calculations were performed on a parallel processing computer. Since the same calculation was being performed on each processor the speed up with increasing numbers of processors used was almost linear. The only alteration made to the model of single particle motion was to change the description of the bed. In the model of single particle movement this was flat, appropriate for comparison with observations. The calculation of particle movements for distributions used a random distribution to describe the heights of the centres of the particles forming the bed. This bed description introduced a range of initial particle positions and increased the likelihood of particle deposition occurring, either by trapping or by increasing the range of heights at which impact could occur.

The multiple calculations of particle movement showed distributions of distance travelled, time in motion and initiation of motion, showing that the particle movements were being affected by the stochastic influences. The behaviour seen in the distributions for each calculated transport stage, and across the range of transport

stages, matched expected behaviour. A comparison of the expression for particle step length of Sekine & Kikkawa (1992) showed similar values for step length but not the same change with transport stage. The differences are probably due to the impact model used here which is simplistic. Sekine & Kikkawa use a more realistic 3 dimensional impact model than the 2 dimensional model used here.

The distributions of particle movements were used in calculations of rate of transport and a model of the movement of sediment over a mobile bed. Once calculated distributions of particle movement could be used in many calculations of sediment transport. For each of these calculations the computing requirements would be less than if the movement of each particle involved in the process was calculated. In order to use the distributions two effects of the mass movement of sediment had to be addressed, particle-particle interactions and particle-flow interactions. For the range of transport stage used here the effects of the first were assumed to be small and ignored, based on the work of Leeder (1983). This is a potential limitation to the technique of using distributions, since as transport stage increases particle- particle interactions start to occur and their effects on particle movement become significant. The effects these interactions have on particle movement could be examined by analysis of observations of particle movement and by numerical experiment. It might be possible to include observed effects in calculation of movements of particles, allowing the use of distributions at high transport stages. The other effect of mass movement of sediment, particle-flow interaction, was addressed using the approach of Owen (1964). Shear stress in the layer where saltation occurred near the bed was partitioned between moving sediment and fluid. Reduction of shear stress at the bed due to particle movement, to the critical shear stress for initiation of motion, acted as a control on particle entrainment, allowing an equilibrium condition to be reached. The balance between fluid and grain shear was used to calculate equilibrium rates of transport and in the calculation of sediment transport over a mobile bed.

The calculations of transport rate were performed using discretised distribution curves of change in particle momentum at impact, equivalent to the momentum extracted from the flow, and the numbers of particles in motion. The calculated transport rates across a range of stages, with different time intervals, agreed with each other but not with observations and calculations of Sekine & Kikkawa (1992). The calculated quantity of material in motion was much higher than observed. Since the basis for the calculation of sediment transport was in both cases the model of Owen (1964) this implies that momentum transfer to the bed in this model was less than in that of Sekine & Kikkawa (1992) and than the actual rate of momentum transfer between particles and the bed. The reasons for this under-prediction of momentum transfer are not obvious, the incorrect calculation of step length might also affect the rate of change of momentum. At high transport stages calculated step lengths were greater than observed, for a particle to keep moving particle momentum would have to be conserved and not transferred to the bed, giving a lower rate of momentum transfer to the bed.

The calculation of sediment transport over a mobile bed used the distributions to calculate entrainment, movement and deposition of sediment. The distributions were used in a discretised form allowing simple iterative calculations to be used to calculate the transport of sediment. The flow over the mobile bed was calculated assuming steady gradually varied flow. Calculations were performed for a steady flow, with no upstream sediment input, showing erosion of the bed and gradual exhaustion of supply.

9.2 Further work

Further work to refine the present models and possible future directions for development will be described in two sections. The first will concentrate on the model of single particle movements, the second on the mass movement of particles, though reference will be made to the model of single particle movements.

9.2.1 Single particle

Comparison of the movement of particles calculated using the existing model with additional observed data would enable the behaviour of the model to be examined more closely and allow further consideration of what should be altered or improved. From the calculations performed using the present version of the model, two components suggest themselves as being the most important to study, the first is the interaction of velocity fluctuations with sediment particles, the second is the modelling of the impact process with the bed.

The method of introducing velocity fluctuations and their effects of the movement of sediment particles into the calculation affected the initiation of motion of particles and particle trajectories, but the number of suspended trajectories occurring was lower than that observed by (Abbott & Francis, 1977). The existing data used to describe the turbulence was limited, in particular the time scales used to describe the turbulence were derived from Eulerian data, since neither measured Lagrangian data, nor empirical conversions for measured Eulerian data were available. Techniques of measurement and analysis of turbulence that are available now could be used to improve the measurements of turbulence over rough beds in open channel flows. The use of electromagnetic current meters to measure turbulent flow over rough beds in rivers has already been mentioned as a source of Eulerian turbulence measurements (Heslop & Allen, 1989, Clifford, 1990). In flumes, Eulerian measurements of turbulence can be made using laser doppler anemometry (LDA), this is a non-invasive technique and can be used in close proximity to the bed without disturbing the flow (Wiberg & Nelson, 1992). Another approach to the measurement of turbulence has been the development of particle based techniques (Adrian, 1991), where a sheet of light is used to illuminate a flow seeded with particles, which are sufficiently small that they follow the flow. The particle positions are recorded and analysed, this method gives Lagrangian measurements of velocity fluctuations and turbulence scales, and can also give insight into the scales of structures involved in turbulence. Such

measurements can be used to supply Lagrangian values for measurements in their own right, or used to derive conversions from Eulerian to Lagrangian statistics in conjunction with LDA measurements. These conversions could then be used with Eulerian measurements of turbulence from rivers.

An alternative, or complementary, approach would be the generation of numerical flow fields, such as those described in Fung *et al.* (1992). The calculated flow behaviour either at a point or following particles can be used to derive Eulerian and Lagrangian statistics for such a flow field, and hence conversions between Eulerian and Lagrangian statistics. The method of Fung *et al.* (1992) can include the effects of boundaries on the flow.

Use of these approaches, either to obtain Lagrangian statistics directly, or to improve conversions from Eulerian to Lagrangian statistics would enable any doubt about the statistics used to describe the turbulence to be eliminated as the reason for the low number of suspended trajectories.

There may also be problems with the method of particle tracking used when it is applied close to boundaries. The flow conditions for eddies are always calculated at the centre of the sediment particle, even though the centre of the eddy might be regarded as being located elsewhere, half the vertical length scale of the eddy away from the bed as a minimum in these calculations. In homogeneous turbulence, or non-isotropic turbulence away from boundaries, the statistics describing the turbulence are the same at all points. The use of the sediment particle centre as the point at which eddy conditions are calculated means that the flow near the bed is sampled preferentially, velocity fluctuations are larger but the mean flow advecting the eddies is slower, which could affect the number of eddies through which a particle passed. If an initial separation of eddy and sediment particle was used in the calculation of eddy size and velocity fluctuations a greater area of the flow could be sampled by the eddies affecting sediment particle movement.

Calculations performed conserving different fractions of particle momentum on impact showed that this could have a large influence on particle movement. In Chapter 5 it was mentioned that the model of impact used here might be a better representation of an immobile, non-fixed bed than of a fixed bed. The appropriate fractions of momentum to conserve on impact may vary with the type of bed with which the impact occurs. The impact process could be studied using experimental work similar to that used in the aeolian environment (Willets & Rice, 1985, Mitha *et al.*, 1986), and by numerical simulations, again similar to those used in aeolian studies (Anderson & Haff, 1988, Werner & Haff, 1988), to determine appropriate fractions of momentum to conserve. The numerical models of particle impact would have to be modified to allow for the much lower relative density in the fluvial environment.

The impact process can also be modified by what happens immediately after impact. In the present model particle rotation only occurs when a particle is in contact with the bed; all rotation stops when the particle loses contact with the bed. If the loss of contact is at the start of a long non-contact movement the effects of friction due to the fluid would be expected to reduce or stop particle movement before contact with the bed occurs again. If the loss of contact is instantaneous then the energy is lost immediately and the particle movement must be affected. This could be important at the initiation of motion and after impact. The rotation could also affect the lift force acting on the particle, but since this is set empirically this is less of a problem.

The other components in the description of particle movement are the drag force, the lift force and the added mass terms. The drag force has been studied and the approximation of the coefficient of drag near a boundary with that for an isolated particle found to be a reasonable approximation (Coleman, 1972). The effect of varying the lift force acting on particles was examined in Chapter 5 and found to have a relatively small effect. The added mass terms were calculated using a single theoretical value for the added mass coefficient, the experimental expression for the

variation of added mass coefficient of Odar & Hamilton (1964) could be used in calculations to examine the effect this would have on calculated particle movements.

The model has at present only been used to calculate the movement of particles which would be expected to move as bedload with their trajectories modified by turbulence. If the model predicted the effects of suspension correctly it could then be used to examine the transition from bedload through to fully suspended movement of particles.

9.2.2 Mass movement of sediment

The work on mass movement of sediment was based on calculations performed using the single particle model, similarly the further work will include modifications to the single particle models for the calculations of distributions.

All the distributions, rate calculations and calculations of sediment movement were for a limited range of particle size, bed particle size, particle density and flow conditions. Calculations of distributions, which could then be used in rate calculations and calculations of sediment transport would enable the variation of transport behaviour to be examined. This would allow direct comparison of observations with the data of Sekine & Kikkawa (1992). For distributions calculated over a wide enough range of conditions the results could be used to run the model of sediment transport over a rough bed with multiple particle sizes. The code is already written to calculate movement of multiple particle sizes.

The calculations of particle movements for distributions were performed for complete particle movements, from initiation of movement to the deposition of the particle. The description of the bed and the model of deposition affect the distributions of movement calculated.

The description of the bed used for both single particle movements and the distributions of movements was based on a single size of sphere, the bed for the distributions of movement has the particle heights selected from a truncated Gaussian distribution. Alternative descriptions have been developed, for example that of Robert (1991); this uses a range of particle sizes, reproducing observed statistical behaviour of bed profiles. A problem with the model of Robert (1991) is that the spheres representing particles forming the bed all have their bases at a single level, the possible positions at which a particle can be trapped are therefore less than with the description of Sekine & Kikkawa (1992). A general problem with these models is that the particle whose motion is being calculated is always entrained from a position on top of an underlying surface whose geometry is being described, rather than from the surface itself. However a model like that of Robert (1991) does give a surface which is more realistic in terms of a range of sizes of particles forming the bed and could be related to the flow.

The model of deposition used in the calculation of distributions allowed particles to be deposited when they had insufficient momentum to continue rolling forward and when the particle centre fell below the zero velocity height. The former is a correct condition for deposition, the latter is due to limitations of the model of particle movement. If the position at which a flow velocity was required was below the zero velocity height the condition was trapped and the calculation stopped, a better treatment would be to set the velocity to zero. This would allow the calculation of particle movement to continue due to the particle momentum and under the influence of any velocity fluctuations acting, the condition for deposition of a particle would then be based on whether a particle had sufficient momentum to continue.

The rate calculations using distributions of particle movement show a higher rate of sediment transport than could be achieved in the model of sediment transport over a mobile bed. The quantity of material which must be entrained at each iteration to reach the equilibrium rate of transport was greater than the available surface

material. This could be due to a number of reasons. The rate calculated using the expression of Sekine & Kikkawa (1992), which gave a good fit to data, was much lower than that calculated using the distributions. The difference could be related to the conditions used, particularly the low particle density, or to the calculated momentum transfer at the bed. If the latter was the case then altering the description of impact and deposition, as described above, could well improve the fit of the model to that of Sekine & Kikkawa (1992) and data. If the lower rates of transport were used the problems with entrainment rates in the model of sediment transport would be reduced. The relation of time interval to entrainment rate could be investigated with further calculations. If necessary the bed structure might have to be modified to match available material to the time interval used in calculations.

The ultimate aim of this work was to examine development of bedforms. At present the model of sediment transport can be regarded as a non-recirculating flume, sediment is entrained from the bed, transported through the flume then trapped at the downstream end. The only type of behaviour such a system could reproduce would be armouring of the bed, and that would require multiple size fractions. If the model was made periodic so that material leaving the downstream boundary re-entered at the upstream end calculations could be performed for longer durations. As long as the calculations of sediment transport allowed equilibrium to become established the effects of perturbations in rate or composition could be examined.

The computational constraints on the calculations performed here are, as always speed, and with the approach used here space. For both of these the trend has been for performance to increase. The approach taken here makes use of this improvement along with the use of parallel processing. The present model of sediment transport was implemented on a single processor. However there is no reason why it should not be implemented on a parallel processing system, as long as computation and communication were balanced. This approach would both speed up calculations and allow the size of the system being described to be increased.

The approach used in the models described in this thesis allowed stochastic influences, important in sediment transport, to be represented both at the scale of individual particle movements and in calculations of sediment transport. The use of parallel processing computers to calculate distributions of particle movements enabled the scale of calculations to be increased from single particle movements to mass transport of sediment. The use of the distributions allowed the effects of stochastic influences on single particle movements to influence mass movements of particles in sediment transport. The calculation of sediment transport over a mobile bed described here was for a simple case. However the approach of using distributions, along with implementation of the sediment transport calculation on a parallel processing system, will allow calculations to be increased in scale, both in time and space. Calculation of sediment transport and bedform development for more realistic systems will then be possible, still retaining the effects of the underlying stochastic influences.

References

Abbott, J. E. & Francis, J. R. D., 1977. Saltation and suspension of solid grains in a water stream. Philosophical Transactions of the Royal Society of London A284, 225 - 254.

Adrian, R. J., 1991. Particle-imaging techniques for experimental fluid mechanics. Annual Review of Fluid Mechanics 23, 261 - 304.

Allen, C. M., 1982. Numerical simulation of contaminant dispersion in estuary flow. Proceedings of the Royal Society London A381, 179 - 194.

Allen, C. M., 1992. Particle tracking models for pollutant dispersion. In: Computer Modelling in the Environmental Sciences, eds. Farmer, D. G., & Rycroft, M. J., Clarendon, Oxford, 65 - 74.

Anderson, R. S. 1987, Eolian sediment transport as a stochastic process: The effects of a fluctuating wind on particle trajectories. Journal of Geology 95, 497 - 512.

Anderson, R. S. & Haff, P. K., 1988. Simulation of eolian saltation. Science 241, 820 - 823.

Antonia, R. A. & Luxton, R. E., 1971. Some statistical properties of turbulence in smooth & rough wall boundary layers. Technical note F-31, Charles Kolling Research Laboratory, University of Sydney.

Ashida, K. & Michiue, M., 1972. Study on hydraulic resistance and bedload transport rate in alluvial streams. Proceedings of the Japanese Society of Civil Engineers 206, 59 - 69.

Ashworth P. J., & Ferguson, R. I., 1989. Size-selective entrainment of bed-load in gravel bed streams. Water Resources Research 25, 627 - 634.

Bagnold, R. A., 1974. Fluid forces on a body in shear flow; experimental use of 'stationary flow'. Proceedings of the Royal Society of London A340, 147 - 171.

Basset, A. B., 1888. Treatise on Hydrodynamics. Vol. 2, Chap. 22, Deighton Bell, London, 285 - 297.

Batchelor, G. K., 1967. An Introduction to Fluid Dynamics. Cambridge University Press, Cambridge.

Beasley, J. D. & Springer, S. G., 1977. Algorithm AS111. The percentage points of the normal distribution. Applied Statistics 26, 118 - 121.

Bennett, J. P. & Nordin, C. F., 1977. Simulation of sediment transport and armouring. Hydrological Sciences Bulletin 22, 555 - 569.

Borah, D. K., Alonso, C. V. & Prasad, S. N., 1982. Routing graded sediments in streams: formulations. Journal of the Hydraulics Division ASCE 108, 1486 - 1503.

Boussinesq, J., 1903. Theorie Analytique de la Chaleur. Vol. 2, L'Ecole Polytechnique, Paris.

Buffington, J. M., Dietrich, W. E. & Kirchner, J. W., 1992. Friction angle measurements on a naturally formed gravel streambed: Implications for critical boundary shear stress. Water Resources Research 28, 411 - 425.

Bunte, K., 1992. Particle number grain-size composition of bedload in a mountain stream. In: Dynamics of Gravel-bed Rivers, eds. Billi, P., Hey, R. D., Thorne, C. R. & Tacconi, P., John Wiley & Sons Ltd., Chichester, 55 - 68.

Carling, P. A., 1989. Bedload transport in two gravel-bedded streams. Earth Surface Processes and Landforms 14, 27 - 39.

Carling, P. A., 1991. An appraisal of the velocity reversal hypothesis for stable pool-riffle sequences in the River Severn, England. Earth Surface Processes & Landforms 16, 19 -31.

Carling, P. A., Kelsey, A. & Glaister, M. S., 1992. Effect of bed roughness, particloe shape and orientation on initial motion criteria. In: Dynamics of Gravel-bed Rivers, eds. Billi, P., Hey, R. D., Thorne, C. R. & Tacconi, P., John Wiley & Sons Ltd., Chichester, 23 - 28.

Chacho, E. F., Burrows, R. L. & Emmett, W. W., 1989. Detection of coarse sediment movement using radio transmitters. In: Hydraulics and the Environment, Fluvial Hydraulics, IAHR XXIII Congress, Ottawa, 367 - 373.

Clifford, N. J., 1990. The formation, nature and maintenance of riffle-pool sequences in gravel-bedded rivers. PhD thesis, University of Cambridge.

Coleman, N. L., 1972. The drag coefficient of a stationary sphere on a boundary of similar spheres. La Houille Blanche 27, 17 - 21.

Correia, L. R. P., Bommanna, G., Krishnappan, G. & Graf, W. H., 1992. Fully coupled unsteady mobile boundary flow model. Journal of Hydraulic Engineering 118, 476 -494.

Csanady, G. T., 1963. Turbulent diffusion of heavy particles in the atmosphere. Journal of atmospheric sciences, 20, 201 - 208.

Crickmore, M. J. & Lean, G. H., 1962. The measurement of sand transport by means of radioactive tracers. Proceedings of the Royal Society of London A266, 402 - 421.

Drake, T. G., Shreve, R. L., Dietrich, W. E., Whiting, P. J. & Leopold, L. B., 1988. Bedload transport of fine gravel observed by motion-picture photography. Journal of Fluid Mechanics 192, 193 - 217.

Einstein, H. A., 1937. Bedload transport as a probability problem (in German) PhD thesis, Federal Institute of Technology, Zurich, Switzerland. (English translation by W. W. Sayre, In: Sedimentation, ed. Shen, H. W., H. W. Shen, Fort Collins, Colorado, USA. 1972)

Einstein, H. A., 1950. The bed-load function for sediment transportation in open channel flows. US Dept of Agriculture Technical Bulletin 1026. (Reprinted in: Sedimentation, ed. Shen, H. W., H. W. Shen, Fort Collins, Colorado, USA. 1972)

Einstein, H. A. & El-Samni, E. A., 1949. Hydrodynamic forces on a rough wall. Review of Modern Physics 21, 520 - 524.

Emmett, W. W. & Myrick, R. M., 1985. Field data describing the movement and storage of sediment in the East Fork River, Wyoming: Part V. Bed-material tracers, 1979 and 1980. US Geological Survey Open-File Report 85-169.

Fernandez Luque, R. & Van Beek, R., 1976. Erosion and transport of bed-load sediment. Journal of Hydraulic Research 14, 127 - 144.

Francis, J. R. D., 1973. Experiments on the motion of solitary grains along the bed of a water stream. Proceedings of the Royal Society London A 332, 443 - 471.

Fread, D. L. & Harbaugh, T. E., 1971. Open-channel profiles by Newton's iteration technique. Journal of Hydrology 13, 70 - 80.

Fung, J. C. H., Hunt, J. C. R., Malik, N. A. & Perkins, R. J., 1992. Kinematic simulation of homogeneous turbulence by unsteady random Fourier modes. Journal of Fluid Mechanics 236, 281 - 318.

Furbish, D. J., 1987. Conditions for geometric similarity of coarse stream-bed roughness. Mathematical Geology 19, 291 - 307.

Gladwell, I., 1979. Initial value routines in the NAG library. ACM Transactions on Mathematical Software 5, 386 - 400.

Gomez, B., Naff, R. L. & Hubbell, D. W., 1989. Temporal variations in bedload transport rates associated with the migration of bedforms. Earth Surface Processes and Landforms 14, 135 - 156.

Gordon, R., Carmichael, J. R. & Isackson, F. J., 1972. Saltation of plastic balls in a 'one-dimensional' flume. Water Resources Research 8, 444 -459.

Graf, W. H., 1971. Hydraulics of Sediment Transport. McGraw-Hill Book Company, New York.

Grass, A. J., 1971. Structural features of turbulent flow over smooth and rough boundaries. Journal of Fluid Mechanics 50, 233 - 255.

Haff, P. K. & Anderson, R. S., 1993. Grain scale simulations of loose sedimentary beds: the example of grain-bed impacts in aeolian saltation. Sedimentology 40, 175 - 198.

Hanna, S. R., 1979. Some statistics of Lagrangian and Eulerian wind fluctuations. Journal of Applied Meteorology 18, 518 - 525.

Hanna, S. R., 1981. Lagrangian & Eulerian time-scale relations in the daytime boundary layer. Journal of Applied Meteorology 20, 242 - 249.

Hanna, S. R., 1982. Applications in air pollution modelling. In: Atmospheric Turbulence and Air Pollution Modelling, eds. Nieuwstadt, F. T. & van Dop, H., Dordrecht, Reidel, 275 - 310.

Hassan, M. A., Church, M. & Schick, A. P., 1991. Distance of movement of coarse particles in gravel bed streams. Water Resources Research 27, 503 - 511.

Hassan, M. A. & Church, M., 1992. The movement of individual grains on the streambed. In: Dynamics of Gravel-bed Rivers, eds. Billi, P., Hey, R. D., Thorne, C. R. & Tacconi, P., John Wiley & Sons Ltd., Chichester, 159 - 173.

Heathershaw, A. D., 1979. The turbulent structure of the bottom boundary layer in a tidal current. Geophysical Journal of the Royal Astronomical Society 58, 395 - 430.

Heslop, S. E. & Allen, C. M., 1989. Turbulence and dispersion in larger UK rivers. In: Hydraulics and the Environment, Environmental Hydraulics, IAHR XXIII Congress, Ottawa, 75 - 82.

Heslop, S. E., Holland, M. J. & Allen, C. M., 1993. Turbulence measurements in the River Severn. In: Mixing and Transport in the Environment, eds. Chatwin, P. C., Beven, K. J. & Millbank, J., John Wiley & Sons Ltd., Chichester, in press.

Hey, R. D., 1979. Flow resistance in gravel-bed rivers. Journal of the Hydraulics Divison ASCE 105, 365 - 379.

Hinze, J. O., 1959, Turbulence. McGraw-Hill, New York.

Hinze, J. O., 1972. Turbulent fluid and particle interaction. Progress in Heat and Mass Transfer 6, 433 - 452.

Hoey, T., 1992. Temporal variations in bedload transport rates and sediment storage in gravel-bed rivers. Progress in Physical Geography 16, 319 - 338

Holly, F. M. & Rahuel, J.-L., 1990. New numerical/physical framework for mobile-bed modelling. Journal of Hydraulic Research 28, 401 - 416.

Hubbell, D. W. & Sayre, W. W., 1964. Sand transport studies with radioactive tracers. Journal of the Hydraulics Division ASCE 90, 39 - 68.

Hunt, J. C. R. & Nalpanis, P., 1985. Saltating and suspended particles over flat and sloping surfaces. I. Modelling concepts. In: Proceedings of the International Workshop on Physics of Blown Sand, Memoirs 8, Vol. I, eds. Barnsdorff-Nielsen, O. E., Moller, J. T., Rasmussen, K. R. & Willets, B. B., Department of Theoretical Statistics, Aarhus University, Denmark, 9 - 36.

Jackson, R. G., 1976. Sedimentological and fluid-dynamic implications of the turbulent bursting phenomenon in geophysical flows. Journal of Fluid Mechanics 77, 531 - 560.

James, C. S., 1990. Prediction of entrainment conditions for nonuniform, noncohesive sediments. Journal of Hydraulic Research 28, 25 - 42.

Jiang, Z. & Haff, P. K., 1993. Multiparticle simulation methods applied to the micromechanics of bed load transport. Water Resources Research 29, 399 - 412.

Kirchner, J. W., Dietrich, W. E. Iseya, F. & Ikeda, H., 1990. The variability of critical shear stress, friction angle, and grain protrusion in water-worked sediments. Sedimentology 37, 647 - 672.

Kirkby, M. J., 1991. Sediment travel distance as an experimental and model variable in particulate movement. Catena Supplement 19, 111 - 128.

Kline, S. J., Reynolds, W. C., Schraub, F. A. & Rundstadler, P. W., 1967. The structure of turbulent boundary layers. Journal of Fluid Mechanics 30, 741 - 773.

Komar, P. D. & Li, Z., 1986. Pivoting analyses of the selective entrainment of sediment by shape and size with application to gravel threshold. Sedimentology 33, 425 - 436.

Komar, P. D. & Li, Z., 1988. Applications of grain-pivoting to selective entrainment of gravel and to flow compentence evaluations. Sedimentology 35, 681 - 695.

Komori, S., Nagaosa, R., Murakami, Y., Chiba, S., Ishii, K., & Kuwahara, K., 1993. Direct numerical-simulation of 3-dimensional open-channel flow with zero-shear gas-liquid interface. Physics of Fluids A-Fluid Dynamics 5, 115 - 125.

Leeder, M. R., 1979. 'Bedload' dynamics: grain-grain interactions in water flows. Earth Surface Processes 4, 229 - 240.

Leeder, M. R., 1983. On the interactions between turbulent flow, sediment transport and bedform mechanics in channelized flows. In: Modern & Ancient Fluvial Systems, eds. Collinson, J. D. & Lewin, J., Special Publication of the International Association of Sedimentologists 6, 5 - 18.

Levi, E, 1983. A universal Strouhal law. Journal of Mechanical Engineering ASCE, 109, 718 - 727.

Levi, E., 1991. Vortices in hydraulics. Journal of Hydraulic Engineering 117, 399 - 413.

Lu, S. S. & Wilmarth, W. W., 1973. Measurements of the Reynolds stress in a turbulent boundary layer. Journal of Fluid Mechanics 60, 481 - 511.

Lynov J.P., Nielsen, A.H., Pecseli, H.L., Rasmussen, J.J., 1991. Studies of the Eulerian-Lagrangian transformation in 2-dimensional random flows. Journal of Fluid Mechanics 224, 485-505.

MacInnes, J. M. & Bracco, F. V., 1991. Stochastic particle dispersion modeling and the tracer-particle limit. Physics of Fluids A - Fluid Dynamics 4, 2809 - 2824.

McEwan, I. K., Willetts, B. B. & Rice, M. A., 1992. The grain/bed collision in sand transport by wind. Sedimentology 39, 971 - 981.

McQuivey, R. S., 1973. Summary of turbulence data from rivers, conveyance channels and laboratory flumes - Turbulence in Water. US Geological Survey Professional Paper 802-B.

McQuivey, R. S. & Keefer, T. N., 1971. Turbulent diffusion and dispersion in open channel flow. In: Stochastic Hydraulics, ed. Chiu, C.-L., University of Pittsburgh, Piitsburgh, 231 - 250.

Marsaglia, G., Zaman, A. & Tsang, W. W., 1989. Toward a universal random number generator. Statistics & Probability Letters 9, 35 - 39.

Maxey, M. R. & Riley, J. J., 1983. Equation of motion for a small rigid sphere in a nonuniform flow. Physics of Fluids 26, 883 - 889.

Meland, N. & Norrman, J. O., 1966. Transport velocities of single particles in bed load motion. Geografiska Annaler 48, 165 - 182.

Milne-Thomson, L. M., 1968. Theoretical Hydrodynamics. 5th ed. Macmillan.

Mitha, S., Tran, M. Q., Werner, B. T. & Haff, P. K., 1986. The grain-bed impact process in aeolian saltation. Acta Mechanica 63, 267 - 278.

Morsi, S. A. & Alexander, A. J., 1972. An investigation of particle trajectories in two phase flow systems. Journal of Fluid Mechanics 55, 193 -208.

Murphy, P. J. & Hooshiari, H., 1982. Saltation in water dynamics. Journal of the Hydraulics Division ASCE 108, 1251 - 1267.

Naden, P., 1987a. An erosion criterion for gravel bed rivers. Earth Surface Processes & Landforms 12, 83 - 93.

Naden, P., 1987b. Modelling gravel-bed topography from sediment transport. Earth Surface Processes & Landforms 12, 353 - 367.

NAG, 1991. NAG Fortran Library Manual, Mark 15, NAG, Oxford.

Nakagawa, H. & Nezu, I., 1977. Prediction of the contribution to Reynolds stress from bursting events in open-channel flow. Journal of Fluid Mechanics 80, 99 - 128.

Nakagawa, H., Tsujimoto, T. & Shimizu, Y., 1988. Velocity profile of flow over rough permeable bed. Proceedings 6th Congress IAHR Kyoto Japan, 20-22 July, 449-456.

Newman, J. N., 1978. Marine Hydrodynamics. MIT Press, Cambridge, Massachusetts.

Odar, F. & Hamilton, W. S., 1964. Forces on a sphere accelerating in a viscous fluid. Journal of Fluid Mechanics 18, 302 - 314.

Oseen, C., 1927. Hydrodynamik. Akademische Verlagsgesellschaft, Leipzig.

Owen, P. R., 1964. Saltation of uniform grains in air. Journal of Fluid Mechanics 20, 225 - 242.

Pasquill, F. & Smith, F. B., 1983. Atmospheric diffusion. 3rd ed, Ellis Horwood Ltd., Chichester

Park, I. & Jain, S. C., 1987. Numerical simulation of degradation of alluvial channel beds. Journal of Hydraulic Engineering 113, 845 - 859.

Parker, G. & Sutherland, A. J., 1990. Fluvial armour. Journal of Hydraulic Research 28, 529 - 544.

Perry, A. E., Henbest, S. & Chong, M. S., 1986. A theoretical and experimental study of wall turbulence. Journal of Fluid Mechanics 165, 163 - 199.

Perry, A. E., Lim, K. L. & Henbest, S. M., 1987. An experimental study of turbulence structure in smooth- and rough-wall turbulent boundary layers. Journal of Fluid Mechanics 177, 437 - 466.

Rahuel, J. L., Holly, F. M., Chollet, J. P., Belleudy, P. J. & Yang, G., 1989. Modeling of riverbed evolution for bedload sediment mixtures. Journal of Hydraulic Engineering 115, 1521 - 1542.

Raudkivi, A. J., 1990. Loose Boundary Hydraulics. 3rd Ed. Pergammon Press, Oxford.

Raupach, M. R., Antonia, R. A. & Rajagopalan, S., 1991. Rough-wall turbulent boundary layers. Applied Mechanics Review 44, 1 - 25.

Reid, I., Frostick, L. E. & Brayshaw, A. C., 1992. Microform roughness elements and the selective entrainment and entrapment of particles in gravel-bed rivers. In: Dynamics of Gravel-bed Rivers, eds. Billi, P., Hey, R. D., Thorne, C. R. & Tacconi, P., John Wiley & Sons Ltd., Chichester, 253 - 266.

Reizes, J. A., 1978. Numerical study of continous saltation. Journal of the Hydraulic Division ASCE 104, 1305 - 1321.

Richards, K. S., 1990. Fluvial geomorphology: initial motion of bed material in gravel-bed rivers. Progress in Physical Geography 14, 395 - 415.

Robert, A., 1988. Statistical properties of sediment bed profiles in alluvial channels. Mathematical Geology 20, 205 -225.

Robert, A., 1991. Fractal properties of simulated bed profiles in coarse-grained channels. Mathematical Geology 23, 367 - 382.

Rumpel, D. A. 1985. Succesive aeolian saltation: studies of idealized collisions. Sedimentology 32, 267 - 280.

Saffman, P. G., 1965. The lift on a small sphere in slow shear flow. Journal of Fluid Mechanics 22, 385 - 400.

Sawford, B. L. & Guest, F. M., 1991. Lagrangian statistical simulation of the turbulent motion of heavy particles. Boundary-Layer Meteorology 54, 147 - 166.

Schmidt, K.-H., & Ergenzinger, P., 1992. Bedload entrainment, travel lengths, step lengths, rest periods-studied with passive (iron, magnetic) and active (radio) tracer techniques. Earth Surface Processes & Landforms 17, 147 - 165.

Sekine, M. & Kikkawa, H., 1988. A fundamental study on the sediment transport in an open channel flow. Memoirs of the School of Science and Engineering 52, Waseda University, 103 - 141.

Sekine, M. & Kikkawa, H., 1992. Mechanics of saltating grains. II. Journal of Hydraulic Engineering 118, 536-558.

Sekine, M. & Parker, G., 1992. Bedload transport on a transverse slope. I. Journal of Hydraulic Engineering 118, 513 - 535.

Shields, A., 1936. Anwendung der aehnlichkeits-mechanik und der turbulenzforschung auf die geschiebebewgung. Preussische Versuchsanstalt fur Wasserbau und Schiffbau, Berlin.

Shuen, J.-S., Solomon, A. S. P., & Faeth, G. M., 1986. Drop-turbulence interactions in a diffusion flame. AIAA Journal 24, 101 - 108.

Soulsby, R. L., 1983. The bottom boundary layer of shelf seas. In: Physical Oceanography of Coastal and Shelf Seas, ed. Johns, B., Elsevier, Amsterdam, 189 - 266.

Snyder, W. H. & Lumley, J. L., 1971. Some measurements of particle velocity autocorrelation functions in a turbulent flow. Journal of Fluid Mechanics 48, 41 - 71.

Sullivan, P. J., 1971. Longitudinal dispersion within a two-dimensional shear flow. Journal of Fluid Mechanics 49, 551 - 576.

Sullivan, P. J., 1974. Instantaneous velocity and length scales in a turbulent shear flow. Advances in Geophysics 18A, 213 - 223.

Sumer, B. M., 1984. Lift forces on moving particles near boundaries. Journal of Hydraulic Engineering 110, 1272 - 1278.

Sumer, B. M. & Deigaard, R., 1981. Particle motions near the bottom in turbulent flow in an open channel. Part 2. Journal of Fluid Mechanics 109, 311 - 338.

Tampieri, F., Scarani, C., Giostra, U., Brusaca, G., Tinarelli, G., Anfossi, D. & Ferrero, E., 1992. On the application of random flight dispersion models in inhomogeneous turbulent flows. Annales Geophysicae-Atmospheres, Hydrospheres & Space Sciences 10, 749 - 758.

Taylor, G. I., 1921. Diffusion by continuous movements. Proceedings of the London Mathematical Society Series 2 20, 196 - 212.

Taylor, G. I., 1938. The spectrum of turbulence. Proceedings of the Royal Society of London A219, 476 - 490.

Tchen, C. M., 1947. Mean value and correlation problems connected with the motion of small particles suspended in a turbulent flow. Ph.D. thesis, Delft.

Thomas, T. G., Williams, J. J. R. & Leslie, D. C., 1992. Development of a conservative 3D free surface code. Journal of Hydraulic Research 30, 107 - 115.

Thompson, R., 1971. Numeric calculation of turbulent diffusion. Quarterly Journal of the Royal Meteorolgical Society 97, 93 - 98.

Thorne, P. D., Williams, J. J. & Heathershaw, A. D., 1989. In situ acoustic measurements of marine gravel threshold and transport. Sedimentology 36, 61 - 74.

Ungar, J. E. & Haff, P. K., 1987. Steady state saltation in air. Sedimentology 34, 289 - 299.

Van Dam, G. C.,1993. The study of shear dispersion in tidal waters by applying discrete particle techniques. In: Mixing and Transport in the Environment, eds. Chatwin, P. C., Beven, K. J. & Millbank, J., John Wiley & Sons Ltd., Chichester, in press.

Van Niekerk, A., Vogel, K. R., Slingerland, R. L. & Bridge, J. S., 1992. Routing of heterogeneous sediments over moveable bed: model dvelopment. Journal of Hydraulic Engineering 118, 246 -262.

Van Rijn, L. C., 1984. Sediment transport, part I: bed load transport. Journal of Hydraulic Engineering 110, 1431 - 1456.

Vogel, K. R., van Niekerk, A., Slingerland, R. L. & Bridge, J. S., 1992. Routing of heterogeneous sediments over moveable bed: model verification. Journal of Hydraulic Engineering 118, 263 - 279.

Werner, B. T., 1987. A physical model of wind-blown sand transport. Ph.D. thesis, California Institute of Technology.

Werner, B. T., 1990. A steady-state model of wind-blown sand transport. Journal of Geology 98, 1 - 17

Werner, B. T. & Haff, P. K., 1988. The impact process in aeolian saltations: two-dimensional simulations. Sedimentology 35, 189 - 196.

White, C. M., 1940. The equilibrium of grains on the bed of a stream. Proceedings of the Royal Society of London A174, 332 - 338.

Wiberg, P. L. & Nelson, J. M., 1992. Unidirectional flow over asymmetric and symmetrical ripples. Journal of Geophysical Research 97, 12745 - 12761.

Wiberg, P. L. & Smith, J. D., 1985. A theoretical model for saltating grains in water. Journal of Geophysical Research 90, 7341 - 7354.

Wiberg, P. L. & Smith, J. D., 1987. Calculations of the critical shear stress for motion of uniform and heterogeneous sediments. Water Resources Research 23, 1471 - 1480.

Wiberg, P. L. & Smith, J. D., 1989. Model for calculating bed load transport of sediment. Journal of Hydraulic Engineering 115, 101 - 123.

Willetts, B. B. & Rice, M. A., 1985. Inter-saltation collisions. In: Proceedings of the International Workshop on Physics of Blown Sand, Memoirs 8, Vol I, eds. Barnsdorff-Nielsen, O. E., Moller, J. T., Rasmussen, K. R. & Willets, B. B., Department of Theoretical Statistics, Aarhus University, Denmark, 83 - 100.

Willetts, B. B., Maizels, J. K. & Florence, J., 1987. The simulation of stream bed armouring and its consequences. Proceedings of the Institute of Civil Engineers Part I 82, 799 - 814.

Williams, G. P., 1970. Flume width and water depth effects in sediment transport experiments. US Geological Survey Professional Paper 562H.

Williams, J.J., 1990. Video observations of marine gravel transport. Geo-Marine Letters 10, 157 -164.

Wilson, J. D. & Zhuang, Y., 1989. Restriction on the timestep to be used in stochastic Lagrangian models of turbulent dispersion. Boundary-Layer Meteorology 49, 309 - 316.

Yalin, M. S., 1977. Mechanics of Sediment Transport. 2nd ed. Pergamon Press, Oxford.

Yvergniaux, P. & Chollet, J. P., 1989. Particle trajectories modelling based on a Lagrangian memory effect. In: IAHR XXIII Congress, Hydraulics and the environment, Turbulence in Hydraulics, 301 - 313.

Zannetti, P., 1990. Air Pollution Modeling: Theories, Computational Methods and Available Software. Van Nostrand Reinhold, New York.

Zhuang, Y., Wilson, J. D. & Lozowski, E. P., 1989. A trajectory-simulation model for heavy particle motion in turbulent flow. Journal of Fluids Engineering 111, 492 - 494.

Nomenclature

A	L^2	surface area, grain projected area
A_E	L^2	area of element (A / h^2)
A_{slab}	L^2	area of slab
Ac		acceleration number ((particle velocity)^2 / (particle acceleration x particle diameter)
b	MT^{-1}	damping coefficient
C_A		coefficient of added mass
C_D		coefficient of drag
C_L		coefficient of lift
C_{L0}		coefficient of lift at reference height
c_s		concentration of sediment
c_*		normalised concentration profile of sediment
$\langle c_s \rangle$		vertically averaged sediment concentration
D_{84}	L	particle diameter for which 84% of sediment by mass is smaller (D_{84} / h)
d	L	particle diameter (d / h)
d_{char}	L	diameter of bed particle (d_{char} / h)
F	MLT^{-2}	body force
F_A	MLT^{-2}	added mass force due to fluid acceleration (F_A/ $\rho U_*^2 h^2$)
$F_{boundary}$	MLT^{-2}	Force acting on boundary per unit width ($F_{boundary}$/ $\rho U_*^2 h^2$)
F_D	MLT^{-2}	drag force (F_D/ $\rho U_*^2 h^2$)
F_L	MLT^{-2}	lift force (F_L/ $\rho U_*^2 h^2$)
f_{dn}		fraction of particles of size d deposited in n iterations
fe_{hd}		fraction of particles of size d entrained from level h
f_n		density function for number of hops
f_t		density function for time
g	LT^{-2}	acceleration due to gravity (gh / U_*^2)
h	L	depth of flow level within bed

k	MT^{-2}	spring constant
k_s	L	Nikuradse roughness length scale (k_s / h)
k_1	L^{-1}	reciprocal of mean step length
k_2	T^{-1}	reciprocal of mean rest period
L	L	step length
$\langle L \rangle$	L	mean step length
L_E	L	Eulerian integral length scale (L_E / h)
L_L	L	Lagrangian integral length scale (L_L / h)
L_s	L	saltation length
L_0	L	$\sigma_L^2 / 2\langle L \rangle$
l	L	streamwise length of bed
	L	mixing length
	L	average distance between grains
M	MLT^{-1}	total momentum extracted from flow during particle movement ($M / \rho h^3 U_{*cr}$)
m	M	mass of particle
m_{slab}	M	mass of slab
N	MLT^{-2}	normal force on rotating particle
n		normal to surface
		power in expression for variation in lift
		number of hops
n_p	L^{-2}	number of particles entrained in a time interval per unit area (h^{-2})
		number of particles travelling a distance greater than x (Kirkby, 1991)
n_{pA}	L^{-2}	number of particles per unit area (h^{-2})
n_{0p}		number of particles initially in motion
n_{total}	L^{-2}	total number of particles per unit area (h^{-2})
nb_{hd}		number of bed particles of size d at level h in the bed
nd_d		number of particles of size d deposited n iterations after it was entrained
ne_d		number of particles of size d entrained
nm_d		number of particles of size d remaining in motion

p	$ML^{-1}T^{-2}$	pressure
		proportion of stones moving at an event
q	LT^{-1}	magnitude of velocity
	L^2T^{-1}	volumetric bedload transport rate per unit width
R		autocorrelation
Re_p		particle Reynolds number ($u_r d/\nu$)
Re_{*k_s}		shear velocity roughness scale Reynolds number ($U_* k_s/\nu$)
Re_{*_p}		shear velocity particle Reynolds number ($U_* d/\nu$)
r		correlation coefficient
S		slope of channel
S_f		friction slope
T_E	T	Eulerian integral time scale ($T_E U_* / h$)
T_L	T	Lagrangian integral time scale ($T_L U_* / h$)
T_{L^*}	T	modified Lagrangian integral time scale
t	T	time (tU_* / h)
t_r	T	particle response time ($t_r U_* / h$)
t_s	T	duration of saltation
U	LT^{-1}	mean streamwise velocity (U / U_*)
U_p	LT^{-1}	mean particle velocity (U_p / U_*)
$U_{U_{*_f}}$	LT^{-1}	mean particle velocity for fluid stage U_{*_f} ($U_{U_{*_f}} / U_{*1.5}$)
U_*	LT^{-1}	mean bed shear velocity
U_{*cr}	LT^{-1}	mean bed shear velocity for initiation of particle movement
$\overline{U}$	LT^{-1}	depth mean flow velocity ($\overline{U} / U_{*1.5}$)
u	LT^{-1}	streamwise instantaneous flow velocity (u / U_*)
u'	LT^{-1}	streamwise fluctuating flow velocity (u' / U_*)
u_p	LT^{-1}	streamwise particle velocity (u_p / U_*)
u_t	LT^{-1}	particle terminal velocity
V	L^3	volume of particle
V_s	L	volume of sediment in motion per unit area

v	LT^{-1}	cross-stream instantaneous flow velocity
$\hat{W}$	LT^{-1}	correlated mean vertical velocity ($\hat{W} / U_*$)
w	LT^{-1}	vertical instantaneous flow velocity (w / U_*)
w'	LT^{-1}	vertical fluctuating flow velocity (w' / U_*)
w_p	LT^{-1}	vertical particle velocity (w_p / U_*)
X		normalised step length
x	L	streamwise direction (x / h)
x_{slab}	L	streamwise distance moved by slab
y	L	cross-stream direction
z	L	vertical distance above velocity distribution zero (z / h)
z_0	L	roughness length scale (z_0 / h)
z_+		wall units ($U_* z/\nu$)
α		shape factor (Ad / V)
β		$\sigma_w T_L / L_E$
Δ		fraction of time scales used at iteration
ΔM	MLT^{-1}	change in momentum at impact (Chapter 7, $\Delta M / \rho h^3 U_*$)
	MLT^{-2}	change in momentum during time interval (Chapter 8, $\Delta M / \rho h^2 U_*^2$)
ΔM_f	MLT^{-1}	flow momentum over an element ($\Delta M_f / \rho h^3 U_{*1.5}$)
ΔM_{ge}	MLT^{-1}	change in momentum sediment above an element ($\Delta M_{ge} / \rho h^3 U_{*1.5}$)
ΔM_n	MLT^{-1}	change in momentum at due to material entrained n iterations before ($\Delta M_n / \rho h^3 U_{*1.5}$)
Δu_p	LT^{-1}	change in streamwise particle velocity at impact ($\Delta u_p / U_*$)
Δt	T	time interval ($\Delta t U_* / h$)
$\Delta x_{deposition}$	L	distance over which deposition occurs during a time interval ($\Delta x_{deposition} / h$)
$\Delta x_{element}$	L	length of downstream element ($\Delta x_{element} / h$)
$\Delta x_{transport}$	L	distance moved by particles during a time interval ($\Delta x_{transport} / h$)
δ		Kronecker delta
	L	particle overlap
ϕ		velocity potential, coordinates fixed

Φ		velocity potential, moving coordinates
Λ	L	length scale of eddies
κ		von Karman's constant
μ	$ML^{-1}T^{-1}$	dynamic viscosity
μ_d		dynamic friction coefficient
μ_t	$ML^{-1}T^{-1}$	eddy viscosity
ν	L^2T^{-1}	kinematic viscosity
θ		angle between particle centres above horizontal
θ_p		pivoting angle
ρ	ML^{-3}	fluid density
ρ_s	ML^{-3}	sediment density (ρ / ρ_s)
σ_l	L	standard deviation of steplength
σ_u	LT^{-1}	standard deviation of streamwise velocity fluctuations (σ_u / U_*)
σ_w	LT^{-1}	standard deviation of vertical velocity fluctuations (σ_w / U_*)
$\hat{\sigma}_w$	LT^{-1}	correlated standard deviation of vertical velocity fluctuations ($\hat{\sigma}_w$ / U_*)
τ	$ML^{-1}T^{-2}$	flow shear stress (τ / ρU_{*cr}^2)
τ_{cr}	$ML^{-1}T^{-2}$	critical shear stress for initiation of particle movement (τ_{cr} / ρU_{*cr}^2)
τ_f	$ML^{-1}T^{-2}$	fluid shear stress
τ_g	$ML^{-1}T^{-2}$	grain shear stress (τ_g / ρU_{*cr}^2)
τ_{gb}	$ML^{-1}T^{-2}$	bed grain shear stress
τ_*		dimensionless shear stress (ρU_*^2 / $g(\rho_s - \rho)h$)
τ_{*cr}		Shields stress for initiation of particle movement(ρU_{*cr}^2 / $g(\rho_s - \rho)d$)
ω	T^{-1}	angular velocity of particle (h / ωU_*)
i subscript		where i =1,2,3 equivalent to x, y, z directions
N subscript		normal component
T subscript		tangential component
x subscript		component in x direction
z subscript		component in z direction

Appendix 1 Rolling motion of particles

Vectors used in rolling model

The rectangular, **i**, **k**, and polar, $\mathbf{r}_1$, θ_1, unit vectors are defined as shown in Figure A1.1.. The conversion from rectangular to polar vectors can then be written:

$$\mathbf{r}_1 = -\cos\theta\,\mathbf{i} + \sin\theta\,\mathbf{k}$$
$$\theta_1 = \sin\theta\,\mathbf{i} + \cos\theta\mathbf{k}$$

where θ is the angle above the horizontal. From these the rate of change of the polar unit vectors with respect to time can be calculated:

$$\frac{d\mathbf{r}_1}{dt} = \frac{\partial \mathbf{r}_1}{\partial r}\frac{\partial r}{\partial t} + \frac{\partial \mathbf{r}_1}{\partial \theta}\frac{\partial \theta}{\partial t}$$
$$= (0)\frac{\partial r}{\partial t} + (\sin\theta\,\mathbf{i} + \cos\theta\,\mathbf{k})\omega$$
$$= \omega\theta_1$$

$$\frac{d\theta_1}{dt} = \frac{\partial \theta_1}{\partial r}\frac{\partial r}{\partial t} + \frac{\partial \theta_1}{\partial \theta}\frac{\partial \theta}{\partial t}$$
$$= (0)\frac{\partial r}{\partial t} + (\cos\theta\,\mathbf{i} - \sin\theta\,\mathbf{k})\omega$$
$$= -\omega\,\mathbf{r}_1$$

The velocity, **v**, can then be calculated

$$\mathbf{v} = \frac{d\mathbf{r}}{dt}$$
$$= \frac{dr}{dt}\mathbf{r}_1 + r\frac{d\mathbf{r}_1}{dt}$$
$$= \frac{dr}{dt}\mathbf{r}_1 + r\omega\theta_1$$

and the acceleration

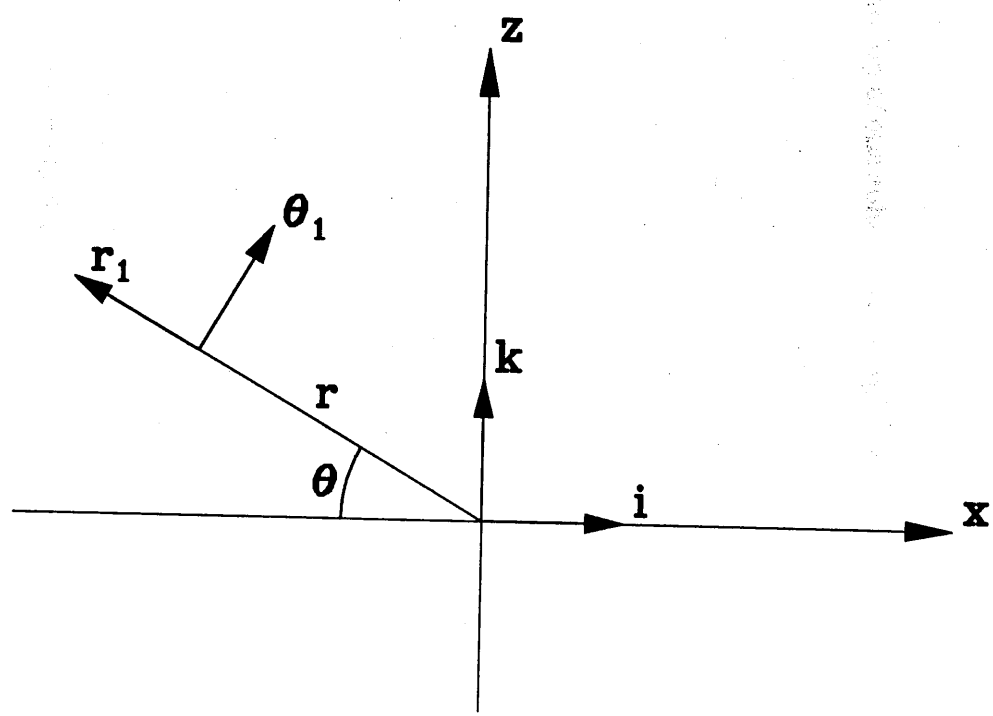

Figure A1.1 Rectangular and polar unit vectors

$$
\begin{aligned}
\mathbf{a} &= \frac{d\mathbf{v}}{dt} \\
&= \frac{d^2r}{dt^2}\mathbf{r}_1 + \frac{dr}{dt}\frac{d\mathbf{r}_1}{dt} + \frac{dr}{dt}\frac{d\theta}{dt}\theta_1 + r\frac{d^2\theta}{dt^2}\theta_1 + r\frac{d\theta}{dt}\frac{d\theta_1}{dt} \\
&= \frac{d^2r}{dt^2}\mathbf{r}_1 + \frac{dr}{dt}\frac{d\theta}{dt}\theta_1 + \frac{dr}{dt}\frac{d\theta}{dt}\theta_1 + r\frac{d^2\theta}{dt^2}\theta_1 - r\left(\frac{d\theta}{dt}\right)^2\mathbf{r}_1 \\
&= \left(\frac{d^2r}{dt^2} - r\left(\frac{d\theta}{dt}\right)^2\right)\mathbf{r}_1 + \left(r\frac{d^2\theta}{dt^2} + 2\frac{dr}{dt}\frac{d\theta}{dt}\right)\theta_1
\end{aligned}
$$

Rolling motion of one sphere over another sphere

For the forces acting in Figure A1.2, using the vectors shown in Figure A1.1

$$
\begin{aligned}
\mathbf{F} &= m\mathbf{a} \\
&= m\left[\left(\frac{d^2r}{dt^2} - r\omega^2\right)\mathbf{r}_1 + \left(r\frac{d\omega}{dt} + 2\frac{dr}{dt}\omega\right)\theta_1\right] \\
&= \mathbf{N} + m\mathbf{g} + \mathbf{F}_x + \mathbf{F}_Z + \mathbf{f} \\
&= \left(N - mg\sin\theta - F_x\cos\theta + F_z\sin\theta\right)\mathbf{r}_1 + \left(-mg\cos\theta + F_x\sin\theta + F_z\cos\theta - f\right)\theta_1
\end{aligned}
$$

where all variables in bold print are vectors, $\mathbf{F}$ is the total force acting on a particle of mass m to give an acceleration of $\mathbf{a}$. The forces acting are the normal reaction, $\mathbf{N}$, horizontal and vertical force components, $\mathbf{F}_x$, $\mathbf{F}_z$, friction force, $\mathbf{f}$, and the acceleration due to gravity, $\mathbf{g}$. The distance between particle centres is r, the angle between particle centres is θ above the horizontal and ω is the angular velocity. The vectors $\mathbf{r}_1$ and θ_1 are the radial and tangential unit vectors already defined. The forces can be resolved into normal and tangential components

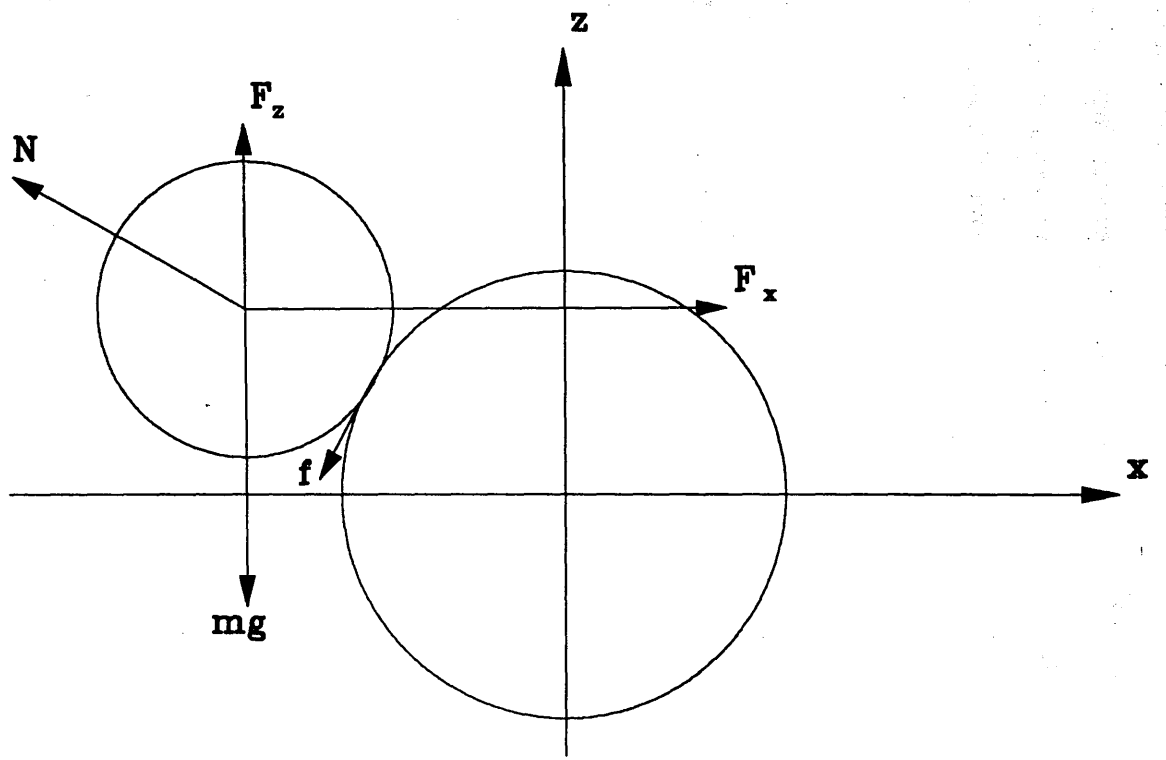

Figure A1.2 Forces acting on moving particle

$$m\left(\frac{d^2r}{dt^2} - r\omega^2\right) = N - mg\sin\theta - F_x\cos\theta + F_z\sin\theta$$

$$m\left(r\frac{d\omega}{dt} + 2\frac{dr}{dt}\omega\right) = -mg\cos\theta + F_x\sin\theta + F_z\cos\theta - f$$

since $r = (d_{char} + d)/2$, the distance between the particle centres, where d_{char} is the diameter of the stationary particle and d is the diameter of the moving particle. For two particles in contact the distance between particle centres does not vary with time, so these expressions become

$$-m\frac{(d_{char} + d)}{2}\omega^2 = N - mg\sin\theta - F_x\cos\theta + F_z\sin\theta$$

$$m\frac{(d_{char} + d)}{2}\frac{d\omega}{dt} = -mg\cos\theta + F_x\sin\theta + F_z\cos\theta - f$$

The total external torque, A, of all the forces about the centre of mass of the rolling sphere is

$$\begin{aligned} \mathrm{A} &= \left(-\frac{d}{2}\mathbf{r}_1\right)\times\mathbf{f} \\ &= \left(-\frac{d}{2}\mathbf{r}_1\right)\times(-f\,\theta_1) \\ &= \frac{d}{2}f\,\mathbf{j} \end{aligned}$$

since **W**, **N**, $\mathbf{F}_x$, $\mathbf{F}_z$ all pass through the centre of the rolling sphere.

The angular acceleration of the rolling sphere about its centre is

$$\alpha = \frac{d^2}{dt^2}(\phi + \varphi)\mathbf{j}$$

where ϕ and φ are the angles defined in Figure A1.3. As there is no slippage between the spheres, only rolling, the lengths of the arcs from the start point of the motion must be equal,

$$\frac{d_{char}}{2}\phi = \frac{d}{2}\varphi$$

From Figure A1.3,

$$\phi = \theta$$
$$\varphi = \frac{d_{char}}{d}\theta$$

so the angular acceleration of the particle

$$\begin{aligned}\alpha &= \frac{\mathrm{d}^2}{\mathrm{d}t^2}(\phi+\varphi)\mathbf{j} \\ &= \frac{\mathrm{d}^2}{\mathrm{d}t^2}\left(\theta+\frac{d_{char}}{d}\theta\right)\mathbf{j} \\ &= \frac{\mathrm{d}\omega}{\mathrm{d}t}\left(\frac{d+d_{char}}{d}\right)\mathbf{j}\end{aligned}$$

The moment of inertia of a sphere about the horizontal axis of rotation of its centre is

$$I = \frac{2}{5}m\left(\frac{d}{2}\right)^2$$

so

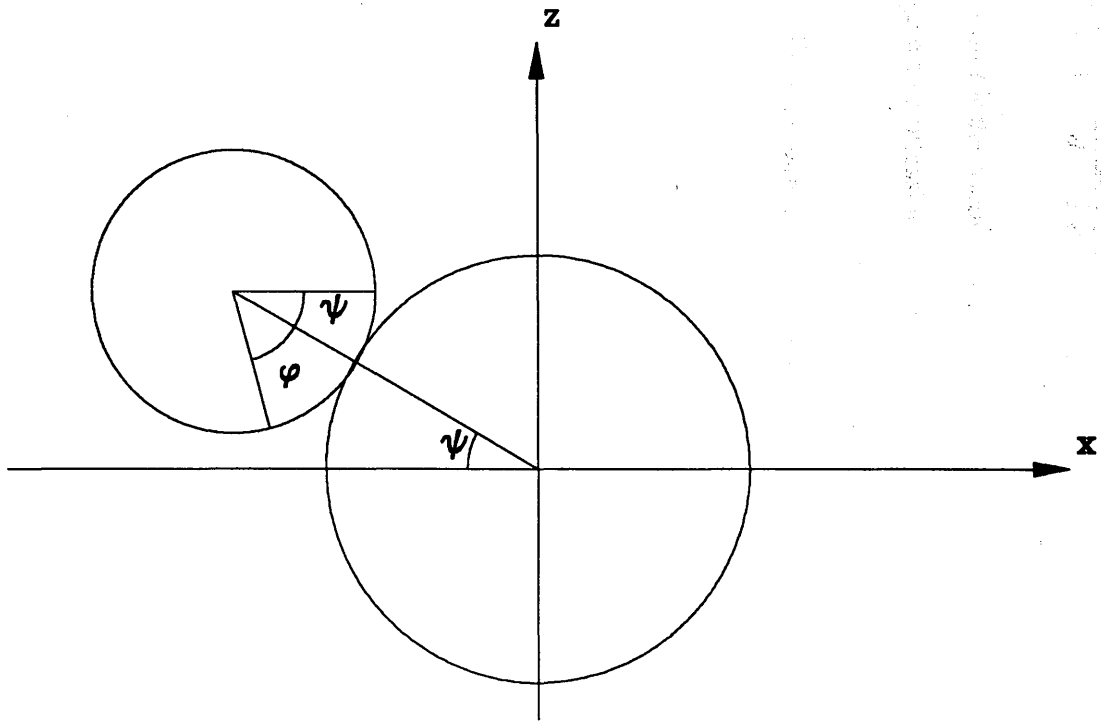

Figure A1.3 Angles of rotation of stationary and moving particles

$$A = I\alpha$$

$$\frac{d}{2} f\mathbf{j} = \frac{2}{5} m\left(\frac{d}{2}\right)^2 \left(\frac{d + d_{char}}{d}\right) \frac{d\omega}{dt} \mathbf{j}$$

$$f = \frac{2}{5} m\left(\frac{d}{2}\right)^2 \left(\frac{d + d_{char}}{d}\right) \frac{d\omega}{dt}$$

This expression for the friction force can be substituted into the tangential force balance to give an expression for particle radial acceleration with no slip

$$\frac{d\omega}{dt} = \frac{5}{7} \frac{2}{m(d_{char} + d)} (-mg\cos\theta + F_x \sin\theta + F_z \cos\theta)$$

The condition for the particle losing contact with the bed particle can be found from the normal force balance

$$N = -m\frac{(d_{char} + d)}{2}\omega^2 + mg\sin\theta + F_x\cos\theta - F_z\sin\theta$$

when the reaction force N becomes positive the moving particle has lost contact with the stationary particle.

Appendix 2 Published paper

Kelsey, A., Allen, C., Beven, K. & Carling, P., 1993. A particle tracking model of sediment transport. In: Mixing and Transport in the Environment, eds. Chatwin, P. C., Beven, K. J. & Millbank, J., John Wiley & Sons Ltd., Chichester, in press.

A PARTICLE TRACKING MODEL OF SEDIMENT TRANSPORT.

Adrian Kelsey, Cath Allen, Keith Beven
Centre for Research on Environmental Systems & Statistics (CRES)
Institute of Environmental & Biological Sciences
Lancaster University
Bailrigg
Lancashire. LA1 4YQ

Paul Carling
Institute of Freshwater Ecology
Windermere Laboratory
Ambleside
Cumbria

Abstract

A particle tracking model of the behaviour of single sediment particles in the fluvial environment is described. The description of sediment behaviour is based on processes of initial motion, rolling, non-contact motion and impact. The interaction of sediment and fluid is modelled by calculating the tracks of sediment and fluid, allowing the effects of turbulent flow to be included. After a description of the model the calculated particle behaviour produced using the model is compared with laboratory observations of single particle behaviour.

1.0: Sediment transport

The total bedload transport of sediment in a river consists of the sum of the movements of individual particles set in motion by the flow. Due to the number of particles in motion it is often possible to describe this transport in a continuum sense (e.g. Holly & Rahuel, 1990). The underlying system though is discrete. The motion of the individual particles is influenced by the flow, the nature of the bed and interactions with other particles, while individual particles movements will in time modify the flow, the bed, and the behaviour of other particles. The system can be described by considering flow, transport and boundary components, together with feedback mechanisms occurring between them (see for example Leeder, 1983, Figure 1).

Both stochastic and physical models of the dynamics of particle motions have been used in the past. Einstein (1937) produced a model of bedload transport based on exponential distributions of the distance moved and the time spent resting by particles, acknowledging the stochastic nature of sediment transport. This approach to sediment transport has also being used by Sayre & Hubbel (1965), Shen & Todorovic (1971), Stelczer (1981) and more recently Hassan et al. (1991). While these applications have shown the possibility of modelling sediment distribution using this technique the number of particles necessary to identify the appropriate distribution is thought to be more than 10^3 (see Hassan et al., 1991) while the downstream distribution of movements will in general be affected by large scale structures in rivers, e.g. pool-riffle structures.

A physical approach to calculating particle movements has being used by Sekine & Kikkawa (1988), Wiberg & Smith (1985) and van Rijn (1982). In all these models the particle trajectory due to the mean flow is calculated. The queueing model of Naden (1987) also uses a physical approach but the particle trajectories used to describe the motion are those observed by Abbott & Francis (1977). In the model of Naden (1987) the probability of initial motion of a particle due to turbulence is calculated, the particle motion is then calculated from the observed saltation characteristics, so incorporating the effects of turbulence on the saltation path. The models in which the particle tracks are calculated directly ignore this influence, though a stochastic element is introduced by including a random element in the impact process, allowing the calculation of a range of saltation trajectories (Sekine & Kikkawa, 1988; Wiberg & Smith, 1985).

Inclusion of the effects of turbulence in fluvial sediment transport of bedload has also been modelled by a range of approaches. Bagnold (1973) splits particle motion into saltation, which he assumes to be purely ballistic with particle trajectories unaffected by turbulence, and suspended, where the turbulent fluctuations of the flow are capable of supporting particles completely. From laboratory observations Abbott & Francis (1977) suggest that while saltations should cover the purely ballistic trajectories there is a region between this and the fully suspended region where saltation trajectories are modified by turbulence, causing upward acceleration of the particle after it has left contact with the bed. They suggested that this region should also be described as suspended and observed that modification of saltation trajectories could occur even at low transport stages, defined as u_*/u_{*cr}, that is the ratio of mean bed shear velocity to the critical shear velocity required to initiate particle motion. Observations in the field (e.g. Drake et al., 1988) also show the importance of turbulence in the transport process, with the high velocity turbulent fluctuations

allowing a range of particles to be entrained into the flow and transported at low transport stages. In modelling the response of particles to turbulence in the aeolian environment this region has been called the region of 'modified saltation' (Anderson, 1987; Hunt & Nalpanis 1985).

The presence of trajectories modified by turbulence at even low transport stages and the importance in entrainment of particles indicates that, if possible, a particle based model of fluvial sediment transport should include the effects of turbulence. Here these effects are included by the use of a particle tracking approach to modelling particle and flow behaviour.

1.1: Particle tracking

In particle tracking models of dispersion the dispersion due to turbulence of a cloud of pollutant or tracer is modelled by tracking a large number of particles for a period of time or over a distance. The particles represent the pollutant or tracer, their position is tracked from a source in a series of steps, taking account of the local mean and turbulent flow conditions at each step. Thus an individual path is calculated for each particle, based on the local flow conditions experienced by that particle. This approach to modelling dispersion is therefore explicitly Lagrangian, with the position of each particle being dependent on its history. Particle tracking models have been developed to model dispersion in the atmosphere, rivers and estuaries. They also offer advantages in modelling dispersion of materials that interact with the environment.

A majority of the work on particle tracking models of dispersion in open channel flow has been for passive pollutants (e.g. Allen, 1982). In these models the behaviour of the particles is identical to that of the fluid, parameters describing the flow can therefore be used directly in calculations describing the dispersion of a tracer. In sediment transport of bedload the particles are non-passive, lagging behind rather than following the flow completely. Particle tracking models have been developed for heavy, non-passive tracers, for example Zhuang et al. (1989) modelled the data of Synder & Lumley (1971); Chollet & Yvergniaux (1989), modelled the behaviour of a single particle moving in suspension in an open channel flow observed by Sumer & Deigaard (1981); Anderson (1987) and Hunt & Nalpanis (1985) have modelled the response of saltating particles to turbulent fluctuations in the aeolian environment. In this paper a particle tracking approach to sediment transport in fluvial environments is developed and applied to the calculation of the movement of single particles observed in laboratory experiments. An extension to multiple particles of different sizes with stochastic boundary conditions is also briefly described.

2.0: Flow modelling

Since the model is 2 dimensional only streamwise and vertical components of flow are calculated, the velocities are non-dimensionalised with respect to the mean bed shear velocity, u_*. The horizontal and vertical components of flow velocity, u, w, are modelled by mean flow components, U, W, to which are added random fluctuating components of velocity, u', w', to represent turbulence.

$$u = U + u'$$
$$w = W + w'$$

At the start of each iteration flow conditions are set according to the position of the particle centre and the flow state, these are then kept constant for the duration of the iteration.

2.1: Mean components of velocity

The mean streamwise component of flow, U, at height z, is calculated from a log law profile for turbulent flow over a rough boundary,

$$U = \frac{1}{\kappa}\log\left(\frac{30z}{k_s}\right)$$

The value of the roughness length, k_s is set from the experimental data used. The zero height is set at 0.2 characteristic diameters, d_{char}, below the tops of the bed particles and the velocity profile is assumed to apply down to the zero velocity height. The velocity profile normally diverges from the logarithmic profile close to the bed due to viscous effects and the presence of the elements making up the bed roughness but these effects are ignored here. The mean vertical component of velocity, W, is zero from continuity considerations.

2.2: Fluctuating components of velocity

The fluctuating components of velocity are calculated from Gaussian distributions, the magnitudes of the fluctuations are set using the values of the standard deviations from the data of McQuivey (1973). The variation with depth has been calculated (after Naden, 1987) as:

$$\frac{\sigma_u}{U} = 0.16\left(\frac{z}{d_{char}}\right)^{-0.65}$$

$$\sigma_w = 0.77\sigma_u$$

where σ_u and σ_w are the standard deviations of the velocity fluctuations u', w' at height z and d_{char} is the characteristic diameter of the bed particles.

2.3: Correlation of turbulent fluctuations

From observations the distributions of horizontal and vertical velocity fluctuations are almost Gaussian, while the distribution of the product of these fluctuations, $u'w'$, is observed to be skewed and have high kurtosis (Heathershaw, 1979). Assuming a Gaussian joint probability and knowledge of a value for the correlation coefficient, r, between u' and w', the values for the conditional mean, $\hat{W}$, and standard deviations ,$\hat{\sigma}_w$, of the vertical velocity at an iteration can be calculated, given the value of the horizontal velocity fluctuation at that iteration.

$$\hat{W} = r\frac{\sigma_w}{\sigma_u}u'$$

$$\hat{\sigma}_w = \sqrt{1-r^2}\,\sigma_w$$

Use of these expressions allows the calculation of turbulence with the same mean correlation coefficient as a set of data. The correlation between the streamwise and vertical velocity fluctuations was initially calculated from a correlation coefficient from Heathershaw (1979), giving a value of -0.18. This is a measurement for turbulent flow over the sea bed in a tidal current and may not be applicable for use in rivers. The correlation coefficient represents a mean value for a trace. However in turbulent flow the mean correlation coefficient is the result of high correlation and activity occurring for short periods of time, separated by periods of relative inactivity. The periods of high activity associated with burst and sweep processes are characterised by high correlations between the velocity components and large contributions to the turbulent shear stress. Observations in the fluvial environment (Drake et al., 1988) and in the marine environment (Williams, 1990) indicate that these structures are important in the sediment transport process, especially close to the threshold for sediment movement.

An attempt has been made to include the effects of these correlated signals by breaking the flow modelling into periods of flow with high negative correlation , corresponding to bursts and sweeps, positively correlated flows corresponding to up-accelerations and down-decelerations and a period of flow with low correlation corresponding to the quiet period.

3.0: Particle processes

The calculation of the track of a sediment particle motion depends on the representation of a number of processes. At the beginning of each iteration the appropriate process is selected, based on the present particle condition. The processes used to describe particle behaviour are entrainment, transport and impact. The transport process consists of 2 components, contact and non-contact motion, depending on the position of the particle with respect to the bed. The calculations performed are all non-dimensional, the parameters used to non-dimensionalise being the fluid density, ρ, the flow depth, h, and the mean bed shear velocity, u_*.

3.1: Entrainment process

The initial motion criterion used is based on the shear stress required to initiate particle motion compared with the instantaneous shear stress due to the turbulent flow. A range of values of shear stress are used, based on the variation observed by Fenton & Abbott (1977), and assuming that the Shields stress, θ_{cr}, for initial motion for a coplanar particle is 0.06. A variation in shear stress for initial motion is expected due to particle position within the bed.

The instantaneous shear stress due to turbulent fluctuations of the flow is calculated from the assumption that the drag force per unit area near the bed is equivalent to the shear stress acting at the bed. Here the appropriate velocity for the calculations is assumed to be that at the particle centre.

The instantaneous shear stress acting at the bed, τ_0, can be calculated as:

$$|\tau_0| = \frac{C_D}{2}u^2$$

$$= \frac{C_D}{2}U^2\left(\left(1+\frac{u'}{U}\right)^2+\left(\frac{w'}{U}\right)^2\right)$$

where C_D is the coefficient of drag of the particle.

From this the mean shear stress, $\bar{\tau}_0$, can be calculated as,

$$\bar{\tau}_0 = \frac{C_D}{2}U^2\left(\left(1+\frac{u'}{U}\right)^2+\left(\frac{w'}{U}\right)^2\right)$$

$$= \frac{C_D}{2}U^2\left(1+\left(\frac{\sigma_u}{U}\right)^2+\left(\frac{\sigma_w}{U}\right)^2\right)$$

Thus, relating these expressions,

$$|\tau_0| = \bar{\tau}_0\frac{\left(\left(1+\frac{u'}{U}\right)^2+\left(\frac{w'}{U}\right)^2\right)}{\left(1+\left(\frac{\sigma_u}{U}\right)^2+\left(\frac{\sigma_w}{U}\right)^2\right)}$$

To calculate whether the instantaneous shear stress is sufficient to initiate motion of a particle the above expression must be divided by the shear stress for initiation of particle motion, τ_{0cr}, giving an equation,

$$\frac{|\tau_0|}{\tau_{0cr}} = \frac{\bar{\tau}_0}{\tau_{0cr}}\frac{\left(\left(1+\frac{u'}{U}\right)^2+\left(\frac{w'}{U}\right)^2\right)}{\left(1+\left(\frac{\sigma_u}{U}\right)^2+\left(\frac{\sigma_w}{U}\right)^2\right)}$$

If this quantity is greater than one then particle motion is initiated.

3.2: Particle transport

Transport of particles by the flow occurs in two modes, a contact mode, where the particle rolls along in contact with the rough bed and a non-contact mode. In both modes fluid forces due to the relative motion of particle and flow are calculated and used to calculate the particle motion. The equations of particle motion are solved

numerically for the duration of an iteration to give particle position and velocity. The particle state at the end of one iteration is used as the initial condition for the next iteration, flow conditions being set for the new particle position.

The transport equations contain coefficients of drag, C_D, lift, C_L, and added mass, C_A. The value of the coefficient of drag is calculated from the curve for an isolated sphere in steady motion, using a fit by Morsi & Alexander (1972), allowing the calculation of coefficient of drag for a range of particle Reynolds number. This ignores any effects due to the particle motion not being steady state, or any variation due to the proximity of a boundary, though measurements by Coleman (1972) and Bagnold (1974) show any variation in coefficient of drag due to the presence of a boundary to be small. There is less information on the coefficient of lift, in particular about the variation of coefficient of lift with particle Reynolds number. In part this is due to the mechanisms generating forces normal to the direction of a flow. These are fluid shear and particle rotation, which can act at the same time for any particle Reynolds number. The presence of different mechanisms generating lift force means that measurement of one contribution to the lift force will often constrain the system in such a way that other contributions cannot be measured. The situation is further confused by the variation in lift observed approaching surfaces (Bagnold, 1974, Sumer, 1984). The range of values of coefficient of lift obtained experimentally is partly due to measurements being of different contributions to the lift force, and partly due to the use of different definitions for the coefficient of lift. The contributions due to different mechanisms acting to generate lift on a particle close to a surface in turbulent flow are hard to determine, as is the variation in lift moving away from the surface. This makes parameterisation of these quantities difficult. Thus the effect of uncertainty in estimated values of these parameters might usefully be examined. In the presence of a fluid the effective mass of an accelerating particle is increased by an amount called the added mass. This extra inertia is due to the fluid accelerated with the particle; for an isolated sphere this added mass is equal to the mass of fluid that would occupy half the volume of the sphere (Milne-Thompson, 1968) , giving an added mass coefficient, C_A, of 1/2.

3.2.1: Contact mode

The calculation of particle movement while in contact with the bed is similar to the description of Francis (1973) and Sekine & Kikkawa (1988), though here solved for flow conditions on an iteration by iteration basis. The equations describe the motion of a sphere rolling over another sphere without slippage. The relative velocities and forces acting are as shown in Figure 1. The tangential components of the forces acting determine the rolling motion of the particle, the normal components

whether the particle remains in contact with the bed. The equations of rolling motion are solved for each iteration after initial motion and also after impact until the particle either loses contact with the bed or stops rolling. If the particle loses contact with the bed the particle position and velocity are used as the initial condition for non-contact motion at the next iteration.

The angular velocity, ω, of the particle due to tangential components of force due to gravity, drag and lift is calculated. The ordinary differential equation for the particle angular velocity is solved numerically, giving values for both the angular velocity and the contact angle θ.

Error! Objects cannot be created from editing field codes.where d is the diameter of the moving particle, ρ_s is the density of the sediment, g is the acceleration due to gravity and u_p and w_p are the horizontal and vertical components of particle velocity respectively.

3.2.2: Non-Contact mode

The non-contact mode solution is for high Reynolds number flow, that is a flow where viscous forces are not important. It is a solution for inviscid, irrotational flow similar to that of Wiberg & Smith (1985) though with the pressure term removed since the magnitude of this component is small. The relative velocities and horizontal and vertical components of the forces acting are shown in Figure 2. The equations of motion of a particle are solved for horizontal and vertical motion due to forces of drag, lift and gravity.

Ordinary differential equations for the velocity components of a single particle can be written as:

$$\frac{\pi d^3}{6}(\rho_s + C_A)\frac{du_p}{dt} = \frac{C_D}{2}\frac{\pi d^2}{4}(u-u_p)\sqrt{(u-u_p)^2+(w-w_p)^2} - \frac{C_L}{2}\frac{\pi d^2}{4}(w-w_p)\sqrt{(u-u_p)^2+(w-w_p)^2}$$

$$\frac{\pi d^3}{6}(\rho_s + C_A)\frac{dw_p}{dt} = \frac{C_D}{2}\frac{\pi d^2}{4}(w-w_p)\sqrt{(u-u_p)^2+(w-w_p)^2} + \frac{C_L}{2}\frac{\pi d^2}{4}(u-u_p)\sqrt{(u-u_p)^2+(w-w_p)^2} - \frac{\pi d^3}{6}(\rho_s - 1)g$$

3.3: Impact process

The impact process is modelled by conserving some fraction of the normal and tangential components of momentum at impact, as shown in Figure 3. Particles can impact during any iteration when a particle is in motion. The vertical particle position at the end of an iteration is checked to see whether the particle could have made contact with the bed. If contact could have occurred then an impact height is chosen from a uniform random distribution, between the zero velocity height and the maximum height at which the particle could have come into contact with the bed, this height specifying a point and hence a contact angle on the bed particle. The non-contact motion equations are solved for this height to give the streamwise position of the particle and its velocity, the normal and tangential components of velocity are then calculated for the contact angle with a sphere of characteristic diameter.

The fraction of momentum conserved on impact is hard to determine and little data exists for the fluvial environment. The work of Gordon et al. (1972) can be interpreted as showing that the normal component of momentum is lost while the tangential momentum is conserved. Abbott & Francis (1977) found that trajectories appeared to be independent of the impact preceding them, although Naden (1987) points out that since most of their observed data included a period of rolling between non-contact motions this was only to be expected. In models of fluvial sediment transport including an impact process Sekine & Kikkawa (1988) set a coefficient of restitution empirically, while Wiberg & Smith (1985) used the coefficients of restitution and friction as a single parameter to fit their model to available data. The fractions of tangential and normal momentum conserved at impact are not well defined and would therefore seem to be ideal parameters to examine the effects of uncertainty in their values in Monte Carlo simulations of particle trajectories.

4.0: Two phase flow

In a particle tracking model of turbulent dispersion, a passive tracer, with similar physical properties to the fluid, is represented by a cloud of particles. The particles are moved according to the local flow conditions in a series of steps giving a Lagrangian model of the dispersion. The data necessary to calculate the dispersion are the magnitude of the turbulent fluctuations, the distribution of the fluctuations and a description of the time and length scales of the turbulence. The fluctuation distributions are usually assumed to be Gaussian, the magnitudes of the fluctuations are then characterised by the standard deviation of the fluctuations. The time and length scales used are related to the Lagrangian integral time and length scales of the flow, these being the time and distance over which the velocity fluctuations remain correlated.

Sediment is a non-passive tracer and its behaviour differs from that of the fluid. When the fluid velocity experienced by a particle changes, a nonpassive particle responds to this change over time. During this time the particle has a velocity relative to the flow and forces due to this velocity will be acting. The particle responses lag behind the behaviour of the fluid and the fluid leaves particles behind due to slippage of the particles; the 'crossing trajectories' effect of Csanady (1963). The time and length scales must then be modified to include the particle response. Approaches to this problem are either to use a modified time scale (Csanady 1963, also used by Hunt & Nalpanis, 1985; Anderson 1987; and Sawford & Guest, 1991), or to track fluid and sediment particles until they diverge to a distance such that the correlation falls to zero (as used by Faeth, 1986; Zhuang et al. 1989; and Yverngniaux & Chollet, 1989). The latter approach is used here.

The time taken by a particle to respond to fluctuations in a flow can be characterised by a particle response time, t_r, Hinze (1972) takes the time for the particle relative velocity to fall to 50% of its initial value. At low particle Reynolds numbers, i.e. Stokes flow:

$$t_r \propto d^2$$

At high particle Reynolds numbers

$$t_r \propto \frac{d}{(u-u_p)^2+(w-w_p)^2}$$

The high Reynolds number form of the particle response time is appropriate for the particles being modelled. The presence of the relative velocity term in the high

Reynolds number response time makes prediction of response times in advance difficult. Comparison of this response time with the time scale of turbulent fluctuations indicates whether a size of particle will respond to the fluctuations of the flow.

The particle trajectories are calculated assuming that the fluctuating components of velocity exist on average for one eddy cycle (Sullivan, 1971). A time interval less than the time scale of the eddy is used to calculate fluid and particle movements, allowing a constant time interval at each iteration while the eddy scale varies.. When a particle enters an eddy the velocity of fluid coincident with the particle centre is calculated, the motion of the fluid and particle during the iteration are then calculated. At the end of each iteration the separation of the fluid and particle and the elapsed time in the eddy are compared with the eddy length and time scales respectively. If the lengths and times are less than these scales the flow conditions are retained, if not a new set of velocities are calculated. Since the scales with which comparisons are made are those for the eddy then when they are exceded no correlation remains with the previous values and the new conditions should be selected from an appropriate random distribution.

There is little Lagrangian data available from measurements in open channel flow. McQuivey & Keefer (1971) report some for surface dispersion, Sullivan (1971) some for particle dispersion through depth. Therefore available Eulerian data may have to be used in a pseudo-Lagrangian way. Sullivan (1971) and Allen (1982) used a time scale, t_L, based on the assumption that a particle moved with velocity σ_w, the standard deviation of the vertical velocity fluctuations, over a distance L_E, the Eulerian integral length scale, giving a time scale

$$t_L = \frac{L_E}{\sigma_w}$$

assuming that the fluctuating component of velocity exists on average for one eddy cycle.

The expression for the streamwise Eulerian integral length scale has been calculated from the data of McQuivey (1973) for flow over rough beds in a flume.

$$L_{Ex} = 2.676 \exp\left(-5.020 \frac{\sigma_u}{U} \right) \qquad (r = -0.744, n = 60)$$

Published data giving information about integral length scales in open channel flow are very limited. The data of McQuivey (1973) only gives values for the streamwise Eulerian length scale, no values for the vertical length scale are given. The vertical Eulerian length scales were calculated as a fraction of the streamwise length scales.

Due to the limited quantity of data of this type available for open channel flow the data used was from turbulence measurements made on the River Severn (Heslop et al., 1992), with L_{Ez}, being set to 50% of the calculated horizontal Eulerian integral length scale, L_{Ex}.

Since the model is to be run many times for the same conditions while calculating the effect of varying parameters the suitability of time interval and influence of turbulence on particle movement can be checked by outputting time scales, time spent in eddies and particle responses to the flow at each iteration. The time scales and time spent in eddies show whether the time interval used is always less than the eddy time scale, while the particle responses indicate whether the inclusion of turbulence in the model is worthwhile.

5.0: Use of model

The paths of single particles were calculated using the model, to produce examples of single particle trajectories and to find an appropriate time interval to use in calculations. The non-dimensional time interval was set to a value of 0.01, the suitability of this value was checked by comparison with calculated time scales for the different transport stages.

To test the effects of uncertainty on the lift and momentum parameters the single particle model was incorporated into a parallel harness, enabling Monte Carlo simulations to be run on the Meiko Computing Surface at Lancaster University. In the Monte Carlo simulations calculations were performed for the same sets of conditions with parameters randomly selected from ranges of values.

The lift parameters varied were the coefficient of lift and a value, n, used as an exponent to alter the variation of the coefficient of lift away from the bed, as used in the expression

$$C_L = C_{L0}\left(\frac{0.5}{z/d}\right)^n$$

where C_{L0} is the coefficient of lift at a reference height at the stream bed. The momentum parameters varied were the coefficients of friction and restitution. The ranges over which the parameters were varied are shown in Table1.

The model was run with 5,000 sets of these varying parameters for each set of conditions used, each parameter set being used for 10 single particle runs. The values of the variable parameters were selected at random from the ranges shown in Table1.

5.1: Data necessary to set model conditions

The data necessary to run the model are flow depth, h, bed roughness length, k_s, and an indication of the size of the particle relative to this quantity, bed shear velocity and particle density. These values are input as a flow Reynolds number, Re_{*_h}, particle Reynolds number, $Re_{*_{k_s}}$, non-dimensional specific particle weight, $g(\rho_s - \rho)h/\rho u_*^2$, and particle relative density, ρ_s/ρ. The other information required is a maximum number of iterations to perform and the time interval used for these iterations, also input in non-dimensional form.

5.2: Data used

The model has been compared with the data of Abbott & Francis (1977), for the movement of single particles over a fixed, flat rough surface in a flume. These data provide information on saltation characteristics, both saltating and partially suspended (by their definition), and data on particle velocity and percentage of time spent in different modes of motion: rolling, saltating and suspended. These are plotted for a range of values of transport stage, (u_*/u_{*cr}) for a known depth over a flat rough bed (figure 11, Abbott & Francis, 1977). The conditions for the different transport stages were set with a critical shear velocity, u_{*cr}, calculated for a Shields stress of 0.06, calculations were performed for transport stages of 1.5, 2, 2.5 and 3.

6.0: Suitability of time interval

The suitability of the constant time interval used at each iteration was checked by comparing it with the calculated vertical and horizontal time scales and the duration of the eddies. The calculated Eulerian and pseudo-Lagrangian time scales in the vertical direction never dropped below the constant value of time interval used (Table 2). The values used were therefore reasonable, if computationally expensive.

6.1: Qualitative model behaviour

The qualitative prediction of particle behaviour made by the model shows similar behaviour to both laboratory and field observations. The calculated particle tracks show the effect of moving from one eddy to another, as seen in Figure 5 (see also Figures 13, 16, Abbott & Francis, 1977). The entrainment and deposition behaviour of the particle showed the possibility of particles remaining immobile for some time before a sufficiently large turbulent fluctuation occurs to initiate particle

motion, travelling for a variable number of hops before coming to rest and then either repeating these processes or coming to rest permanently.

6.2: Presentation of results

The variables output for each set of parameters are those shown in Figure 12 of Abbott & Francis (1977), that is saltation and suspension lengths and mean maximum heights, mean particle velocities and the percentage of time that a particle spends rolling, at rest and in suspension. The mean particle velocity for a track was calculated as the distance travelled by a particle divided by the time spent travelling. The trajectory lengths and heights were calculated from the particle tracks, calculating the distance between contacts with the bed, and the highest point between these contacts. The split between saltating and partially suspended trajectories was calculated by checking for the occurrence of any upward accelerations in the particle trajectory between contacts with the bed.

To compare observed and calculated results the normalised square of the residual was calculated, then subtracted from one, that is

$$\text{fit} = 1 - \left(\frac{y - y_c}{y} \right)^2$$

where y is the observed value of a quantity and y_c is the mean of the calculated values for a given set of conditions for the same quantity. This expression gives a value of 1 for a perfect fit and can be used to rank values in order of closeness to the observed value.

The results for the 5,000 sets of parameters calculated for each transport stage were sorted using the sum of the values for the fit for the mean particle velocity, saltation and suspension length, divided by three. The number of variables was limited to three so that poor results for one variable were not averaged out by the other variables used. The lengths and heights of trajectories are positively correlated over the whole parameter set, for each transport stage, so using these variables in the overall fit would give no useful increase in information (see Tables 3, 4).

6.3: Effects of uncertainty in parameters

The parameters varied to check the effect of uncertainty on their values were those affecting the lift force acting on a particle and those affecting momentum conservation on impact.

The effect of uncertainty on the coefficient of lift and the variation in lift away from the bed is shown in Figure 5. The region of best fit forms a diagonal with positive slope. In this region increases in the coefficient of lift and hence lift force are matched by decreases in persistence of lift force away from the bed. In the region above the diagonal particle motions are too short, low and slow, while below the diagonal the particle motions are too long, high and faster. The observed behaviour can be simulated by a range of coefficients of lift and different curves for the variation in lift away from the bed.

The variation of the coefficients of friction and restitution does not give rise to any structure across the range of parameter values used. From their observations Abbott & Francis (1977) found initial particle velocity at the start of a trajectory to be independent of any prior rolling and little difference between maximum trajectory heights from rest and those after an impact, they therefore asserted that momentum was not conserved on impact. This work was reviewed by Naden (1985) who points out that the existence of the rolling and saltating motion does not eliminate the possibility of momentum being conserved and that the view of Abbott & Francis (1977) was based on rather sparse data. The model used here allows momentum to be conserved at impact but assumes that a period of rolling, however short, occurs after an impact. The momentum conservation may therefore be important in the continuation or otherwise of particle motion but the period of rolling appears to decouple the impact at the end of one saltation from the trajectory of the next saltation.

6.4: Model output

The fit of the calculated values from the model to the observed data as expressed by the sum of fits described earlier shows a trend of better fits with increasing transport stage, the better fits occurring at lower values of coefficient of lift and higher values of n, that is lower values of coefficient of lift away from the wall (see Figure 6). The plots in Figure 6 only show variation in goodness of fit with the lift parameters, since only with these is there any structured variation. The coefficients of friction and restitution were also varied in these calculations but caused no structure in the goodness of fit.

When the components of the fit are examined it is found that the predicted particle velocity is always lower than the observed, while the length scales show a range of fits from under- to over-estimation. The regions of best fit for each parameter don't overlay each other completely, which accounts for some of the lack of overall fit for the model, but the main limitation on the accuracy of the model fit appears to be

due to the poor fit to the mean particle velocity. Examining the interaction of this variable with the parameter sets and other calculated variables gives an indication of why the calculated mean particle velocity is always low.

The variation of particle velocity with the lift parameters shows increasing accuracy of fit with increasing coefficient of lift and these higher values of coefficient of lift persisting away from the bed. The calculated particle velocity shows a positive correlation with the saltation and suspended trajectory length scales, for the best 500 fits, though the correlations are poor (see Tables 5, 6). The other comparisons that may be made are of the time a particle spends in the different modes of transport.

The time spent rolling and hence the time spent near to the bed is over-estimated at all transport stages. The distance travelled while rolling will be less than the distance that would be travelled if a particle was saltating or partially suspended, this therefore reduces the mean particle velocity. The variation of time spent rolling with particle velocity shows a trend of increasing particle velocity with decreasing time spent rolling at all the calculated transport stages, though the scatter of points below this line shows that other factors also affect the mean particle velocity. The time spent in modified saltation shows the reverse trend of increasing particle velocity with increasing time spent in modified saltation, though again the scatter of points shows that other factors are affecting the mean particle velocity.

The over-estimation of time spent rolling at all transport stages could be due to the near bed velocity modelling or the rolling model or some combination of both. The improved fit of the model with increasing stage can be at least partially explained by reduced time spent in contact with and close to the bed in comparison with lower transport stages. The alteration in the fit with the variation in the uncertain parameters can also be seen to be due to decreased time in contact with the bed. Here this is caused by the lift force being large enough to reduce the time a particle spends in contact with the bed.

The rolling model used is very simple, sphere rolling over sphere with no slippage. However inclusion of a percentage slip factor in the calculation of particle rolling had very little effect on the overall results, though the conditions under which particles lose contact with the bed could also affect the time spent close to the bed.

The near bed velocity has been modelled using a logarithmic flow profile to calculate the mean streamwise velocities. This profile breaks down close to boundaries, but to allow calculation of forces on particles set into the surface of the bed the profile is here assumed to apply down to the zero velocity height. The use of a

flow model which correlates the velocity fluctuations to give a degree of structure to the turbulence improves the fit of the model, more so at low transport stages than at high transport stages. At higher transport stages fluctuations in shear stress about the mean value need not be as large for the flow to become competent to cause sediment transport, fluctuations are therefore not as important in starting the transport process. The structure in the turbulence is only represented by different values of the correlation coefficient, assuming constant values for the standard deviations of the velocity fluctuations. Any systematic differences in these values during the high shear stress events is therefore ignored. The distributions used for horizontal and vertical fluctuations are still Gaussian so shear stress contributions due to a few large events or lots of small events will not be modelled adequately. Since the model is failing due to particles spending too much time near the bed, the inclusion of such effects, causing the particle to be displaced from this region might well improve the model further.

The low particle velocities are likely to be a result of a combination of the effects of these processes. The equations used to describe non-contact particle motion are simplified with terms that only made small contributions to the force acting on a particle not being included. They give reasonable predictions of the particle motion away from the bed, as can be seen from the predictions at higher transport stages. The accuracy of the rest of the model may be examined by consideration of the results for a transport stage of 3, at this stage the observed time spent rolling was 4%, so the distance travelled in this mode of motion would also be expected to be small in comparison to the distances travelled in saltation and partially suspended saltation. If the mean particle velocity is modified by using only the observed time spent rolling and the calculated time spent in the other modes of motion this gives better fits, as shown in Figure 7 in comparison with those in Figure 5. A similar calculation may be performed for the lower transport stages which does improve the calculated fit to the mean particle velocity. At lower transport stages the time spent rolling increases and so the distance travelled in this mode of transport becomes more significant, the fit remains worse at lower transport stages.

7.0: Discussion

The present model predicts the behaviour of single particles across a range of transport stages, though the quantitative results are not accurate at low transport stages and improve as the transport stage increases. The fit to the saltation characteristics is much better than to the mean particle velocities. The variation of goodness of fit with the coefficient of lift in these calculations shows that particle behaviour can be effectively reproduced by a range of values. Calculation of the

behaviour of single particles allows calculated particle behaviour to be compared with available data, the results obtained may then be used in other calculations. The single particle models of van Rijn (1984) and Wiberg & Smith (1989) have been used to calculate total bedload transport, based on the profiles of sediment distribution through depth obtained from the models. Another use of particle models of sediment transport is in calculating the development of bedforms, as in Naden (1987).

The ability to run a model many times in parallel can be used to perform multiple calculations across a range of parameters, investigating the effect of uncertainty on these parameters, as has been described here. Alternatively the parameters may be fixed and multiple calculations performed for a single set of conditions. These multiple calculations allow the production of distributions in space and time for the motion of a single particle, as shown in Figure 7. These calculations may be repeated for a range of combinations of particle size, bed roughness and transport stage. In this way distributions for a range of particles representative of a sediment distribution over a related range of bed roughnesses may be calculated. Calculation of sediment transport by direct calculation of the behaviour of a sufficient number of particles to represent a system would require large quantities of computer time, which would not be available with present facilities. Pre-calculation of the distribution functions for a range of particles, for a range of conditions allows sediment movement to be calculated from these distributions, removing the restriction on the number of particles whose behaviour can be calculated.

The calculation of distribution curves has similarities with the stochastic approaches to calculating sediment transport. In this approach distributions are calculated from dispersion of sediment tracers in flumes or rivers (Kirkby, 1991), but there are problems in retrieval of the tracer and in identifying the effects of interactions of bedforms with the sediment transport process and hence in the number of particles necessary to identify distributions (see for example Hassan et al. 1991). In comparison the modelled system is a simplification of the particle transport processes and in its representation of the bed as a flat rough surface with no bedforms present. The distributions produced are not distorted by any interactions with bedforms and the final position of all particles is calculated. The assumptions made make the initial calculations of sediment distributions simple but mean that the effects of any interactions with the bed when routing sediment may be superimposed later. This distribution function approach to modelling total bedload transport is being explored in further studies of the particle tracking model.

Acknowledgements

AK was in receipt of a NERC research studentship (GT4/89/AAPS/30) during this work.

References

Abbott, J. E. & Francis, J. R. D., 1977. Saltation and suspension of solid grains in a water stream. Philosophical Transactions of the Royal Society of London, 284A, 225 - 254.

Allen, C. M., 1982. Numerical simulation of contaminant dispersion in estuary flow. Proceedings of the Royal Society of London A381, 179 - 194.

Anderson, R. S., 1987. Eolian sediment transport as a stochastic process: The effects of a fluctuating wind on particle trajectories. Journal of Geology 95, 497 - 512.

Anderson, R. S., 1989. Saltation of sand: a qualitative review with biological analogy. Proceedings of the Royal Society of Edinburgh, 96B, 149 - 165.

Bagnold, R. A., 1973. The nature of saltation and of 'bed load' transport in water. Proceedings of the Royal Society of London A332, 473 - 504.

Bagnold, R. A., 1974. Fluid forces on a body in shear flow; experimental use of 'stationary flow'. Proceedings of the Royal Society of London A340, 147 - 171.

Coleman, N. L., 1972. The drag coefficient of a stationary sphere on a boundary of similar spheres. La Houille Blanche 27, 17 - 21.

Csanady, G. T., 1963. Turbulent diffusion of heavy particles in the atmosphere. Journal of the Atmospheric Sciences 20, 201 - 208.

Drake, T. G., Shreve, R. L., Dietrich, W. E., Whiting, P. J. + Leopold, L. B., 1988. Bedload transport of fine gravel observed by motion - picture photography. Journal of Fluid Mechanics 192, 193 - 217.

Einstein, H. A., 1937. Bed load transport as a probability problem. D. Sc. Thesis, Federal Institute of Technology, Zurich, Switzerland. Reprinted in, Chen, H. W., (ed), Sedimentation - Symposium in Honour of Prof. H. A. Einstein, C1 - C105.

Fenton, J. D. & Abbott, J. E., 1977. Initial movement of grains on a stream bed: the effect of relative protrusion. Proceedings of the Royal Society of London A352, 523 - 537.

Gordon, R., Carmichael, J. B. & Isackson, F. J., 1972. Saltation of plastic balls in a 'one-dimensional flume'. Water Resources Research 8, 444 - 459.

Hassan, M. A., Church, M. & Schick, A. P., 1991. Distance of movement of coarse particles in gravel bed streams. Water Resources Research 27, 503 - 511.

Holly, F. M. & Rahuel, J. L., 1990. New numerical/physical framework for mobile bed modelling. Part I: Numerical and physical principles. Journal of Hydraulic Research 28, 401 - 416.

Heslop, S. Holland, M. J. & Allen, C. M. Turbulence measurements in the River Severn. In this volume.

Heathershaw, A. D., 1979. The turbulent structure of the bottom boundary layer in a tidal current. Geophysical Journal of the Royal Astronomical Society 58, 395 - 430.

Hunt, J. C. R. & Nalpanis, P., 1985. Saltating and suspended particles over flat and sloping surfaces. I. Modelling concepts. In Proceeding of International Workshop on the Physics of blown Sand, Barndorff-Nielsen, O. E. et al. (eds) Vol 1, 9 - 36. University of Aarhus.

Hinze, J. O., 1972. Turbulent fluid and particle interaction. Progress in Heat and Mass Transfer 6, 433 - 452.

Leeder, M. R., 1983. On the interactions between turbulent flow, sediment transport and bedform mechanics in channelized flows. In Collinson, J. D. & Lewin, J., (eds), Modern & ancient fluvial systems. International Association of Sedimentologists Special Publication 6, 5 - 18.

McQuivey, R. S., 1973. Summary of turbulence data from rivers, conveyance channels and laboratory flumes - Turbulence in Water. U.S. Geological Survey Prof. Pap. 802-B.

McQuivey, R. S. & Keefer, T. N., 1971. Turbulent diffusion and dispersion in open channel flow. In Chiu, C.-L. (ed), Stochastic Hydraulics, University of Pittsburgh, 231 - 250.

Milne-Thomson, L. M., 1968. Theoretical Hydrodynamics. 5th ed., Macmillan & Co. Ltd., London.

Morsi, S. A. & Alexander, A. J., 1972. An investigation of particle trajectories in two phase flow systems. Journal of Fluid Mechanics 55, 193 208.

Naden, P. S., 1985. Gravel bedforms - the development of a sediment transport model. PhD thesis, University of Leeds.

Naden, P. S., 1987. An erosion criterion for gravel bed rivers. Earth Surface Processes & Landforms, 12, 83 - 93.

Naden, P. S., 1987. Modelling gravel - bed topography from sediment transport. Earth Surface Processes & Landforms, 12, 353 - 367.

Sayre, W. W. & Hubbell, W. W., 1965. Transport and dispersion of labelled bed material North Loup River, Nebraska. U.S. Geological Survey Professional paper 433-C.

Sawford, B. L. & Guest, F. M., 1991. Lagrangian statistical simulation of the turbulent motion of heavy particles. Boundary-layer meterorology 54, 147-166

Sekine, M. & Kikkawa, H., 1988. A fundamental study on the sediment transport in an open channel flow. Memoirs of the School of Science and Engineering, Waseda University, No. 52.

Shen, H. W. & Todorovic, P., 1971. A general stochastic model for the transport of sediment bed material. In Chiu, C.-L. (ed), Stochastic hydraulics, University of Pittsburgh, 489 - 503.

Shuen, J.-S., Solomon, A. S. P., & Faeth, G. M., 1986. Drop-turbulence interactions in a diffusion flame. AIAA Journal 24, 101 - 108.

Snyder, W. H. & Lumley, J. L., 1971. Some measurements of particle velocity autocorrelation functions in a turbulent flow. Journal of Fluid Mechanics 48, 41 - 71.

Stelczer, K., 1981. Bed-load Transport, Theory and Practice. Water Resources Publications.

Sumer, B. M., 1984. Lift forces on moving particles near boundaries. Journal of Hydraulic Engineering 110, 1272 - 1278.

Sumer, B. M. & Deigaard, R., 1981. Particle motions near the bottom in turbulent flow in an open channel Part 2. Journal of Fluid Mechanics 109, 311 - 338.

Sullivan, P. J., 1971. Longitudinal dispersion within a two-dimensional shear flow. Journal of Fluid Mechanics 49, 551 - 576.

Van Rijn, L. C., 1984. Sediment transport, Part I: Bed Load Transport. Journal of Hydraulic Engineerinng 110, 1431 - 1456.

Wiberg, P. L. & Smith, J. D., 1985. A theoretical model for saltating grains in water. Journal of Geophysical Research 90, 7341 - 7354.

Wiberg, P. L. & Smith, J. D., 1989. Model for calculating bed load transport of sediment. Journal of Hydraulic Engineering 115, 101 - 123.

Williams, J. J., 1990. Video observations of marine gravel transport. GeoMarine Letters 10, 157 - 164.

Yvergniaux, P. & Chollet, J. P., 1989. Particle trajectories modelling based on a Lagrangian memory effect. In IAHR XXIII Congress: Hydraulics and the environment, A: Turbulence in Hydraulics 301 - 313.

Zhuang, Y, Wilson, J. D. & Lozowski, E. P., 1989. A trajectory simulation model for heavy particle motion in turbulent flow. Journal of Fluids Engineering 111, 492 - 494.

Nomenclature

C_A	Added mass coefficient
C_D	Coefficient of drag
C_L	Coefficient of lift
C_{L0}	Coefficient of lift at reference height
d	Particle diameter
d_{char}	Characteristic particle diameter
g	Acceleration due to gravity
h	Flow depth
k_S	Roughness length
L_{Ex}	Horizontal Eulerian integral length scale
L_{Ez}	Vertical Eulerian integral length scale
Re_{*_h}	Flow Reynolds number = $\frac{u_* h}{\upsilon}$
$Re_{*_{ks}}$	Particle Reynolds number = $\frac{u_* k_s}{\upsilon}$

t_l	Eddy time scale
t_r	Particle response time
U	Mean streamwise component of velocity at height z
u	Instantaneous streamwise component of velocity at height z
u'	Fluctuating streamwise component of velocity at height z
u_*	Mean bed shear velocity
u_{*cr}	Critical shear velocity to initiate particle motion
u_p	Streamwise particle velocity
W	Mean vertical component of velocity at height z
$\hat{W}$	Conditional mean vertical component of velocity at height z at an iteration
w	Instantaneous vertical component of velocity at height z
w'	Fluctuating vertical component of velocity at height z
w_p	Vertical particle velocity
y	Observed value of quantity
y_c	Calculated value of quantity
z	Height above velocity zero
γ_s	Specific weight of sediment $= \dfrac{g(\rho_s - \rho)h}{\rho u_*^2}$
θ	Contact angle
θ_{cr}	Shields stress $= \dfrac{\rho u_{*cr}^2}{g(\rho_s - \rho)d}$
ω	Angular velocity of particle $= \dfrac{d\theta}{dt}$
υ	Kinematic velocity
ρ	Density of fluid
ρ_s	Density of sediment
σ_u	Standard deviation of streamwise velocity fluctuations at height z
σ_w	Standard deviation of vertical velocity fluctuations at height z
$\hat{\sigma}_w$	Correlated standard deviation of vertical velocity fluctuations at height z
τ_0	Shear stress
τ_{0cr}	Critical shear stress to initiate particle motion

Table 1. Ranges of parameters used in uncertainty calculations.

Coefficient of lift	0.2 - 0.6
'n'	1.0 - 5.0
Coefficient of friction	0.0 - 1.0
Coefficient of restitution	0.0 - 1.0

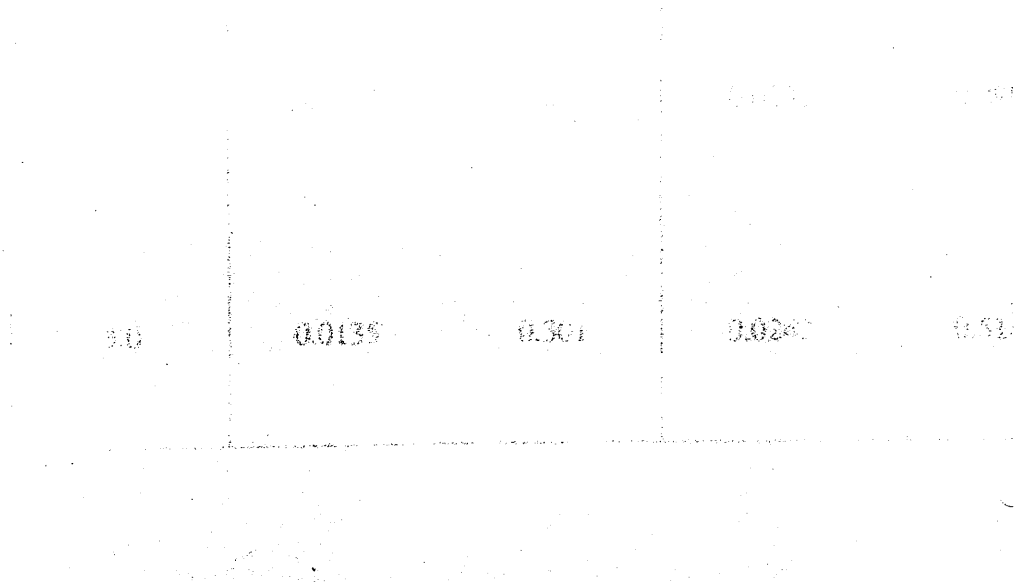

Table 2. Vertical Eulerian and pseudo-Lagrangian timescales.

Transport stage (u_* / u_{*cr})	Vertical Eulerian Timescale		Vertical pseudo-Lagrangian Timescale	
	Minimum	Mean	Minimum	Mean
1.5	0.0135	0.127	0.0265	0.212
2.0	0.0135	0.027	0.0277	0.288
2.5	0.0137	0.028	0.0237	0.290
3.0	0.0135	0.301	0.0242	0.514

Table 3. Correlation of mean maximum saltation heights with saltation lengths.

Transport stage (u_* / u_{*cr})	Regression slope	Regression constant	Correlation coefficient
1.5	0.786	0.144	0.869
2.0	0.719	0.155	0.917
2.5	0.596	0.159	0.966
3.0	-	-	-

Table 4. Correlations of mean maximum trajectory heights with suspended trajectory lengths.

Transport stage (u_* / u_{*cr})	Regression slope	Regression constant	Correlation coefficient
1.5	1.209	0.030	0.978
2.0	0.970	0.034	0.985
2.5	0.868	0.037	0.989
3.0	0.750	0.078	0.988

Table 5. Correlations of saltation lengths with mean particle velocities for best 500 fits.

Transport stage (u_* / u_{*cr})	Regression slope	Regression constant	Correlation coefficient
1.5	0.228	0.451	0.064
2.0	1.112	0.121	0.314
2.5	1.454	0.261	0.368
3.0	-	-	-

Table 6. Correlations of suspended trajectory lengths with mean particle velocities for best 500 fits.

Transport stage (u_* / u_{*cr})	Regression slope	Regression constant	Correlation coefficient
1.5	0.685	0.085	0.253
2.0	1.013	0.096	0.315
2.5	1.095	0.252	0.344
3.0	1.846	-0.067	0.575

Figure1. Rolling motion of particle. a) Flow and particle velocities determining relative velocity. b) Forces due to flow and due to gravity, components showing normal component, determining whether rolling particle remains in contact and tangential component affecting motion.

Figure 2. Non-contact motion of particle. a) Flow and particle velocities determining relative velocity. b) Forces due to flow and due to gravity, components showing contributions to horizontal and vertical forces acting.

Figure 3. Effect of impact on particle velocities. a) Particle velocity and components immediately before impact. b) Particle velocity and components immediately after impact, fractions of the normal and tangential components of velocity conserved.

Figure 4. Saltations modified by the effects of turbulence. Calculated particle heights at each iteration are shown plotted against time for transport stages of a) 2.0, b) 2.5. Units are non-dimensionalised with respect to flow depth and mean bed shear velocity.

Figure 5. Effect of uncertainty in the values of coefficient of lift on calculated fits, transport stage = 3.

Figure 6. Variation in calculated fit of model to observed behaviour due to uncertainty in parameters used in model. The graphs show the calculated fits at transport stages from 1.5 to 3 for the range of values of variation in lift and coefficient of lift shown in Table 1.

Figure 7. Fit modified to account for excess time spent rolling, transport stage = 3. Observed time spent rolling at this transport stage is 4%, fit is modified assuming distance travelled while rolling is small compared with that saltating and that mean particle velocity can be altered by scaling time in motion.

Figure 8. Calculated distribution of time particles spend in motion. The distributions are generated from calculations of the movement of 10,000 particles at a transport stage = 2. Each particle track is calculated for a particle initially at rest, the calculation is continued until the particle stops moving, giving values for single particle motions. The distribution only includes those particles that move from the initial rest position.

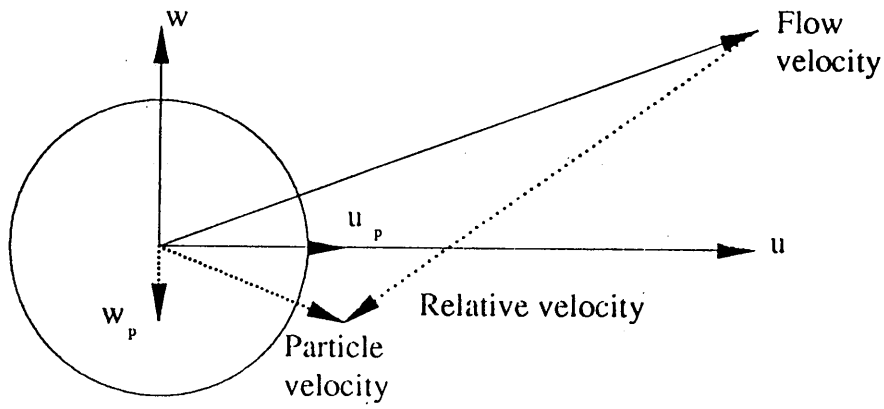

a) Velocities

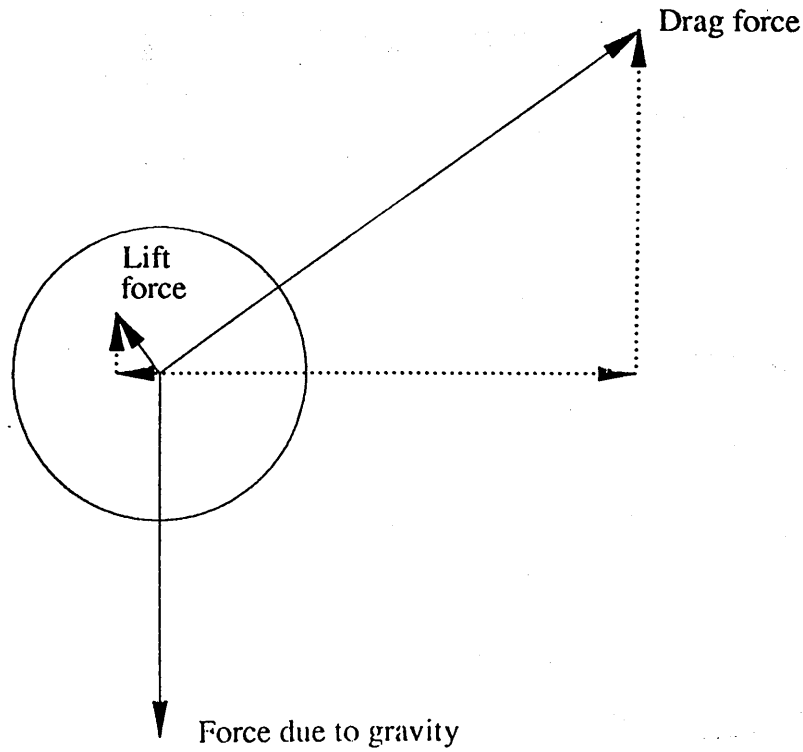

b) Forces

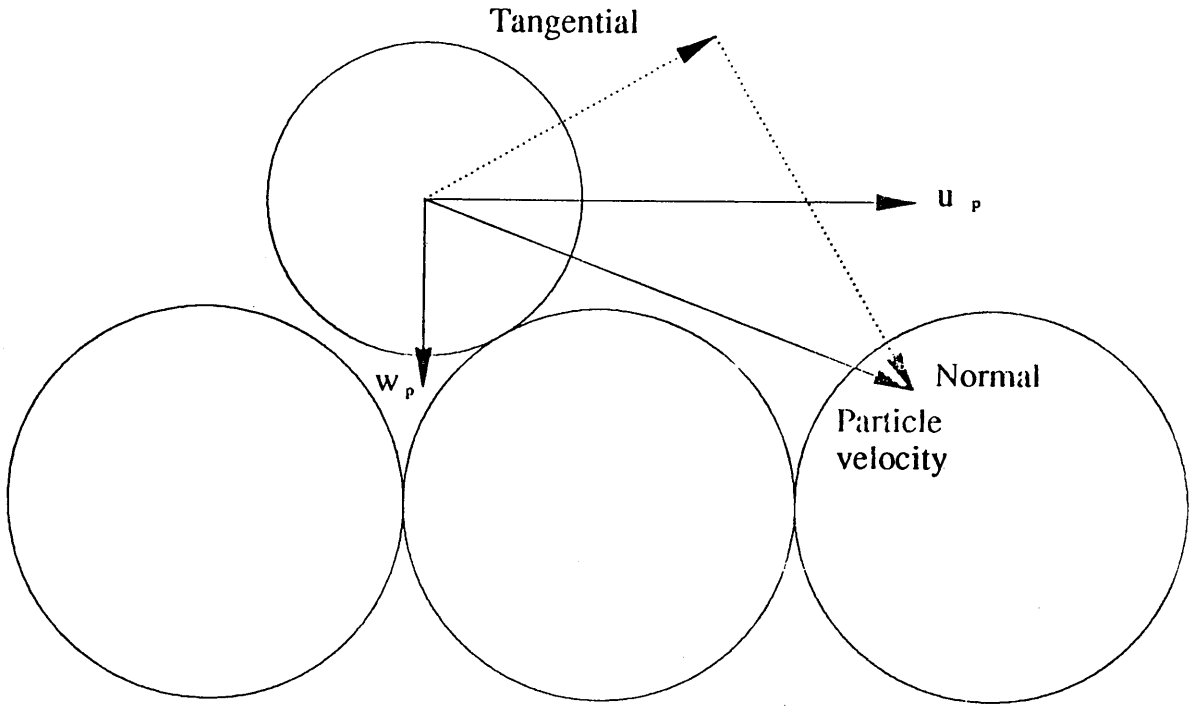

a) Velocities immediately before impact

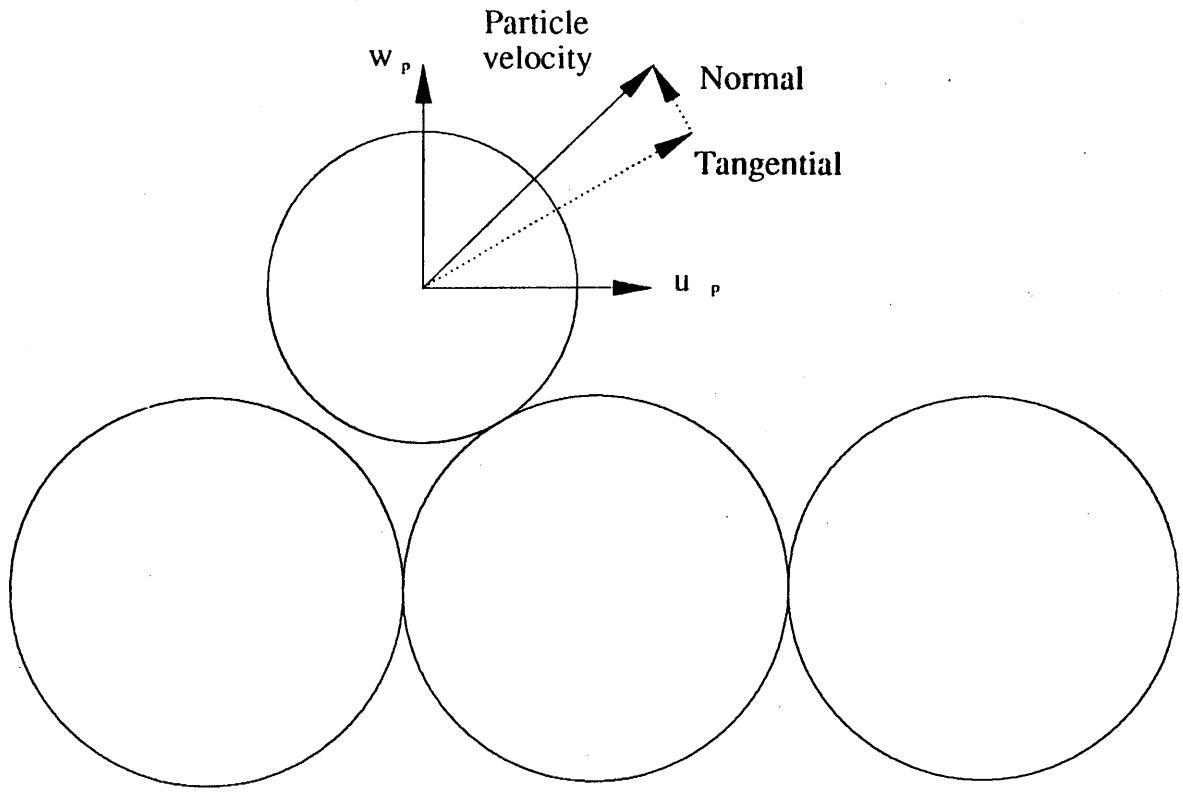

b) Velocities immediately after impact

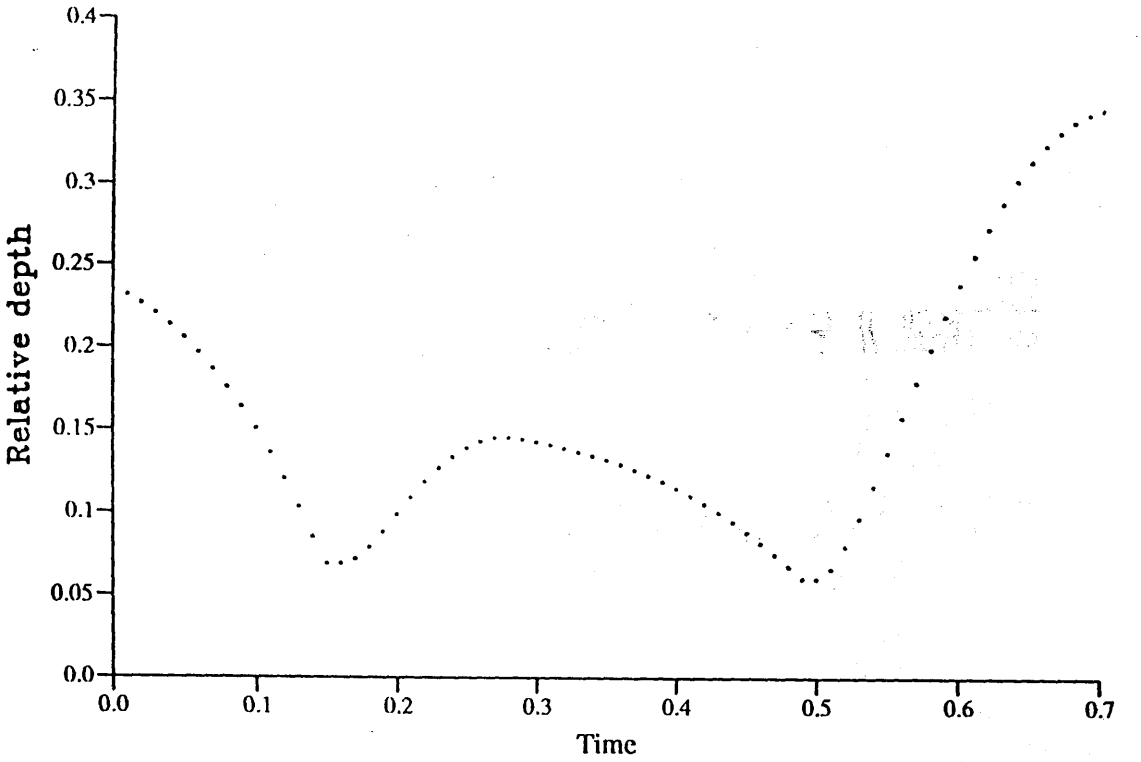

a) Transport stage = 2.0

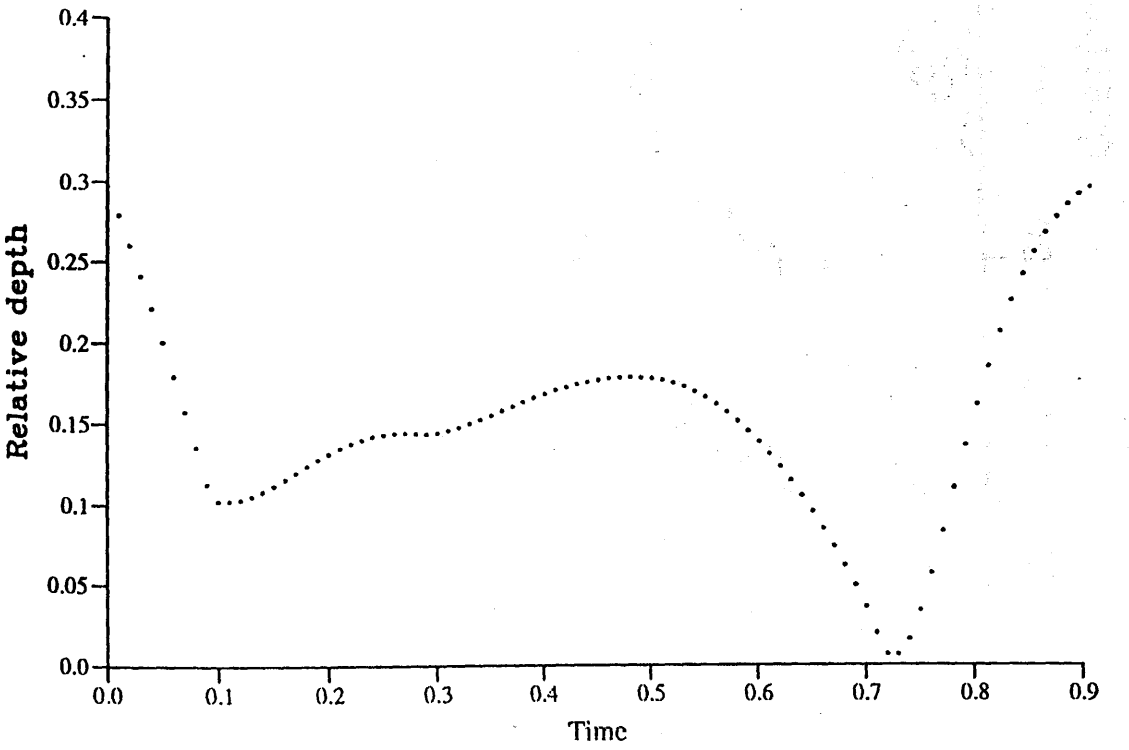

b) Transport stage = 2.5

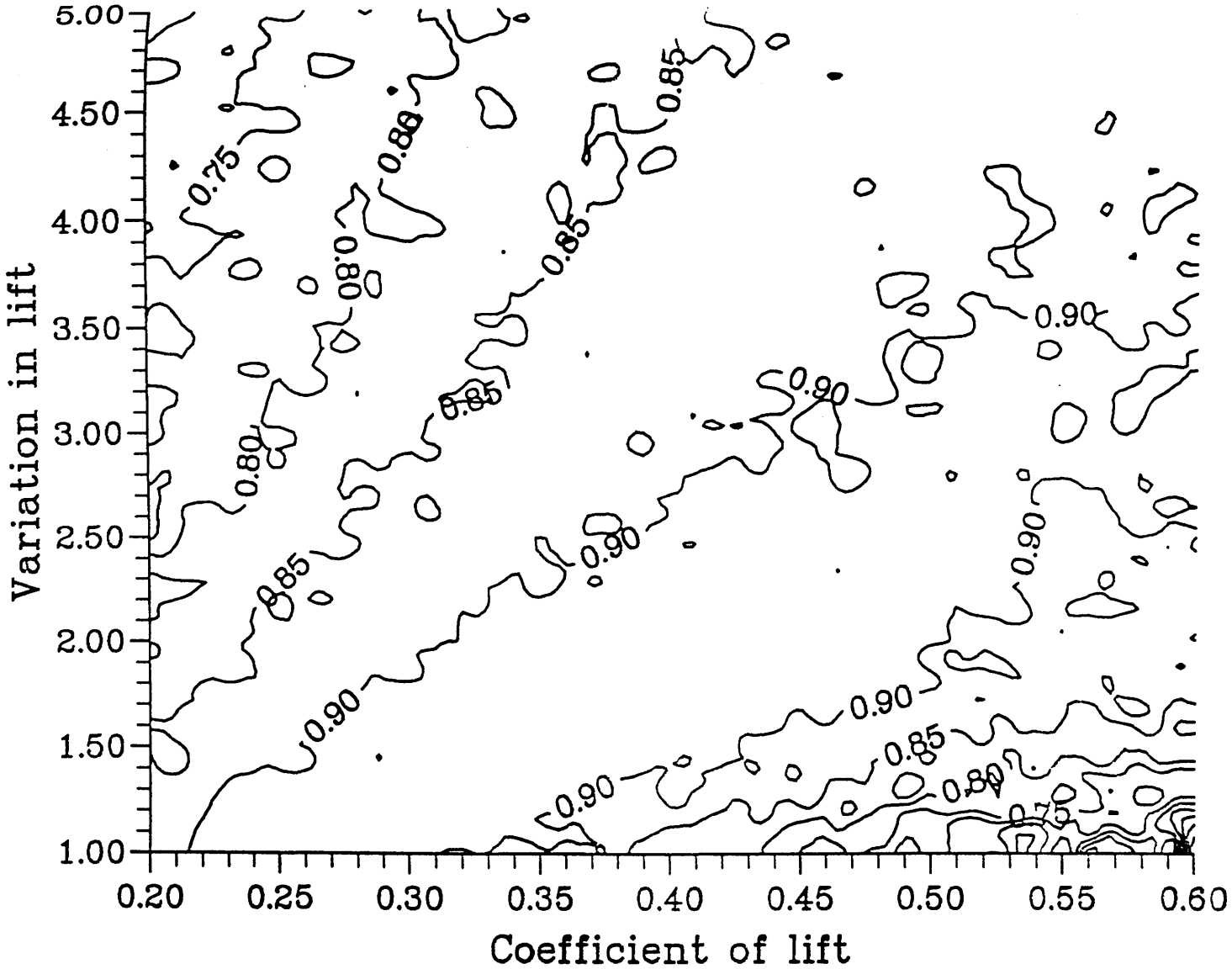

Transport stage

3.0

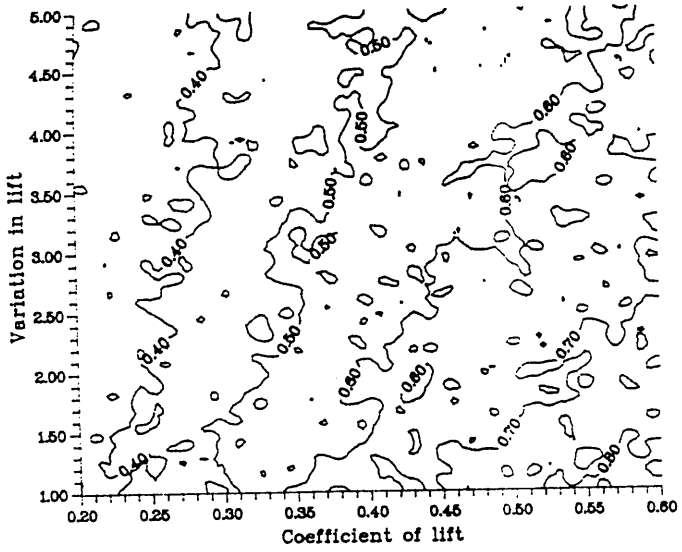
Variation in lift
Coefficient of lift
Transport stage

1.5

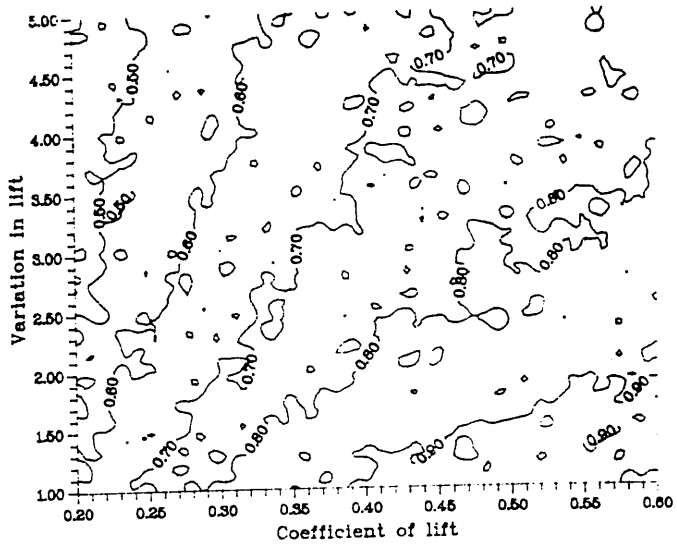
Variation in lift
Coefficient of lift
Transport stage

2.0

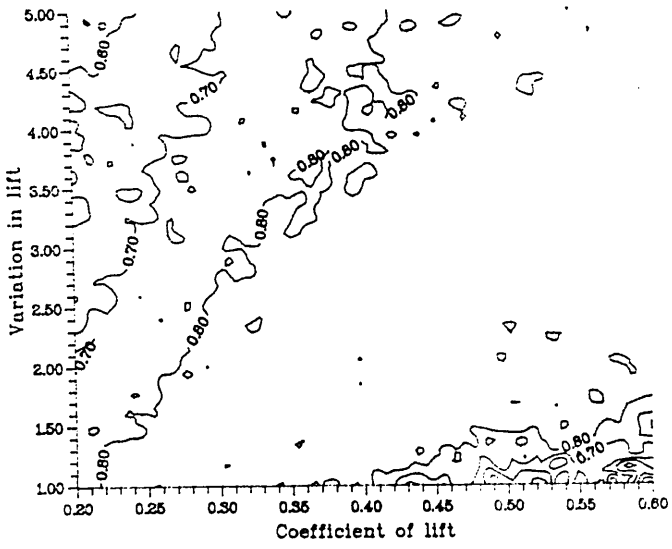
Variation in lift
Coefficient of lift
Transport stage

2.5

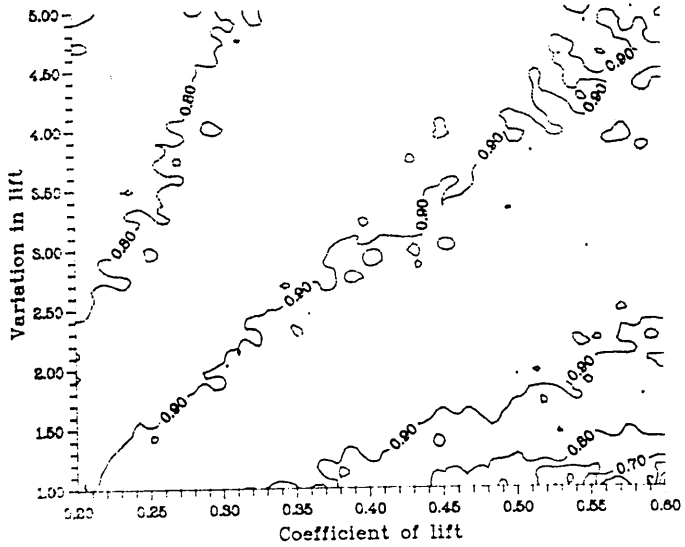
Variation in lift
Coefficient of lift
Transport stage

3.0

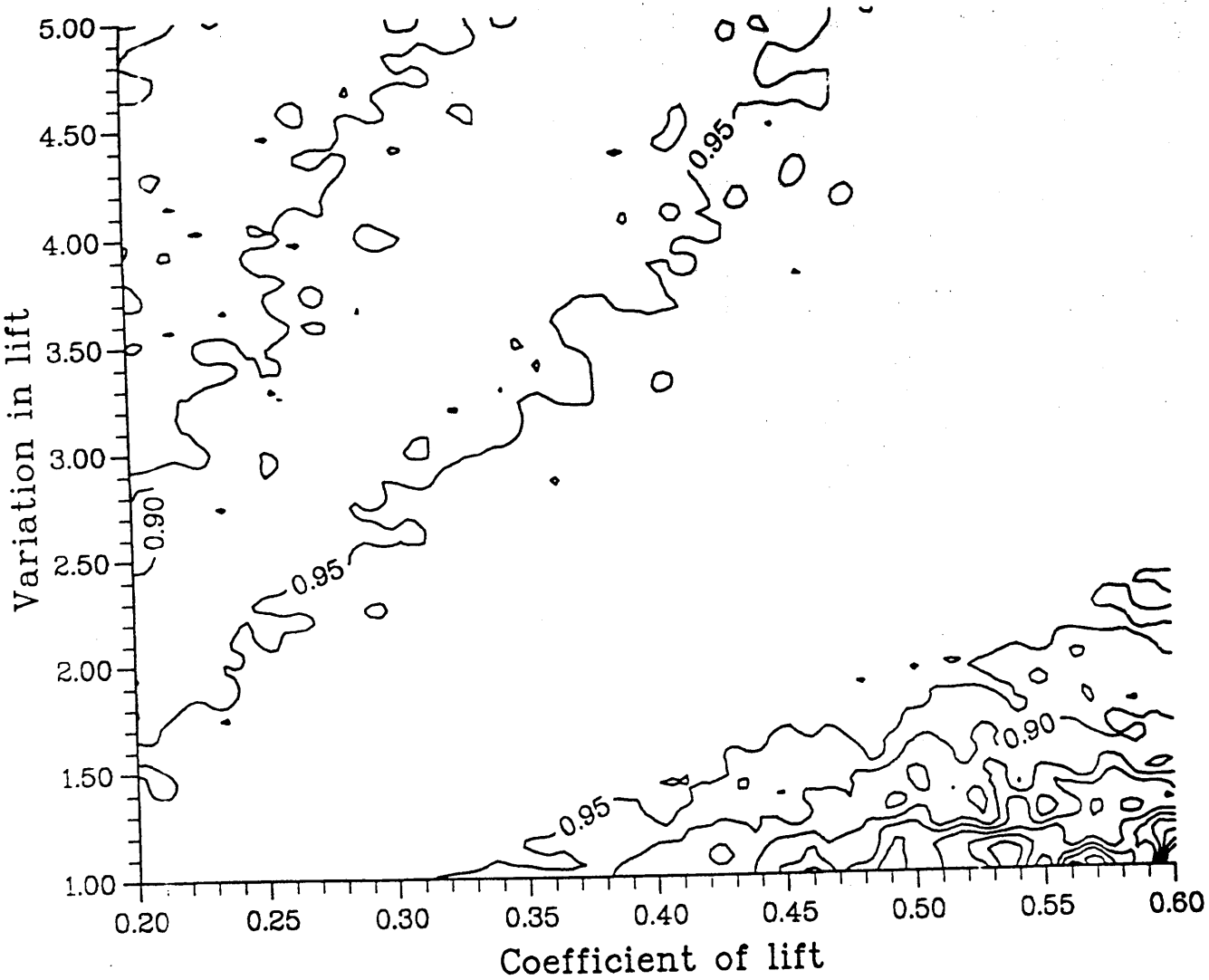

Transport stage

3.0

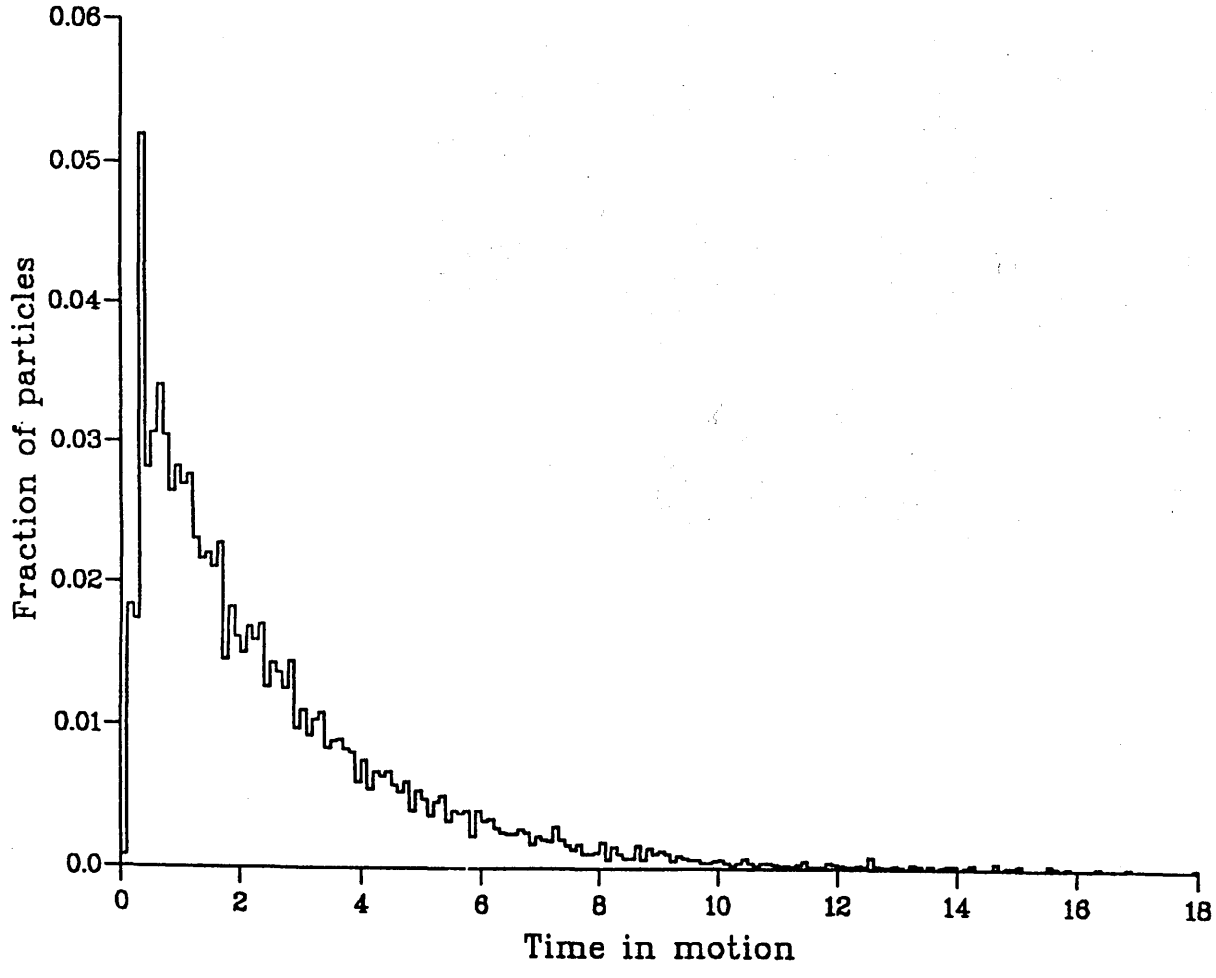
0.06
0.05
0.04
0.03
0.02
0.01
0.0
Fraction of particles
0
2
4
6
8
10
12
14
16
18
Time in motion